Qualitative methods for heterogeneous media

Lorenzo Audibert

École Doctorale de l'École Polytechnique

THÈSE

présentée en vue de l'obtention du titre de

Docteur de l'École Polytechnique

Spécialité : **Mathématiques Appliquées**

par

Lorenzo Audibert

Qualitative methods for heterogeneous media

Thèse soutenue publiquement le 17 septemble 2015 devant le jury composé de :

Directeurs de thèse :	Houssem Haddar	-	INRIA Saclay
	Alexandre Girard	-	EDF R&D
Rapporteurs :	Shari Moskow	-	Drexel University
	Chrysoula Tsogka	-	University of Crete
Examinateurs :	Rainer Kress	-	University of Göttingen
	Josselin Garnier	-	Université Paris Diderot
	Grégoire Allaire	-	Ecole Polytechnique
	Marc Bonnet	-	CNRS ENSTA

Remerciements

Au moment de conclure ce manuscrit je voudrais dire toute ma gratitude aux trois personnes qui ont rendu cette thèse possible, Alexandre, Guy et Houssem. Merci Alexandre, ingénieur au savoir encyclopédique, toujours disponible pour discuter d'obscur point théorique ou pour trouver l'astuce pratique qui fait marcher le numérique. Merci Guy de m'avoir fait confiance et d'avoir su convaincre les « hautes sphères » d'EDF de la pertinence de cette thèse. Merci Houssem, finalement quelle chance cela a été de travailler avec toi, je suis heureux de t'avoir fourni des excuses pour te détourner de tes tâches administratives et d'avoir pu bénéficier de tes avis bienveillants et de ta clairvoyance. A ton contact j'ai aimé dépasser la bonne idée pour passer à l'analyse, il ne me reste plus qu'à écrire les preuves comme un mathématicien et non comme un ingénieur. A tous les trois mille mercis pour la confiance que vous m'avez accordée et les conseils que vous m'avez donnés pendant ces trois années.

Je voudrais remercier également Chrysoula Tsogka et Shari Moskow pour avoir accepté d'être rapporteuses de cette thèse. Je suis conscient que me lire en anglais, n'a pas du être de tout repos et leur en suis reconnaissant.

Je suis honoré que Grégoire Allaire, Josselin Garnier, Rainer Kress et Marc Bonnet aient accepté de faire partie de mon jury.

Je remercie Didier Boldo, Steven Kerzale et Mégane Boudineau pour leur aide sur l'aspect numérique de cette thèse. L'élasticité serait sans doute plus obscure pour moi sans Drossos Gintides avec qui j'ai eu le plaisir de travailler lors de sa présence au CMAP.

Ecrire cette thèse ce fut aussi un peu abandonner les collègues d'EDF pendant trois ans, heureusement leur sympathie et les nombreuses pauses café m'ont permis de garder un pied dans la recherche industrielle. A présent qu'il est temps d'y revenir, je ne doute pas que cela se fera facilement grâce à eux.

Le quotidien de la thèse a été à la fois joyeux et stimulant grâce aux autres étudiants de l'équipe DEFI, Nicolas, Simona, Thi Phong, Mohamed, Zixian, Lucas et les nombreux visiteurs du Delaware. En parlant du Delaware je tiens à remercier Fioralba Cakoni pour la bonne humeur quelle amenait toujours avec elle lors de chacune de ses visites. Incapable de situer le Delaware sur une carte, je ne perds pas espoir de lui rendre visite à mon tour maintenant qu'elle se trouve dans le New Jersey.

Bien entendu le CMAP ne se limite pas à l'équipe DEFI. L'atmosphère qui y règne est à la fois chaleureuse et studieuse et si l'on peut y découvrir le contrôle optimal, l'algèbre tropicale, la modélisation des populations de chenilles...on peut tout autant y créer une équipe de foot soudée qui aurait clairement mérité la victoire lors du tournoi des labos, aussi l'échec subi fut-il le plus dur de mes années de thèse. Bien évidemment rien ne marcherait si Nasséra, Jessica et Alexandra n'étaient pas là pour nous faciliter la vie au quotidien et nous guider dans les méandres administratif de l'école, je me suis entièrement reposé sur vous encore merci.

Faire des sciences ça ne coule pas de source, je tiens à saluer ici les professeurs qui me les ont fait découvrir et aimer: M. Joly, M. Briançon, Mme Picard et M. Riddell.

Mais ne soyons pas trop rabat-joie, une grande partie de ces trois années de recherche s'est aussi passée à l'extérieur du labo et il serait bien injuste d'oublier tous mes amis de longues dates (je ne les citerais pas de peur d'oublier quelqu'un)... qui m'ont écouté leur parler de maths (et d'autres choses) avec le même sourire patient.

Pour conclure, mes remerciements s'adressent tout particulièrement à mon père, qui attend toujours mon prochain brevet et ma future start-up, à ma sœur, sociologue en herbe qui aura lu l'ensemble de ma production mathématique, à ma mère, sans qui je n'aurais jamais été aussi loin (je ne doute pas que tu as déjà dans un coin de ta tête un nouveau sommet à atteindre) et à Emma pour m'aimer malgré les réveils au milieu de la nuit, persuadé que j'étais d'avoir prouvé un théorème.

Contents

Chapter 1

Introduction

Concrete is a wide spread material, usually associated to building, because of its availability, its small cost and its simplicity of use. Often associated to reinforce steel bar (but not always) it ensures primarily the structural behavior of the engineering structure. However concrete is often used to ensure other functions which are not necessarily of secondary importance. For example dams are concrete structures where concrete should also be impermeable (at least the leaking should be controlled). In France the reactor building of nuclear power plants (of electrical power 1300 MW and 1450 MW) is made of a double-wall of reinforced concrete. This double-wall containment have to be impermeable to gases up to a pressure of six bar (or at least they are tested at this pressure) in order to avoid contamination of the environment by radioactive materials in case of an accident. This secondary function ensured by concrete structures on those examples is a crucial function and the infrastructure could not be operated without the guarantee that this function is working. Assessing the state of those structures is therefore a necessity and the use of non destructive inspection techniques would be the best way to proceed. The requirements of nuclear safety are very high on the capabilities that non destructive inspection should achieve: as we will see in the following those expectations could not be matched with classical methods.

As several key infrastructures are built in concrete and are getting older and older, the issue of using them safely as long as possible starts to be an important one. This creates active research in several fields from experimental work in physics and engineering up to applied mathematics. This is mainly due to the properties of concrete that are very attractive from the building point of view, but are very complex from the inspection viewpoint.

The first main difficulty is that concrete is by construction a composite material, at any space scale, and this is true for several types of properties: mechanical, electromagnetic, chemical,... . Secondly, concrete changes in many ways over time, undergoing moisturising, chemical reactions,

Figure 1.1: On the left dam of and on the right the nuclear power plant of St Alban

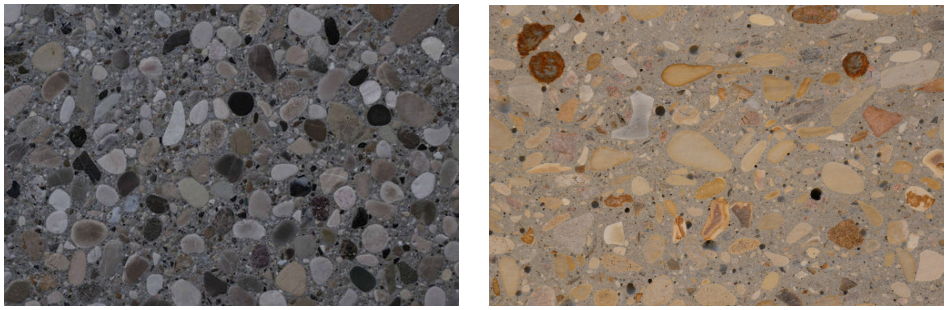

Figure 1.2: pictures of concrete

or cracking - in the form of either large cracks or multiple small ones. Moreover some of those evolutions are not dangerous and can be described as normal in the "life" of the material. Finally those degradations are not by themselves of interest to the engineers that are in charge of the structure. They will prefer to know the speed of the leaking process than the number of cracks found in one piece of material. All those challenges are creating a fairly recent active field of research on non destructive testing of concrete material and more globally on the understanding and modelling of physical processes in this material. A large number of techniques are tested and studied in order to overcome the aforementioned difficulties and try to formulate at least partial answers. Some have looked into electromagnetic waves to probe the material (from Electrical Impedance measurement to Radar and even MRI), or chemical devices and mechanical waves such as ultrasound measurement.

We are interested in ultrasound measurements because from the operational point of view they are easy to set up and the waves are directly influenced by the material properties we are interested in. The main difficulty using ultrasound in concrete is the heterogeneity between the celerities of the induced waves inside the aggregates and the cement paste. This composite aspect of concrete can be seen from a simple picture such as figure 1.2 , where one can see aggregates bonded together by cement paste.

In solids such as concrete the wave propagation can be modelled in the frequency domain by the equation of linear elasticity,

$$\mathrm{div}(2\mu \mathrm{e}(u) + \lambda \mathrm{div}(u) Id) + \rho\omega^2 u = 0$$

which might be simplified by considering only the longitudinal waves that solve the scalar wave equation

$$\Delta u + k^2 n u = 0$$

We have to use a wavelength of the same size than defects. It happens that the defects we are interested in are similar in size with the aggregates. This wavelength requirement implies that the aggregates' microstructure creates an important and unpredictable scattering which makes the signature of the defect extremely difficult to find.

To picture how the background masks the signature of the defect (making it more difficult to spot) we provide an example of measurement of ultrasound in concrete, in figure 1.3. Our

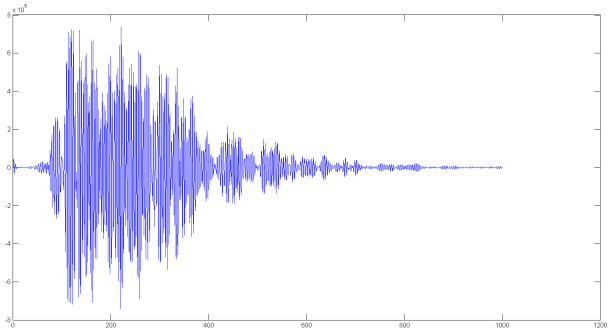

Figure 1.3: Recorded field from CEOS experiment

targeted defect size makes impossible the use of techniques relying on estimation of the background: for example homogenization or random medium techniques do not seem to be suited to our case of study.

To overcome the lack of clear signature of the defect in the measurement of the scattered field, the works of [41] and [48] (and the more theoretically oriented work of [6]) use differential measurement. In these works they compare measurements that are taken at different states of loading. The loading process will primarily have an influence on cracks, therefore the difference between the measurements will mainly originate from the defects. All these works rely on an analysis of the propagation of energy through the material to construct an indicator or an image of the defect. More precisely the work of [41] relies on the approximation of the propagation of waves' energy in an heterogeneous medium by the radiative transfer equation. Based on this analysis they construct a linearised inversion scheme to reconstruct the parameter of the radiative transfer equation or diffusion equation and identify a defect (actually a crack) as a decrease in diffusivity (because the crack is blocking the propagation of energy). They work on multistatic measurements taken at two different static loading states. This acquisition method simplified the analysis compared to [48]. Indeed in this work they used a dynamic low frequency excitation to modify the medium and an ultrasonic (high frequency) wave to probe it. They then constructed an indicator of defect by looking at roughly the amount of time that it takes for energy to propagate through the material with respect to the low frequency wave. Analysing this experiment is much more complicated as the process involves non-linear interaction between the two waves, through the intermediary of constantly changing cracks whose scattering properties are affected by the low frequency waves. Clearly these two works show that differential measurements are feasible and allow to overcome the difficulty introduced by the heterogeneity in concrete.

Unlike these works we take a more applied maths and inverse problems point of view of the question. And more precisely in the vast literature of inverse problems for wave equation our work should be compared to other qualitative or geometrical methods. We choose this class of methods because in its final algorithmic implementation it does not depend on the type of defects, which permits to cope with the wide variety of degradations affecting concrete. Moreover they are simple and efficient in terms of implementation. The disadvantage however is that they

are only able to give geometrical information of the defects. We do not work on the fact that they can also give information on the nature of the obstacle if one has access to several frequency data [32]. As featured previously several works have used differential measurement to overcome the heterogeneous nature of concrete. In this thesis we will also overcome the unknown nature of the material using differential measurement however we won't need to use an energy framework to analyse our method. The fact that our analysis relies on the wave equation allows to use only one frequency of multi static measurement. Since we do not use diffusion approximation, it might give a better resolution. On the other hand we retain the advantages of working in the framework of qualitative methods, namely flexibility and scalability in term of final numerical algorithm. After elaborating a new theoretical framework (chapter 2), we demonstrate that it permits to compare two different datasets (chapter 3). This comparison leads to the construction of a differential imaging method. We then extend the previous results to limited aperture data (chapter 4), and run numerical simulations on concrete-like material (chapter 5). Finally, we extend the application of the method to anisotropic medium and linear elasticity (chapters 6 and 7). Chapters are organized as follows.

Outline of the Thesis

Chapter 2 : Generalized Linear Sampling Method(GLSM)

In this chapter we restrict ourselves to the scattering of scalar waves by an isotropic obstacle. We consider plane wave incident field and farfield measurement and a full aperture acquisition. In this classical setting we revisit the Linear Sampling Method (LSM) first introduced by Colton and Kirsch in [24] in order to have an exact characterization of the support of the obstacle. Such a result has already been proven by Arens and Lechleiter in [3] using the theory of the factorization method. The classical LSM was using the farfield equation as a data fidelity term with a classical Tikhonov regularization which does not bring any theoretical guarantee. The factorization method aims at modifying the data fidelity term in order to obtain theoretical guarantee with a classical Tikhonov regularization. We concentrate instead on the regularization term in order to obtain an exact characterization while keeping the data fidelity term of the LSM. We clarify the link with the factorization method more deeply. We also provide an exact characterization in the case of noisy measurement. Finally our numerical results show superior reconstruction of the obstacle through our framework.

Chapter 3 : Imaging a change in the medium using differential measurement In this chapter again we consider the simpler case of the scattering of scalar waves by an isotropic medium. Our interest is to use two sets of measurement in order to image the change that appears in-between those measurements. We will in fact obtain an exact characterization of the connected component that contains the change. To obtain this result we need to strengthen the connection between the farfield equation and the minimizing sequence we construct within the GLSM framework. Under assumptions on the physical parameter we were able to demonstrate that the sequence we construct actually converges to the solution of some interior transmission problem. Using this asymptotic property of the GLSM we were able to compare the solution of the GLSM constructed from each data set and to obtain an asymptotical characterization of the connected part that contains the change. Finally we construct from the data an indicator

function that takes advantage of this asymptotic behaviour to give an exact characterization. From the numerical implementation we obtain a method that is equivalent to the computing cost of applying the GLSM to each set of measurement.

Chapter 4 : GLSM for non symmetric factorization : In this chapter we extend the GLSM to the case of non symmetric factorization, that arise for example when one considers limited aperture measurement. First we extend the result on strong convergence to the solution of the underlying interior transmission problem under the same assumptions as the characterization of the obstacle. We then propose a method within the GLSM framework to treat the case of non-symmetric factorization, this method uses an a priori estimate of the area where lies the obstacle. Under those weak assumptions we obtain the exact characterization of the scatter and the strong convergence to the solution of the underlying interior transmission problem. In this chapter we still consider the simpler case of the scattering of scalar waves by an isotropic medium, however we improve the condition on the physical parameter under which the GLSM method works. To the best of our knowledge it is the first time that such a result is proven under assumptions on the physical parameter near the boundary of the obstacle only. As a consequence of the results of this chapter we treat the case of nearfield data. From the numerical point of view we introduce a second order method to minimize the GLSM functional which proves to be very efficient in terms of computation time and discuss the difficulties in the case of non-symmetric factorization.

Chapter 5 : Application to a concrete like microstructure The contributions of this chapter are twofolds. First we present the software we built to generate concrete-like microstructures. This software works using only open source packages and is part of the research project of EDF R&D on non destructive testing of concrete. It allows to build a microstructure that occupies a given space in 3D. The microstructure will respect a prescribed distribution of size which is known a priori (in practice from the conception of concrete). One can mesh such a geometry and simulate non destructive testing acquisition on this type of medium. Using such a medium we provide numerical evidence that differential imaging gives promising results on concrete like microstructure.

Chapter 6 : Extension to Orthoptic media In this chapter we consider the scattering of scalar waves by an orthoptic medium. The main contribution of this chapter is to extend the result of chapter 4 under which assumptions the GLSM method works, again we obtain that the conditions on the physical parameters are restricted to the boundary of the obstacle. We also discuss the extension of the result we obtain in chapter 3. This result and the result of chapter 4 on non-symmetric factorization allow us to obtain a complete result in the case of known heterogeneous background.

Chapter 7 : Extension to Elasticity In this chapter we extend the result of the previous chapter to linear elasticity. We also introduce the problem of limited polarization, the case when only one type of polarization is used as sources and measurements. This type of acquisition gives rise to an interior-exterior transmission problem which we were not able to solve and to a non symmetric factorization that do not fall into the theory we developed in chapter 4.

Chapter 2

Generalized Linear Sampling Method

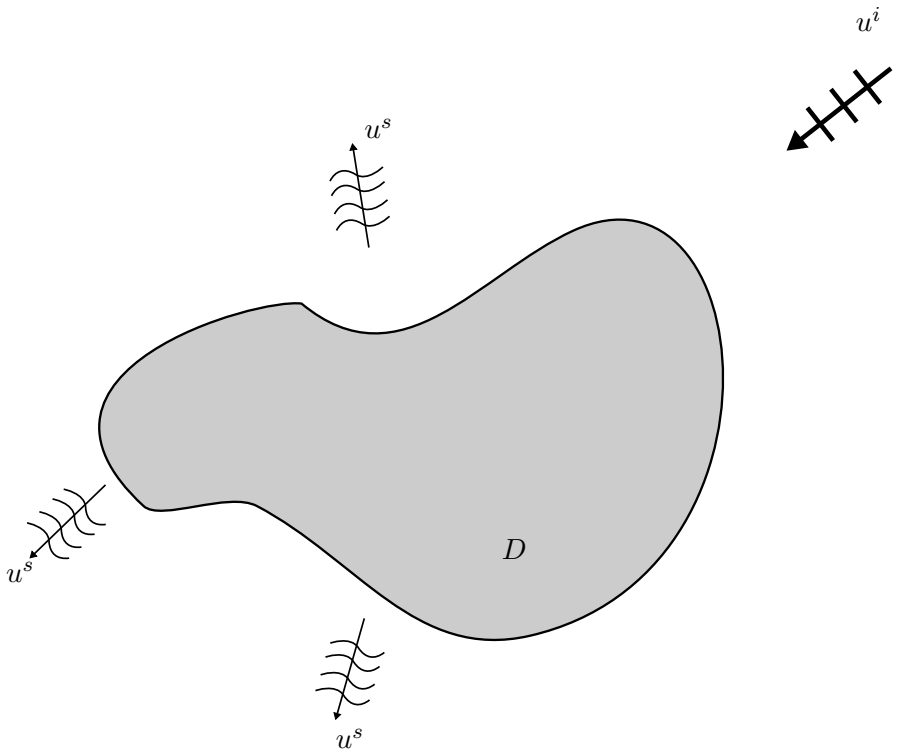

Contents

This chapter is the article [5], published in Inverse Problems. From this article we have slightly modified Theorem 6 to have a little bit more generality. We have also corrected the proof where we have made a small error that does not affect the rightfulness of the theorem. Finally we add a numerical example on the determination of interior transmission eigenvalues. This chapter gives an exact characterization of the support of an obstacle D from multistatic measurement of the farfield pattern of the scattered wave generated by a plane wave. Such measurement can be analyzed using the farfield operator and characterization of the obstacle can be cast as a range characterization as explained in section 2.2. Therefore the problem is to demonstrate (in section 2.3) that one can obtain an exact characterization of the range of a compact operator G as long as one knows $F = GH$ and $B = H^*TH$, where H is dense and T is coercive. This characterization is formulated using the minimizer of a cost functional that involves F as a data fidelity term and B as the regularization term. In section 2.3.2 we show that our theory shares similarity with the factorization method and we extended it to the case of noisy measurement in section 2.3.4. Finally we applied our range characterization to determine the support of an isotropic obstacle that scattered scalar waves and numerical results demonstrate that our formulation gives good reconstruction results.

2.1 Introduction

This work can be seen as a contribution to the development of so-called qualitative methods [25, 40, 15] for solving inverse scattering problems for extended targets from fixed frequency multi-static data. More specifically, we introduce and analyze a new formulation of the so-called Linear Sampling Method (LSM) [24, 23], that we will refer to as Generalized Linear Sampling Method (GLSM). GLSM is based on a new exact characterization of the targets shape in terms of the so-called farfield operator (at a fixed frequency). This characterization is based on constructing nearby solutions to the farfield equation as minimizing sequences of a special cost functional and uses two (complementary) factorizations of the farfield operator. The first one is the basic factorization used in the theoretical justification behind LSM and the second one is the one used by the factorization method (FM) [39, 40]. This combination allows us for instance to require less restrictive assumptions than FM. It also turns out that one can establish a direct link between our method and FM for a special setting of GLSM and this also provides a direct link with the analysis in [2, 3] justifying the use of LSM in some particular configurations. Although not directly inspired by them, the GLSM shares some similarities with the so-called inf-criterion [40] or the formulation of this criterion in [44] as well as the probe method [38, 28].

The main idea behind our method is to explicitly construct the nearby solution of the LSM by adding to a standard least squares misfit functional a penalty term proportional to an appropriate norm of the associated Herglotz wave. Using the second factorization of the farfield operator (as used in FM), we express this term using the measured farfield operator. The main issues to address are first how to cope with the fact that the penalty term is compact and second how to address the case of noisy operators. Here comes the role of the first factorization generally used for LSM. For more details we refer to the third section where the general formulation of the method is presented as well as the analysis for different configurations. In order to introduce the main ideas behind GLSM as well as a concrete application, we choose to present the case

of scalar inverse scattering from inhomogeneous inclusions. We show for this example how the method can be applied and we also indicate other possible straightforward applications (which are roughly speaking all cases where FM applies, or more generally where the inf-criterion and LSM apply).

The impact of our method on the numerical side is twofold. In fact, the analysis of GLSM for noisy farfield operators suggests a different indicator function for LSM than the one usually used. This new indicator function is similar to the one proposed in [2] but contains an additional term that correctly fixes the behavior of the indicator function outside the obstacle for noisy operators. The superiority of this new indicator function is demonstrated through some numerical results. The second alternative is to directly use the minimizing sequence constructed by GLSM, which is computationally more expensive but leads to better results for multi-connected objects. In fact the second numerical method can be used as a post-processing of the first one since, from numerical experiments, we observed that only few iterations are needed to update the initial guess provided by LSM.

The article is organized as follows. In Section 2.2 a model problem is introduced to motivate GLSM after recalling the basis of the LSM and the factorization method. The theoretical foundation of the GLSM is given in Section 2.3. Section 2.4 provides an example of application of GLSM by completely treating the model problem introduced in Section 2.2 and indicating other possible applications. The last section (Section 2.5) is devoted to the introduction of two numerical algorithms issued from Section 2.3 along with validating numerical results and comparing with other algorithms.

2.2 A model problem and motivation for GLSM

In order to introduce the ideas and motivations behind the proposed new algorithm below, namely GLSM, we choose to present as a model problem the scalar inverse time harmonic scattering problem from inhomogenous targets. For a wave number $k > 0$, the total field solves the Helmholtz equation

$$\Delta u + k^2 n u = 0 \text{ in } \mathbb{R}^d$$

with $d = 2$ or 3 and with $n \in L^\infty(\mathbb{R}^d)$ denoting the refractive index such that the support of $n-1$ is equal to $\overline{D}$ with D a bounded domain with Lipschitz boundary and connected complement and such that $\Im(n) \geq 0$. We are interested in the cases where the total field is generated by plane waves, $u^i(\theta, x) := e^{ikx\cdot\theta}$ with $x \in \mathbb{R}^d$ and $\theta \in \mathbb{S}^{d-1}$ (the unit sphere) and we denote by u^s the scattered field defined by

$$u^s(\theta, \cdot) = u - u^i(\theta, \cdot) \quad \text{in } \mathbb{R}^d,$$

which is assumed to be satisfying the Sommerfeld radiation condition,

$$\lim_{r\to\infty} \int_{|x|=r} \left| \frac{\partial u^s}{\partial r} - iku^s \right|^2 ds = 0.$$

Our data for the inverse problem will be formed by noisy measurements of so called farfield pattern $u^\infty(\theta, \hat{x})$ defined by

$$u^s(\theta, x) = \frac{e^{ik|x|}}{|x|^{(d-1)/2}} (u^\infty(\theta, \hat{x}) + O(1/|x|))$$

as $|x| \to \infty$ for all $(\theta, \hat{x}) \in \mathbb{S}^{d-1} \times \mathbb{S}^{d-1}$. The goal is to be able to reconstruct D from these measurements (without knowing n) using a new sampling algorithm. The foundation of this algorithm is inspired by the Linear Sampling Method and the Factorization Method that we shall briefly review here in the context of this special scattering problem. These methods are based on the farfield operator $F : L^2(\mathbb{S}^{d-1}) \to L^2(\mathbb{S}^{d-1})$, defined by

$$Fg(\hat{x}) := \int_{\mathbb{S}^{d-1}} u^\infty(\theta, \hat{x}) g(\theta) ds(\theta).$$

Let us define for $\psi \in L^2(D)$, the unique function $w \in H^1_{\text{loc}}(\mathbb{R}^d)$ satisfying

$$\begin{cases} \Delta w + nk^2 w = k^2(1-n)\psi \text{ in } \mathbb{R}^d, \\ \lim\limits_{r\to\infty} \int\limits_{|x|=r} \left|\frac{\partial w}{\partial r} - ikw\right|^2 ds = 0. \end{cases} \tag{2.1}$$

By linearity of the forward scattering problem, Fg is nothing but the farfield pattern of w solution of (2.1) with $\psi = v_g$ in D, where

$$v_g(x) := \int_{\mathbb{S}^{d-1}} e^{ikx\cdot\theta} g(\theta) ds(\theta), \ g \in L^2(\mathbb{S}^{d-1}), \ x \in \mathbb{R}^d.$$

Now consider the (compact) operator $H : L^2(\mathbb{S}^{d-1}) \to L^2(D)$ defined by

$$Hg := v_g|_D, \tag{2.2}$$

and the (compact) operator $G : \overline{\mathcal{R}(H)} \subset L^2(D) \to L^2(\mathbb{S}^{d-1})$ defined by

$$G\psi := w^\infty,$$

where w^∞ is the farfield of $w \in H^1_{\text{loc}}(\mathbb{R}^d)$ solution of (2.1) and where $\overline{\mathcal{R}(H)}$ denotes the closure of the range of H in $L^2(D)$. Then clearly

$$F = GH.$$

The basis of the Linear Sampling Method is the following characterization of D in terms of the range of G. This characterization is based on the solvability of so called interior transmission problem defined by $(u, v) \in L^2(D) \times L^2(D)$ such that $u - v \in H^2(D)$ and

$$\begin{cases} \Delta u + k^2 n u = 0 \quad \text{in } D, \\ \Delta v + k^2 v = 0 \quad \text{in } D, \\ (u - v) = f \quad \text{on } \partial D, \\ \frac{\partial}{\partial \nu}(u - v) = g \quad \text{on } \partial D, \end{cases} \tag{2.3}$$

for given $f \in H^{\frac{1}{2}}(\partial D)$ and $g \in H^{-\frac{1}{2}}(\partial D)$. We shall make the following assumption

Hypothesis 1. *We assume that $k^2 \in \mathbb{R}_+$ and $n \in L^\infty(D)$ are such that, $\Im(n) \geq 0$ and such that for all $f \in H^{\frac{1}{2}}(\partial D)$ and $g \in H^{-\frac{1}{2}}(\partial D)$ problem (2.22) has a unique solution $(u, v) \in L^2(D) \times L^2(D)$ such that $u - v \in H^2(D)$.*

It is well known for instance that if in addition, $1/(n-1) \in L^\infty(D)$ and $\Re(n-1)$ is positive definite or negative definite in a neighborhood of ∂D, then Hypothesis 1 is verified for all $k \in \mathbb{R}$ except a countable set without any finite accumulation point [52]. Defining

$$\phi_z(\hat{x}) := e^{-ik\hat{x}\cdot z},$$

the main ingredient of LSM is the following.

Theorem 1. *Under Hypothesis 1, $\phi_z \in \mathcal{R}(G)$ if and only if $z \in D$.*

The proof of this theorem is rather straightforward using the important result of Lemma 1 (see [49]) and the fact that ϕ_z is the farfield of $\Phi(\cdot; z)$, the fundamental solution of the Helmholtz equation satisfying the Sommerfeld radiation condition.

Lemma 1. $\overline{\mathcal{R}(H)} = \{v \in L^2(D); \Delta v + k^2 v = 0 \text{ in } D\}$.

From Theorem 1 one can deduce the following statement, which is the basic theoretical justification of the LSM.

Theorem 2. *Under Hypothesis 1, the operator F is injective with dense range. Moreover, the following holds.*

- *If $z \in D$ then there exists g_z^ϵ such that $\|Fg_z^\epsilon - \phi_z\|_{L^2(\mathbb{S}^{d-1})} \leq \epsilon$ and $\limsup_{\epsilon\to 0} \|Hg_z^\epsilon\|_{L^2(D)} < \infty$.*
- *If $z \notin D$ then for all g_z^ϵ such that $\|Fg_z^\epsilon - \phi_z\|_{L^2(\mathbb{S}^{d-1})} \leq \epsilon$, $\lim_{\epsilon\to 0} \|Hg_z^\epsilon\|_{L^2(D)} = \infty$.*

This theorem thus suggests to use a nearby solution to $Fg_z^\epsilon \simeq \phi_z$ for different sampling points z to obtain an indicator of D. Two problematic issues are then raised: the first one is that the indicator function (provided by the theorem) should be $\|Hg_z^\epsilon\|_{L^2(D)}$ which depends on D and the second one is that the theorem does not give explicit construction of g_z^ϵ. In practice, a Tikhonov regularization is usually used to build a nearby solution (as suggested by the first statement in Theorem 2) and $\|g_z^\epsilon\|_{L^2(\mathbb{S}^{d-1})}$ is used in replacement of $\|Hg_z^\epsilon\|_{L^2(D)}$. In [2] it is proved, based on the Factorization method, that Tikhonov regularization provides the good solution as soon as $\Im(n) = 0$ and in that case one can replace $\|Hg_z^\epsilon\|_{L^2(D)}$ with $|Hg_z^\epsilon(z)|$. As it will be seen later, the proposed GLSM gives an alternative solution independent from the Factorization method (although inspired by this method) and, more importantly, that efficiently treats the case of noisy operator.

The idea behind GLSM is as simple as reconstructing a nearby solution of the LSM by using a least squares misfit functional with a penalty term that controls $\|Hg_z^\epsilon\|^2_{L^2(D)}$. This is feasible thanks to the second factorization of the farfield operator, which is the starting point of the Factorization method. More precisely, for the case under consideration, since the farfield operator of w has the following expression ([25])

$$w^\infty(\hat{x}) = -\int_{\mathcal{D}} e^{-iky.\hat{x}}(1-n)k^2(\psi(y) + w(y))dy,$$

one simply has $G = H^*T\psi$ where $H^* : L^2(D) \to L^2(\mathbb{S}^{d-1})$ is the adjoint of H given by

$$H^*\varphi(\hat{x}) := \int_D e^{-iky.\hat{x}}\varphi(y)dy, \ \varphi \in L^2(D), \ \hat{x} \in \mathbb{S}^{d-1},$$

and where T: $L^2(D) \to L^2(D)$ is defined by

$$T\psi := -k^2(1-n)(\psi + w), \tag{2.4}$$

with $w \in H^1_{\text{loc}}(\mathbb{R}^d)$ being the solution of (2.1). Finally we get

$$F = H^* T H,$$

which indicates that $(Fg, g)_{L^2(\mathbb{S}^{d-1})} = (T(Hg), Hg)_{L^2(D)}$. Therefore, if the operator T satisfies some appropriate coercivity property, the term $(Fg, g)_{L^2(\mathbb{S}^{d-1})}$ would be equivalent to $\|Hg_z^\epsilon\|^2_{L^2(D)}$. One then can use $\left|(Fg, g)_{L^2(\mathbb{S}^{d-1})}\right|$ as a penalty term and also as a criterion for building the indicator function. This is the starting point of GLSM. The detailed formulation and analysis of the method are given in the next section.

2.3 Theoretical Foundations of GLSM

In this section we shall give the theoretical foundations of the Generalized Linear Sampling Method. The general framework is given by the following assumptions. We shall denote by X and Y two (complex) reflexive Banach spaces with duals X^* and Y^* respectively and shall denote by $\langle , \rangle$ a duality product that refers to $\langle X^*, X\rangle$ or $\langle Y^*, Y\rangle$ duality. We consider two bounded linear operators $F : X \to X^*$ and $B : X \to X^*$ that are assumed to be bounded. Moreover we shall assume that the following factorizations hold

$$F = GH \quad \text{and} \quad B = H^* T H \tag{2.5}$$

where the operators $H : X \to Y$, $T : Y \to Y^*$ and $G : \overline{\mathcal{R}(H)} \subset Y \to X^*$ are bounded, with $\overline{\mathcal{R}(H)}$ the closure of the range of H in Y.

2.3.1 Formulation of GLSM for noise free measurements

Let $\alpha > 0$ be a given parameter and $\phi \in X^*$. The GLSM (for noisy free measurements) is based on considering minimizing sequences of the functional $J_\alpha(\phi; \cdot) : X \to \mathbb{R}$

$$J_\alpha(\phi; g) := \alpha|\langle Bg,\, g\rangle| + \|Fg - \phi\|^2 \quad \forall g \in X. \tag{2.6}$$

Indeed this functional has not a minimizer in general. However, since $J_\alpha(\phi; \cdot) \geq 0$ one can define

$$j_\alpha(\phi) := \inf_{g \in X} J_\alpha(\phi; g). \tag{2.7}$$

Then the first simple observation is the following.

Lemma 2. *Assume that F has dense range. Then for all $\phi \in X^*$, $j_\alpha(\phi) \to 0$ as $\alpha \to 0$.*

Proof. Since F has dense range, for a given $\epsilon > 0$ there exists g_ϵ such that $\|Fg_\epsilon - \phi\| < \frac{\epsilon}{2}$. Then one can choose $\alpha_0(\epsilon)$ such for all $\alpha \leq \alpha_0(\epsilon)$, $\alpha|\langle Bg_\epsilon,\, g_\epsilon\rangle| < \frac{\epsilon}{2}$ so that $j_\alpha(\phi) < \epsilon$, which proves the claim. □

The central theorem for noise free GLSM is the following characterization of the range of G in terms of F and B.

Theorem 3. *We assume in addition that*

- *G is compact and $F = GH$ has dense range.*
- *T satisfies the coercivity property*

$$|\langle T\varphi,\, \varphi\rangle| > \mu \,\|\varphi\|^2 \quad \forall\, \varphi \in \mathcal{R}(H), \tag{2.8}$$

where $\mu > 0$ is a constant independent of φ. Let $C > 0$ be a given constant (independent of α) and consider for $\alpha > 0$ and $\phi \in X^*$, $g_\alpha \in X$ such that

$$J_\alpha(\phi; g_\alpha) \leq j_\alpha(\phi) + C\,\alpha. \tag{2.9}$$

Then $\phi \in \mathcal{R}(G)$ if and only if $\limsup_{\alpha\to 0} |\langle Bg_\alpha,\, g_\alpha\rangle| < \infty$ which is true if and only if $\liminf_{\alpha\to 0} |\langle Bg_\alpha,\, g_\alpha\rangle| < \infty$.

Proof.

- Assume that $\phi \in \mathcal{R}(G)$. Then, by definition one can find $\varphi \in \overline{\mathcal{R}(H)}$ such that $G\varphi = \phi$. for $\alpha > 0$, $\exists g_0 \in X$ such that $\|Hg_0 - \varphi\|^2 < \alpha$. Then by continuity of G, $\|Fg_0 - \phi\|^2 < \|G\|^2\alpha$. On the other hand the continuity of T implies

$$|\langle Bg_0,\, g_0\rangle| = |\langle THg_0,\, Hg_0\rangle| \leq \|T\|\,\|Hg_0\|^2 < 2\,\|T\|\,(\alpha + \|\varphi\|^2)$$

From the definitions of $j_\alpha(\phi)$ and g_α we have

$$\alpha|\langle Bg_0,\, g_0\rangle| + \|Fg_0 - \phi\|^2 > j_\alpha(\phi) > J_\alpha(\phi, g_\alpha) - C\alpha.$$

We then deduce from the definition of J_α and previous inequalities

$$\alpha|\langle Bg_\alpha,\, g_\alpha\rangle| \leq J_\alpha(\phi, g_\alpha) \leq C\alpha + 2\alpha\,\|T\|\,(\alpha + \|\varphi\|^2) + \alpha\|G\|^2.$$

Therefore $\limsup_{\alpha\to 0} |\langle Bg_\alpha,\, g_\alpha\rangle| < \infty$. This also implies $\liminf_{\alpha\to 0} |\langle Bg_\alpha,\, g_\alpha\rangle| < \infty$.

- Assume that $\phi \notin \mathcal{R}(G)$ and assume (by a contradiction argument) that $\liminf_{\alpha\to 0} |\langle Bg_\alpha,\, g_\alpha\rangle| < \infty$. Then, (for some extracted subsequence g_α) $|\langle Bg_\alpha,\, g_\alpha\rangle| < A$ for some constant A independent of $\alpha \to 0$. The coercivity of T implies that $\|Hg_\alpha\|$ is also bounded. Since Y is reflexive, then one can assume that, up to an extracted subsequence, Hg_α weakly converges to some φ in Y. In fact $\varphi \in \overline{\mathcal{R}(H)}$ since the latter is a convex set. Since G is compact, we obtain that GHg_α strongly converges to $G\varphi$ as $\alpha \to 0$. On the other hand, Lemma 2 and the definition $J_\alpha(\phi, g_\alpha)$ imply that $\|Fg_\alpha - \phi\| \leq J_\alpha(\phi, g_\alpha) \leq j_\alpha(\phi) + C\alpha \to 0$ as $\alpha \to 0$. Since $Fg_\alpha = GHg_\alpha$ we obtain that $G\varphi = \phi$ which is a contradiction. We then conclude that if $\phi \notin \mathcal{R}(G)$ then $\liminf_{\alpha\to 0} |\langle Bg_\alpha,\, g_\alpha\rangle| = \infty$. The latter also implies $\limsup_{\alpha\to 0} |\langle Bg_\alpha,\, g_\alpha\rangle| = \infty$.

□

As indicated in the previous section, the range of the operator G characterizes the inclusion D. Therefore this theorem would lead to a characterization of D in terms of the operators F and B. It also stipulates that an indicator function is given by $|\langle Bg_\alpha, g_\alpha\rangle|$ for small values of α. Let us note that the parameter α does not play the role of a regularization parameter, since for foreseen applications, the operator B is in general compact. However, constructing a sequence (g_α) satisfying (2.9) for fixed $\alpha > 0$ may be viewed as a regularization of the minimization of $J_\alpha(\phi;\cdot)$ that can be used for numerics. A different regularization procedure that would be more suited for noisy operators is introduced in the following subsection.

Let us finally remark that in most of the applications that we have in mind, taking $B = F$ would be sufficient. In this particular case one can state the following straightforward corollary.

Corollary 1. *Assume that $G(\varphi) = H^*T(\varphi)$ for all $\varphi \in \mathcal{R}(H)$ and assume in addition that*

- *H is compact and F has dense range,*
- *T satisfies the coercivity property (2.8).*

Let $C > 0$ be a given constant (independent of α) and consider for $\alpha > 0$ and $\phi \in X^*$, $g_\alpha \in X$ such that

$$J_\alpha(\phi; g_\alpha) \leq j_\alpha(\phi) + C\,\alpha. \tag{2.10}$$

Then $\phi \in \mathcal{R}(G)$ if and only if $\limsup_{\alpha\to 0} |\langle Fg_\alpha, g_\alpha\rangle| < \infty$ which is true if and only if $\liminf_{\alpha\to 0} |\langle Fg_\alpha, g_\alpha\rangle| < \infty$.

The assumptions required in this corollary are weaker than the ones required by the Factorization method but are similar to those of so-called inf-criterion (See [40]). Indeed the main advantage of GLSM with respect to the inf-criterion (as it will explained in the numerical section) is that it leads to a more tractable numerical inversion algorithms. In some special configurations there is a direct link between GLSM and the factorization method as explained below.

We also remark that according to Lemma 2 the sequence (g_α) provides a nearby solution to $Fg \simeq \phi$ satisfying

$$\|Fg_\alpha - \phi\| \leq j_\alpha(\phi) + C\,\alpha.$$

The reader then easily observes from the proof that one obtains the same conclusion in Corollary 1 if we replace the indicator function $|\langle Fg_\alpha, g_\alpha\rangle|$ by $|\langle \phi, g_\alpha\rangle|$. The latter criterion coincides with the one proposed in [2] and has been analyzed in [2] and [3] based on the $(F^*F)^{\frac{1}{4}}$ method.

2.3.2 Link with the $(F^*F)^{\frac{1}{4}}$ method

We found it useful to indicate a link between the GLSM and the first version of the factorization method, namely the so-called $(F^*F)^{\frac{1}{4}}$-method [39]. This method applies when X is a Hilbert space with a scalar product denoted $(\cdot,\cdot)$, and $F : X \to X$ is compact, normal, injective and with dense range. Then it is shown that F can be factorized as

$$F = (F^*F)^{\frac{1}{4}} J (F^*F)^{\frac{1}{4}}$$

with $J : X \to X$ a coercive operator. Among others, two possibilities are of interest:

- A first possibility is to apply the GLSM with $B = F$, $H = (F^*F)^{\frac{1}{4}}$ and $G = (F^*F)^{\frac{1}{4}}J$. We then obtain that $\phi \in \mathcal{R}((F^*F)^{\frac{1}{4}})$ if and only if $\limsup_{\alpha\to 0} |\langle Fg_\alpha, g_\alpha\rangle| < \infty$ where g_α satisfies (2.9). Therefore, whenever one can use the range of $(F^*F)^{\frac{1}{4}}$ to characterize the shape of the scattering object, one can also use GLSM with $B = F$ to obtain a different characterization.

- Another (more informative) possibility is to apply GLSM with $B = (F^*F)^{\frac{1}{2}}$. In this case, using the system $(\lambda_i, \psi_i)_{i\geq 1}$ of eigenvalues and eigenvectors of the normal operator F, we observe that

$$\begin{aligned} J_\alpha(\phi; g) &= \alpha|((F^*F)^{\frac{1}{2}}g, g)| + \|Fg - \phi\|^2 \\ &= \alpha \sum_i |\lambda_i||(g, \psi_i)|^2 + \sum_i (\lambda_i(g, \psi_i) - (\phi, \psi_i))^2. \end{aligned}$$

  Hence, $J_\alpha(\phi; \cdot)$ has a minimizer given by

$$g_\alpha = \sum_i \frac{\bar{\lambda_i}(\phi, \psi_i)}{\alpha|\lambda_i| + |\lambda_i|^2}\psi_i.$$

  It is clear that this g_α satisfies (2.9). Let us now define

$$g_\alpha^{\mathrm{FM}} = \sum_i \frac{|\lambda_i|^{\frac{1}{2}}}{|\lambda_i| + \alpha}(\phi, \psi_i)\psi_i,$$

  which is the minimizer of the Tikhonov functional $\alpha \|g\|^2 + \left\|(F^*F)^{\frac{1}{4}}g - \phi\right\|^2$. Then one observes that the GLSM indicator is nothing but

$$|((F^*F)^{\frac{1}{2}}g_\alpha, g_\alpha)| = \sum_i \frac{|\lambda_i|(\phi, \psi_i)^2}{(\alpha + |\lambda_i|)^2} = \left\|g_\alpha^{\mathrm{FM}}\right\|^2.$$

We finally remark that one obtains a similar link with the so called $F_\#$ method (when it applies) and GLSM by taking $B = F_\#$ and replacing F by $F_\#$ in the GLSM setting. But when the $F_\#$ method applies one can also apply GLSM with only $B = F$.

2.3.3 Regularized formulation of GLSM

As it will be clearer later, the previous formulation of GLSM has to be adapted to the case of noisy operators since in general a noisy operator B does not satisfy a factorization of the form (2.5) (with a middle operator satisfying a coercivity property similar to (2.8)). In order to cope with this issue we introduce a regularized version of J_α which allows similar range characterization and where one controls both the noisy criteria and the noisy misfit term. Among several other options, it turned out that a convenient way to introduce this regularization is to consider for $\alpha > 0$ and $\epsilon > 0$ (that will later be linked with the noise level) and for $\phi \in X^*$, the functional $J_\alpha^\varepsilon(\phi; \cdot) : X \to \mathbb{R}$ defined by

$$J_\alpha^\varepsilon(\phi; g) = \alpha(|\langle Bg, g\rangle| + \varepsilon \|g\|^2) + \|Fg - \phi\|^2. \tag{2.11}$$

Lemma 3. *Assume that B is compact. Then for all $\alpha > 0$, $\epsilon > 0$ and $\phi \in X^*$ the functional $J^\varepsilon_\alpha(\phi;\cdot)$ has a minimizer $g^\varepsilon_\alpha \in X$. If we assume in addition that F has dense range, then*

$$\lim_{\alpha\to 0}\lim_{\varepsilon\to 0} J^\varepsilon_\alpha(\phi; g^\varepsilon_\alpha) = \lim_{\varepsilon\to 0}\limsup_{\alpha\to 0} J^\varepsilon_\alpha(\phi; g^\varepsilon_\alpha) = 0.$$

Proof. The existence of minimizer is clear: for fixed $\alpha > 0$, $\epsilon > 0$ and $\phi \in X^*$, any minimizing sequence (g^n) of $J^\varepsilon_\alpha(\phi;\cdot)$ is bounded and therefore one can assume that it is weakly convergent in X to some $g^\varepsilon_\alpha \in X$. The lower semi-continuity of the norm with respect to weak convergence and the compactness property of B then imply

$$J^\varepsilon_\alpha(\phi; g^\varepsilon_\alpha) \le \liminf_{n\to\infty} J^\varepsilon_\alpha(\phi; g^n) \le \inf_{g\in X} J^\varepsilon_\alpha(\phi; g),$$

which proves that g^ε_α is a minimizer of $J^\varepsilon_\alpha(\phi;\cdot)$ on X.
Now assume in addition that F has dense range. By Lemma 2, $j_\alpha(\phi) \to 0$ as $\alpha \to 0$. Showing that $\lim_{\varepsilon\to 0} J^\varepsilon_\alpha(\phi; g^\varepsilon_\alpha) = j_\alpha(\phi)$ will then prove that $\lim_{\alpha\to 0}\lim_{\varepsilon\to 0} J^\varepsilon_\alpha(\phi; g^\varepsilon_\alpha) = 0$. We observe that

$$J^\varepsilon_\alpha(\phi; g) = J_\alpha(\phi; g) + \alpha\varepsilon\|g\|^2 \tag{2.12}$$

and therefore $|J^\varepsilon_\alpha(\phi; g) - J_\alpha(\phi; g)| \to 0$ as $\varepsilon \to 0$. For $\eta > 0$ one can choose g such that $|J_\alpha(\phi; g) - j_\alpha(\phi)| \le \eta/2$. For this g one then has for ε sufficiently small $|J^\varepsilon_\alpha(\phi; g) - J_\alpha(\phi; g)| < \eta/2$. We obtain by triangular inequality that for ε sufficiently small $J^\varepsilon_\alpha(\phi; g) \le j_\alpha(\phi) + \eta$. We now observe from the definitions of g^ε_α and j_α and from (2.12),

$$j_\alpha(\phi) \le J_\alpha(\phi; g^\varepsilon_\alpha) \le J^\varepsilon_\alpha(\phi; g^\varepsilon_\alpha) \le J^\varepsilon_\alpha(\phi; g),$$

which proves the claim.
We now prove $\lim_{\varepsilon\to 0}\limsup_{\alpha\to 0} J^\varepsilon_\alpha(\phi; g^\varepsilon_\alpha) = 0$. First consider g_ε a minimizer on X of the Tikhonov functional $\varepsilon^2\|g\|^2 + \|Fg - \phi\|^2$ and set $j^\varepsilon = \varepsilon^2\|g_\varepsilon\|^2 + \|Fg_\varepsilon - \phi\|^2$ which goes to zero as ε goes to zero (classical result for Tikhonov regularization, see also Lemma 2 which is valid for any bounded operator B). We have that $\alpha \le \varepsilon$, $J^\varepsilon_\alpha(g) \le \varepsilon^2\|g\|^2 + \|Fg - \Phi\|^2 + \alpha(|(Bg, g)|$. By taking the upper limit we have

$$\limsup_{\alpha\to 0} J^\varepsilon_\alpha(g^\varepsilon_\alpha) \le \limsup_{\alpha\to 0} J^\varepsilon_\alpha(g_\varepsilon) = j^\varepsilon,$$

which concludes the proof. □

Theorem 4. *Under the assumptions of Theorem 3 and the additional assumption that B is compact the following holds. If g^ε_α denotes the minimizer of $J^\varepsilon_\alpha(\phi;\cdot)$ (defined by (2.11)) for $\alpha > 0$, $\varepsilon > 0$ and $\phi \in X^*$, then $\phi \in \mathcal{R}(G)$ if and only if $\limsup_{\alpha\to 0}\limsup_{\varepsilon\to 0} |\langle Bg^\varepsilon_\alpha, g^\varepsilon_\alpha\rangle| < \infty$ which is true if and only if $\liminf_{\alpha\to 0}\liminf_{\varepsilon\to 0} |\langle Bg^\varepsilon_\alpha, g^\varepsilon_\alpha\rangle| < \infty$.*

Proof. The proof is similar to the proof of Theorem 3.

- Assume that $\phi = G(\varphi)$ for some $\varphi \in \overline{\mathcal{R}(H)}$. We consider the same g_0 as in the first part of the proof of Theorem 3 (that depends on α but is independent from ε). Then we choose ε such that $\varepsilon\|g_0\|^2 \le 1$. Then

$$J^\varepsilon_\alpha(\phi; g^\varepsilon_\alpha) \le J^\varepsilon_\alpha(\phi; g_0) \le J_\alpha(\phi; g_0) + \alpha \tag{2.13}$$

Consequently

$$\alpha|\langle Bg_\alpha^\varepsilon,\, g_\alpha^\varepsilon\rangle| \le J_\alpha^\varepsilon(\phi; g_\alpha^\varepsilon) \le \alpha + 2\alpha\,\|T\|\,(\alpha + \|\varphi\|^2) + \alpha\|G\|^2$$

which proves $\limsup_{\alpha\to 0}\limsup_{\varepsilon\to 0}|\langle Bg_\alpha^\varepsilon,\, g_\alpha^\varepsilon\rangle| < \infty$.

- Assume $\phi \notin \mathcal{R}(G)$ and assume that $\liminf_{\alpha\to 0}\liminf_{\varepsilon\to 0}|\langle Bg_\alpha^\varepsilon,\, g_\alpha^\varepsilon\rangle|$ is finite. The coercivity of T implies that $\liminf_{\alpha\to 0}\liminf_{\varepsilon\to 0}\|Hg_\alpha^\varepsilon\|^2$ is also finite. This means the existence of a subsequence $(\alpha', \varepsilon(\alpha'))$ such that $\alpha' \to 0$ and $\varepsilon(\alpha') \to 0$ as $\alpha' \to 0$ and $\left\|Hg_{\alpha'}^{\varepsilon(\alpha')}\right\|^2$ is bounded independently from α'. On the other hand, the second part of Lemma 3 (namely the first limit), indicates that one can choose this subsequence such that $J_{\alpha'}^{\varepsilon(\alpha')}(g_{\alpha'}^{\varepsilon(\alpha')}) \to 0$ as $\alpha' \to 0$ and therefore $\left\|Fg_{\alpha'}^{\varepsilon(\alpha')} - \phi\right\| \to 0$ as $\alpha' \to 0$. The compactness of G implies that a subsequence of $GHg_{\alpha'}^{\varepsilon(\alpha')}$ converges for some $G\varphi$ in X^*. The uniqueness of the limit implies that $G\varphi = \phi$ which is a contradiction.

□

In this theorem ε should be viewed as the regularization parameter (and not α which is rather used to construct an indicator function with a limiting process). As indicated by (2.13), this regularization parameter serves in the construction of the minimizing sequence of Theorem 3.

This theorem with regularization stipulates that a criterion to localize the target is given by $|\langle Bg_\alpha^\varepsilon,\, g_\alpha^\varepsilon\rangle|$ for small values of ϵ and α. The reader can easily see from the first part of the proof that the result holds true if we replace this by $(|\langle Bg_\alpha^\varepsilon,\, g_\alpha^\varepsilon\rangle| + \varepsilon\|g_\alpha^\varepsilon\|^2)$. This latter criterion is more suited to the case of noisy measurements as indicated in the section below.

2.3.4 The GLSM for noisy data

In this section we will consider the case where there may be noise in the data. More precisely, we shall assume that one has access to two noisy operators B^δ and F^δ such that

$$\left\|F^\delta - F\right\| \le \delta\|F\| \quad \text{and} \quad \left\|B^\delta - B\right\| \le \delta\|B\|$$

for some $\delta > 0$. We also assume in this section that the operators, B, B^δ F^δ and F are compact. We then consider for $\alpha > 0$ and $\phi \in X^*$, the functional $J_\alpha^\delta(\phi;\cdot) : X \to \mathbb{R}$,

$$J_\alpha^\delta(\phi; g) := \alpha(|\langle B^\delta g,\, g\rangle| + \delta\|B\|\,\|g\|^2) + \left\|F^\delta g - \phi\right\|^2 \quad \forall\, g \in X, \tag{2.14}$$

which coincides with a regularized noisy functional J_α^ε with a regularization parameter $\epsilon = \delta\|B\|$. According to Lemma 3 one can consider g_α^δ a minimizer of $J_\alpha^\delta(\phi; g)$. We first observe (similarly to in the second part of the proof of Lemma 3)

Lemma 4. *Assume in addition that F has dense range. Then for all $\phi \in X^*$,*

$$\lim_{\alpha\to 0}\limsup_{\delta\to 0} J_\alpha^\delta(\phi; g_\alpha^\delta) = 0.$$

Proof. We observe that for all $g \in X$,

$$J_\alpha^\delta(\phi; g) \leq J_\alpha(\phi; g) + (2\alpha\delta\|B\| + \delta^2\|F\|^2)\,\|g\|^2\,. \tag{2.15}$$

Since $(2\alpha\delta\|B\| + \delta^2\|F\|^2) \to 0$ as $\delta \to 0$, then as in the proof of Lemma 3, for any $\eta > 0$ (α fixed), one can choose $g \in X$ such that for sufficiently small δ,

$$J_\alpha^\delta(\phi; g) \leq j_\alpha(\phi) + \eta$$

Consequently, from the definition of g_α^δ,

$$J_\alpha^\delta(g_\alpha^\delta; \phi) \leq j_\alpha(\phi) + \eta$$

This proves the claim, since $j_\alpha(\phi) \to 0$ as $\alpha \to 0$ (by Lemma 2).

□

Theorem 5. *Assume that the assumptions of Theorem 3 and the additional assumptions of this subsection hold true. Let g_α^δ be the minimizer of $J_\alpha^\delta(\phi;\cdot)$ (defined by (2.14)) for $\alpha > 0$, $\delta > 0$ and $\phi \in X^*$. Then $\phi \in \mathcal{R}(G)$ if and only if $\limsup_{\alpha\to 0}\limsup_{\delta\to 0}\left(\left|\langle B^\delta g_\alpha^\delta, g_\alpha^\delta\rangle\right| + \delta\|B\|\left\|g_\alpha^\delta\right\|^2\right) < \infty$ which is true if and only if $\liminf_{\alpha\to 0}\liminf_{\delta\to 0}\left(\left|\langle B^\delta g_\alpha^\delta, g_\alpha^\delta\rangle\right| + \delta\|B\|\left\|g_\alpha^\delta\right\|^2\right) < \infty$.*

Proof. The proof of this theorem follows the lines of the proof of Theorem 4.

- Assume that $\phi = G(\varphi)$ for some $\varphi \in \overline{\mathcal{R}(H)}$. We consider the same g_0 as in the first part of the proof of Theorem 3 (that depends on α but is independent from δ). Choosing δ sufficiently small such that

  $$(2\alpha\delta\|B\| + \delta^2\|F\|^2)\,\|g_0\|^2 \leq \alpha$$

  we get

  $$J_\alpha^\delta(\phi; g_\alpha^\delta) \leq J_\alpha^\delta(\phi; g_0) \leq J_\alpha(\phi; g_0) + \alpha. \tag{2.16}$$

  Consequently

  $$\alpha\left(|\langle Bg_\alpha^\delta, g_\alpha^\delta\rangle| + \delta\|B\|\left\|g_\alpha^\delta\right\|^2\right) \leq J_\alpha^\delta(\phi; g_\alpha^\delta) \leq \alpha + 2\alpha\,\|T\|\,(\alpha + \|\varphi\|^2) + \alpha\|G\|^2,$$

  which proves $\limsup_{\alpha\to 0}\limsup_{\delta\to 0}\left(\left|\langle B^\delta g_\alpha^\delta, g_\alpha^\delta\rangle\right| + \delta\|B\|\left\|g_\alpha^\delta\right\|^2\right) < \infty$.

- Assume $\phi \notin \mathcal{R}(G)$ and assume that $\liminf_{\alpha\to 0}\liminf_{\varepsilon\to 0}\left(\left|\langle B^\delta g_\alpha^\delta, g_\alpha^\delta\rangle\right| + \delta\|B\|\left\|g_\alpha^\delta\right\|^2\right)$ is finite. The coercivity of T implies that

  $$\mu\left\|Hg_{\alpha(\delta)}^\delta\right\|^2 \leq |\langle Bg_\alpha^\delta, g_\alpha^\delta\rangle| \leq |\langle B^\delta g_\alpha^\delta, g_\alpha^\delta\rangle| + \delta\|B\|\left\|g_\alpha^\delta\right\|^2.$$

  Therefore $\liminf_{\alpha\to 0}\liminf_{\delta\to 0}\left\|Hg_\alpha^\delta\right\|^2$ is also finite. This means the existence of a subsequence $(\alpha', \delta(\alpha'))$ such that $\alpha' \to 0$ and $\delta(\alpha') \to 0$ as $\alpha' \to 0$ and $\left\|Hg_{\alpha'}^{\delta(\alpha')}\right\|^2$ is bounded independently from α'. One can also choose $\delta(\alpha')$ such that $\delta(\alpha') \leq \alpha'$.

On the other hand Lemma 4 indicates that one can choose this subsequence such that $J_{\alpha'}^{\delta(\alpha')}(g_{\alpha'}^{\delta(\alpha')}) \to 0$ as $\alpha' \to 0$ and therefore $\left\|F^\delta g_{\alpha'}^{\delta(\alpha')} - \phi\right\| \to 0$ as $\alpha' \to 0$ and $\alpha'\delta(\alpha')\|g_{\alpha'}^{\delta(\alpha')}\|^2 \to 0$ as $\alpha' \to 0$. By a triangular inequality and $\delta(\alpha') \leq \alpha'$ we then deduce that $\left\|Fg_{\alpha'}^{\delta(\alpha')} - \phi\right\| \to 0$ as $\alpha' \to 0$. The compactness of G implies that a subsequence of $GHg_{\alpha'}^{\delta(\alpha')}$ converges for some $G\varphi$ in X^*. The uniqueness of the limit implies that $G\varphi = \phi$ which is a contradiction.

□

It is clear from the proof of the theorem that any strategy of regularization $\varepsilon(\delta)$ satisfying $\epsilon(\delta) \geq \delta\|B\|$ and $\epsilon(\delta) \to 0$ as $\delta \to 0$ would be convenient to obtain a similar result. From the numerical perspective this theorem indicates that a criterion to localize the object would be

$$|\langle B^\delta g_\alpha^\delta,\, g_\alpha^\delta\rangle| + \delta\|B\| \left\|g_\alpha^\delta\right\|^2$$

for small values of α. Indeed the theorem only says that this criterion would be efficient for sufficiently small noise. Building explicit link between the value of α and the noise level δ (in the fashion of a posteriori regularization strategies) would be of valuable theoretical interest but this seems to be challenging (due to the compactness of the operator B). One can see from the proof that adding the term $\delta\|B\| \left\|g_\alpha^\delta\right\|^2$ is important to conclude when ϕ is not in the range of G. This means that this term is important for correcting the behavior of the indicator function outside the inclusion, which is corroborated by the numerical experiments below.

2.4 Some applications of GLSM

We turn back to our model problem and consider the notation and assumptions of Section 2.2. We shall apply GLSM with $B = F$. The central additional theorem needed for this case is the following coercivity property of the operator T. This theorem holds true under the following assumptions on the refractive index.

Hypothesis 2. *We assume that $n \in L^\infty(\mathbb{R}^d)$, $\mathrm{supp}(n-1) = \overline{D}$, $\Im(n) \geq 0$ and there exist constants $n_0, \alpha > 0$ such that $1 - \Re(n(x)) + \alpha\Im(n(x)) \geq n_0$ for a.e. $x \in D$ or $\Re(n(x)) - 1 + \alpha\Im(n(x)) \geq n_0$ for a.e. $x \in D$.*

We recall that the values of $k^2 \in \mathbb{R}_+$, for which Hypothesis 1 does not hold, form a discrete set without finite accumulation point. The values $k^2 \in \mathbb{R}_+$ for which Hypothesis 1 does not hold will be referred in the sequel as transmission eigenvalues.

Theorem 6. *Assume that Hypothesis 2 holds and that $k^2 \in \mathbb{R}_+$ is not a transmission eigenvalue. Then the operator T defined by (2.4) satisfies the coercivity property (2.8) with $X = X^* = L^2(D)$ and the operator H defined by (2.2).*

Proof. For the reader convenience we start by proving a useful (classical) identity related to the imaginary part of T. With $(\cdot,\cdot)$ denoting $L^2(D)$ scalar product, for $\psi \in L^2(D)$ and $w \in H^1_{\mathrm{loc}}(\mathbb{R}^d)$ solution of (2.1),

$$(T\psi, \psi) = -k^2 \int_D (1-n)(\psi + w)\overline{\psi}\, dx. \tag{2.17}$$

We remark that by elliptic regularity, $w \in H^2_{\rm loc}(\mathbb{R}^d)$. Multiplying (2.1) with $\overline{w}$ and integrating by part over B_R: a ball of radius R containing D,

$$k^2 \int_D (1-n)(\psi+w)\overline{w}\, dx = -\int_{B_R} |\nabla w|^2 - k^2|w|^2 dx + \int_{|x|=R} \frac{\partial w}{\partial r}\overline{w}\, ds.$$

The Sommerfeld Radiation condition indicates that

$$\lim_{R\to\infty} \Im \int_{|x|=R} \frac{\partial w}{\partial r}\overline{w}\, ds = k \int_{\mathbb{S}^{d-1}} |w^\infty|^2 ds,$$

Therefore, taking the imaginary part then letting $R \to \infty$ yields

$$k^2 \Im \int_D (1-n)(\psi+w)\overline{w}\, dx = k \int_{\mathbb{S}^{d-1}} |w^\infty|^2 ds.$$

Consequently, decomposing $(\psi+w)\overline{\psi} = |\psi+w|^2 - (\psi+w)\overline{w}$, we obtain the important identity,

$$\Im(T\psi,\psi) = \int_D k^2 \Im(n)(|\psi+w|^2) dx + k\int_{\mathbb{S}^{d-1}} |w^\infty|^2 ds. \tag{2.18}$$

We are now in position to prove the coercivity property using a contradiction argument. Assume for instance the existence of a sequence $\psi_\ell \in \mathcal{R}(H)$ such that

$$\|\psi_\ell\|_{L^2(D)} = 1 \quad \text{ and } |(T\psi_\ell,\psi_\ell)| \to 0 \text{ as } \ell \to \infty.$$

We denote by $w_\ell \in H^2_{\rm loc}(\mathbb{R}^d)$ solution of (2.1) with $\psi = \psi_\ell$. Elliptic regularity implies that $\|w_\ell\|_{H^2(D)}$ is bounded uniformly with respect to ℓ. Then up to changing the initial sequence, one can assume that ψ_ℓ weakly converges to some ψ in $L^2(D)$ and w_ℓ converges weakly in $H^2_{\rm loc}(\mathbb{R}^d)$ and strongly in $L^2(D)$ to some $w \in H^2_{\rm loc}(\mathbb{R}^d)$. It is then easily seen (using distributional limit) that w and ψ satisfy (2.1), and since $\psi_\ell \in \mathcal{R}(H)$

$$\Delta\psi + k^2\psi = 0 \quad \text{ in } D. \tag{2.19}$$

Identity (2.18) and $|(T\psi_\ell,\psi_\ell)| \to 0$ imply that $w_\ell^\infty \to 0$ in $L^2(\mathbb{S}^{d-1})$ and therefore $w^\infty = 0$. The Rellich theorem and unique continuation principle implies $w = 0$ outside D and consequently $w \in H^2_0(D)$. With the help of equation (2.19) we get that $u = w+\psi \in L^2(D)$ and $v = \psi \in L^2(D)$ are such that $u - v \in H^2(D)$ and are solution of the interior transmission problem (2.22) with $f = g = 0$. We then infer that $w = \psi = 0$. Identity (2.17) applied to ψ_ℓ and w_ℓ implies

$$|(T\psi_\ell,\psi_\ell)| \geq k^2 \left| \int_D (1-n)|\psi_\ell|^2 dx \right| - k^2 \left| \int_D (1-n) w_\ell \overline{\psi}_\ell\, dx \right|.$$

Therefore, since $\int_D (1-n) w_\ell \overline{\psi}_\ell dx \to \int_D (1-n) w\overline{\psi} dx = 0$, and using the assumptions on n,

$$\lim_{\ell\to 0} |(T\psi_\ell,\psi_\ell)| \geq k^2 n_0/2 > 0,$$

which is a contradiction. □

Let $C > 0$ be a given constant (independent of α) and consider for $\alpha > 0$ and $z \in \mathbb{R}^d$, $g_\alpha^z \in L^2(\mathbb{S}^{d-1})$ such that

$$\alpha|(Fg_\alpha^z, g_\alpha^z)| + \|Fg_\alpha^z - \phi_z\|^2 \leq j_\alpha(\phi_z) + C\,\alpha, \tag{2.20}$$

where

$$j_\alpha(\phi_z) = \inf_{g \in L^2(\mathbb{S}^{d-1})} \left(\alpha|(Fg, g)| + \|Fg - \phi_z\|^2\right).$$

Combining the results of Theorems 6 and 1 and the first claim of Theorem 2, we obtain the following as a straightforward application of Corollary 1.

Theorem 7. *Assume that Hypothesis 2 holds and that $k^2 \in \mathbb{R}_+$ is not a transmission eigenvalue. Then $z \in D$ if and only if $\limsup_{\alpha\to 0} |(Fg_\alpha^z, g_\alpha^z)| < \infty$ which is true if and only if $\liminf_{\alpha\to 0} |(Fg_\alpha^z, g_\alpha^z)| < \infty$.*

For applications, it is important to rather use the criterion provided in Theorem 5. Consider $F^\delta : L^2(\mathbb{S}^{d-1}) \to L^2(\mathbb{S}^{d-1})$ a compact operator such that

$$\left\|F^\delta - F\right\| \leq \delta,$$

then consider for $\alpha > 0$ and $\phi \in L^2(\mathbb{S}^{d-1})$, the functional $J_\alpha^\delta(\phi; \cdot) : L^2(\mathbb{S}^{d-1}) \to \mathbb{R}$,

$$J_\alpha^\delta(\phi; g) := \alpha(|(F^\delta g, g)| + \delta \|g\|^2) + \left\|F^\delta g - \phi\right\|^2 \quad \forall\, g \in L^2(\mathbb{S}^{d-1}). \tag{2.21}$$

Then as a direct consequence of Theorem 5, we have the following characterization of D.

Theorem 8. *Assume that Hypothesis 2 holds and that $k^2 \in \mathbb{R}_+$ is not a transmission eigenvalue. For $z \in \mathbb{R}^d$ let us denote by $g_{\alpha,\delta}^z$ the minimizer of $J_\alpha^\delta(\phi_z; \cdot)$ over $L^2(\mathbb{S}^{d-1})$. Then $z \in D$ if and only if $\limsup_{\alpha\to 0} \limsup_{\delta\to 0} \left(\left|(F^\delta g_{\alpha,\delta}^z, g_{\alpha,\delta}^z)\right| + \delta \left\|g_{\alpha,\delta}^z\right\|^2\right) < \infty$ which is true if and only if $\liminf_{\alpha\to 0} \liminf_{\delta\to 0} \left(\left|(F^\delta g_{\alpha,\delta}^z, g_{\alpha,\delta}^\delta)\right| + \delta \left\|g_{\alpha,\delta}^z\right\|^2\right) < \infty$.*

The numerical algorithm associated with this theorem is given in next section. Let us note again as conclusion of this section that the results of Theorems 7 and 8 in fact apply whenever the so called $F_\#$ method apply. For instance the result holds true for obstacle scattering with Dirichlet boundary conditions, Neumann boundary conditions or impedance boundary conditions [40, 21]. One has just to remove assumption 2 and instead of excluding transmission eigenvalues, one has to exclude the resonant eigenfrequencies associated with the interior problem. One can also apply GLSM to cracks as a consequence of the work in [12]. For Maxwell's equations one can in principle also treat the inverse medium problem but the GLSM method does not allow to treat (in its current form) the case of inverse obstacle scattering (i.e. for instance perfectly or imperfectly conducting obstacles).

2.5 Numerical algorithms issued from GLSM and validation

Minimizing J_α^δ (defined in equation 2.14) with $B = F$ may be computationally expensive and not straightforward (see Section 2.5.2). Thus we first propose to use the indicator function of the GLSM with the solution of the LSM, which can be seen as a generalisation of [3] in the case of noisy measurement. Then we introduce a second algorithm which is a post processing in the sense that it uses the solution of the LSM both to initialize the optimization algorithm that minimize J_α^δ and to initialise the parameter α.

In order to fix the ideas, we shall restrict ourselves to the two dimensional case and will introduce the algorithms for the discrete version of GLSM. We identify $\mathbb{S}^1$ with the interval $[0, 2\pi[$. In order to collect the data of the inverse problem we solve numerically (2.1) for N incident fields $u^i(\frac{2\pi j}{\mathrm{N}}, \cdot)$, $j \in \{0...\mathrm{N}-1\}$ using the surface integral equation forward solver available in [35]. The discret version of F is then the matrix $F_\mathrm{N} := (u^\infty(\frac{2\pi j}{\mathrm{N}}, \frac{2\pi k}{\mathrm{N}}))_{0\leq j,k\leq \mathrm{N}-1}$. We add some noise to the data to build a noisy far field matrix F_N^δ where $(F_\mathrm{N}^\delta)_{j,k} = (F_\mathrm{N})_{j,k}(1+\sigma N_{ij})$ for $\sigma > 0$ and N_{ij} an uniform complex random variable in $[-1, 1]^2$. We denote $\Phi_{z,\mathrm{N}} \in \mathbb{C}^\mathrm{N}$, the vector defined by $\Phi_{z,\mathrm{N}}(j) = \phi_z(\frac{2\pi j}{\mathrm{N}})$ for $0 \leq j \leq \mathrm{N}-1$.

2.5.1 The use of GLSM as a new indicator function for the LSM

We introduce the Tikhonov regularized solution of the far field equation

$$g_{z,\mathrm{N}}^{\eta,\mathrm{LSM}} := argmin_{g_\mathrm{N}} \eta \|g_\mathrm{N}\|^2_{L^2(\mathbb{S}^1)} + \left\|F_\mathrm{N}^\delta g_\mathrm{N} - \Phi_{z,\mathrm{N}}\right\|^2_{L^2(\mathbb{S}^1)},$$

where the regularization parameter η is chosen using the Morozov discrepancy principle, i.e. η is defined as the unique solution of

$$\left\|F_\mathrm{N}^\delta g_{z,\mathrm{N}}^{\eta,\mathrm{LSM}} - \Phi_{z,\mathrm{N}}\right\|_{L^2(\mathbb{S}^1)} = \delta \left\|g_{z,\mathrm{N}}^{\eta,\mathrm{LSM}}\right\|_{L^2(\mathbb{S}^1)}.$$

Solving the same two equations with $F_\#^{\frac{1}{2}}$ or $(F^*F)^{\frac{1}{4}}$, depending of the nature of the scatter, instead of F will give the solution of the factorization method $g_{z,\mathrm{N}}^{\eta,\mathrm{FM}}$. To solve both the LSM and the FM equations we rely on the singular value decomposition of F_N^δ, which gives an explicit solution like in 2.3.2.

As proposed in [3],[39] and [24], from these two problems three indicator functions can be computed:

$$\mathcal{I}^{\mathrm{LSM}}(z) = \frac{1}{\left\|g_{z,\mathrm{N}}^{\eta,\mathrm{LSM}}\right\|_{L^2(\mathbb{S}^1)}}$$

$$\mathcal{I}^{\mathrm{HLSM}}(z) = \frac{1}{\sqrt{|Hg_{z,\mathrm{N}}^{\eta,\mathrm{LSM}}(z)|}} = \frac{1}{\sqrt{|(\Phi_{z,\mathrm{N}}, g_{z,\mathrm{N}}^{\eta,\mathrm{LSM}})_{L^2(\mathbb{S}^1)}|}}$$

$$\mathcal{I}^{\mathrm{FM}}(z) = \frac{1}{\left\|g_{z,\mathrm{N}}^{\eta,\mathrm{FM}}\right\|_{L^2(\mathbb{S}^1)}}$$

As shown in the previous sections, a fourth indicator function is relevant, namely

$$\mathcal{I}^{\mathrm{GLSM}}(z) = \frac{1}{\sqrt{\left|(F_{\mathrm{N}}^{\delta} g_{z,\mathrm{N}}^{\eta,\mathrm{LSM}}, g_{z,\mathrm{N}}^{\eta,\mathrm{LSM}})\right|_{L^2(\mathbb{S}^1)} + \delta \left\| g_{z,\mathrm{N}}^{\eta,\mathrm{LSM}} \right\|^2_{L^2(\mathbb{S}^1)}}}$$

This indicator is indeed motivated by GLSM. However let us note that since $g_{z,\mathrm{N}}^{\eta,\mathrm{LSM}}$ is not the minimizer of $J_\alpha^\delta(\phi;\cdot)$ (defined in equation (2.14)) the theory developed here does not apply for this indicator function (a last indicator function covered by the theory will be built in section 2.5.2 using a more computationally complex method). The numerical experiments presented below indicate in the same time that this indicator function provides results comparable to the Factorization method.

We will present two simulations: a first one where two ellipses have Dirichlet boundary conditions and the other one where $n = 2 + 0.5i$ in one ellipse and $2 + 0.1i$. In both examples $\mathrm{N} = 100$ and we will consider $\frac{\|F_{\mathrm{N}}^{\delta} - F_{\mathrm{N}}\|}{\|F_{\mathrm{N}}\|} = 0,\ 1$ and 5%.

Figures 2.1 and 2.2 show the results of the four indicator functions. First we see that $\mathcal{I}^{\mathrm{HLSM}}$ is not robust to noise, the area outside the obstacle shows artefact where the indicator function is greater than inside the obstacle. This is an expected result since as stated at the end of 2.3.1 one can easily replace $|\langle F g_\alpha, g_\alpha\rangle|$ by $|\langle \phi, g_\alpha\rangle|$, which is not a valid indicator function in the presence of noise. Finally $\mathcal{I}^{\mathrm{LSM}}$ recover with less precision the border of the shape than $\mathcal{I}^{\mathrm{FM}}$ and $\mathcal{I}^{\mathrm{GLSM}}$ which exhibit comparable results.

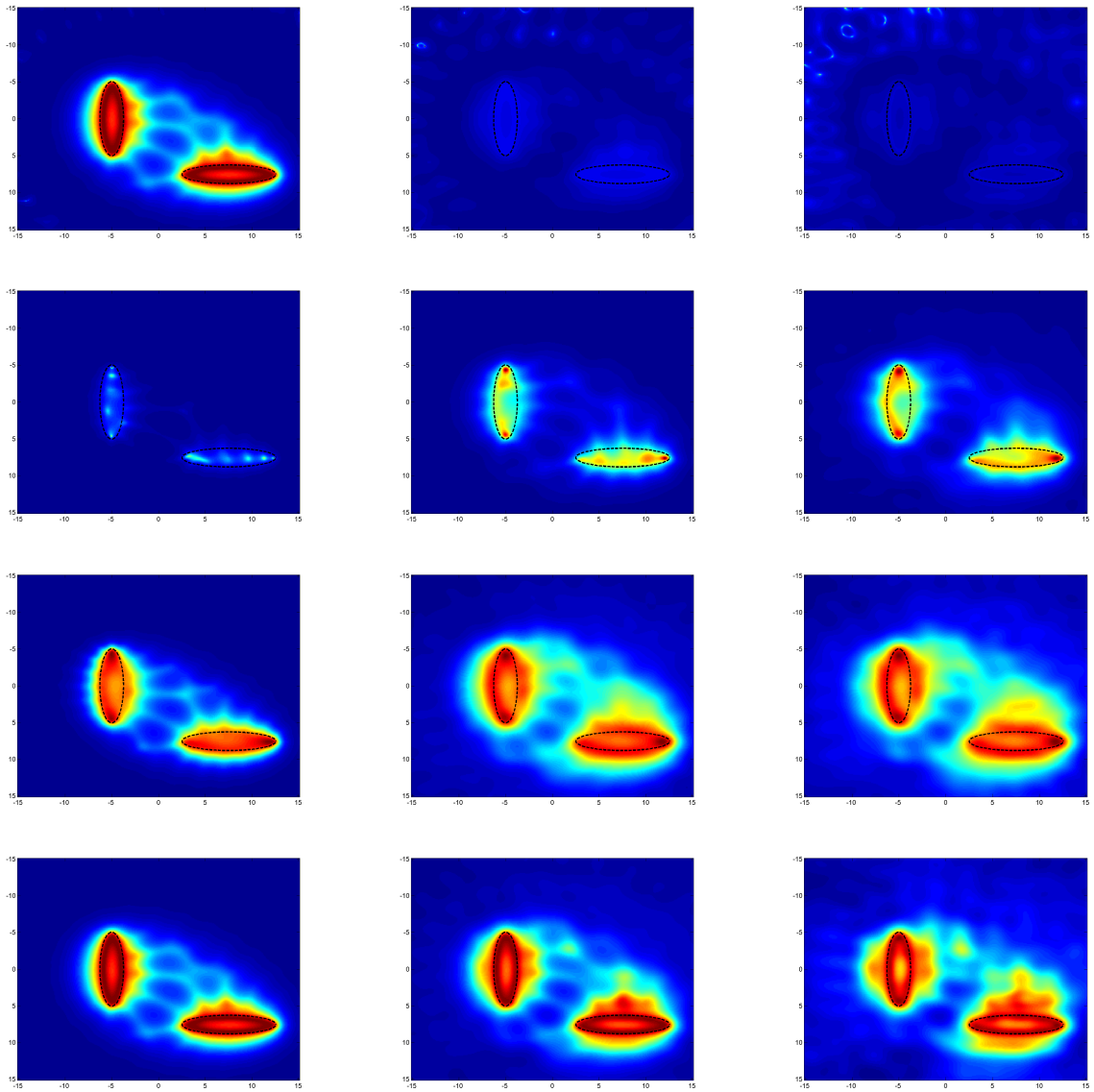

Figure 2.1: $\mathcal{I}^{\text{HLSM}}$ (first line), $\mathcal{I}^{\text{LSM}}$ (second line), $\mathcal{I}^{\text{FM}}$ (third line) and $\mathcal{I}^{GLSM}$ (forth line) applied to the Dirichlet scatters for 0, 1 and 5% of noise (from left to right)

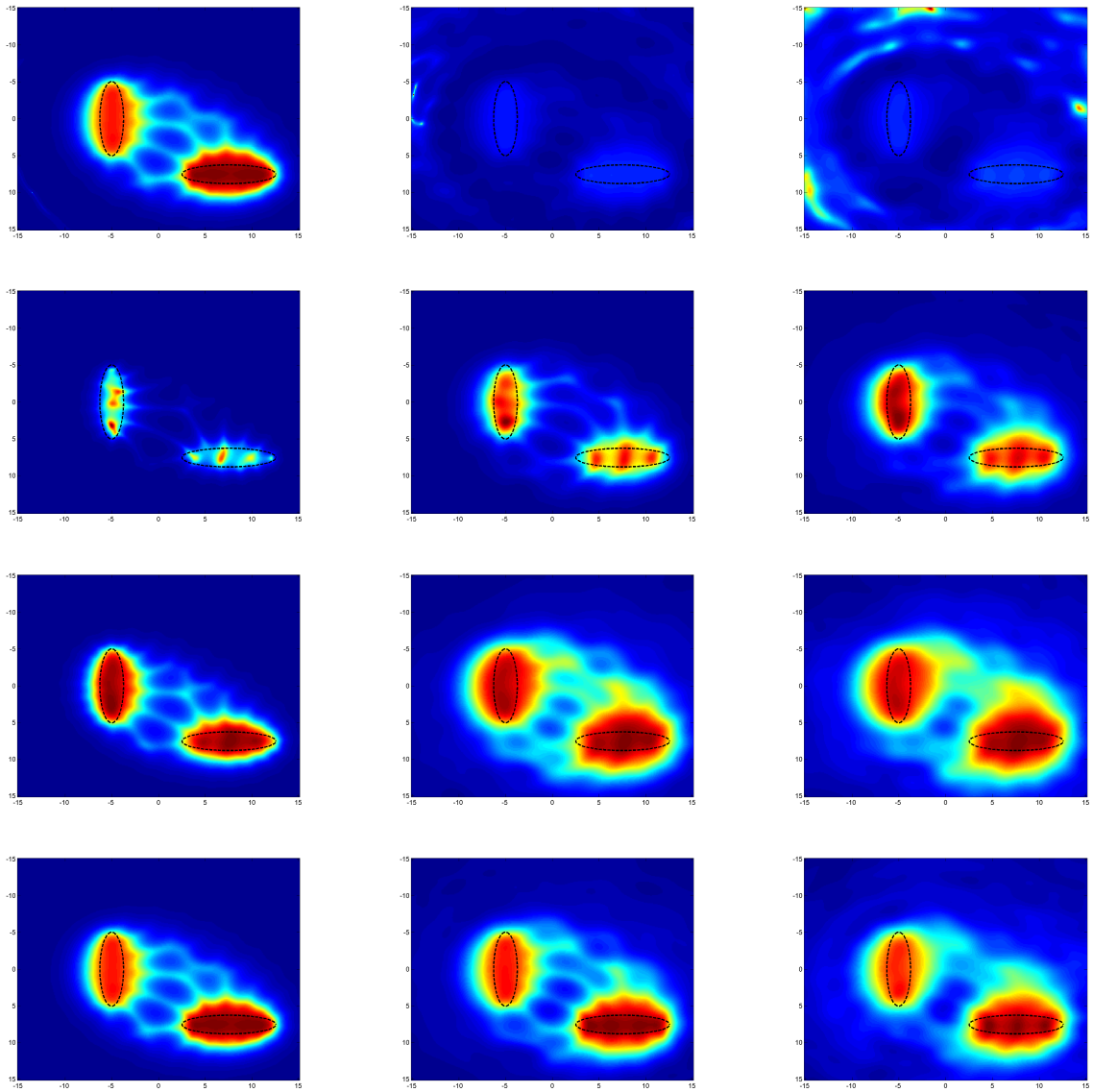

Figure 2.2: $\mathcal{I}^{\mathrm{HLSM}}$ (first line), $\mathcal{I}^{\mathrm{LSM}}$ (second line), $\mathcal{I}^{\mathrm{FM}}$ (third line) and $\mathcal{I}^{\mathrm{GLSM}}$ (forth line) applied to penetrable scatters for 0, 1 and 5% of noise (from left to right))

2.5.2 Minimizing J_α^δ: a post-processing

In order to apply Theorem 8, we should find the minimizer of $J_\alpha^\delta(\phi;\cdot)$ (defined in equation (2.14)). There are two main difficulties in this theorem. First, we do not have an analytic solution of the minimizer thus we will rely on an optimisation algorithm and as already mentioned in 2.3.4 and second we do not have an a priori method to link α to the noise level. Because of the good performance of the Morozov discrepancy principle we look for an heuristic that stays close to

this principle. Since we have $\alpha(|(F^\delta g, g)| + \delta \|g\|^2) \leq \alpha(\|F^\delta\| + \delta)\|g\|^2$, we choose:

$$\alpha = \frac{\eta_{\text{LSM}}}{\|F^\delta\| + \delta}$$

where η_{LSM} is the parameter found when one applies the Morozov discrepancy principle to the Tikhonov formulation of the LSM.

Remark 1. *The inequality $|(F^\delta g, g)| \leq \|F^\delta\| \|g\|^2$ we use to find the previous heuristic will reduce the strength of the penalty term compared to the Tikhonov-LSM. Moreover the fact that this inequality is coarser for eigenvector corresponding to small eigenvalue means that the penality term will be smaller for points outside the obstacle. This is shown by figure 2.3, where we see that after the optimisation process the solution deviates from the Morozov discrepancy principle mainly outside the obstacle.*

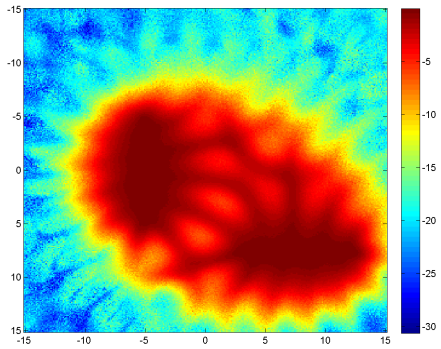

Figure 2.3: $\|F^\delta_{\text{N}} g_{\text{N}} - \Phi_{z,\text{N}}\| - \delta \|g_{\text{N}}\|$ after minimisation on the Dirichlet scatters with 5% of noise.

Minimizing $J^\delta_\alpha(\phi;\cdot)$ in $\mathbb{C}^{\text{N}}$ is not an easy task since it is a not differentiable nor a convex cost functionnal. However we can hope that $g^{\eta,\text{LSM}}_{z,\text{N}}$ will be close to a minimum which makes it worth to try a gradient method. As explained in [50] gradient method extended well for complex variable if one looks at $J^\delta_\alpha(\phi; g_{\text{N}})$ as a function of two variables, g_{N} and $\bar{g}_{\text{N}}$, knowing that one can compute the gradient of J^δ_α with respect to g_{N} :

$$\nabla_{\bar{g}_{\text{N}}} J^\delta_\alpha(\phi; g_{\text{N}}, \bar{g}_{\text{N}}) := \alpha\left(\frac{F^\delta_{\text{N}} g_{\text{N}} \cdot \bar{g}_{\text{N}}}{|F^\delta_{\text{N}} g_{\text{N}} \cdot \bar{g}_{\text{N}}|} F^\delta_{\text{N}} g_{\text{N}} + \delta g_{\text{N}}\right) + F^{\delta *}_{\text{N}}(F^\delta_{\text{N}} g_{\text{N}} - \Phi_{\text{N}})$$

where $\cdot$ is the standard scalar product between vectors. We do not change the absolute value with a differentiable surrogate because, with the initial guess we use it is not necessary, this is supported by the fact that for the unperturbed operator F the coercivity implies that $|(Fg, g)|$ is never zero when g is not zero.

Finally to do the optimization we use the non-linear conjugate gradient implemented in [51] with a modified Hestenes-Stiefel heuristic to update the direction descent, which is described in algorithm 1. We choose drastic stopping rules in order to ensure the convergence of the

algorithm however we observe that convergence occurs before those stopping rules are satisfied. The design of a tailored method and set of parameters to minimize J_α^δ would be an interesting perspective for this work.

Algorithm 1 Minimizing J_α^δ

for all z **do**
  $g^0 = g_{z,\mathrm{N}}^{\eta,\mathrm{LSM}}$ and $\alpha = \frac{\eta_{\mathrm{LSM}}(z)}{\left\|F_{\mathrm{N}}^\delta\right\|+\delta}$
  while $\left\|g^{t+1}-g^t\right\| \leq 10^{-10}\left\|g^t\right\|$ **or** $J_\alpha^\delta(g^{t+1}) - J_\alpha^\delta(g^t) \leq 10^{-10} J_\alpha^\delta(g^0)$ **or** $t < 200$ **do**
    $\Delta g^t = -\nabla_g J_\alpha^\delta(g^t, \bar{g}^t)$
    $\beta_{HS}^t = max(0, -\frac{\Re(\Delta g^{t\top}(\Delta g^t - \Delta g^{t-1}))}{\Re(s^{t-1\top}(\Delta g^t - \Delta g^{t-1}))})$
    $s^t = \Delta g^t + \beta_{HS}^t s^{t-1}$
    $\tau^t = \arg\min_{\tau\in\mathbb{R}} J_\alpha^\delta(g^t + \tau s^t)$
    $g^{t+1} = g^t + \tau^t s^t$
    $t \leftarrow t+1$
  $g_{z,\mathrm{N}}^{\alpha,\mathrm{GLSM}} = g^t$

The result of this optimization performed for each z, gives us a new set: $g_{z,N}^{\alpha,\mathrm{GLSM}}$ which ultimately creates a new indicator function:

$$\mathcal{I}^{\mathrm{GLSMoptim}}(z) = \frac{1}{\sqrt{\left|(F_{\mathrm{N}}^\delta g_{z,\mathrm{N}}^{\alpha,\mathrm{GLSM}}, g_{z,\mathrm{N}}^{\alpha,\mathrm{GLSM}})\right| + \delta\left\|g_{z,N}^{\alpha,\mathrm{GLSM}}\right\|^2}}$$

Figures 2.4 and 2.5 show that this post processing increases the quality of the reconstruction especially in the space in-between the two scatters. Moreover figure 2.6 shows that the improvement on an isolated scatter, a kite of contrast $n = 2 + 0.5i$, is less impressive (i.e. we do not improve the reconstruction of the non-convex part of the kite).

Remark 2. *In the (less general) case where the $F_\#$ method is valid, one could choose $B^\delta = F_\#^\delta = |\Re(F^\delta)| + |\Im(F^\delta)|$ in equation (2.14). We know that $F_\#^\delta$ is a positive and self-adjoint operator then one can drop the absolute value in the definition of J_α^δ :*

$$J_\alpha^\delta(\phi; g) := \alpha(\left\|(F_\#^\delta)^{\frac{1}{2}} g\right\|^2 + \delta_\# \|g\|^2) + \left\|F^\delta g - \phi\right\|^2$$

and find $g_{z,\mathrm{N}}^{\alpha,\mathrm{GLSM}}$ easily by solving the following (iteration-free) problem:

$$\alpha((F_\#^\delta)^{\frac{1}{2}*}(F_\#^\delta)^{\frac{1}{2}} g_N + \delta_\# g_N) + F^{\delta *}(F^\delta g_N - \Phi_N) = 0.$$

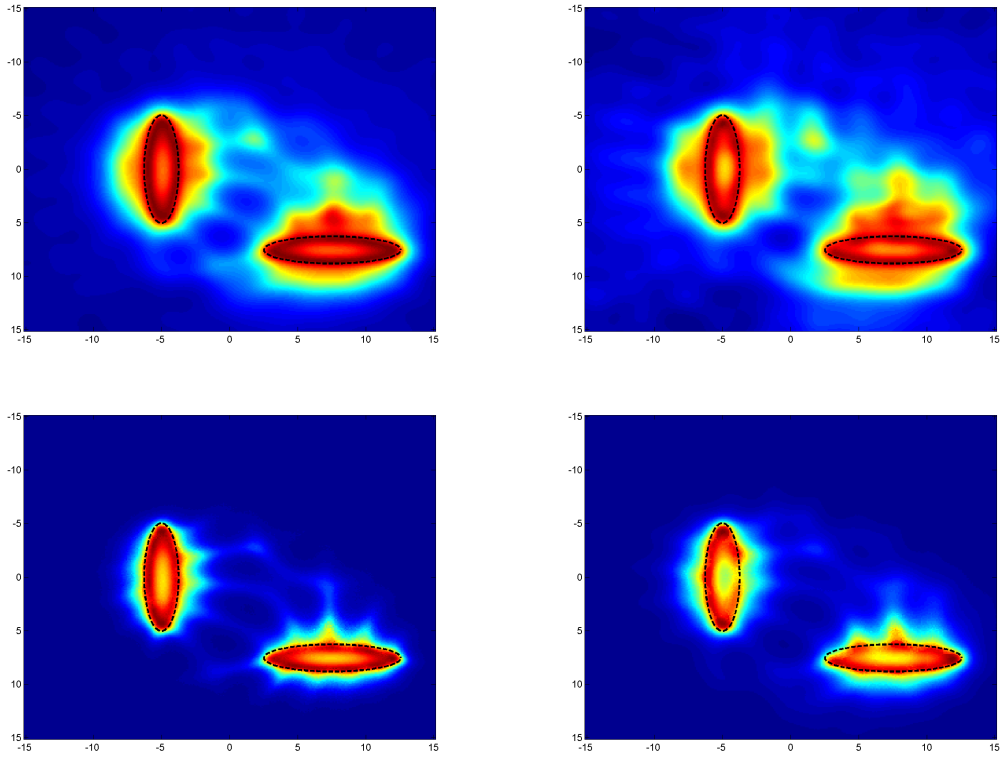

Figure 2.4: $\mathcal{I}^{\mathrm{GLSM}}$ (first line) and $\mathcal{I}^{\mathrm{GLSMoptim}}$ (second line) applied to the Dirichlet scatters for 1 and 5% of noise (from left to right)

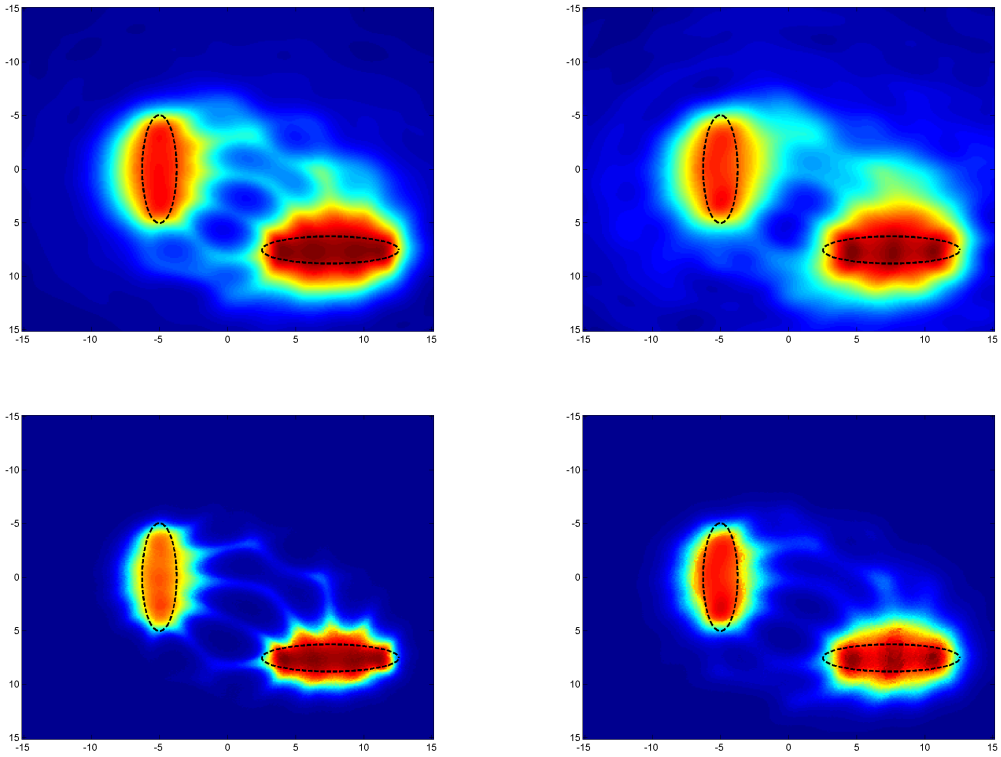

Figure 2.5: $\mathcal{I}^{\mathrm{GLSM}}$ (first line) and $\mathcal{I}^{\mathrm{GLSMoptim}}$ (second line) applied to the penetrable scatters for 1 and 5% of noise (from left to right)

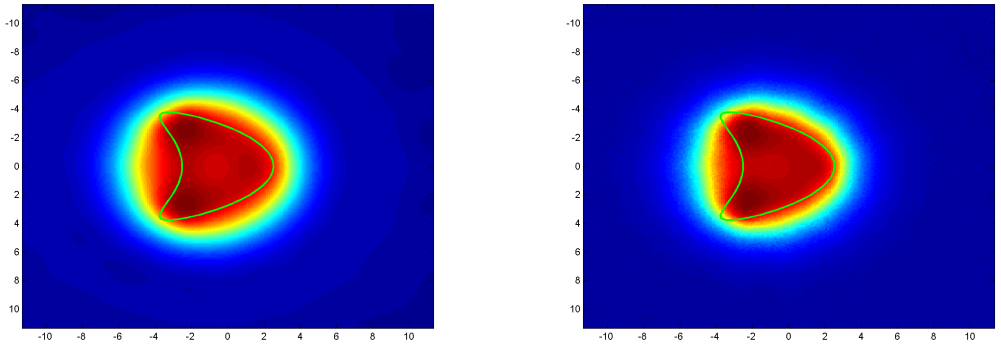

Figure 2.6: $\mathcal{I}^{\mathrm{GLSM}}$ and $\mathcal{I}^{\mathrm{GLSMoptim}}$ (from left to right) with 1% of noise

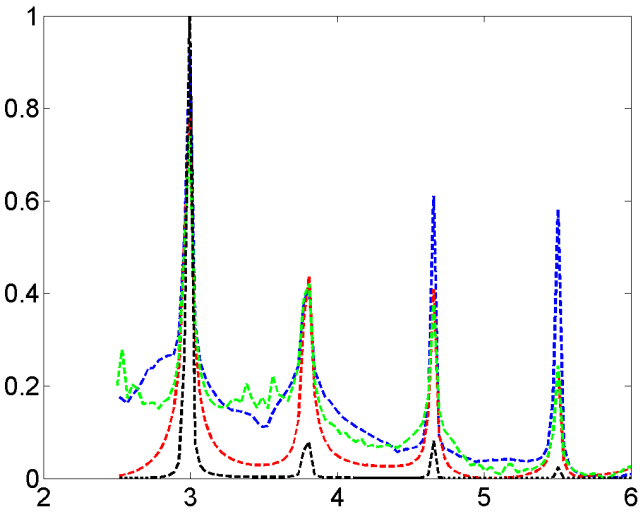

Figure 2.7: The mean value for z inside the obstacle of $\|Hg_z^\alpha\|^2_{L^2(D)}$ (black), $|\langle Fg^{z,\alpha}, g^{z,\alpha}\rangle|$ (red), $\|g_\alpha^z\|$ (blue) and $|\langle F_\# g^{z,\alpha}, g^{z,\alpha}\rangle|$ (green)

2.6 Determination of the transmission eigenvalue from far field data

In [16] it is shown that the norm of Hg_z^α can not stay bounded if k is an interior transmission eigenvalue. This result relies on the hypothesis that F has dense range even at an interior transmission eigenvalue (assuming this is related to the existence of non scattering waves [8]). When k is not a transmission eigenvalue we extensively use the fact that $|\langle Bg^{z,\alpha}, g^{z,\alpha}\rangle|$ actually controls the norm of Hg_z^α. If we take $B = F_\#$, in [43] they demonstrate that $T_\#$ is coercive even if k is a transmission eigenvalue. If we take $B = F$, this control depends on the coercivity of T which we only prove when k is not a transmission eigenvalue. Therefore we can conclude that the sequence we have construct using the GLSM framework will give us an exact characterization of the interior transmission eigenvalue as the failure of the indicator function only when $B = F_\#$. However when $B = F$ as we have an exact characterization of the support of the scatter when k is not a transmission eigenvalue value we can compute $\|Hg_z^\alpha\|^2_{L^2(D)}$ after determining D from the data. In figure 2.7 we show the mean value of $|\langle Fg^{z,\alpha}, g^{z,\alpha}\rangle|$, $\|g_\alpha^z\|$, $\|Hg_z^\alpha\|^2_{L^2(D)}$ and $|\langle F_\# g^{z,\alpha}, g^{z,\alpha}\rangle|$ for z inside a sphere (same example as in [32]).

For the convenience of the reader we reproduce the theorem given in [16] when $n-1$ does not change sign in all D. We denote $g^{z,\alpha}$, the minimizing sequence of the GLSM cost functional with $B = F_\#$.

Theorem 9. *Let k be a transmission eigenvalue and assume that F has dense range. Then for almost every $z \in D$, $\liminf_{\alpha\to 0}\liminf_{\delta\to 0}\|Hg_z^\alpha\|^2_{L^2(D)}$ or $\liminf_{\alpha\to 0}\liminf_{\delta\to 0}|\langle F_\# g^{z,\alpha}, g^{z,\alpha}\rangle|$ cannot be bounded.*

Proof. Assume that for a set of points $z \in D$ which has a positive measure, $\mu\,\|Hg_z^\alpha\|^2_{L^2(D)} \leq$

$\langle F_{\#} g^{z,\alpha},\, g^{z,\alpha}\rangle| \leq M$ (where M may depend on z but not on α and δ). Therefore we deduce that there exist v_z such that $Gv_z = \phi_z^\infty$. We can then deduce that v_z and u_z solve :

$$\begin{cases} \Delta u_z + k^2 n u_z = 0 \quad \text{in } D, \\ \Delta v_z + k^2 v_z = 0 \quad \text{in } D, \\ (u_z - v_z) = \Phi_z \quad \text{on } \partial D, \\ \frac{\partial}{\partial \nu}(u_z - v_z) = \frac{\partial}{\partial \nu}\Phi_z \quad \text{on } \partial D, \end{cases} \tag{2.22}$$

and introduced $w_z = u_z - v_z - \theta_z$ which is an element of $V = \{u \in H^2(D), u = 0, \frac{\partial}{\partial \nu} u = 0 \; on \; \partial D\}$ that solves a fourth order problem which is equivalent to the following variational formulation [16][equation (10)] on which the Fredholm alternative holds:

$$\int_D \frac{1}{n-1}\{(\Delta + k^2 n)(u_z - \theta_z)\}\{(\Delta + k^2)\varphi\} dx = 0 \qquad \text{for all } \varphi \in V_0(D). \tag{2.23}$$

where $\theta_z \in H^2(D)$ is a lifting function that verifies $\theta_z = \Phi_z$ and $\frac{\partial}{\partial \nu}\theta_z = \frac{\partial}{\partial \nu}\Phi_z$ on∂D. Since k is an interior transmission eigenvalue, we introduce $w_0 \in V$ any interior transmission eigenfunction. The Fredholm alternative leads to

$$\int_D \frac{1}{n-1}\{(\Delta + k^2 n)(\theta_z)\}\{(\Delta + k^2) w_0\} dx = 0 \qquad \text{for all } \varphi \in V_0(D). \tag{2.24}$$

Integrating by parts we obtain:

$$\int_{\partial D} \frac{1}{n-1}(\Delta + k^2 n) w_0 \, \frac{\partial \Phi(\cdot\,, z)}{\partial \nu} \, ds - \int_{\partial D} \frac{\partial}{\partial \nu}\left(\frac{1}{n-1}(\Delta + k^2 n) w_0\right) \Phi(\cdot\,, z) \, ds = 0, \tag{2.25}$$

where these integrals have to be understood in the sense of $H^{\mp 1/2}$ (resp. $H^{\mp 3/2}$) duality pairing. Defining $\psi(x) := \frac{1}{n-1}(\Delta + k^2 n(x)) w_0(x)$ in D then, ψ is in $L^2(D)$ and satisfies $(\Delta + k^2)\psi(x) = 0$ in D. Classical interior elliptic regularity results and the Green's representation theorem implies that

$$\psi(z) = \int_{\partial D} \left(\psi(x) \frac{\partial \Phi(x,z)}{\partial \nu} - \frac{\partial \psi(x)}{\partial \nu}\Phi(x,z)\right) ds_x \qquad \text{for } z \in D. \tag{2.26}$$

Equation (2.25) and the unique continuation principle now show that $\psi = 0$ in D. Therefore $(\Delta + k^2 n(x)) u_0(x) = 0$ in D. Since $u_0 \in V$ one deduces from Green's representation theorem that $u_0 = 0$ in D, which is a contradiction.

□

Chapter 3

Identifying defects in an unknown background using differential measurements

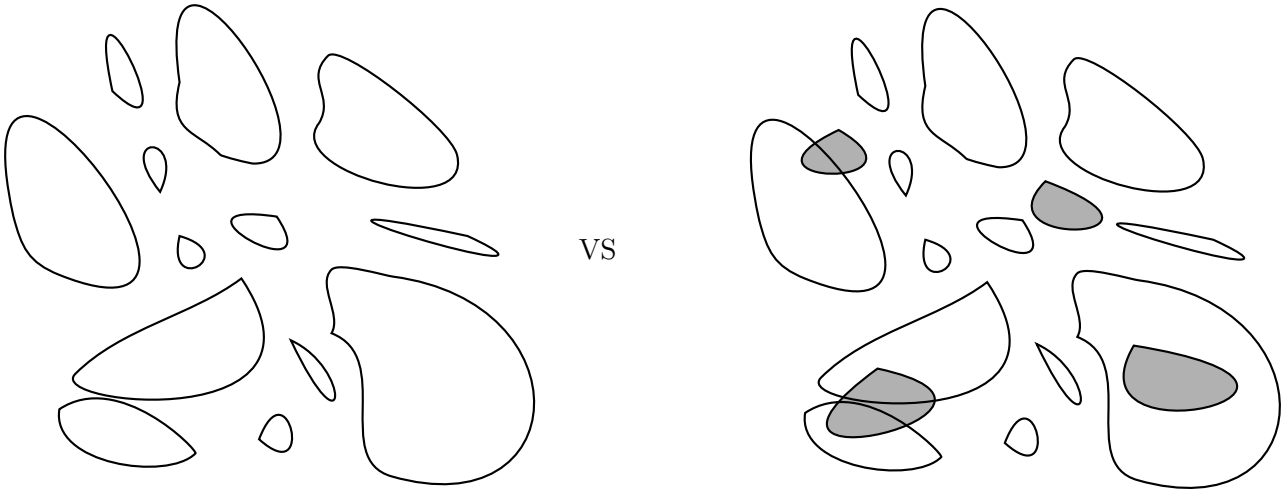

Contents

Except for section 3.6, this chapter is made of the article published in Inverse Problems and Imaging [4]. The main theoretical contribution of this chapter is to give a clear connection between the GLSM framework introduced in the previous chapter and the solution to the interior transmission problem. To do so we slightly adapt, in section 3.3, the GLSM cost functional to be able to prove the strong convergence of the sequence of minimizer to the solution of the

underlying interior transmission problem. One application of this result is to be able to give the asymptotic behaviour of the indicator function inside the obstacle (section 3.6). More importantly it allows one to compare the solution of two different data sets, for example data taken on the same unknown medium before and after the appearance of a defect. In section 3.4, we consider the case of an unknown medium made of several disjoint parts and obtain an exact characterization of the connected parts that have been modified. Thanks to the strong convergence results of section 3.3 we are able to construct from the data an indicator function that images the connected parts of the unknown medium that have been modified by the defect. In section 3.5 we illustrate this behaviour on simulated data.

3.1 Introduction

We are interested in the design of a numerical inversion algorithm capable of identifying defects in an unknown background from multistatic measurements of waves at a fixed frequency. The original motivation of our work is the identification of defects in concrete like materials using ultrasounds, but the methodology that we propose can be applied to a wider range of non destructive testing applications. The two main specificities of our setting are the following. We first assume that the background is made of finitely many disjoint unknown inhomogeneities with a size larger or comparable to the wavelength of the probing wave as shown in figure 3.1. The material properties of these inhomogeneities are also not known a priori and therefore one cannot obtain reliable estimators of the background Green function. This setting implies in particular that classical qualitative/imaging methods cannot be directly applied (see for instance [45, 33, 25, 40, 15, 30, 10, 11, 6] and references therein). In order to overcome this lack of a priori information, we second assume that two sets of measurements, respectively corresponding to defect-free and defect-containing backgrounds, are available. Our approach then relies on a special combination of the indicator functions provided by the generalized linear sampling method GLSM (introduced in [5]) when applied to the two sets of measurements independently. The link between these indicator functions and solutions to so-called interior transmission problems allows us to introduce an additional filtered difference term that is capable of characterizing the components of the background that have non empty intersections with these defects.

In these first investigations we shall consider the scalar time harmonic wave equation and address the case where the measurements are given by the full aperture far field measurements associated with incident plane waves. We first recall the basis of the GLSM algorithm and specify the link between the indicator function and the solution to an appropriate interior transmission problem under some additional convexity assumptions. The analysis of the noisy measurements case also requires a slight modification of the regularizing scheme introduced in [5]. We then introduce a filtered difference term associated with the farfield operator of the defect free background. The analysis of this term relies on the well posedness of some specific interior transmission problems which (implicitly) imposes restrictions on the refraction indexes of the background and the defect(s) as well as on their geometry. Under those hypotheses we construct an indicator function that gives exact characterization of the defects support and the components of the background that have non empty intersections with these defects. We shall analyze both the noise free and the noisy cases. In practice, the construction of the indicator

function requires the minimization of a convex functional that turns out to be quadratic for special choices of the penalty terms.

We numerically test and validate our method in a two dimensional setting. We compare different strategies to build the indicator function provided by the theory and test the robustness of the method against the complexity of the background.

The article is organized as follows. In Section 3.2 a model problem is introduced and the main results of the GLSM are recalled in Section 3.3. The theoretical analysis of our method is given in Section 3.4. The last section (Section 3.5) is devoted to the introduction of numerical algorithms issued from Section 3.4 along with validating numerical results.

3.2 A model problem and motivation

We choose to consider as a model problem the scalar inverse time harmonic scattering problem from inhomogenous media. The goal would be to identify a local change in the index of refraction between two measurements campaigns. The first set of measurements then corresponds with our background medium defined by its refractive index n_0. We assume that this index has the following properties : $n_0 \in L^\infty(\mathbb{R}^d)$, $\Im(n_0) \geq 0$ and $n_0 = 1$ in $\mathbb{R}^d \setminus D_0$ where D_0 is a union of simply connected bounded domains with Lipschitz boundaries and such that $\mathbb{R}^d \setminus D_0$ is connected. The second set of measurements is obtained for a medium with a refractive index n that satisfies similar properties as n_0 and $n = 1$ in $\mathbb{R}^d \setminus D$ where D is a union of simply connected bounded domains with Lipschitz boundaries and such that $\mathbb{R}^d \setminus D$ is connected. We shall later further assume that $D_0 \subset D$ and denote by $\Omega \subset D$ the smallest union of simply connected domains such that $\overline{D} = \overline{\Omega} \cup \overline{D_0}$, $n = n_0$ in $\mathbb{R}^d \setminus \Omega$. The domain Ω is the target we want to retrieve without knowing n_0 and n.

For a wave number $k > 0$, the respective total fields $u_0 \in H^1_{loc}(\mathbb{R}^d)$ and $u \in H^1_{loc}(\mathbb{R}^d)$ associated with these two set of measurements solve the following Helmholtz equations:

$$\Delta u_0 + k^2 n_0 u_0 = 0 \text{ and } \Delta u + k^2 n u = 0 \text{ in } \mathbb{R}^d$$

with $d = 2$ or 3. We are interested in the cases where the total field is generated by plane waves, $u^i(\theta, x) := e^{ikx\cdot\theta}$ with $x \in \mathbb{R}^d$ and $\theta \in \mathbb{S}^{d-1}$ (the unit sphere) and we denote by u_0^s and u^s the scattered fields defined by

$$u_0^s(\theta, \cdot) = u_0 - u^i(\theta, \cdot) \text{ and } u^s(\theta, \cdot) = u - u^i(\theta, \cdot) \quad \text{in } \mathbb{R}^d,$$

which are assumed to be satisfying the Sommerfeld radiation condition,

$$\lim_{r\to\infty} \int_{|x|=r} \left| \frac{\partial u_0^s}{\partial r} - iku_0^s \right|^2 ds = 0 \text{ and } \lim_{r\to\infty} \int_{|x|=r} \left| \frac{\partial u^s}{\partial r} - iku^s \right|^2 ds = 0.$$

Our data for the inverse problem will be formed by noisy measurements of so called farfield patterns $u_0^\infty(\theta, \hat{x})$ and $u^\infty(\theta, \hat{x})$ defined by

$$u_0^s(\theta, x) = \frac{e^{ik|x|}}{|x|^{(d-1)/2}} (u_0^\infty(\theta, \hat{x}) + O(1/|x|))$$

$$u^s(\theta,x)=\frac{e^{ik|x|}}{|x|^{(d-1)/2}}(u^\infty(\theta,\hat{x})+O(1/|x|))$$

as $|x|\to\infty$ for all $(\theta,\hat{x})\in\mathbb{S}^{d-1}\times\mathbb{S}^{d-1}$. The goal is to be able to reconstruct an approximation of Ω from these measurements (without knowing n_0 and n) using a new sampling algorithm. The algorithm takes advantage of the recently introduced algorithm GLSM [5] applied to each set of measurements. We therefore need to consider the two farfield operators F_0 and $F:L^2(\mathbb{S}^{d-1})\to L^2(\mathbb{S}^{d-1})$, respectively defined by

$$F_0g(\hat{x}):=\int_{\mathbb{S}^{d-1}}u_0^\infty(\theta,\hat{x})g(\theta)ds(\theta)\text{ and }Fg(\hat{x}):=\int_{\mathbb{S}^{d-1}}u^\infty(\theta,\hat{x})g(\theta)ds(\theta).$$

Let us define for $\psi_0\in L^2(D_0)$, the unique function $w_0\in H^1_{\text{loc}}(\mathbb{R}^d)$ satisfying

$$\begin{cases}\Delta w_0+n_0k^2w_0=k^2(1-n_0)\psi_0\text{ in }\mathbb{R}^d,\\ \lim\limits_{r\to\infty}\int\limits_{|x|=r}\left|\dfrac{\partial w_0}{\partial r}-ikw_0\right|^2ds=0.\end{cases}\tag{3.1}$$

and for $\psi\in L^2(D)$ we denote by $w\in H^1_{\text{loc}}(\mathbb{R}^d)$ the unique solution of the same equations with n_0 replaced by n and ψ_0 replaced by ψ. By linearity of the forward scattering problem, F_0g (resp. Fg) is nothing but the farfield pattern of w_0 (resp. w) with $\psi_0=v_g$ in D_0 (resp. $\psi=v_g$ in D), where

$$v_g(x):=\int_{\mathbb{S}^{d-1}}e^{ikx\cdot\theta}g(\theta)ds(\theta),\ g\in L^2(\mathbb{S}^{d-1}),\ x\in\mathbb{R}^d.$$

Now consider the (compact) operators $H_0:L^2(\mathbb{S}^{d-1})\to L^2(D_0)$ and $H:L^2(\mathbb{S}^{d-1})\to L^2(D)$ respectively defined by

$$H_0g:=v_g|_{D_0}\text{ and }Hg:=v_g|_D,\tag{3.2}$$

and the (compact) operators $G_0:\overline{\mathcal{R}(H_0)}\subset L^2(D_0)\to L^2(\mathbb{S}^{d-1})$ and $G:\overline{\mathcal{R}(H)}\subset L^2(D)\to L^2(\mathbb{S}^{d-1})$ respectively defined by

$$G_0\psi_0:=w_0^\infty\text{ and }G\psi:=w^\infty$$

where w_0^∞ (resp. w^∞) is the farfield of w_0 (resp. w) and $\overline{\mathcal{R}(H_0)}$ (resp. $\overline{\mathcal{R}(H)}$) denotes the closure of the range of H_0 in $L^2(D_0)$ (resp. H in $L^2(D)$). Then clearly

$$F_0=G_0H_0\text{ and }F=GH.$$

This is the first factorization needed by GLSM. We recall that [49]

$$\overline{\mathcal{R}(H)}=\{v\in L^2(D);\Delta v+k^2v=0\text{ in }D\},$$

and one has a similar characterization for $\overline{\mathcal{R}(H_0)}$. On the other hand, since the farfield patterns of w_0 and w respectively have the following expressions ([25])

$$w_0^\infty(\hat{x})=-\int_{D_0}e^{-iky\cdot\hat{x}}(1-n_0)k^2(\psi_0(y)+w_0(y))dy,$$

$$w^\infty(\hat{x}) = -\int_D e^{-iky\cdot\hat{x}}(1-n)k^2(\psi(y)+w(y))dy,$$

one simply has $G_0 = H_0^* T_0 \psi$ and $G = H^* T\psi$, where $H_0^* : L^2(D_0) \to L^2(\mathbb{S}^{d-1})$ and $H^* : L^2(D) \to L^2(\mathbb{S}^{d-1})$ are respectively the adjoints of H_0 and H given by

$$H_0^*\varphi(\hat{x}) := \int_{D_0} e^{-iky\cdot\hat{x}}\varphi(y)dy,\ \varphi \in L^2(D_0),\ \hat{x} \in \mathbb{S}^{d-1},$$

$$H^*\varphi(\hat{x}) := \int_{D} e^{-iky\cdot\hat{x}}\varphi(y)dy,\ \varphi \in L^2(D),\ \hat{x} \in \mathbb{S}^{d-1},$$

and where T_0: $L^2(D_0) \to L^2(D_0)$ and T: $L^2(D) \to L^2(D)$ are defined by

$$T\psi_0 := -k^2(1-n_0)(\psi_0 + w_0) \text{ and } T\psi := -k^2(1-n)(\psi + w), \tag{3.3}$$

with $w_0, w \in H^1_{\text{loc}}(\mathbb{R}^d)$ being obtained from ψ and ψ_0 as indicated in (3.1). Finally we get

$$F_0 = H_0^* T_0 H_0 \text{ and } F = H^* T H, \tag{3.4}$$

which give the second factorization needed by GLSM. As we shall later observe, other factorizations are possible and are more suited for the analysis of our method.

3.3 A modified version of the GLSM for noisy measurements

In this section we will review the case of noise free data as it is presented in [5] and complement it with an explicit convergence result, then give a slightly modified version of the noisy case in order to ensure an additional property needed in section 3.4. We present the method in an abstract form. We denote by X and Y two (complex) reflexive Banach spaces with duals X^* and Y^* respectively and shall denote by $\langle\cdot,\cdot\rangle$ a duality product that refers to $\langle X^*, X\rangle$ or $\langle Y^*, Y\rangle$ duality. We consider two linear operators $F : X \to X^*$ and $B : X \to X^*$ that are assumed to be bounded. Moreover we shall assume that the following factorizations hold

$$F = GH \quad \text{and} \quad B = H^* T H \tag{3.5}$$

where the operators $H : X \to Y$, $T : Y \to Y^*$ and $G : \overline{\mathcal{R}(H)} \subset Y \to X^*$ are bounded, where $\overline{\mathcal{R}(H)}$ is the closure of the range of H in Y. Note that we allow the operator B to be different from F, which will be exploited in numerical algorithms introduced later. Let $\alpha > 0$ be a given parameter and $\phi \in X^*$. The GLSM (for noise free measurements) is based on considering minimizing sequences of the functional $J_\alpha(\phi;\cdot) : X \to \mathbb{R}$

$$J_\alpha(\phi; g) := \alpha|\langle Bg, g\rangle| + \|Fg - \phi\|^2 \quad \forall g \in X. \tag{3.6}$$

We observe that if F has dense range then, for all $\phi \in X^*$,

$$j_\alpha(\phi) := \inf_{g\in X} J_\alpha(\phi; g) \to 0 \text{ as } \alpha \to 0. \tag{3.7}$$

The central theorem in the case of noise free measurement is then the following characterization of the range of G in terms of F and B (see [5, Theorem 3]).

Theorem 10. *We assume in addition that*

- *G is compact and $F = GH$ has dense range and is injective,*
- *T satisfies the coercivity property*

$$|\langle Th,\, h\rangle| > \mu \,\|h\|^2 \quad \forall\, h \in \mathcal{R}(H), \tag{3.8}$$

where $\mu > 0$ is a constant independent of h. Consider for $\alpha > 0$ and $\phi \in X^*$, $g_\alpha \in X$ such that

$$J_\alpha(\phi; g_\alpha) \leq j_\alpha(\phi) + p(\alpha) \tag{3.9}$$

where $\frac{p(\alpha)}{\alpha}$ is bounded with respect to α. Then

- *$\phi \in \mathcal{R}(G)$ implies $\limsup_{\alpha\to 0} |\langle Bg_\alpha,\, g_\alpha\rangle| < \infty$,*
- *$\phi \notin \mathcal{R}(G)$ implies $\liminf_{\alpha\to 0} |\langle Bg_\alpha,\, g_\alpha\rangle| = \infty$.*

If we suppose in addition that $h \mapsto \sqrt{|\langle Th,\, h\rangle|}$ is a uniformly convex function on $\overline{\mathcal{R}(H)}$ and that $\frac{p(\alpha)}{\alpha} \to 0$ as $\alpha \to 0$, then $\phi \in \mathcal{R}(G)$ if and only if $\lim_{\alpha\to 0} |\langle Bg_\alpha,\, g_\alpha\rangle| < \infty$. In the case $\phi = G\varphi$, the sequence Hg_α converges strongly to φ in Y.

Proof. The first part of the theorem has been proved in [5]. We shall prove the convergence of Hg_α to φ when $\phi = G\varphi$ for $\varphi \in Y$. The coercivity of T combined with the first part of the theorem imply that $\|Hg_\alpha\|^2$ is bounded. Second, from (3.6) and (3.9) and the injectivity of G we infer that the only possible weak limit of (any subsequence of) Hg_α is φ. Thus the whole sequence Hg_α weakly converges to φ. Since $\varphi \in \overline{\mathcal{R}(H)}$ we have

$$j_\alpha(\phi) = \inf_{g\in X)} J_\alpha(g, \phi) = \inf_{h\in\overline{\mathcal{R}(H)}} \left(\alpha|\langle Th,\, h\rangle| + \|Gh - \phi\|^2\right) \leq \alpha|\langle T\varphi,\, \varphi\rangle|.$$

Thus

$$|\langle Bg_\alpha,\, g_\alpha\rangle| \leq |\langle T\varphi,\, \varphi\rangle| + \frac{p(\alpha)}{\alpha},$$

which implies (as $\frac{p(\alpha)}{\alpha} \to 0$)

$$\limsup_{\alpha\to 0} |\langle THg_\alpha,\, Hg_\alpha\rangle| \leq |\langle T\varphi,\, \varphi\rangle|. \tag{3.10}$$

The uniform convexity of $h \mapsto \sqrt{|\langle Bh,\, h\rangle|}$ and the continuity and coercivity properties of T ensure that $\overline{\mathcal{R}(H)}$ equipped with $\sqrt{|\langle Th,\, h\rangle|}$ is a uniformly convex Banach space. We deduce from (3.10) and the weak convergence that Hg_α strongly converges to φ (see for instance [14, Chap. 3, Prop. 3.32]).

□

For practical applications one needs to consider the case with noisy data. More precisely, we shall assume that one has access to two noisy operators $B^\delta : X \to X^*$ and $F^\delta : X \to X^*$ such that

$$\left\|F^\delta - F\right\| \leq \delta\|F\| \quad \text{and} \quad \left\|B^\delta - B\right\| \leq \delta\|B\|$$

for some $\delta > 0$. We also assume that the operators, B, B^δ F^δ and F are compact.

Let $\eta \in]0,1[$ be a constant parameter. We define for $\alpha > 0$ and $\phi \in X^*$ the regularized functional

$$J_\alpha^\delta(\phi; g) := \alpha |\langle B^\delta g,\, g\rangle| + \alpha^{1-\eta}\delta \|B\|\, \|g\|^2 + \left\| F^\delta g - \phi \right\|^2 \quad \forall\, g \in X. \tag{3.11}$$

As indicated in Remark 3 below, this functional coincides with the one introduced in [5] for $\eta = 0$. It exhibits qualitatively similar properties: e.g., due to the compactness of B^δ it has a minimizer

$$g_\alpha^\delta = \arg\min_{g \in X} J_\alpha^\delta(\phi; g) \tag{3.12}$$

and we also have

$$\lim_{\alpha\to 0} \limsup_{\delta \to 0} J_\alpha^\delta(\phi; g_\alpha^\delta) = 0. \tag{3.13}$$

Theorem 11. *Assume that the first two assumptions of Theorem 10 hold true. Let g_α^δ be the minimizer of $J_\alpha^\delta(\phi;\cdot)$ (defined by (3.11)) for $\alpha > 0$, $\delta > 0$ and $\phi \in X^*$.*

Then

- *$\phi \in \mathcal{R}(G)$ implies $\limsup_{\alpha\to 0} \limsup_{\delta\to 0} \left(|\langle B^\delta g_\alpha^\delta,\, g_\alpha^\delta\rangle| + \delta\alpha^{-\eta}\|B\| \left\| g_\alpha^\delta \right\|^2 \right) < \infty$.*
- *$\phi \notin \mathcal{R}(G)$ implies $\liminf_{\alpha\to 0} \liminf_{\delta\to 0} \left(|\langle B^\delta g_\alpha^\delta,\, g_\alpha^\delta\rangle| + \delta\alpha^{-\eta}\|B\| \left\| g_\alpha^\delta \right\|^2 \right) = \infty$.*

Moreover, when $\phi \in \mathcal{R}(G)$ we also have

$$\limsup_{\alpha\to 0} \limsup_{\delta\to 0} \delta\|B\| \left\| g_\alpha^\delta \right\|^2 = 0. \tag{3.14}$$

If in addition the last assumptions of Theorem 10 hold true and $G\varphi = \phi$, then there exists $\delta_0(\alpha)$ such that for all $\delta(\alpha) \le \delta_0(\alpha)$, $Hg_\alpha^{\delta(\alpha)}$ converges strongly to φ as α goes to zero.

Proof. The proof follows the lines of the proof of [5, Theorem 5].

- Assume that $\phi = G(\varphi)$ for some $\varphi \in \overline{\mathcal{R}(H)}$. We consider g_0 (that depends on α but is independent from δ) such that $\|Hg_0 - \varphi\|^2 < \alpha$. Choosing δ sufficiently small such that

  $$(\alpha\delta\|B\| + \alpha^{1-\eta}\delta\|B\| + \delta^2\|F\|^2)\, \|g_0\|^2 \le \alpha$$

  we get

  $$J_\alpha^\delta(\phi; g_\alpha^\delta) \le J_\alpha^\delta(\phi; g_0) \le J_\alpha(\phi; g_0) + \alpha. \tag{3.15}$$

  Consequently

  $$\alpha \left(|\langle B^\delta g_\alpha^\delta,\, g_\alpha^\delta\rangle| + \alpha^{-\eta}\delta\|B\| \left\| g_\alpha^\delta \right\|^2 \right) \le J_\alpha^\delta(\phi; g_\alpha^\delta) \le \alpha + 2\alpha\, \|T\|\, (\alpha + \|\varphi\|^2) + \alpha\|G\|^2,$$

  which proves $\limsup_{\alpha\to 0} \limsup_{\delta\to 0} \left(|\langle B^\delta g_\alpha^\delta,\, g_\alpha^\delta\rangle| + \alpha^{-\eta}\delta\|B\| \left\| g_\alpha^\delta \right\|^2 \right) < \infty$. We also have, as a consequence of the inequalities above, that

  $$\delta\|B\| \left\| g_\alpha^\delta \right\|^2 \le C\alpha^\eta$$

which proves $\limsup_{\alpha\to 0}\limsup_{\delta\to 0}\delta\|B\|\left\|g_\alpha^\delta\right\|^2=0$.

Now assume that the last assumptions of Theorem 10 hold true. We recall that

$$J_\alpha^\delta(\phi;g)\leq J_\alpha(\phi,g)+(\alpha\delta\|B\|+\alpha^{1-\eta}\delta\|B\|+\delta^2\|F\|^2)\left\|g\right\|^2.$$

If we use the sequence g_α from Theorem 10, and choose $\delta_0(\alpha)$ small enough such that $\limsup_{\alpha\to 0}(\alpha\delta_0(\alpha)\|B\|+\alpha^{1-\eta}\delta_0(\alpha)\|B\|+\delta_0(\alpha)^2\|F\|^2)\frac{\|g_\alpha\|^2}{\alpha}=0$. Then, from the convergence properties of sequence Hg_α, we clearly obtain for $\delta(\alpha)\leq\delta_0(\alpha)$,

$$\limsup_{\alpha\to 0}|\left\langle Bg_\alpha^{\delta(\alpha)},\,g_\alpha^{\delta(\alpha)}\right\rangle|\leq|\langle T\varphi,\,\varphi\rangle|.$$

We then conclude as in the proof of Theorem 10 that $Hg_\alpha^{\delta(\alpha)}$ converges strongly to φ as α goes to zero.

- Assume $\phi\notin\mathcal{R}(G)$ and assume that $\liminf_{\alpha\to 0}\liminf_{\delta\to 0}\left(|\left\langle B^\delta g_\alpha^\delta,\,g_\alpha^\delta\right\rangle|+\alpha^{-\eta}\delta\|B\|\left\|g_\alpha^\delta\right\|^2\right)$ is finite. The coercivity of T and $\alpha<1$ implies that

$$\mu\left\|Hg_{\alpha(\delta)}^\delta\right\|^2\leq|\left\langle Bg_\alpha^\delta,\,g_\alpha^\delta\right\rangle|\leq|\left\langle B^\delta g_\alpha^\delta,\,g_\alpha^\delta\right\rangle|+\alpha^{-\eta}\delta\|B\|\left\|g_\alpha^\delta\right\|^2.$$

Therefore $\liminf_{\alpha\to 0}\liminf_{\delta\to 0}\left\|Hg_\alpha^\delta\right\|^2$ is also finite. This means the existence of a subsequence $(\alpha',\delta(\alpha'))$ such that $\alpha'\to 0$ and $\delta(\alpha')\to 0$ as $\alpha'\to 0$ and $\left\|Hg_{\alpha'}^{\delta(\alpha')}\right\|^2$ is bounded independently from α'. One can also choose $\delta(\alpha')$ such that $\delta(\alpha')\leq\alpha'^{1-\eta}$.

On the other hand Equation (3.13) indicates that one can choose this subsequence such that $J_{\alpha'}^{\delta(\alpha')}(g_{\alpha'}^{\delta(\alpha')})\to 0$ as $\alpha'\to 0$ and therefore $\left\|F^\delta g_{\alpha'}^{\delta(\alpha')}-\phi\right\|\to 0$ as $\alpha'\to 0$ and $\alpha'^{1-\eta}\delta(\alpha')\|g_{\alpha'}^{\delta(\alpha')}\|^2\to 0$ as $\alpha'\to 0$. By a triangular inequality and $\delta(\alpha')\leq\alpha'^{1-\eta}$ we then deduce that $\left\|Fg_{\alpha'}^{\delta(\alpha')}-\phi\right\|\to 0$ as $\alpha'\to 0$. The compactness of G implies that a subsequence of $GHg_{\alpha'}^{\delta(\alpha')}$ converges for some $G\varphi$ in X^*. The uniqueness of the limit implies that $G\varphi=\phi$ which is a contradiction.

□

Remark 3. *The treatment of noisy cases has been done in [5] with $\eta=0$. This choice does not guarantee the extra property (3.14) which is needed to ensure the convergence of our algorithm in Section 3.4.*

3.4 Identification of modifications in a given unknown background

We first recall how GLSM can be applied to F (resp. F_0) in order to image D (resp. D_0). Since the treatment is the same for F and F_0 we present it only for F. The first step is to

obtain a characterization of D in terms of the range of the operator G. This characterization is linked to solutions to so-called interior transmission problems (ITP). For a Lipschitz bounded domain D, an index of refraction n as in Section 3.2 and two boundary data $f \in H^{\frac{3}{2}}(\partial D)$ and $g \in H^{\frac{1}{2}}(\partial D)$ we define the interior transmission problem $\mathrm{ITP}(D, f, g, n)$ as the problem of seeking $(u, v) \in L^2(D) \times L^2(D)$ such that $u - v \in H^2(D)$ and

$$\mathrm{ITP}(D, f, g, n) : \begin{cases} \Delta u + k^2 n u = 0 & \text{in } D, \\ \Delta v + k^2 v = 0 & \text{in } D, \\ (u - v) = f & \text{on } \partial D, \\ \frac{\partial}{\partial \nu}(u - v) = g & \text{on } \partial D. \end{cases} \tag{3.16}$$

We denote by $\sigma(D, n)$ the set of transmission eigenvalues that we define here as the set of wave numbers $k \in \mathbb{R}$ for which $\mathrm{ITP}(D, f, g, n)$ is not well posed for all $f \in H^{\frac{3}{2}}(\partial D)$ and $g \in H^{\frac{1}{2}}(\partial D)$. It is known for instance that if $1/(n-1) \in L^\infty(D)$ and $\Re(n-1)$ is positive definite or negative definite in a neighborhood of ∂D, then $\sigma(D, n)$ is a countable set without any finite accumulation point [52]. Defining

$$\phi_z(\hat{x}) := e^{-ik\hat{x}\cdot z}, \tag{3.17}$$

the farfield of $\Phi(\cdot; z)$, the fundamental solution of the Helmholtz equation satisfying the Sommerfeld radiation condition, we have the following theorem [15].

Theorem 12. *Assume that $k \notin \sigma(D, n)$. Then G is compact, injective with dense range and $\phi_z \in \mathcal{R}(G)$ if and only if $z \in D$. Moreover, if $z \in D$ then $G(v) = \phi_z$ if and only if there exists $u \in L^2(D)$ such that (u, v) is a solution of $\mathrm{ITP}(D, \Phi_z, \frac{\partial \Phi_z}{\partial \nu}, n)$.*

We recall also that under some hypotheses on n, for instance those in Hypothesis 3, the operator T satisfies the coercivity property (3.8) if $k \notin \sigma(D, n)$ [5]. Using equations (3.4) one can apply the theory in Section 3.3 with $B = F$ and deduce a characterization of D (resp. D_0) from the knowledge of F (resp. F_0).

Hypothesis 3. *The index of refraction n and the domain D satisfy $n \in L^\infty(\mathbb{R}^d)$, $\mathrm{supp}(n-1) = \overline{D}$, $\Im(n) \geq 0$ and there exist two constants $n_* > 0$ and $\alpha \geq 0$ such that $1 - \Re(n(x)) + \alpha \Im(n(x)) \geq n_*$ for a.e. $x \in D$ or $\Re(n(x)) - 1 + \alpha \Im(n(x)) \geq n_*$ for a.e. $x \in D$.*

However, the choice of $B = F$ does not guarantee the convexity assumption required to ensure the strong convergence of the Herglotz waves to solutions of interior transmission problems (see conclusions of Theorems 10 and 11). This property is needed to treat the case of differential measurements. This is why, in the latter case, we will rather use $B = F_\# := |\Re(F)| + |\Im(F)|$ under slightly stronger assumptions on the refractive index.

3.4.1 Comparison of ITP solutions

The main ingredient of our algorithm is based on the following results on the solutions of the interior transmission problems related to D and D_0. Let us first further specify the assumptions on these domains. We suppose that D_0, D and Ω are the smallest domains with connected complement that respectively verify $\mathrm{supp}(n_0 - 1) \subset \bar{D}_0$, $\mathrm{supp}(n-1) \subset \bar{D}$ and $\mathrm{supp}(n - n_0) \subset \bar{\Omega}$. We also assume that $D_0 \subset D$ which implies in particular that $D = \Omega \cup D_0$. We denote by $D_{0,i}$,

$i = 1, \dots, M_0$ and D_i, $i = 1, \dots, M$ the simply connected components of respectively D_0 and D. We introduce $\mathcal{F} = \{i \text{ such that } \exists j \ D_{0,i} = D_j \text{ and } D_{0,i} \cap \Omega = \emptyset\}$ and define $\hat{D}_0 := \bigcup_{i \in \mathcal{F}} D_{0,i}$ which is the part of D_0 that has not been modified between the two measurements campaigns. We set $\tilde{D}_0 := D_0 \setminus \hat{D}_0$.
We then define $\mathcal{G} = \left\{ i \textit{ such that } \ D_i \cap \tilde{D}_0 \neq \emptyset \right\}$ and set $\tilde{D} := \bigcup_{i \in \mathcal{G}} D_i$ which represents the component of D that intersects with $\tilde{D}_0$. We then set $\tilde{\Omega} := \Omega \cap \tilde{D}$ and $\hat{\Omega} := D \setminus \left\{ \tilde{D} \cup \hat{D}_0 \right\}$.
One can remark that $\tilde{D} = \tilde{D}_0 \cup \tilde{\Omega}$ and that we have the following non-intersecting partitions (See Fig. 3.1, 3.2 and 3.3)

$$D = \tilde{D} \cup \hat{\Omega} \cup \hat{D}_0, \quad \Omega = \hat{\Omega} \cup \tilde{\Omega} \quad \text{and} \quad D_0 = \hat{D}_0 \cup \tilde{D}_0.$$

As we shall later observe, our algorithm will not exactly recover Ω (shaded region in Fig. 3.2) but rather reconstruct either $\tilde{D}_0$ (shaded region in Fig. 3.1) or the bigger domain

$$\Omega_T := \Omega \cup \tilde{D}_0 = \hat{\Omega} \cup \tilde{D}.$$

containing Ω (shaded region in Fig. 3.3).

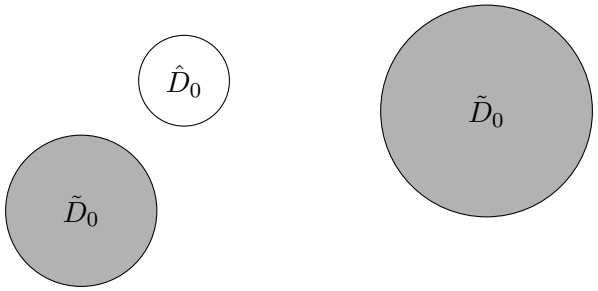

Figure 3.1: Sketch of a possible configuration for D_0 (the part $\tilde{D}_0$ is shaded).

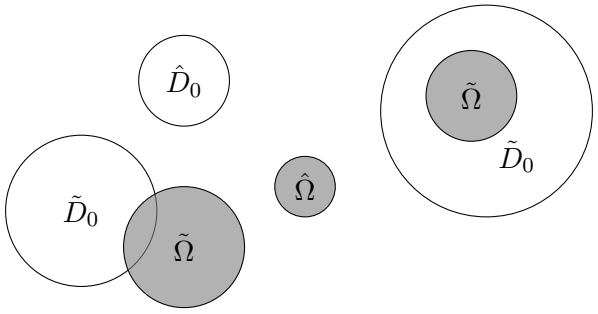

Figure 3.2: Sketch of a possible configuration for D. The defect Ω is represented by the shaded region ($\tilde{D} = \tilde{\Omega} \cup \tilde{D}_0$).

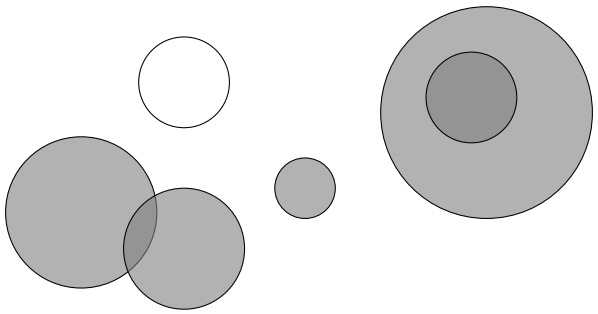

Figure 3.3: Sketch of Ω_T (shaded region) associated with D_0 (Fig. 3.1) and Ω (Fig. 3.2).

Let us denote by $\mathrm{ITP}(D, f, g, n, n')$ the problem $\mathrm{ITP}(D, f, g, n)$ where the equation for v is replaced with

$$\Delta v + k^2 n' v = 0 \quad \text{in } D, \tag{3.18}$$

and by $\sigma(D, n, n')$ the set of associated transmission eigenvalues (defined similarly to $\sigma(D, n)$).

Theorem 13. *Assume that $k \notin \sigma(D, n) \cup \sigma(D_0, n_0) \cup \sigma(\tilde{\Omega}, n, \tilde{n})$ where $\tilde{n}$ is defined in $\tilde{D} \supset \tilde{\Omega}$ by:*

$$\tilde{n} := \begin{cases} n_0 & \text{in } \tilde{D}_0, \\ 1 & \text{in } \tilde{D} \setminus \tilde{D}_0. \end{cases} \tag{3.19}$$

Let $z \in D$ and consider $(u, v) \in L^2(D) \times L^2(D)$ (resp. $(u_0, v_0) \in L^2(D_0) \times L^2(D_0)$) solutions of $\mathrm{ITP}(D, \Phi_z, \frac{\partial \Phi_z}{\partial \nu}, n)$ (resp. $\mathrm{ITP}(D_0, \Phi_z, \frac{\partial \Phi_z}{\partial \nu}, n_0)$). Then:

- *If $z \in \hat{D}_0$ then $v = v_0$ in D_0.*
- *If $z \in \tilde{D}_0$, then $v \neq v_0$ in D_0.*

Proof. We first consider the case where $z \in \hat{D}_0$. In $D \setminus \hat{D}_0$, the function Φ_z satisfies $\Delta \Phi_z + k^2 \Phi_z = 0$ and therefore the ITP solutions in this domain are given by $v = v_0 = -\Phi_z$ and $u = u_0 = 0$. On the other hand, by definition of $\hat{D}_0$, $n = n_0$ in $\hat{D}_0$ meaning that $\mathrm{ITP}(\hat{D}_0, \Phi_z, \frac{\partial \Phi_z}{\partial \nu}, n) \equiv \mathrm{ITP}(\hat{D}_0, \Phi_z, \frac{\partial \Phi_z}{\partial \nu}, n_0)$ and thus $v = v_0$ in $\hat{D}_0$.

We now consider the case $z \in \tilde{D}_0$. Using the same arguments as above we have $v = v_0$ in $D_0 \setminus \tilde{D}_0$. Let us assume that $v = v_0$ in $\tilde{D}_0$ (and conclude using a contradiction argument).

We now introduce $\tilde{u}$ defined on $\tilde{D}$:

$$\tilde{u} := \begin{cases} u_0 & \text{in } \tilde{D}_0, \\ v + \Phi_z & \text{in } \tilde{D} \setminus \tilde{D}_0. \end{cases} \tag{3.20}$$

Since we suppose that $v = v_0$ in $\tilde{D}_0$ and using the boundary conditions satisfied by $u_0 - v_0$ on $\partial \tilde{D}_0$, we obtain that the jump of $\tilde{u}$ and the jump of its normal derivative are zero on $\partial \tilde{D}_0 \setminus \partial \tilde{D}$ (the trace of $\tilde{u}$ and the trace of its normal derivative on $\partial \tilde{D}_0$ are defined as elements of respectively $H^{-1/2}(\partial \tilde{D}_0)$ and $H^{-3/2}(\partial \tilde{D}_0)$). Therefore, $\tilde{u} \in L^2(\tilde{D})$ and is solution to the Helmholtz equation with index of refraction $\tilde{n}$. Moreover, by construction, the Cauchy data of $u - \tilde{u}$ are equal to zero on $\partial \tilde{D}$. In addition, in the domain $\tilde{D}_0$, $u - \tilde{u} = u - u_0 = u - v - (u_0 - v_0) \in H^2(\tilde{D}_0)$ and in $\tilde{D} \setminus \tilde{D}_0$, $u - \tilde{u} = u - v - \Phi_z \in H^2(\tilde{D} \setminus \tilde{D}_0)$. The continuity of the Cauchy data of

$u-\tilde{u}$ across $\partial\tilde{D}_0 \setminus \partial\tilde{D}$ then implies $u-\tilde{u} \in H^2(\tilde{D})$. Finally we have that $(u,\tilde{u})$ are solution of ITP$(\tilde{D},0,0,n,\tilde{n})$.

In order to finish the proof we need to look at two cases. Let us introduce the simply connected domain $\tilde{D}_{0,i}$ where z belongs. First we suppose that $\tilde{D}_{0,i}$ is not included in any simply connected part of Ω. Then clearly $\partial\tilde{D} \cap \partial\tilde{D}_0$ has a non zero measure, which means that ITP$(\tilde{D},0,0,n,\tilde{n})$ is not well posed (n and $\tilde{n}$ are both equal to n_0 on this part of the boundary). The equality of the Cauchy data means that $u=\tilde{u}$ in $\tilde{D}_0 \setminus \tilde{\Omega}$, where $\tilde{\Omega} = \Omega \cap \tilde{D}$. This yields that the Cauchy data of $u-\tilde{u}$ are equal to zero on $\partial\tilde{\Omega}$. Consequently $(u,\tilde{u})|_{\tilde{\Omega}}$ are solution of ITP$(\tilde{\Omega},0,0,n,\tilde{n})$. Our hypothesis on k implies $u=\tilde{u}=0$ in $\tilde{\Omega}$, which implies that $u=0$ in $\tilde{\Omega}$. Using a unique continuation argument we get $u=0$ in $\tilde{D}$. This yields that the Cauchy data of v and $-\Phi_z$ coincides on $\partial\tilde{D}$ which give $v_0 = v = -\Phi_z$ in $\tilde{D}_0 \setminus \{z\}$. We obtain a contradiction since $v_0 = v_0 - u_0 \in H^2(\tilde{D}_0)$ while $\Phi_z \notin H^2(\tilde{D}_0)$.

The second case is when $\tilde{D}_{0,i} \subset \tilde{\Omega}_i \subset \tilde{D}_i$, where $\tilde{\Omega}_i \subset \tilde{\Omega}$ and $\tilde{D}_i$ are simply connected components of respectively Ω and $\tilde{D}$. Since the interior transmission problems of disconnected components are independent from each other, we already have that $(u,\tilde{u})$ are solution of ITP$(\tilde{D}_i,0,0,n,\tilde{n})$. In the cases where $\tilde{\Omega}_i$ is not equal to $\tilde{D}_i$ (for example when $\tilde{D}_{0,i} \neq \tilde{D}_i \cap \tilde{D}_0$) one can use the same reasoning as for the first case (replacing $\tilde{D}$ by $\tilde{D}_i$ and $\tilde{\Omega}$ by $\tilde{\Omega}_i$) to infer that $(u,\tilde{u})$ are solution of ITP$(\tilde{\Omega}_i,0,0,n,\tilde{n})$. Therefore $\tilde{u}_0 = 0$ in $\tilde{\Omega}_i$. This yields that the Cauchy data of v_0 and $-\Phi_z$ coincide on $\partial\tilde{D}_{0,i}$ which gives $v_0 = -\Phi_z$ in $\tilde{D}_{0,i} \setminus \{z\}$. We obtain a contradiction since $v_0 = v_0 - u_0 \in H^2(\tilde{D}_{0,i})$ while $\Phi_z \notin H^2(\tilde{D}_{0,i})$. □

Remark 4. *The assumption of Theorem 13 is to be understood as an implicit assumption on n and n_0. This theorem is indeed meaningful only when $\sigma(D,n) \cup \sigma(D_0,n_0) \cup \sigma(\tilde{\Omega},n,\tilde{n})$ forms a discrete set without finite accumulation points. We remark that the latter is true when $\Re(n-1)$, $\Re(n_0-1)$ and $\Re(n-\tilde{n})$ are positive definite quantities in a neighborhood of respectively ∂D, ∂D_0 and $\partial\tilde{\Omega}$. We also remark that if $\tilde{D}_{0,i} \subset \Omega_i$ and $\partial\tilde{D}_{0,i} \cap \partial\Omega_i$ has a non zero surface measure, then $\sigma(\tilde{\Omega},n,\tilde{n}) = \mathbb{R}$ and therefore one has to exclude this configuration.*

3.4.2 Characterization of Ω_T and $\tilde{D}_0$ in terms of F and F_0

We assume in this section that hypotheses of Theorem 13 on the wave number k hold true. We shall also assume that one can respectively obtain from F and F_0 two operators B and $B_0 : L^2(\mathbb{S}^{d-1}) \to L^2(\mathbb{S}^{d-1})$ such that $B_0 = H_0^* T_{B_0} H_0$, $B = H^* T_B H$ where T_{B_0} and T_B are respectively defined on $L^2(D_0)$ and $L^2(D)$ and satisfy the coercivity and uniform convexity assumptions of Theorem 10.

An example of such construction is $B = |\Re(F)| + |\Im(F)|$ and $B_0 = |\Re(F_0)| + |\Im(F_0)|$. It is for instance shown in [40] that under Hypothesis 4, the operator $B = H^* T_\# H$, with $T_\#$ a strictly positive and selfadjoint operator which satisfies the coercivity property (3.8) if $k \notin \sigma(D,n)$. It is then clear that $h \mapsto \sqrt{|\langle T_\# h,\, h\rangle|} = \left\| T_\#^{1/2} h \right\|^2_{L^2(D)}$ satisfies the uniform convexity assumption. Similar considerations apply to B_0.

Hypothesis 4. *The index of refraction n and the domain D satisfy $n \in L^\infty(\mathbb{R}^d)$, $\mathrm{supp}(n-1) = \overline{D}$, $\Im(n) \geq 0$ and there exist constants $n_* > 0$ and $\Re((n(x)-1)) \geq n_*$ for a.e. $x \in D$.*

Remark 5. *If $\Im n(x) > \gamma > 0$ in D, then one can simply use $B = \Im F$. A similar comment applies to n_0, D_0, B_0 and F_0.*

In the following $(\cdot,\,\cdot)$ and $\|\cdot\|$ will respectively denote the L^2 scalar product and the associated norm (the domain is not indicated if clear from the context).

For a point $z \in \mathbb{R}^d$ and ϕ_z given by (3.17), we consider the two functionals defined on $L^2(\mathbb{S}^{d-1})$ by

$$J_{0,\alpha}(\phi_z; g) = \alpha|(B_0 g,\, g)| + \|F_0 g - \phi_z\|^2$$

and

$$J_{\alpha}(\phi_z; g) = \alpha|(B g,\, g)| + \|F g - \phi_z\|^2$$

and denote by $g^{\alpha}_{0,z}$ and g^{α}_{z} two sequences of $L^2(S^{d-1})$ respectively satisfying (like in (3.9)),

$$J_{0,\alpha}(\phi_z; g^{\alpha}_{0,z}) \leq \inf_{g \in L^2(S^{d-1})} J_{0,\alpha}(\phi_z; g) + p(\alpha) \tag{3.21}$$

and

$$J_{\alpha}(\phi_z; g^{\alpha}_{z}) \leq \inf_{g \in L^2(S^{d-1})} J_{\alpha}(\phi_z; g) + p(\alpha), \tag{3.22}$$

where $\frac{p(\alpha)}{\alpha}$ goes to 0 as $\alpha \to 0$. For g and g_0 in $L^2(\mathbb{S}^{d-1})$, we introduce the key quantities will be used in the following :

$$\begin{aligned} &\mathcal{A}(g) := |(Bg,\, g)|, \quad \mathcal{A}_0(g) := |(B_0 g,\, g)| \quad \text{and the coupling term} \\ &\mathcal{D}(g, g_0) := |(B_0(g - g_0),\, g - g_0)|. \end{aligned} \tag{3.23}$$

Theorem 14. *For g^{α}_{z} and $g^{\alpha}_{0,z}$ satisfying (3.22), (3.21), we have the following results.*

- *If $z \in \hat{D}_0$ then $\lim_{\alpha \to 0} \mathcal{D}(g^{\alpha}_{z}, g^{\alpha}_{0,z}) = 0$.*
- *If $z \in \tilde{D}_0$ then $0 < \lim_{\alpha \to 0} \mathcal{D}(g^{\alpha}_{z}, g^{\alpha}_{0,z}) < \infty$.*
- *If $z \in \Omega \setminus \tilde{D}_0$ then $\lim_{\alpha \to 0} \mathcal{D}(g^{\alpha}_{z}, g^{\alpha}_{0,z}) = \infty$.*

Proof. For fixed $z \in D$ (resp. $z \in D_0$), we denote by (u, v) (resp (u_0, v_0)) the solution of $\mathrm{ITP}(D, \Phi_z, \frac{\partial \Phi_z}{\partial \nu}, n)$ (resp. of $\mathrm{ITP}(D_0, \Phi_z, \frac{\partial \Phi_z}{\partial \nu}, n_0)$).

- If $z \in \hat{D}_0$ we actually know from the application of Theorem 10 that $H g^{\alpha}_{z} \to v$ in $L^2(D)$ and $H_0 g^{\alpha}_{0,z} \to v_0$ in $L^2(D_0)$. Therefore, using the boundedness of T_{B_0} and the fact that $D_0 \subset D$,

$$\mathcal{D}(g^{\alpha}_{z}, g^{\alpha}_{0,z}) \to \left|(T_{B_0}(v - v_0),\, (v - v_0))_{L^2(D_0)}\right| \text{ as } \alpha \to 0. \tag{3.24}$$

  Theorem 13 indicates that $v = v_0$ in D_0 which proves the desired result.

- If $z \in \tilde{D}_0$, we still have $H g^{\alpha}_{z} \to v$ in $L^2(D)$ and $H g^{\alpha}_{0,z} \to v_0$ in $L^2(D_0)$ and therefore (3.24) still holds. However, this time $v \neq v_0$ in D_0 (according to Theorem 13). The coercivity and continuity of T_{B_0} imply (for some constant $\mu_0 > 0$)

$$\mu_0 \|v - v_0\|^2_{L^2(D_0)} \leq \left|(T_{B_0}(v - v_0),\, (v - v_0))_{L^2(D_0)}\right| \leq \|T_{B_0}\| \, \|v - v_0\|^2_{L^2(D_0)}$$

  which gives the desired result.

- If $z \in \Omega \setminus \tilde{D}_0$, we still have that $Hg_z^\alpha \to v$ in $L^2(D)$ but $\left\|H_0 g_{0,z}^\alpha\right\|_{L^2(D_0)}$ is now unbounded. Since
$$\mu_0 \left\|H_0 g_{0,z}^\alpha - H_0 g_z^\alpha\right\|^2_{L^2(D_0)} \leq \left|\left(B_0(g_z^\alpha - g_{0,z}^\alpha),\, (g_z^\alpha - g_{0,z}^\alpha)\right)\right|$$
we clearly get $\lim_{\alpha\to 0} \mathcal{D}(g_z^\alpha, g_{0,z}^\alpha) = \infty$.

□

Let us introduce the two functionals

$$\mathcal{I}_T(g, g_0) := \frac{1}{\sqrt{\mathcal{A}(g)\left(1 + \mathcal{A}(g)\mathcal{D}(g, g_0)^{-1}\right)}} \tag{3.25}$$

$$\mathcal{I}_{\mathrm{MB}}(g, g_0) := \frac{1}{\sqrt{\mathcal{A}_0(g_0) + \mathcal{A}(g)\left(1 + \mathcal{A}_0(g_0)\mathcal{D}(g, g_0)^{-1}\right)}}. \tag{3.26}$$

The previous Theorem together with the application of Theorems 10 and 12 can be used to prove that $\mathcal{I}_T(g_z^\alpha, g_{0,z}^\alpha)$ and $\mathcal{I}_{\mathrm{MB}}(g_z^\alpha, g_{0,z}^\alpha)$ respectively provide some indicator functions of Ω_T and $\tilde{D}_0$ (the subscript "MB" stands for modified background since $\tilde{D}_0$ corresponds to the simply connected components of D_0 that have non empty intersections with Ω).

Corollary 2. *For those g_z^α and $g_{0,z}^\alpha$ satisfying (3.22) and (3.21), we have the following characterizations:*

- *$z \in \Omega_T$ if and only if $\lim_{\alpha\to 0} \mathcal{I}_T(g_z^\alpha, g_{0,z}^\alpha) > 0$.*
- *$z \in \tilde{D}_0$ if and only if $\lim_{\alpha\to 0} \mathcal{I}_{\mathrm{MB}}(g_z^\alpha, g_{0,z}^\alpha) > 0$.*

Proof. Theorems 10 and 12 imply that $z \in D$ (respectively $z \in D_0$) if and only if $\lim_{\alpha\to 0} \mathcal{A}(g_z^\alpha) < \infty$ (respectively $\lim_{\alpha\to 0} \mathcal{A}_0(g_{0,z}^\alpha) < \infty$). These results imply that $\lim_{\alpha\to 0} \mathcal{I}_T(g_z^\alpha, g_z^\alpha) = 0$ (resp. $\lim_{\alpha\to 0} \mathcal{I}_{\mathrm{MB}}(g_z^\alpha, g_{0,z}^\alpha) = 0$) when $z \in \mathbb{R}^d \setminus D$ (resp. $z \in \mathbb{R}^d \setminus D_0$). The first point of theorem 14 imply that for $z \in \hat{D}_0$, $\lim_{\alpha\to 0} \mathcal{I}_T(g_z^\alpha, g_z^\alpha) = 0$ (resp. $\lim_{\alpha\to 0} \mathcal{I}_{\mathrm{MB}}(g_z^\alpha, g_{0,z}^\alpha) = 0$). Equations (3.25) and (3.26) and the fact that $\mathbb{R}^d = \{\mathbb{R}^d \setminus D\} \cup \hat{D}_0 \cup \tilde{D}_0 \cup \{\Omega \setminus \tilde{D}_0\}$ together with the last two points of theorem 14 conclude the proof. □

3.4.3 The case of noisy operators

We shall extend here the result of previous section to the case of noisy operators. In addition to the assumptions of Section 3.4.2, we suppose that one has access to F^δ, F_0^δ, B^δ and B_0^δ that are compact operators on $L^2(\mathbb{S}^{d-1})$ and satisfy

$$\|B - B^\delta\| \leq \delta,\ \|B_0 - B_0^\delta\| \leq \delta,\ \|F - F^\delta\| \leq c\delta \text{ and } \|F_0 - F_0^\delta\| \leq c\delta$$

for some constant $c > 0$, where δ plays the role of some upper bound on the norm of the absolute noise level in B^δ and B_0^δ. Following Theorem 11, we consider for $z \in \mathbb{R}^d$ and ϕ_z given by (3.17), the functions $g_{0,z}^{\alpha,\delta}$ and $g_z^{\alpha,\delta}$ in $L^2(\mathbb{S}^{d-1})$ defined by

$$g_{0,z}^{\alpha,\delta} := \arg \min_{g\in L^2(\mathbb{S}^{d-1})} \left[\alpha\left(|(B_0^\delta g,\, g)| + \alpha^{1-\eta}\delta \|g\|^2\right) + \left\|F_0^\delta g - \phi_z\right\|^2\right], \tag{3.27}$$

$$g_z^{\alpha,\delta} = \arg \min_{g\in L^2(\mathbb{S}^{d-1})} \left[\alpha\left(|(B^\delta g,\, g)| + \alpha^{1-\eta}\delta \|g\|^2\right) + \left\|F^\delta g - \phi_z\right\|^2\right] \tag{3.28}$$

where $\eta \in (0,1)$ is fixed and α is a small parameter. Similarly to (3.23) we define

$$\begin{aligned} &\mathcal{A}^{\alpha,\delta}(g) := |(B^\delta g,\, g)| + \alpha^{-\eta}\delta \|g\|^2, \quad \mathcal{A}_0^{\alpha,\delta}(g) := |(B_0^\delta g,\, g)| + \alpha^{-\eta}\delta \|g\|^2, \\ &\mathcal{D}^\delta(g, g_0) := |(B_0^\delta(g-g_0),\, g-g_0)| + \delta \|g-g_0\|^2. \end{aligned} \tag{3.29}$$

Theorem 15. *For $g_{0,z}^{\alpha,\delta}$ and $g_z^{\alpha,\delta}$ defined by (3.27) and (3.28) we have the following results:*

- *If $z \in \hat{D}_0$ then $\lim_{\alpha\to 0} \liminf_{\delta\to 0} \mathcal{D}^\delta(g_z^{\alpha,\delta}, g_{0,z}^{\alpha,\delta}) = 0$.*
- *If $z \in \tilde{D}_0$ then $0 < \lim_{\alpha\to 0} \liminf_{\delta\to 0} \mathcal{D}^\delta(g_z^{\alpha,\delta}, g_{0,z}^{\alpha,\delta}) < \infty$.*
- *If $z \in \Omega \setminus \tilde{D}_0$ then $\lim_{\alpha\to 0} \liminf_{\delta\to 0} \mathcal{D}^\delta(g_z^{\alpha,\delta}, g_{0,z}^{\alpha,\delta}) = \infty$.*

Proof. Let $z \in D_0$. From Theorem 11 and Theorem 12 (applied respectively to $(F^\delta,\, B^\delta)$ and $(F_0^\delta,\, B_0^\delta)$) one deduces the existence of a sequence $\delta(\alpha)$ such that $Hg_z^{\alpha,\delta(\alpha)} \to v$ in $L^2(D)$ where v is the solution of the $ITP(D, \Phi_z, \frac{\partial \Phi_z}{\partial \nu}, n)$ and $H_0 g_{0,z}^{\alpha,\delta(\alpha)} \to v_0$ in $L^2(D_0)$ where v_0 is the solution of $ITP(D_0, \Phi_z, \frac{\partial \Phi_z}{\partial \nu}, n_0)$ (it is obvious from Theorem 11 that one can choose a same subsequence $\delta(\alpha)$ for $Hg_z^{\alpha,\delta}$ and $H_0 g_z^{\alpha,\delta}$). Following the same proof as for Theorem 14 we deduce (using Theorem 13) that

$$\lim_{\alpha\to 0} \mathcal{D}(g_z^{\alpha,\delta(\alpha)}, g_{0,z}^{\alpha,\delta(\alpha)}) = 0$$

for $z \in \hat{D}_0$ and

$$0 < \lim_{\alpha\to 0} \mathcal{D}(g_z^{\alpha,\delta(\alpha)}, g_{0,z}^{\alpha,\delta(\alpha)}) = \left|(T_{B_0}(v-v_0),\, (v-v_0))_{L^2(D_0)}\right| < \infty$$

for $z \in \tilde{D}_0$. Obviously

$$|\mathcal{D}(g, g_0) - \mathcal{D}^\delta(g, g_0)| \le 4\delta(\|g_0\|^2 + \|g\|^2).$$

Therefore, using Theorem 11 we deduce that

$$\mathcal{D}(g_z^{\alpha,\delta(\alpha)}, g_{0,z}^{\alpha,\delta(\alpha)}) - \mathcal{D}^{\delta(\alpha)}(g_z^{\alpha,\delta(\alpha)}, g_{0,z}^{\alpha,\delta(\alpha)}) \to 0 \text{ as } \alpha \to 0.$$

This proves the first two statements of the theorem (using the fact that the above considerations apply for any subsequence of $(F^\delta,\, B^\delta)$ and $(F_0^\delta,\, B_0^\delta)$).

For $z \in \Omega \setminus \tilde{D}_0$, the statement of the theorem follows from the coercivity property

$$\mu_0 \left\|H_0 g_{0,z}^{\alpha,\delta} - H_0 g_z^{\alpha,\delta}\right\|_{L^2(D_0)}^2 \le \mathcal{D}^\delta(g_z^{\alpha,\delta}, g_{0,z}^{\alpha,\delta})$$

(for some constant $\mu_0 > 0$) and the fact that (using the first part of Theorem 11)

$$\limsup_{\alpha\to 0} \liminf_{\delta\to 0} \left\|H_0 g_z^{\alpha,\delta}\right\|_{L^2(D_0)}^2 < \infty,$$

while

$$\liminf_{\alpha\to 0}\liminf_{\delta\to 0}\left\|H_0 g_{0,z}^{\alpha,\delta}\right\|^2_{L^2(D_0)}=\infty.$$

□

We now consider

$$\mathcal{I}_T^{\alpha,\delta}(g,g_0)=\frac{1}{\sqrt{\mathcal{A}^{\alpha,\delta}(g)\left(1+\mathcal{A}^{\alpha,\delta}(g)\mathcal{D}^{\delta}(g,g_0)^{-1}\right)}} \tag{3.30}$$

$$\mathcal{I}_{\mathrm{MB}}^{\alpha,\delta}(g,g_0)=\frac{1}{\sqrt{\mathcal{A}_0^{\alpha,\delta}(g_0)+\mathcal{A}^{\alpha,\delta}(g)\left(1+\mathcal{A}_0^{\alpha,\delta}(g_0)\mathcal{D}^{\delta}(g,g_0)^{-1}\right)}}. \tag{3.31}$$

The previous Theorem together with the application of Theorems 11 and 12 imply the following characterizations.

Corollary 3. *For $g_{0,z}^{\alpha,\delta}$ and $g_z^{\alpha,\delta}$ defined by (3.27) and (3.28) we have*

- *$z\in\Omega_T$ if and only if $\lim_{\alpha\to 0}\liminf_{\delta\to 0}\mathcal{I}_T^{\alpha,\delta}(g_z^{\alpha,\delta},g_{0,z}^{\alpha,\delta})>0$.*
- *$z\in\tilde{D}_0$ if and only if $\lim_{\alpha\to 0}\liminf_{\delta\to 0}\mathcal{I}_{\mathrm{MB}}^{\alpha,\delta}(g_z^{\alpha,\delta},g_{0,z}^{\alpha,\delta})>0$.*

Proof. Theorems 11 and 12 imply that $z\in D$ (respectively $z\in D_0$) if and only if $\lim_{\alpha\to 0}\liminf_{\delta\to 0}\mathcal{A}^{\alpha,\delta}(g_z^{\alpha,\delta})<\infty$ (respectively $\lim_{\alpha\to 0}\liminf_{\delta\to 0}\mathcal{A}_0^{\alpha,\delta}(g_{0,z}^{\alpha,\delta})<\infty$). The results are then straightforwardly deduced using Theorem 15. □

3.5 Numerical results

In order to fix the ideas, we shall limit ourselves to the two dimensional case and will introduce the algorithms for the discrete setting. We identify $\mathbb{S}^1$ with the interval $[0,2\pi[$. In order to collect the data of the inverse problem we solve numerically (3.1) for N incident fields $u^i(\frac{2\pi j}{\mathrm{N}},\cdot)$, $j\in\{0...\mathrm{N}-1\}$ using the surface integral equation forward solver available in [35]. The discrete version of F is then the matrix $F:=(u^\infty(\frac{2\pi j}{\mathrm{N}},\frac{2\pi k}{\mathrm{N}}))_{0\le j,k\le \mathrm{N}-1}$. We add some noise to the data to build a noisy far field matrix F^δ where $(F^\delta)_{j,k}=(F)_{j,k}(1+\sigma N_{ij})$ for $\sigma>0$ and N_{ij} an uniform complex random variable in $[-1,1]^2$. We similarly generate F_0^δ. In all our simulation we use a relative noise level of 1%. We denote by $\phi_z\in\mathbb{C}^{\mathrm{N}}$, the vector defined by $\phi_z(j)=exp(-ik(z_1\cos(\frac{2\pi j}{\mathrm{N}})+z_2\sin(\frac{2\pi j}{\mathrm{N}}))$ for $0\le j\le \mathrm{N}-1$.

The analysis of previous sections applied with $B^\delta=F_\sharp^\delta:=|\Re(F^\delta)|+|\Im(F^\delta)|$ suggests to consider

$$g_z^{\mathrm{GLSM}}:=\mathrm{argmin}_{g\in L^2(\mathbb{S}^1)}\left(\alpha\left\|(F_\sharp^\delta)^{\frac{1}{2}}g\right\|^2_{L^2(\mathbb{S}^1)}+\alpha^{1-\eta}\delta\left\|g\right\|^2_{L^2(\mathbb{S}^1)}+\left\|F^\delta g-\phi_z\right\|^2_{L^2(\mathbb{S}^1)}\right).$$

The minimizer is explicitly given by

$$g_z^{\mathrm{GLSM}}=(\alpha F_\sharp^\delta+\alpha^{1-\eta}\delta Id+F^{\delta *}F^\delta)^{-1}F^{\delta *}\phi_z.$$

We similarly construct $g_{0,z}^{\mathrm{GLSM}}$ using F_0^δ. In our numerical simulations we choose $\eta = 0$ (which corresponds to the one used in [5]) as we were not able to find an automatic way to choose its value and do not observe a significant influence of this parameter. We recall that the theory works for all $0 < \eta < 1$ and that the condition $\eta > 0$ is purely technical. The numerical simulations show that the reconstructions are not sensitive to this parameter. However the choice of α is important. Unfortunately, for the noisy case, we have no theory that relates the choice of α to the noise parameter δ. A heuristic choice is given by (3.34). Then (as in section 3.4) we introduce the following quantities

$$\mathcal{A}^{\mathrm{GLSM}}(z) = \left\| (F_\sharp^\delta)^{\frac{1}{2}} g_z^{\mathrm{GLSM}} \right\|^2 + \alpha^{-\eta}\delta \left\| g_z^{\mathrm{GLSM}} \right\|^2,$$

$$\mathcal{A}_0^{\mathrm{GLSM}}(z) = \left\| (F_{0,\sharp}^\delta)^{\frac{1}{2}} g_{0,z}^{\mathrm{GLSM}} \right\|^2 + \alpha^{-\eta}\delta \left\| g_{0,z}^{\mathrm{GLSM}} \right\|^2,$$

$$\mathcal{D}^{\mathrm{GLSM}}(z) = \left\| (F_\sharp^\delta)^{\frac{1}{2}} (g_z^{\mathrm{GLSM}} - g_{0,z}^{\mathrm{GLSM}}) \right\|^2 + \delta \left\| g_z^{\mathrm{GLSM}} - g_{0,z}^{\mathrm{GLSM}} \right\|^2$$

and construct the two indicator functions (see Corollary 3)

$$\mathcal{I}_{\mathrm{T}}^{\mathrm{GLSM}}(z) = \frac{1}{\sqrt{\mathcal{A}^{\mathrm{GLSM}}(z)(1 + \mathcal{A}^{\mathrm{GLSM}}(z)\mathcal{D}^{\mathrm{GLSM}}(z)^{-1})}}, \tag{3.32}$$

$$\mathcal{I}_{\mathrm{MB}}^{\mathrm{GLSM}}(z) = \frac{1}{\sqrt{\mathcal{A}_0^{\mathrm{GLSM}}(z) + \mathcal{A}^{\mathrm{GLSM}}(z)(1 + \mathcal{A}_0^{\mathrm{GLSM}}(z)\mathcal{D}^{\mathrm{GLSM}}(z)^{-1})}}. \tag{3.33}$$

Finally we will also look at the performance of the GLSM in reconstructing D and D_0 using respectively the following indicator functionals:

$$\mathcal{I}^{\mathrm{GLSM}}(z) = \frac{1}{\sqrt{\mathcal{A}^{\mathrm{GLSM}}(z)}}, \quad \mathcal{I}_0^{\mathrm{GLSM}}(z) = \frac{1}{\sqrt{\mathcal{A}_0^{\mathrm{GLSM}}(z)}}.$$

Similarly to [5] a heuristic choice of α in the GLSM algorithm that roughly keeps the same level of regularization as for the Tikhonov regularization would be

$$\alpha = \frac{\alpha_{\mathrm{LSM}}}{\left\| F_\sharp^\delta \right\| + \delta \alpha_{\mathrm{LSM}}^{-\eta}}, \tag{3.34}$$

where α_{LSM} is computed using the Morozov principle on the Tikhonov regularization. This is the choice we adopt in our numerical simulations. In the examples shown below, we consider a background medium made of several inclusions of constant index of refraction n_0. The targets Ω (represented with dashed lines) are inclusions of constant index of refraction n and their support can intersect the support of n_0. The scale on all the graphs is normalized by the wavelength.

We first consider an example where $D = D_0$, meaning that $\Omega \subset D_0$. Figure 3.4 shows that the numerical simulation exhibit the behavior demonstrated in Corollary 3, i.e. one is capable of selecting the component of D_0 that contains Ω.

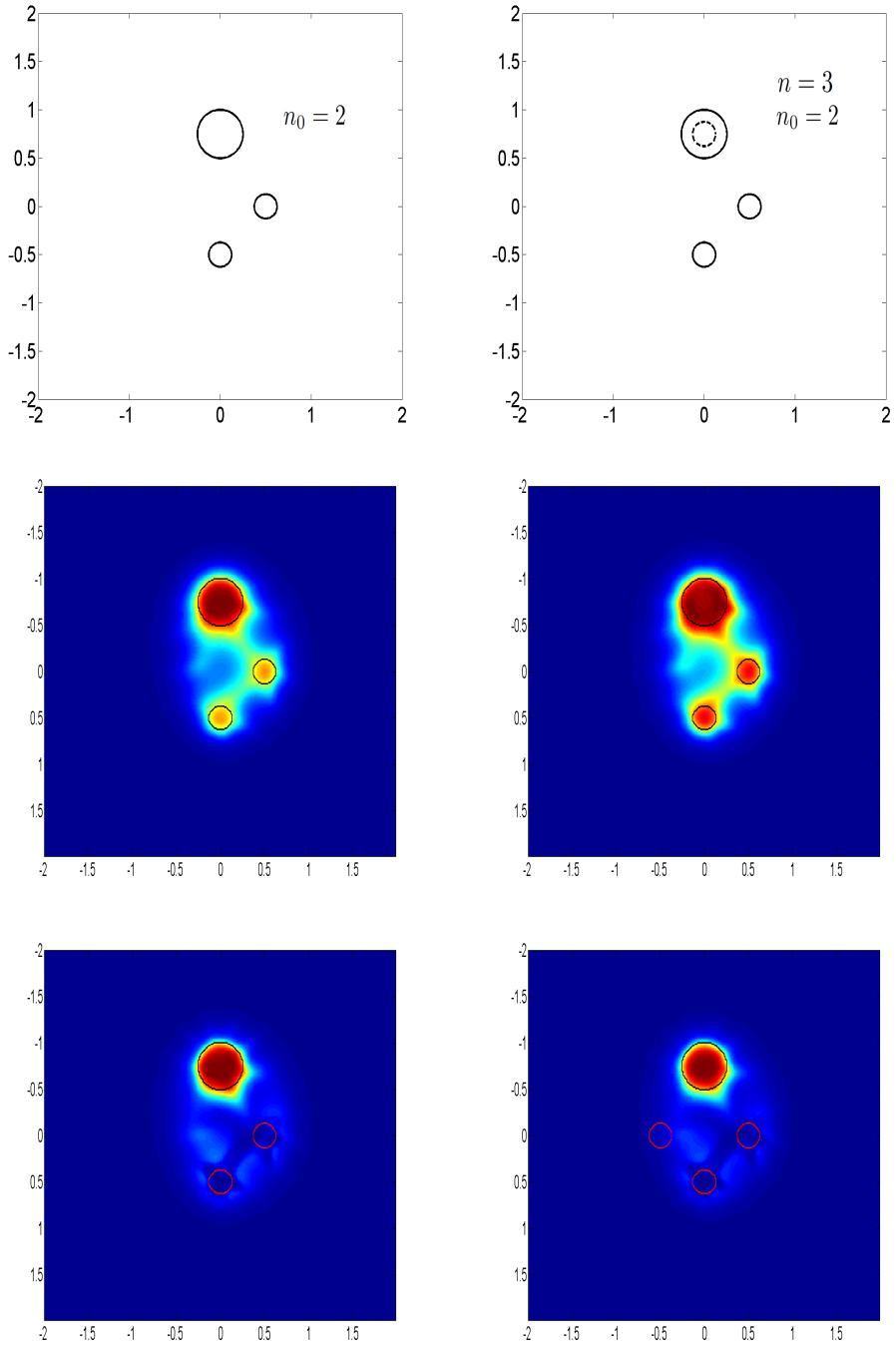

Figure 3.4: $(n_0, n) = (2, 3)$ from left to right and top to bottom : $\mathcal{I}_0^{\mathrm{GLSM}}$, $\mathcal{I}^{\mathrm{GLSM}}$, $\mathcal{I}_{\mathrm{T}}^{\mathrm{GLSM}}$ and $\mathcal{I}_{\mathrm{MB}}^{\mathrm{GLSM}}$

A more complicated case corresponds with $D \neq D_0$. In our examples, Ω is made in this case of two components: a first one included in D_0 and a second one that does not intersect with D_0.

Figure 3.5 shows that the result predicted by the theory is still valid.

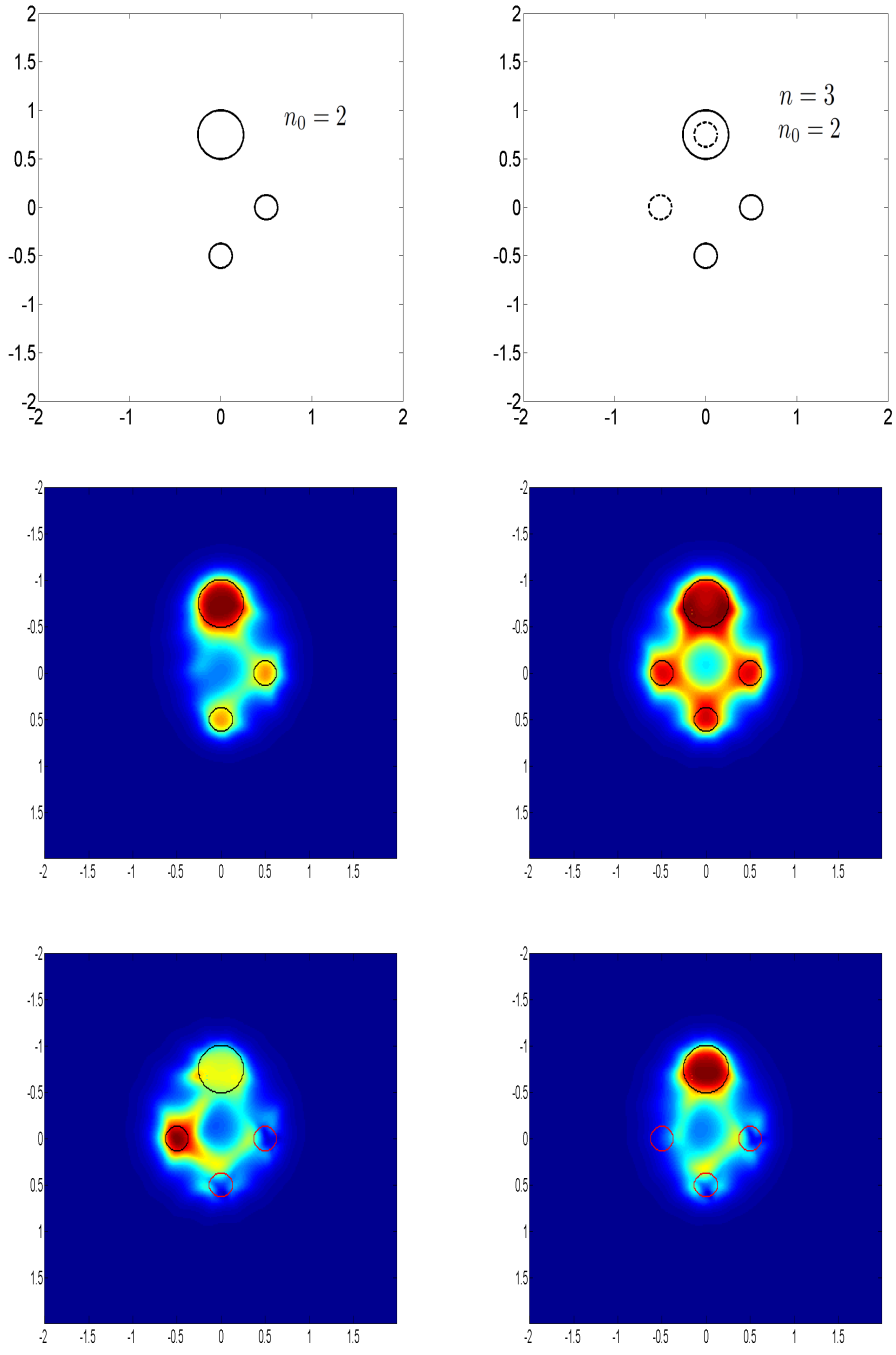

Figure 3.5: $(n_0, n) = (2, 3)$ from left to right and top to bottom : $\mathcal{I}_0^{\mathrm{GLSM}}$, $\mathcal{I}^{\mathrm{GLSM}}$, $\mathcal{I}_{\mathrm{T}}^{\mathrm{GLSM}}$ and $\mathcal{I}_{\mathrm{MB}}^{\mathrm{GLSM}}$

Our theory works also for absorbing background components (this case was excluded in the

study of known inhomogeneous background [33]). The results presented in figure 3.6 shows that we still obtain good reconstructions for this case that also exhibit a larger spacing between heterogeneities. Finally, let us mention that one would obtain similar numerical results if $g_{0,z}$ and g_z have been computed using the classical Tikhonov-Morozov regularization of the LSM equation ([5]) or (and) one uses $B^\delta = F^\delta$ instead of $B^\delta = F^\delta_\#$. However, this scheme is not covered by the theoretical part of this paper.

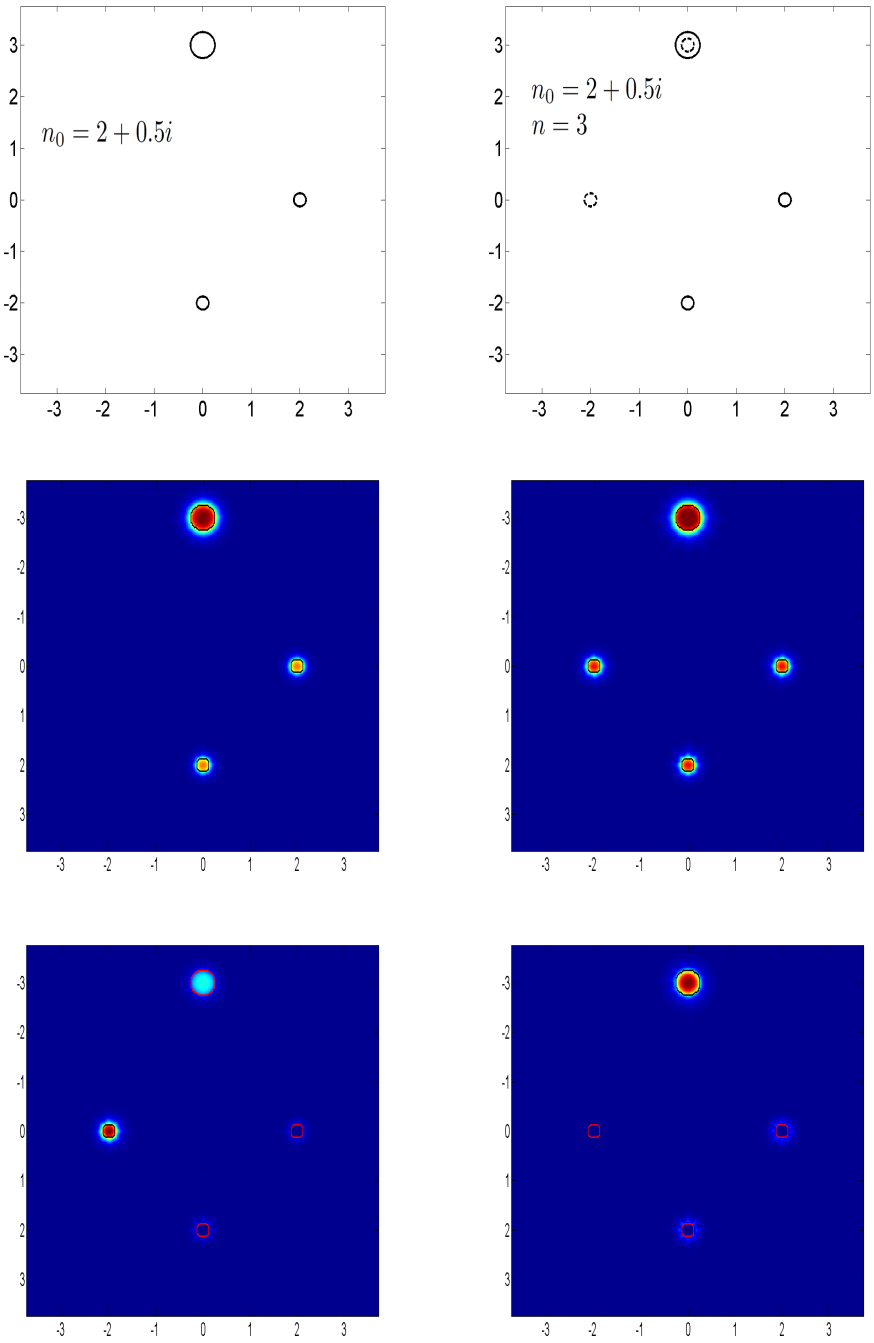

Figure 3.6: $(n_0, n) = (2 + 0.5i, 3)$ from left to right and top to bottom : $\mathcal{I}_0^{\mathrm{GLSM}}$, $\mathcal{I}^{\mathrm{GLSM}}$, $\mathcal{I}_{\mathrm{T}}^{\mathrm{GLSM}}$ and $\mathcal{I}_{\mathrm{MB}}^{\mathrm{LSM}}$

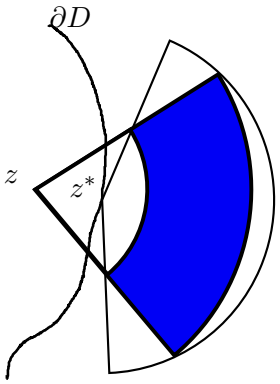

Figure 3.7: The area in blue is the area on which we do the integration.

3.6 Asymptotic behaviour of the indicator function inside D

In this section we would like to give an insight on what type of reconstruction one might expect from the GLSM. This result is far from a resolution analysis but it gives the asymptotic behaviour of our indicator function inside D, such an approach have been proposed in [3]. One might think of this result as the best indicator function that this technique may attain. First it shows that the GLSM framework cannot provide a step like image of the support of the obstacle in the sense that the imaging functional tends to infinity as z goes to the boundary of D from inside.

From previous section we know that using GLSM framework for z inside D we construct a sequence of Herglotz wave functions that strongly converge to the solution v_z of the interior transmission problem (3.16) with $(f, g) = (\Phi_z, \frac{\partial}{\partial \nu}\Phi_z)$.

The scattered field associated to v_z defined by $u_z^s = u_z - v_z$ can be extend outside D as $u_z^s = \Phi_z$ and it verifies the Lippman Schwinger equation:

$$u_z^s(x) = \int_D k^2(1-n)u_z(z)\Phi(x,z)dz$$

In [25][Theorem 8.2 p. 269] Colton and Kress give the boundness of the volume potential operator from $L^2(D)$ to $H^2(G)$ where G is a bounded domain, which implies

$$\|u_z^s\|_{H^2(G)} \leq C \underbrace{\left\|k^2(1-n)u_z\right\|_{L^2(D)}}_{=\|Tv_z\|_{L^2(D)}} \leq C\|T\|\|v_z\| \tag{3.35}$$

We should now specify G. Our first requirement would be to choose a domain which do not intersect D in order to exploit the fact that $u_z^s = \Phi_z$ outside D. Since Φ_z exhibits radial symmetry it would be easier to choose G as an angular portion of an annulus of center z. If we suppose D to be Lipschitz, there exist R and θ such that for all $z^* \in \partial D$ one can found a cone of radius R, summit z^* and angle 4θ such that this cone do not intersect D. We consider z such that $|z - z^*| = \varepsilon$. We thus extract the portion of cone depicted in figure 3.7, and call it C_z. It is a portion of the cone of center z, with half-angle $\theta^* = \arctan(\frac{R\sin(\theta/2)}{\delta + R\cos(\theta/2)})$ and radius between $R_1 = \frac{\delta\tan(\theta)R_2}{\tan(\theta)\cos(\theta) - \sin(\theta/2))R + \delta\tan(\theta)}$ and $R_2 = (\delta^2 + R^2 + 2\delta R\cos(\theta/2))^{\frac{1}{2}}$. We will be considering

the case when $z \to z^*$ which means ε goes to 0. First we see that $R_1 = O(\varepsilon)$, $R_1 = O(1)$ and $\theta = O(1)$. In order to apply (3.35) in C_z we first need to compute the H^2 norm of Φ_z and extract its leading term.

- In 2D $\Phi_z = \frac{i}{4}H_0^{(1)}(kr)$ where $r = |x - z|$, we have the asymptotic expansion $\Phi_z = \frac{1}{2\pi}ln(\frac{1}{r}) + \frac{i}{4} - \frac{1}{2\pi}\ln(\frac{k}{2}) - \frac{C}{2\pi} + O(r^2 ln(\frac{1}{r}))$ as r goes to 0 . We concentrate on the leading term

$$\int_{C_z \setminus D} |\Phi_z|^2 \approx \int_{C_z} \frac{1}{(2\pi)^2} ln(\frac{1}{r})^2 r dr d\theta$$
$$\approx \frac{2\theta^*}{4(2\pi)^2}(R_2^2(2\ln^2(R_2) - 2\ln(R_2) + 1) - R_1^2(2\ln^2(R_1) - 2\ln(R_1) + 1))$$

$$\int_{C_z} |\nabla \Phi_z|^2 \approx \int_{C_z} \frac{1}{(2\pi)^2 r} dr d\theta + O() = \frac{2\theta^*}{(2\pi)^2}(ln(R_2) - ln(R_1))$$

$$\int_{C_z} |\nabla^2 \Phi_z|^2 \approx \int_{C_z} \frac{1}{(2\pi)^2 r^3} dr d\theta + O() = \frac{2\theta^*}{(2\pi)^2}(\frac{1}{R_1^2} - \frac{1}{R_2^2})$$

- in 3D $\Phi_z = \frac{\exp(ikr)}{r}$ where $r = |x - z|$, the formulas below become

$$\int_{C_z} |\Phi_z|^2 = \int_{C_z} \frac{1}{r^2} r^2 sin(\theta) dr d\theta d\psi = (cos(\theta_1) - cos(\theta_2))\Delta\psi(R_2 - R_1)$$

$$\begin{aligned}\int_{C_z} |\nabla \Phi_z|^2 =& (cos(\theta_1) - cos(\theta_2))\Delta\psi \int_{C_z} |\frac{ike^{ikr}}{r} - \frac{e^{ikr}}{r^2}|^2 r^2 dr \\ =& (cos(\theta_1) - cos(\theta_2))\Delta\psi \int_{C_z} (\frac{1}{r^2} + k^2) dr \\ =& (cos(\theta_1) - cos(\theta_2))\Delta\psi(\frac{1}{R_1^2} - \frac{1}{R_2^2} + k^2 R_2 - k^2 R_1)\end{aligned}$$

$$\begin{aligned}\int_{C_z} |\nabla^2 \Phi_z|^2 =& (cos(\theta_1) - cos(\theta_2))\Delta\psi \int_{C_z} |\frac{-2ike^{ikr}}{r^2} + 2\frac{e^{ikr}}{r^3} - \frac{k^2 e^{ikr}}{r}|^2 r^2 dr \\ =& (cos(\theta_1) - cos(\theta_2))\Delta\psi \int_{C_z} (\frac{4}{r^4} + k^4) dr \\ =& (cos(\theta_1) - cos(\theta_2))\Delta\psi(\frac{4}{R_1^3} - \frac{4}{R_1^3} + k^4 R_2 - k^4 R_1)\end{aligned}$$

If we keep only the leading terms and apply those formula to (3.35) we obtain :

$$\frac{1}{\varepsilon^d} \leq C^2 \|T\|^2 \|v_z\|^2 \leq C^2 \frac{\|T\|^2}{\mu} |(Tv,\, v)| \tag{3.36}$$

where $d = 2$ or 3 is the dimension. Therefore we saw that our method will at best (when the regularization parameter α and the noise level δ go to zero) give an indicator function with a known behaviour near the boundary (unfortunately not step like).

Chapter 4

GLSM for non-symmetric factorization

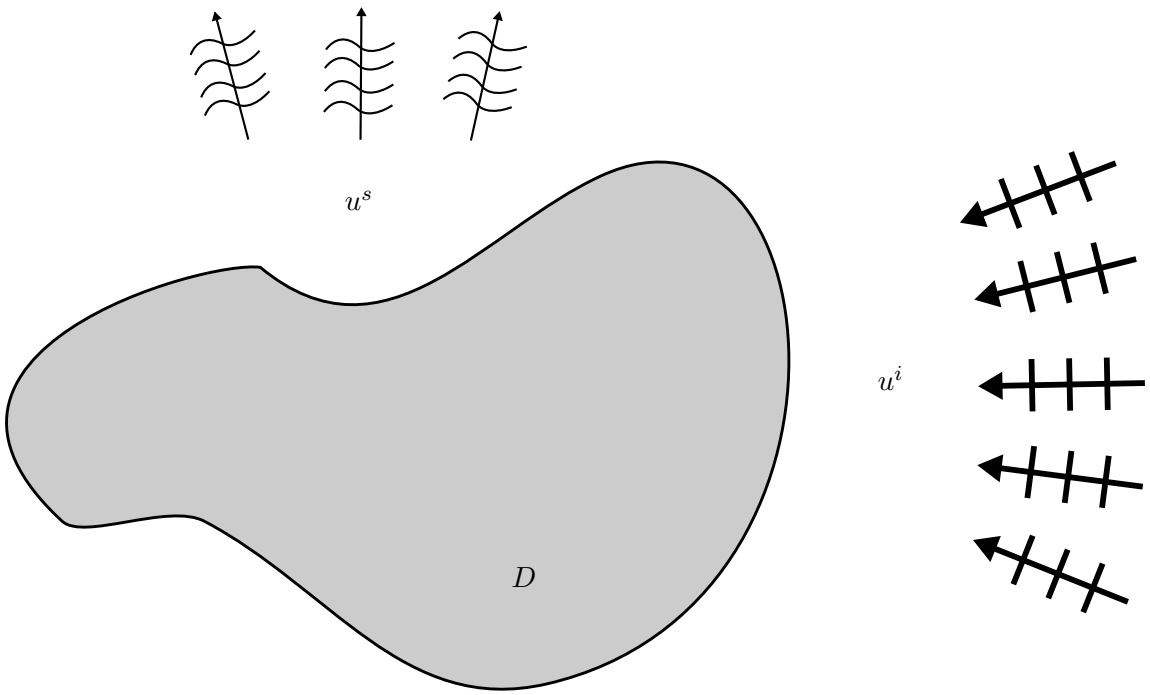

Contents

The analysis in chapters 2 and 3 extensively rely on the symmetric factorization of the farfield operator F in order to conclude on both the characterization of the domain shape and also on the strong convergence of Herglotz waves to the solutions of ITP. For the latter we even require a uniform convexity for the middle operator T. In this chapiter we will concentrate on extending the analysis to the cases of non symmetric factorizations of F such as the one that appears for limited aperture measurements, that we take as our model problem in section 4.1. Before adressing the case of non symmetric factorizations, we shall first propose in section 4.2.1 a new setting for the GLSM for which the strong convergence of Herglotz waves to the solutions of ITP is guaranteed without the assumption of uniform convexity. Our new framework is valid for the case $B = F$. In section 4.2.2 we extend the new setting of GLSM to non symmetric factorizations. In section 4.3 we give a new proof of the coercivity of the middle operator T under a much weaker assumption on the index of refraction n: we basically require that n does not change sign only in a neighborhood of the boundary of the inhomogeneity. We then discuss the model of nearfield measurement which is an other type of setting for the inverse problem where non symmetric factorizations occur. Finally we give some numerical results for limited aperture data and introduce a second order scheme to optimize the GLSM functional.

As mentioned in the general introduction, we tried to make each chapter selfcontained and therefore some repetitions for notation and setting are observed at the introductory sections (and sometimes in the proofs).

4.1 A model problem for limited aperture data

Similarly to previous chapters for a wave number $k > 0$, the total field solve the following scalar wave equation:

$$\Delta u + k^2 n u = 0 \text{ in } \mathbb{R}^d$$

with $d = 2$ or 3 and with $n \in L^\infty(\mathbb{R}^d)$ denoting the refractive index such that the support of $n - 1$ is included inside $\overline{D}$ with D a bounded domain with Lipschitz boundary and connected complement and such that $\Im(n) \geq 0$.

We are interested in the cases where the total field is generated by plane waves, $u^i(\theta, x) := e^{ikx\cdot\theta}$ with $x \in \mathbb{R}^d$ and $\theta \in \Gamma_s$ ($\Gamma_s \subset \mathbb{S}^{d-1}$ the unit sphere) and we denote by u^s the scattered field defined by

$$u^s(\theta, \cdot) = u - u^i(\theta, \cdot) \quad \text{in } \mathbb{R}^d,$$

which is assumed to be satisfying the Sommerfeld radiation condition,

$$\lim_{r\to\infty} \int_{|x|=r} \left| \frac{\partial u^s}{\partial r} - iku^s \right|^2 ds = 0.$$

Our data for the inverse problem will be formed by noisy measurements of the so called farfield pattern $u^\infty(\theta, \hat{x})$ defined by

$$u^s(\theta, x) = \frac{e^{ik|x|}}{|x|^{(d-1)/2}} (u^\infty(\theta, \hat{x}) + O(1/|x|))$$

as $|x| \to \infty$ for all $(\theta, \hat{x}) \in \Gamma_s \times \Gamma_m$, where Γ_m is a subset of $\mathbb{S}^{d-1}$ possibly different from Γ_s. The goal is to be able to reconstruct D from these measurements (without knowing n). We shall extend the results of chapters 2 and 3 to the case of farfield operators $F : L^2(\Gamma_s) \to L^2(\Gamma_m)$, defined by

$$Fg(\hat{x}) := \int_{\Gamma_s} u^\infty(\theta, \hat{x}) g(\theta) ds(\theta), \ \hat{x} \in \Gamma_m$$

where $\Gamma_s \neq \Gamma_m$. Let us define, for $\psi \in L^2(D)$, the unique function $w \in H^1_{\text{loc}}(\mathbb{R}^d)$ satisfying

$$\begin{cases} \Delta w + nk^2 w = -k^2(n-1)\psi \text{ in } \mathbb{R}^d, \\ \lim\limits_{r\to\infty} \int\limits_{|x|=r} \left| \frac{\partial w}{\partial r} - ikw \right|^2 ds = 0. \end{cases} \tag{4.1}$$

By linearity of the forward scattering problem, Fg is nothing but the farfield pattern of w solution of (4.1) with $\psi = v_g$ in D, where

$$v_g(x) := \int_{\Gamma_s} e^{ikx\cdot\theta} g(\theta) ds(\theta), \ g \in L^2(\Gamma_s), \ x \in \mathbb{R}^d.$$

Now consider the (compact) operator $H_s : L^2(\Gamma_s) \to L^2(D)$ defined by

$$H_s g := v_g|_D, \tag{4.2}$$

and the (compact) operator $G_m : \overline{\mathcal{R}(H_s)} \subset L^2(D) \to L^2(\Gamma_m)$ defined by

$$G_m \psi := w^\infty|_{\Gamma_m} \tag{4.3}$$

where w^∞ is the farfield of $w \in H^1_{\text{loc}}(\mathbb{R}^d)$ solution of (4.1) and where $\overline{\mathcal{R}(H_s)}$ denotes the closure of the range of H_s in $L^2(D)$. Then clearly

$$F = G_m H_s$$

One can still decompose F to get the second factorisation of the farfield operator. More precisely, for the case under consideration, since the farfield pattern of w has the following expression ([15])

$$w^\infty(\hat{x}) = -\int_D e^{-iky.\hat{x}} (1-n) k^2 (\psi(y) + w(y)) dy,$$

one simply has $G_m = H_m^* T\psi$, where $H_m^* : L^2(D) \to L^2(\Gamma_m)$ is the adjoint of H_m (defined as H_s but on Γ_m) given by

$$H_m^* \varphi(\hat{x}) := \int_D e^{-iky.\hat{x}} \varphi(y) dy, \ \varphi \in L^2(D), \ \hat{x} \in \Gamma_m,$$

and T: $L^2(D) \to L^2(D)$ is defined by

$$T\psi := -k^2(1-n)(\psi + w), \tag{4.4}$$

with $w \in H^1_{\text{loc}}(\mathbb{R}^d)$ being the solution of (4.1). Finally we get

$$F = H_m^* T H_s, \tag{4.5}$$

This factorization is not "symmetric" in the sense that $H_m^* \neq H_s^*$ in general. This is the main challenge in the case of limited aperture.

Remark 6. *First we should stress that T does not depend on the aperture. This middle operator does even not depend on the type of sources and measurements that are used (this will be briefly discussed in Section 4.4). Second, when $\Gamma_s = \Gamma_m$ we clearly have $H_m = H_s$ and then we end up with a setting similar to the full aperture case, $F = H_s^* T H_s$. The GLSM as formulated in chapter 2 then applies to this special case that correspond in physical experiments to sources and receivers on symmetric opposite sides of the target (as shown in figure 4.1).*

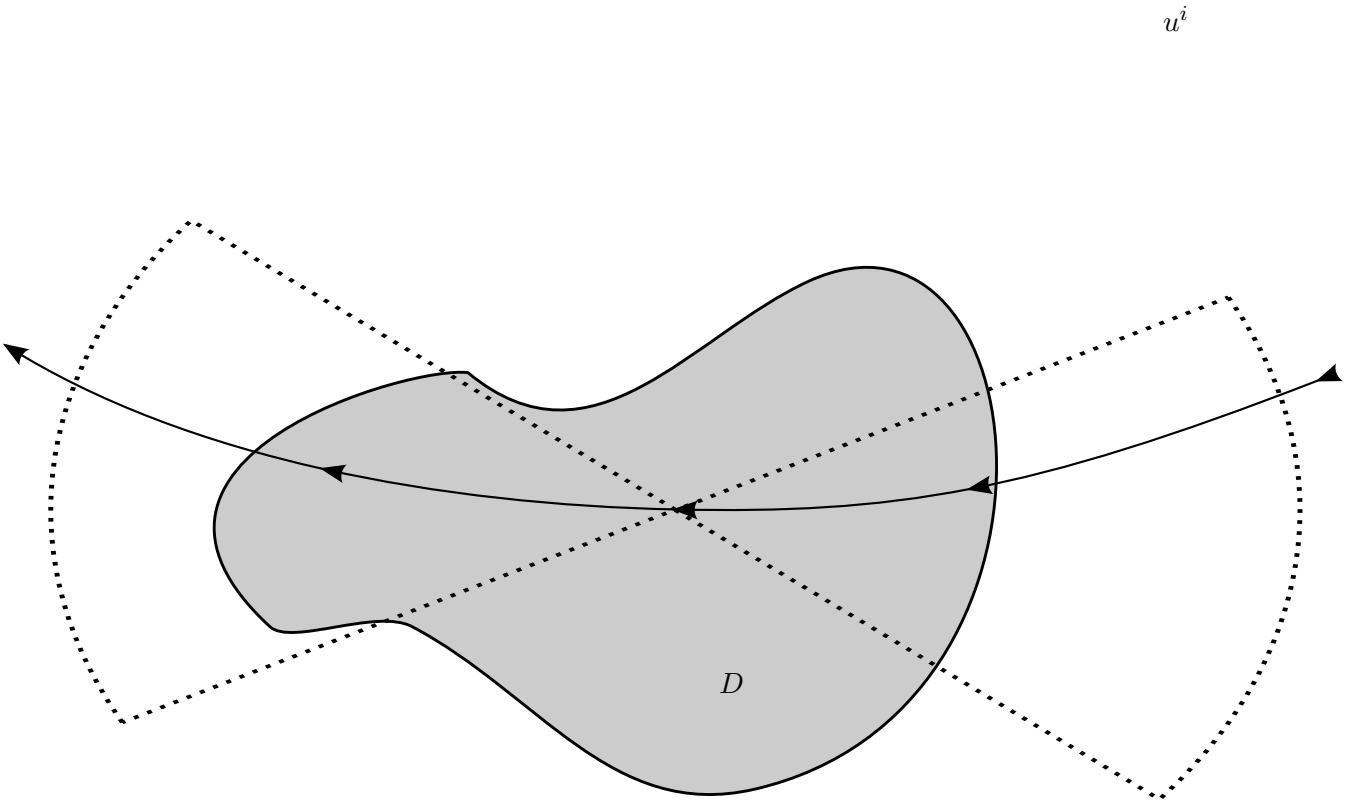

Figure 4.1: The arrow goes from the sources to the measurement. In this case the factorization is symmetric.

4.2 Theoretical foundation of the GLSM for limited aperture

In this section we shall give the theoretical foundation of the extension of the Generalized Linear Sampling Method to non symmetric factorizations. We will adopt an abstract framework as we want to use the results for other cases such as in Section 4.4 and in Section 6.4. In Section 4.1 we saw that the factorization of the farfield operator in the limited aperture problem lacks of symmetry. This symmetry is of primary importance in the GLSM framework of Chapter 2. It seems to us that it is not possible to restore this symmetry by carefully designing an operator B as it appears in the theory for GLSM. This approach has been adopted in the case of known heterogeneous background and near field data as in Section 4.4 (see also [33] and [19] for the case of the Factorization method). For a general setting we will only rely on the choice $B = F$ (i.e. $\Gamma_s = \Gamma_m$). We already saw that in this setting one cannot guarantee the strong

convergence of Herglotz waves to the solution of the interior transmission problem (when the sampling point is inside D). This is why we shall first modify the setting of GLSM so that one obtain this convergence result even in the case $B = F$ (the strong convergence result which is essential for Chapter 3). The idea is to add an extra (carefully chosen) penalty term that is inspired from difficulties encountered in establishing the overmentioned convergence result in the classical setting of GLSM.

4.2.1 A new formulation of the GLSM for symmetric factorizations

Analysis of the noiseless case

We denote as usual by X and Y two (complex) reflexive Banach spaces with duals X^* and Y^* respectively and shall denote by $(,\,)$ a duality product that refers to $(X^*,\,X)$ or $(Y^*,\,Y)$ duality. We consider the linear operator $F : X \to X^*$. Moreover we shall assume that the following factorization holds

$$F = H^*TH \tag{4.6}$$

where the operators $H : X \to Y$ and $T : Y \to Y^*$ are bounded. We denote by $G : \overline{\mathcal{R}(H)} \subset Y \to X^*$ the linear operator H^*T restricted to $\overline{\mathcal{R}(H)}$.

Let $\alpha > 0$ be a given parameter and $\phi \in X^*$.

The new GLSM (for noise free measurements) is based on considering minimizing sequences of the functional $J_\alpha(\phi;\cdot) : X \to \mathbb{R}$

$$J_\alpha(\phi; g) := \alpha|(Fg,\, g)| + \alpha^{1-\eta}|(Fg - \phi,\, g)| + \|Fg - \phi\|^2 \quad \forall g \in X, \tag{4.7}$$

where $\eta \in]0, 1]$ is a fixed parameter.

Following the lines of the proofs in Chapter 2 we first observe that

$$j_\alpha(\phi) := \inf_{g\in X} J_\alpha(\phi; g) \to 0 \text{ as } \alpha \to 0. \tag{4.8}$$

for all $\phi \in X^*$ if one assumes that F has dense range. In that case, for a given $\varepsilon > 0$ there exists g_ε such that $\|Fg_\varepsilon - \phi\| < \frac{\varepsilon}{2}$. Then one can choose $\alpha_0(\varepsilon)$ such for all $\alpha \le \alpha_0(\varepsilon)$, $\alpha|(Fg_\varepsilon,\, g_\varepsilon)| + \alpha^{1-\eta}|(Fg - \phi,\, g)| < \frac{\varepsilon}{2}$ so that $j_\alpha(\phi) < \varepsilon$, which proves (4.8).

One then can prove the following characterization of the range of G in terms of F (compare with Theorem 3 of Chapter 2).

Theorem 16. *We assume the following:*

- *H is compact, G is injective and $F = H^*TH$ is injective with dense range.*
- *T satisfies the coercivity property*

$$|(Th,\, h)| > \mu \|h\|^2 \quad \forall\, h \in \mathcal{R}(H), \tag{4.9}$$

where $\mu > 0$ is a constant independent of h. Consider for $\alpha > 0$ and $\phi \in X^*$, $g_\alpha \in X$ such that

$$J_\alpha(\phi; g_\alpha) \le j_\alpha(\phi) + p(\alpha) \tag{4.10}$$

where $\frac{p(\alpha)}{\alpha}$ is bounded with respect to α. Then

- $\phi \in \mathcal{R}(G)$ *implies* $\limsup_{\alpha\to 0} |(Fg_\alpha,\, g_\alpha)| < \infty$,
- $\phi \notin \mathcal{R}(G)$ *implies* $\liminf_{\alpha\to 0} |(Fg_\alpha,\, g_\alpha)| = \infty$.

In the case $\phi = G\varphi$, the sequence Hg_α converges strongly to φ in Y as α goes to zero.

Proof. Assume that $\phi \in \mathcal{R}(G)$ and let $\varphi \in \overline{\mathcal{R}(H)}$ such that $G\varphi = \phi$. For $\alpha > 0$ one can choose $\exists g_0 \in X$ such that $\|Hg_0 - \varphi\|^2 < \alpha^2$. Then by continuity of G, $\|Fg_0 - \phi\|^2 < \|G\|^2\alpha^2$. On the other hand the continuity of T implies

$$|(Fg_0,\, g_0)| = |(THg_0,\, Hg_0)| \le \|T\|\, \|Hg_0\|^2 < 2\,\|T\|\,(\alpha^2 + \|\varphi\|^2)$$

and

$$|(Fg_0 - \phi,\, g_0)| = |(T(Hg_0 - \varphi),\, Hg_0)| \le \|T\|\, \|Hg_0 - \varphi\|\, \|Hg_0\| < 2\,\|T\|\,\alpha(\alpha + \|\varphi\|).$$

From the definitions of $j_\alpha(\phi)$ and g_α we have

$$\alpha|(Fg_0,\, g_0)| + \alpha^{1-\eta}|(Fg_0 - \phi,\, g_0)| + \|Fg_0 - \phi\|^2 > j_\alpha(\phi) > J_\alpha(\phi, g_\alpha) - p(\alpha).$$

We then deduce from the definition of J_α the fact that $\eta \in]0, 1]$ and previous inequalities

$$\alpha|(Fg_\alpha,\, g_\alpha)| \le J_\alpha(\phi, g_\alpha) \le p(\alpha) + 2\alpha\,\|T\|\,(\alpha^2 + \|\varphi\|^2) + \alpha^2\|G\|^2 + 2\,\|T\|\,\alpha^{2-\eta}(\alpha + \|\varphi\|). \quad (4.11)$$

Therefore $\limsup_{\alpha\to 0} |(Fg_\alpha,\, g_\alpha)| < \infty$.

The coercivity of T implies that $\|Hg_\alpha\|^2$ is bounded. From (4.8) and (4.10) and the injectivity of G we infer that the only possible weak limit of (any subsequence of) Hg_α is φ. Thus the whole sequence Hg_α weakly converges to φ. On the other hand we have that :

$$\begin{aligned}\|Hg_\alpha - \varphi\|^2 &\le |(T(Hg_\alpha - \varphi),\, Hg_\alpha - \varphi)| \\ &\le |(T(Hg_\alpha - \varphi),\, Hg_\alpha)| + |(T(Hg_\alpha - \varphi),\, \varphi)| \\ &\le |(Fg_\alpha - \phi,\, g_\alpha)| + |(T(Hg_\alpha - \varphi),\, \varphi)|\end{aligned}$$

The last term goes to zero due to the weak convergence. The first term goes to zero since equation (4.11) implies that $|(Fg_\alpha - \phi,\, g_\alpha)| \le \alpha^\eta$. Therefore we conclude that Hg_α strongly converges to φ.

We now consider the case $\phi \notin \mathcal{R}(G)$. Assume that $\liminf_{\alpha\to 0} |(Fg_\alpha,\, g_\alpha)| < \infty$. Then, (for some extracted subsequence g_α) $|(Fg_\alpha,\, g_\alpha)| < A$ for some constant A independent of $\alpha \to 0$. The coercivity of T implies that $\|Hg_\alpha\|$ is also bounded and therefore one can assume that, up to an extracted subsequence, Hg_α weakly converges to some φ in Y. In fact $\varphi \in \overline{\mathcal{R}(H)}$ since the latter is a convex set. Since G is compact, we obtain that GHg_α strongly converges to $G\varphi$ as $\alpha \to 0$. On the other hand, (4.8) and the definition of $J_\alpha(\phi, g_\alpha)$ imply that $\|Fg_\alpha - \phi\| \le J_\alpha(\phi, g_\alpha) \le j_\alpha(\phi) + C\alpha \to 0$ as $\alpha \to 0$. Since $Fg_\alpha = GHg_\alpha$ we obtain that $G\varphi = \phi$ which is a contradiction. We then conclude that if $\phi \notin \mathcal{R}(G)$ then $\liminf_{\alpha\to 0} |(Fg_\alpha,\, g_\alpha)| = \infty$. The latter also implies $\limsup_{\alpha\to 0} |(Fg_\alpha,\, g_\alpha)| = \infty$. □

Remark 7. *The extension proposed in Theorem 16 requires indeed less assumptions than the one proposed in chapter 3. However the result from 3 is still interesting for practical applications (when applicable) since it uses a convex cost functional which is easier to minimize numerically.*

Analysis of the noisy case

Let $F^\delta : X \to X^*$ be the operator associated with noisy farfield measurements such that

$$\left\| F^\delta - F \right\| \leq \delta \|F\|$$

for some $\delta > 0$. We assume that the operators F^δ and F are compact.

Again let $\eta \in]0, 1]$ be a fixed parameter. We define for $\alpha > 0$ and $\phi \in X^*$ the regularized functional

$$J_\alpha^\delta(\phi; g) := \alpha |\big(F^\delta g,\, g\big)| + \alpha^{1-\eta} |\big(F^\delta g - \phi,\, g\big)| + \alpha^{1-\eta}\delta\|F\|\,\|g\|^2 + \left\| F^\delta g - \phi \right\|^2 \quad \forall\, g \in X. \tag{4.12}$$

As indicated in Chapter 2, this functional has a minimizer

$$g_\alpha^\delta = \arg\min_{g \in X} J_\alpha^\delta(\phi; g) \tag{4.13}$$

and we also have

$$\lim_{\alpha \to 0} \limsup_{\delta \to 0} J_\alpha^\delta(\phi; g_\alpha^\delta) = 0. \tag{4.14}$$

Theorem 17. *Assume that the first two assumptions of Theorem 16 hold true. Let g_α^δ be the minimizer of $J_\alpha^\delta(\phi; \cdot)$ (defined by (4.12)) for $\alpha > 0$, $\delta > 0$ and $\phi \in X^*$.*

Then

- *$\phi \in \mathcal{R}(G)$ implies $\limsup_{\alpha \to 0} \limsup_{\delta \to 0} \left(\left| \big(F^\delta g_\alpha^\delta,\, g_\alpha^\delta\big) \right| + \delta \alpha^{-\eta} \|F\| \left\| g_\alpha^\delta \right\|^2 \right) < \infty$.*
- *$\phi \notin \mathcal{R}(G)$ implies $\liminf_{\alpha \to 0} \liminf_{\delta \to 0} \left(\left| \big(F^\delta g_\alpha^\delta,\, g_\alpha^\delta\big) \right| + \delta \alpha^{-\eta} \|F\| \left\| g_\alpha^\delta \right\|^2 \right) = \infty$.*

Moreover, when $\phi \in \mathcal{R}(G)$ we also have

$$\limsup_{\alpha \to 0} \limsup_{\delta \to 0} \delta \|F^\delta\| \left\| g_\alpha^\delta \right\|^2 = 0.$$

If $G\varphi = \phi$, then there exists $\delta_0(\alpha)$ such that for all $\delta(\alpha) \leq \delta_0(\alpha)$, $Hg_\alpha^{\delta(\alpha)}$ converges strongly to φ as α goes to zero.

Proof. The proof follows the lines of the proof of Theorem 16.

Assume that $\phi = G(\varphi)$ for some $\varphi \in \overline{\mathcal{R}(H)}$. We consider g_0 (that depends on α but is independent from δ) such that $\|Hg_0 - \varphi\|^2 < \alpha^2$. Choosing δ sufficiently small such that

$$(\alpha\delta\|F\| + \alpha^{1-\eta}\delta\|F\| + \alpha^{1-\eta}\delta\|F\| + \delta^2\|F\|^2)\,\|g_0\|^2 \leq \alpha$$

we get

$$J_\alpha^\delta(\phi; g_\alpha^\delta) \leq J_\alpha^\delta(\phi; g_0) \leq J_\alpha(\phi; g_0) + \alpha. \tag{4.15}$$

Consequently

$$\alpha\left(|\left(F^\delta g_\alpha^\delta,\, g_\alpha^\delta\right)| + \alpha^{-\eta}\delta\|F^\delta\|\left\|g_\alpha^\delta\right\|^2\right) \leq J_\alpha^\delta(\phi; g_\alpha^\delta) \leq C\alpha,$$

which proves $\limsup_{\alpha\to 0}\limsup_{\delta\to 0}\left(\left|\left(F^\delta g_\alpha^\delta,\, g_\alpha^\delta\right)\right| + \alpha^{-\eta}\delta\|F^\delta\|\left\|g_\alpha^\delta\right\|^2\right) < \infty$. We also have, as a consequence of the inequalities above, that

$$\delta\|F\|\left\|g_\alpha^\delta\right\|^2 \leq C\alpha^\eta,$$

which proves $\limsup_{\alpha\to 0}\limsup_{\delta\to 0}\delta\|F^\delta\|\left\|g_\alpha^\delta\right\|^2 = 0$. We also have

$$|\left(F^\delta g_\alpha^\delta - \phi,\, g_\alpha^\delta\right)| \leq C\alpha^\eta$$

which proves, with the estimate on $\delta\|F\|\left\|g_\alpha^\delta\right\|^2$ given above above,

$$\limsup_{\alpha\to 0}\limsup_{\delta\to 0}|\left(Fg_\alpha^\delta - \phi,\, g_\alpha^\delta\right)| = 0.$$

We then conclude as in the proof of Theorem 16 that $Hg_\alpha^{\delta(\alpha)}$ converges strongly to φ as α goes to zero.

Now assume that $\phi \notin \mathcal{R}(G)$ and $\liminf_{\alpha\to 0}\liminf_{\delta\to 0}\left(\left|\left(F^\delta g_\alpha^\delta,\, g_\alpha^\delta\right)\right| + \alpha^{-\eta}\delta\|F\|\left\|g_\alpha^\delta\right\|^2\right)$ is finite. The coercivity of T and $\alpha < 1$ implies that

$$\mu\left\|Hg_{\alpha(\delta)}^\delta\right\|^2 \leq |\left(Fg_\alpha^\delta,\, g_\alpha^\delta\right)| \leq |\left(F^\delta g_\alpha^\delta,\, g_\alpha^\delta\right)| + \alpha^{-\eta}\delta\|F\|\left\|g_\alpha^\delta\right\|^2.$$

Therefore $\liminf_{\alpha\to 0}\liminf_{\delta\to 0}\left\|Hg_\alpha^\delta\right\|^2$ is also finite. This means the existence of a subsequence $(\alpha', \delta(\alpha'))$ such that $\alpha' \to 0$ and $\delta(\alpha') \to 0$ as $\alpha' \to 0$ and $\left\|Hg_{\alpha'}^{\delta(\alpha')}\right\|^2$ is bounded independently from α'. One can also choose $\delta(\alpha')$ such that $\delta(\alpha') \leq \alpha'^{1-\eta}$.

On the other hand Equation (4.14) indicates that one can choose this subsequence such that $J_{\alpha'}^{\delta(\alpha')}(g_{\alpha'}^{\delta(\alpha')}) \to 0$ as $\alpha' \to 0$ and therefore $\left\|F^\delta g_{\alpha'}^{\delta(\alpha')} - \phi\right\| \to 0$ as $\alpha' \to 0$ and $\alpha'^{1-\eta}\delta(\alpha')\|g_{\alpha'}^{\delta(\alpha')}\|^2 \to 0$ as $\alpha' \to 0$. By a triangular inequality and $\delta(\alpha') \leq \alpha'^{1-\eta}$ we then deduce that $\left\|Fg_{\alpha'}^{\delta(\alpha')} - \phi\right\| \to 0$ as $\alpha' \to 0$. The compactness of G implies that a subsequence of $GHg_{\alpha'}^{\delta(\alpha')}$ converges for some $G\varphi$ in X^*. The uniqueness of the limit implies that $G\varphi = \phi$ which is a contradiction.

□

4.2.2 A formulation for non symmetric factorizations

In this section we shall extend the theoretical foundations of the Generalized Linear Sampling Method to the case of non symmetric factorisation. In this case the general framework is given by the following assumptions. We shall denote by X_1, X_2 and Y three (complex) reflexive Banach spaces with duals X_1^*, X_2^* and Y^* respectively and shall denote by $(,)$ a duality product that refers to (X_1^*, X_1), (X_2^*, X_2) or (Y^*, Y) duality. We also set $X := X_1 \times X_2$. We consider

a linear operator $F : X_2 \to X_1^*$ that is assumed to be bounded. Moreover we shall assume that the following factorizations hold

$$F = U^*TV \tag{4.16}$$

where the operators $V : X_2 \to Y$, $T : Y \to Y^*$ and $U : X_1 \to Y$ are bounded. We set $G : \overline{\mathcal{R}_Y(V)} \subset Y \to X_1^*$ the restriction of U^*T to where $\overline{\mathcal{R}_Y(V)}$ where $\overline{\mathcal{R}_Y(V)}$ is the closure of the range of V in Y (and similar notation for U).

Moreover we assume the existence of a space $\hat{Y}$ such that U and V can be extended to bounded operators $V : X_2 \to \hat{Y}$ and $U : X_1 \to \hat{Y}$ such that

$$\|Vg_2 + Ug_1\|_Y \leq \|Vg_2 + Ug_1\|_{\hat{Y}}, \quad \forall (g_1, g_2) \in X. \tag{4.17}$$

We finally assume that

$$\overline{\mathcal{R}_Y(V)} = \overline{\mathcal{R}_Y(U)} \quad \text{and} \quad \overline{\mathcal{R}_{\hat{Y}}(V)} = \overline{\mathcal{R}_{\hat{Y}}(U)}. \tag{4.18}$$

Typically one has $X_2 = L^2(\Gamma_s)$, $X_1 = L^2(\Gamma_m)$, $Y = L^2(D)$, $\hat{Y} = L^2(\Sigma)$ with $D \subset \Sigma$ (or L^2 replaced with other Sobolev spaces). For the purpose of the inverse problem of determining D, the domain Σ is assumed to be known and therefore the operators $V : X_2 \to \hat{Y}$ and $U : X_1 \to \hat{Y}$ are also known a priori.

Analysis of the noiseless case

Let $\alpha > 0$ be a given parameter and $\phi \in X_1^*$. We redefine the functional J_α as $J_\alpha(\phi; \cdot) : X = X_1 \times X_2 \to \mathbb{R}$

$$J_\alpha(\phi; g) := \alpha |(Fg_2,\, g_1)| + \alpha^{1-\eta} \|Vg_2 - Ug_1\|_{\hat{Y}}^2 + \alpha^{1-\eta} |(Fg_2 - \phi,\, g_1)| + \|Fg_2 - \phi\|^2 \tag{4.19}$$

for all $g = (g_1, g_2) \in X$ where $\eta \in]0, 1[$ is again a fixed parameter. We also define

$$j_\alpha(\phi) := \inf_{g \in X} J_\alpha(\phi; g). \tag{4.20}$$

Then again the first simple observation is the following.

Lemma 5. *Assume that F has dense range. Then for all $\phi \in X_1^*$, $j_\alpha(\phi) \to 0$ as $\alpha \to 0$.*

Proof. Since F has dense range, for a given $\varepsilon > 0$ there exists g_2^ε such that

$$\|Fg_2^\varepsilon - \phi\| \leq \varepsilon/3. \tag{4.21}$$

Using (4.18) and (4.17) we can choose g_1^ε such that:

$$\|Vg_2^\varepsilon - Ug_1^\varepsilon\|_Y^2 < \|Vg_2^\varepsilon - Ug_1^\varepsilon\|_{\hat{Y}}^2 < \varepsilon/3 \tag{4.22}$$

One then can choose α small enough such that

$$\alpha |(Fg_2^\varepsilon,\, g_1^\varepsilon)| + \alpha^{1-\eta} |(Fg_2^\varepsilon - \phi,\, g_1^\varepsilon)| \leq \varepsilon/3. \tag{4.23}$$

Together with equations (4.23) and (4.22) the latter inequality implies

$$j_\alpha(\phi) \leq J_\alpha(g^\varepsilon, \phi) \leq \varepsilon$$

for sufficiently small α where $g^\varepsilon = (g_1^\varepsilon, g_2^\varepsilon)$. □

The central theorem for non symmetric factorizations of F is the following characterization of the range of G in terms of F and U and V as operators with values in $\hat{Y}$.

Theorem 18. *We assume that*

- $G : \overline{\mathcal{R}_Y(V)} \subset Y \to X_1^*$ *is injective and that* F *has dense range.*
- T *satisfies the coercivity property*

$$|(T\varphi,\, \varphi)| > \mu \|\varphi\|^2 \quad \forall\, \varphi \in \overline{\mathcal{R}(U)} = \overline{\mathcal{R}(V)}, \tag{4.24}$$

where $\mu > 0$ *is a constant independent of* φ*. Let* $p(\alpha)$ *be a given function such that* $\frac{p(\alpha)}{\alpha} = O(1)$ *and consider for* $\alpha > 0$ *and* $\phi \in X_1^*$, $g^\alpha = (g_1^\alpha, g_2^\alpha) \in X$ *such that*

$$J_\alpha(\phi; g^\alpha) \leq j_\alpha(\phi) + p(\alpha). \tag{4.25}$$

Then $\phi \in \mathcal{R}(G)$ *implies* $\limsup_{\alpha\to 0} |(Fg_2^\alpha,\, g_1^\alpha)_1| + \alpha^{-\eta} \|Vg_2^\alpha - Ug_1^\alpha\|_{\hat{Y}}^2 < \infty$ *and* $\phi \notin \mathcal{R}(G)$ *implies* $\liminf_{\alpha\to 0} |(Fg_2^\alpha,\, g_1^\alpha)_1| + \alpha^{-\eta} \|Vg_2^\alpha - Ug_1^\alpha\|_{\hat{Y}}^2 = \infty$*. In the case* $\phi = G\varphi$*, the two sequences* Vg_2^α *and* Ug_1^α *converge strongly to* φ *in* Y*.*

Proof. The proof follows again roughly the same steps and ideas as the proof of similar results for the case of symmetric factorizations. We start with the case $\phi \in \mathcal{R}(G)$. We consider $\varphi \in \overline{\mathcal{R}_Y(V)}$ such that $G\varphi = \phi$ and $h_2^\alpha \in X_2$ such that $\|Vh_2^\alpha - \varphi\|_Y^2 \leq \alpha^2$. According to (4.18) and (4.17), there exists $h_1^\alpha \in X_1$ such that:

$$\|Vh_2^\alpha - Uh_1^\alpha\|_Y^2 < \|Vh_2^\alpha - Uh_1^\alpha\|_{\hat{Y}}^2 < \alpha^\eta. \tag{4.26}$$

We also have

$$\begin{aligned} |(Fh_2^\alpha,\, h_1^\alpha)_1| =& |(TVh_2^\alpha,\, Uh_1^\alpha)| \\ \leq& |(TVh_2^\alpha,\, Vh_2^\alpha)| + |(TVh_2^\alpha,\, Uh_1^\alpha - Vh_2^\alpha)| \\ \leq& \|T\| \|Vh_2^\alpha\|_Y^2 + \|T\| \|Vh_2^\alpha\|_Y \sqrt{\alpha^\eta} \end{aligned} \tag{4.27}$$

and

$$|(Fh_2^\alpha - \phi,\, h_1^\alpha)| = |(T(Vh_2^\alpha - \varphi),\, Uh_1^\alpha)| \leq \|T\| \|Vh_2^\alpha - \varphi\| \|Uh_1^\alpha\| < 2\|T\| \alpha(\alpha + \|\varphi\| + \sqrt{\alpha^\eta}).$$

The two previous inequalities and the definitions g^α and $j_\alpha(\phi)$ lead to

$$\alpha(|(Fg_2^\alpha,\, g_1^\alpha)_1| + \alpha^{-\eta} \|Vg_2^\alpha - Ug_1^\alpha\|_{\hat{Y}}^2 + \alpha^{-\eta}|(Fh_2^\alpha - \phi,\, h_1^\alpha)|) \leq j_\alpha(\phi) + p(\alpha) \leq C\alpha,$$

where C is bounded independently of α. This implies the first part of the Theorem. We also have

$$\|Vg_2^\alpha - Ug_1^\alpha\|_{\hat{Y}}^2 \leq C\alpha^\eta \tag{4.28}$$

and

$$|(Fg_2^\alpha - \phi,\, g_1^\alpha)| \leq C\alpha^\eta. \tag{4.29}$$

We shall prove now the convergence of Vg_2^α to φ when $\phi = G\varphi$ for $\varphi \in Y$. The coercivity of T implies

$$\mu \|Vg_2^\alpha\|_Y^2 \leq |(TVg_2^\alpha,\, Vg_2^\alpha)| \leq |(TVg_2^\alpha,\, Vg_2^\alpha) + (TVg_2^\alpha,\, Ug_1^\alpha - Vg_2^\alpha)| + |(TVg_2^\alpha,\, Ug_1^\alpha - Vg_2^\alpha)|$$

On the one hand

$$|(TVg_2^\alpha,\, Vg_2^\alpha) + (TVg_2^\alpha,\, Ug_1^\alpha - Vg_2^\alpha)| = |(Fg_2^\alpha,\, g_1^\alpha)_1| \leq C$$

and on the other hand

$$|(TVg_2^\alpha,\, Ug_1^\alpha - Vg_2^\alpha)| \leq \|T\|\, \|Vg_2^\alpha\|_Y\, \|Vg_2^\alpha - Ug_1^\alpha\|_{\hat{Y}} \leq \|T\|\, C\alpha^\eta\, \|Vg_2^\alpha\|_Y$$

These inequalities show that $\|Vg_2^\alpha\|_Y$ is bounded. Second, from Lemma 5 and (4.25) and the injectivity of G we infer that the only possible weak limit of (any subsequence of) Vg_2^α in Y is φ. Thus the whole sequence Vg_2^α weakly converges to φ in Y. Following the idea of proof of Theorem 16 we use the formula:

$$|(T(Vg_2^\alpha - \varphi),\, Vg_2^\alpha - \varphi)| \leq |(T(Vg_2^\alpha - \varphi),\, \varphi)| + \underbrace{|(T(Vg_2^\alpha - \varphi),\, Vg_2^\alpha - Ug_1^\alpha)|}_{\geq \|T\|(\|Vg_2^\alpha\| + \|\varphi\|)\|Vg_2^\alpha - Ug_1^\alpha\|_Y} + |(Fg_2^\alpha - \phi,\, g_1^\alpha)|$$

The first term on the right hand side goes to zero thanks to the the weak convergence, the second terms goes to zero thanks to (4.28) and the third term goes to zero thanks to (4.29). The coercivity of T implies that Vg_2^α converges strongly to φ in Y. The strong convergence of Ug_1^α to φ in Y is a direct consequence of (4.28).

We now consider the case $\phi \notin \mathcal{R}(G)$ and assume that $\liminf_{\alpha\to 0} |(Fg_2^\alpha,\, g_1^\alpha)_1| + \alpha^{-\eta}\, \|Vg_2^\alpha - Ug_1^\alpha\|_{\hat{Y}}^2 < \infty$. Then, (for some extracted subsequence g^α) $|(Fg_2^\alpha,\, g_1^\alpha)_1| + \alpha^{-\eta}\, \|Vg_2^\alpha - Ug_1^\alpha\|_{\hat{Y}}^2 \leq A$ for some A independent of α as α goes to 0. Using the same reasoning as in the first part of the theorem this implies that $\|Vg_2^\alpha\|_Y$ is bounded. We then obtain a contradiction exactly in the same way as in the proof of the second part of Theorem 16.

□

Analysis of the case with noise

We now consider the case of noisy data and/or non exact models. The noise in the data is modeled with an operator F^δ such that

$$\left\|F^\delta - F\right\| \leq \delta\, \|F\|$$

for some $\delta > 0$. We can also assume error in the "model" by considering perturbed operators U^δ, V^δ and right hand sides ϕ^δ such that

$$\left\|U^\delta - U\right\| \leq \delta\, \|U\|\,, \quad \left\|V^\delta - V\right\| \leq \delta\, \|V\| \quad \text{and} \quad \left\|\phi^\delta - \phi\right\| \leq \delta\, \|\phi\|\,.$$

We introduce the counterpart of (4.19) in the noisy case (for a constant $\eta \in]0,\ 1[$) :

$$\begin{aligned} J_\alpha^\delta(\phi; g) := \alpha|\left(F^\delta g_2,\, g_1\right)_1| + \delta\alpha^{1-\eta}\, \|F\|\, (\|g_1\|_{X_1}^2 + \|g_2\|_{X_2}^2) + \alpha^{1-\eta}|\left(F^\delta g_2 - \phi,\, g_1\right)_1| \\ + \alpha^{1-\eta} \left\|V^\delta g_2 - U^\delta g_1\right\|_{\hat{Y}}^2 + \left\|F^\delta g_2 - \phi^\delta\right\|_{X_1^*}^2 \quad \forall g = (g_1, g_2) \in X. \end{aligned} \tag{4.30}$$

One can first remark that

$$J_\alpha^\delta(\phi; g) \leq J_\alpha(\phi; g) + n(\delta, \alpha, g), \tag{4.31}$$

where

$$\begin{aligned} n(\delta,\alpha,g) =& \delta(\alpha+\alpha^{1-\eta})\,\|F\|\,(\|g_1\|_{X_1}^2+\|g_2\|_{X_2}^2)+\delta^2(\|F\|\,\|g_2\|_{X_2}^2 \\ &+\alpha^{1-\eta}(\|U\|^2\,\|g_1\|_{X_1}^2+\|V\|^2\,\|g_2\|_{X_2}^2)+\|\phi\|^2). \end{aligned} \tag{4.32}$$

Lemma 6. *For all $\alpha,\delta>0$ the functional $J_\alpha^\delta(\phi;\cdot)$ has a minimizer $g^{\alpha,\delta}$. In addition we have that:*

$$\lim_{\alpha\to 0}\lim_{\delta\to 0} J_\alpha^\delta(\phi,g^{\alpha,\delta}) = \lim_{\delta\to 0}\limsup_{\alpha\to 0} J_\alpha^\delta(\phi,g^{\alpha,\delta}) = 0.$$

Proof. The existence of a minimizer is clear: for a fixed $\alpha>0$, $\delta>0$ and ϕ, any minimizing sequence g^n of $J_\alpha^\delta(\phi;\cdot)$ is bounded and therefore there exists a weakly convergent subsequence to some $g^{\alpha,\delta}$. The lower semi-continuity of the norm with respect to the weak convergence and the compactness property of the operators then imply:

$$J_\alpha^\delta(\phi,g^{\alpha,\delta}) \le \liminf_{n\to+\infty} J_\alpha^\delta(\phi,g^n) \le \inf_g J_\alpha^\delta(\phi,g)$$

which proves that $g^{\alpha,\delta}$ is a minimizer of $J_\alpha^\delta(\phi;\cdot)$. Equation (4.31) together with a choice of δ such that, for any $\varepsilon>0$:

$$n(\delta,\alpha,g^\varepsilon)\le\varepsilon$$

where g^ε is the same as introduced in the proof of Lemma 6, we finally get that:

$$J_\alpha^\delta(\phi,g^{\alpha,\delta})\le 2\varepsilon.$$

□

We can then state the theorem that characterise the range of G in the case of noisy data (as the noise goes to 0).

Theorem 19. *Let $g^{\alpha,\delta}$ be the minimizer of $J_\alpha^\delta(\cdot,\phi)$ (defined by (4.30)), we denote*

$$R(g^{\alpha,\delta},\alpha,\delta) = |\left(F^\delta g_2^{\alpha,\delta},\, g_1^{\alpha,\delta}\right)_1| + \delta\alpha^{-\eta}\,\|F\|\,(\left\|g_1^{\alpha,\delta}\right\|_{X_1}^2+\left\|g_2^{\alpha,\delta}\right\|_{X_2}^2)+\alpha^{-\eta}\left\|V^\delta g_2-U^\delta g_1\right\|_{\hat{Y}}^2$$

then

- $\phi\in\mathcal{R}(G)$ *implies* $\limsup_{\alpha\to 0}\limsup_{\delta\to 0} R(g^{\alpha,\delta},\alpha,\delta)<\infty$
- $\phi\notin\mathcal{R}(G)$ *implies* $\liminf_{\alpha\to 0}\liminf_{\delta\to 0} R(g^{\alpha,\delta},\alpha,\delta)=\infty$

  Moreover, when $\phi\in\mathcal{R}(G)$, we also have

$$\limsup_{\alpha\to 0}\limsup_{\delta\to 0}\delta\|F\|(\left\|g_1^{\alpha,\delta}\right\|_{X_1}^2+\left\|g_2^{\alpha,\delta}\right\|_{X_2}^2)=0. \tag{4.33}$$

  If $G\varphi=\phi$, then there exists $\delta_0(\alpha)$ such that for all $\delta(\alpha)\le\delta_0(\alpha)$, $Vg_2^{\alpha,\delta(\alpha)}$ and $Ug_1^{\alpha,\delta(\alpha)}$ converge strongly to φ as α goes to zero.

Proof. The case $\phi \in \mathcal{R}(G)$: We consider the same h^α as in the first part of the proof of Theorem 18 (that only depends on α). If we choose $\delta(\alpha)$ such that :

$$n(\delta(\alpha), \alpha, h^\alpha) \leq \alpha$$

then we get

$$J_\alpha^\delta(g^{\alpha,\delta}, \phi) \leq C\alpha + \alpha.$$

Consequently we have

$$R(g^{\alpha,\delta}, \alpha, \delta) \leq C$$

which proves the first assertion of the theorem. We also have, as a consequence of the inequalities above, that

$$\delta \|F\| (\left\|g_1^{\alpha,\delta}\right\|_{X_1}^2 + \left\|g_2^{\alpha,\delta}\right\|_{X_2}^2) \leq C\alpha^\eta$$

which proves $\limsup_{\alpha\to 0} \limsup_{\delta\to 0} \delta \|F\| (\left\|g_1^{\alpha,\delta}\right\|_{X_1}^2 + \left\|g_2^{\alpha,\delta}\right\|_{X_2}^2) = 0$. For the same reason if $\eta > 0$ we have $\limsup_{\alpha\to 0} \limsup_{\delta\to 0} \left\|V^\delta g_2 - U^\delta g_1\right\|_{\hat{Y}}^2 = 0$.

Now assume that the last assumptions of Theorem 18 hold true. We recall that

$$J_\alpha^\delta(\phi; g) \leq J_\alpha(\phi, g) + n(\delta, \alpha, g).$$

If we use the sequence h^α from Theorem 18, and choose $\delta_0(\alpha)$ small enough such that, $\limsup_{\alpha\to 0} n(\delta_0(\alpha), \alpha, h^\alpha) = 0$.

Then, from the convergence properties of the sequences $Vg_2^{\alpha,\delta}$ and $Ug_1^{\alpha,\delta}$, we clearly obtain for $\delta(\alpha) \leq \delta_0(\alpha)$ that the quantity $\left(TVg_2^{\alpha,\delta}, Vg_2^{\alpha,\delta}\right)$ is bounded. To conclude as in the proof of Theorem 18 that $Vg_2^{\alpha,\delta}$ and $Ug_1^{\alpha,\delta}$ converges strongly to φ as α goes to zero we just need to remark that

$$\|Vg_2 - Ug_1\|_{\hat{Y}}^2 \leq \left\|V^\delta g_2 - U^\delta g_1\right\|_{\hat{Y}}^2 + \delta^2 \|U\| \|g_1\|_{X_1}^2 + \delta^2 \|V\| \|g_2\|_{X_2}^2 \to 0$$

and

$$|(Fg_2 - \phi,\, g_1)_1| \leq |\left(F^\delta g_2 - \phi,\, g_1\right)_1| + \delta \|F\| (\|g_1\|_{X_1}^2 + \|g_2\|_{X_2}^2) \to 0.$$

The case $\phi \notin \mathcal{R}(G)$: Assume that $\liminf_{\alpha\to 0} \liminf_{\delta\to 0} R(g^{\alpha,\delta}, \alpha, \delta)$ is finite. We then have :

$$\begin{aligned} |\left(Fg_2^{\alpha,\delta}, g_1^{\alpha,\delta}\right)_1| &\leq |\left(F^\delta g_2^{\alpha,\delta}, g_1^{\alpha,\delta}\right)_1| + \delta \|F\| \left\|g_1^{\alpha,\delta}\right\|_{X_1} \left\|g_2^{\alpha,\delta}\right\|_{X_2} \\ &\leq |\left(F^\delta g_2^{\alpha,\delta}, g_1^{\alpha,\delta}\right)_1| + \frac{\delta}{2} \|F\| \left\|g_1^{\alpha,\delta}\right\|_{X_1}^2 + \frac{\delta}{2} \|F\| \left\|g_2^{\alpha,\delta}\right\|_{X_2}^2. \end{aligned} \tag{4.34}$$

The assumption also implies that $\left\|Vg_2^{\alpha,\delta} - Ug_1^{\alpha,\delta}\right\|_{\hat{Y}}^2$ staya bounded, meaning that, similarly to the second part of the proof of Theorem 18, that $\left\|Vg_2^{\alpha,\delta}\right\|_Y^2$ stays bounded. This leads to the same contradiction as in the case of noise free measurements. □

4.3 Application to inverse scattering

The purpose of this section is to apply the result of section 4.2 to the case described in section 4.1. This will be possible if $D \subset \Sigma$ where Σ is some bounded known domain. We then define $\hat{Y}$ from section 4.2 to be $L^2(\Sigma)$ and set $V = H_s$ and $U = H_m$. We shall also revisit Theorem 6 and significanlty weaken the required conditions on the coercivity of T, which turned out to finally be the same as the one under which the interior transmission problem is well posed [52].

4.3.1 Preliminary results

As in Chapter 2 the basis of the GLSM is the characterization of the obstacle D in term of the range of G_m. This characterization is based on the solvability of the following interior transmission problem for $u, v \in L^2(D)$ such that $u - v \in H^2(D)$,

$$\begin{cases} \Delta u + k^2 n u = 0 & \text{in } D, \\ \Delta v + k^2 v = 0 & \text{in } D, \\ (u - v) = f & \text{on } \partial D, \\ \frac{\partial}{\partial \nu}(u - v) = g & \text{on } \partial D, \end{cases} \tag{4.35}$$

for a given $f \in H^{\frac{1}{2}}(\partial D)$ and $g \in H^{-\frac{1}{2}}(\partial D)$. Similarly to Chapter 2 we should make the following assumption

Hypothesis 5. *We assume that $k^2 \in \mathbb{R}_+$ is such that for all $f \in H^{\frac{1}{2}}(\partial D)$ and $g \in H^{-\frac{1}{2}}(\partial D)$ problem (4.35) has a unique solution in $(u, v) \in L^2(D) \times L^2(D)$ and $u - v \in H^2(D)$.*

We recall that it is known that if $n-1$ positive definite or negative definite in a neighborhood of ∂D, Hypothesis 5 is verified for all $k \in \mathbb{R}$ except a countable set without finite accumulation point.
Defining

$$\phi_z(\hat{x}) := e^{-ik\hat{x}\cdot z} \ for \ \hat{x} \in \Gamma_m$$

we have:

Theorem 20. *Under Hypothesis 5, $\phi_z \in \mathcal{R}(G_m)$ (for G_m defined in (4.3)) if and only if $z \in D$.*

The proof of this theorem is rather straightforward using the result of Lemma 7 (see [40]) and the fact that ϕ_z is the farfield of $\Phi(\cdot, z)$, the fundamental solution of the Helmholtz equation satisfying the Sommerfeld radiation condition.

Lemma 7. $\overline{\mathcal{R}(H_s)} = \{v \in L^2(D) \ s.t. \ \Delta v + k^2 v = 0 \ in \ D\}$

In order to apply the theory developped in Section 4.2 it remains to prove that T is coercive which will be done in the following under weaker assumptions than in Theorem 6. Let $C > 0$ be a given constant (independent of α) and consider $\alpha > 0$ and $z \in \mathbb{R}^d$, $g^{z,\alpha} = (g_1^{z,\alpha}, g_2^{z,\alpha}) \in L^2(\Gamma_m) \times L^2(\Gamma_s)$ such that :

$$\begin{aligned} J_\alpha(\phi_z, g^{z,\alpha}) = \alpha |(F g_2^{z,\alpha}, \, g_1^{z,\alpha})_1| + \alpha^{1-\eta} \left\| H_s g_2^{z,\alpha} - H_m g_1^{z,\alpha} \right\|^2_{L^2(\Sigma)} \\ + \alpha^{1-\eta} |(F g_2^{z,\alpha} - \phi_z, \, g_1^{z,\alpha})_1| + \left\| F g_2^{z,\alpha} - \phi_z \right\|^2 \\ \leq j_\alpha(\phi_z) + C\alpha, \end{aligned}$$

where $\eta \in]0,1[$ and

$$j_\alpha(\phi_z) = \inf_{g \in L^2(\Gamma_m)\times L^2(\Gamma_s)} J_\alpha(\phi_z, g)$$

.

Combining the results of Theorems 18 and 20 we obtain the following theorem:

Theorem 21. *Assume that Hypothesis 5 holds and that T verifies*

$$|(Th,\, h)| \geq \mu \, \|h\|_{L^2(D)}$$

for $h \in \overline{\mathcal{R}(H_s)}$. Then $z \in D$ if and only if $\limsup_{\alpha\to 0} |(Fg_2^{z,\alpha},\, g_1^{z,\alpha})_1| + \alpha^{-\eta} \, \|H_s g_2^{z,\alpha} - H_m g_1^{z,\alpha}\|^2_{L^2(\Sigma)} < \infty$.
Moreover, if $z \in D$ then the sequence of Herglotz wave functions associated to $g^{z,\alpha}$ converges strongly to the solution v of (4.35) with $(f,g) = (\Phi_z, \frac{\partial \Phi_z}{\partial \nu})$ as α goes to zero.

For applications, it is rather important to rather use the criterion provided in Theorem 19. Consider $F^\delta : L^2(\Gamma_s) \to L^2(\Gamma_m)$ a compact operator such that:

$$\left\| F^\delta - F \right\| \leq \delta.$$

Then consider for $\alpha > 0$ and $\phi \in L^2(\Gamma_m)$ the functional $J^\delta_\alpha(\phi, \cdot) : L^2(\Gamma_s) \times L^2(\Gamma_m) \to \mathbb{R}$,

$$\begin{aligned} J^\delta_\alpha(\phi_z, g) = \alpha |\left(F^\delta g_2,\, g_1\right)_1| + \alpha^{1-\eta} \, \|H_s g_2 - H_m g_1\|^2_{L^2(\Sigma)} + \alpha^{1-\eta}\delta \, \|g\|^2 \\ + \alpha^{1-\eta} |\left(F^\delta g_2 - \phi_z,\, g_1\right)_1| + \left\| F^\delta g_2 - \phi_z \right\|^2 \end{aligned}$$

where $\eta \in]0,1[$. Then as a direct consequences of Theorem 19 we obtain the following characterization of D,

Theorem 22. *Assume that the hypothesis of Theorem 21 hold true. For $z \in \mathbb{R}^d$ denote by $g^{z,\alpha,\delta}$ the minimizer of $J^\delta_\alpha(\phi, \cdot)$ over $L^2(\Gamma_s) \times L^2(\Gamma_m)$. Then $z \in D$ if and only if*

$$\limsup_{\alpha\to 0} \limsup_{\delta \to 0} |\left(F^\delta g_2^{z,\alpha,\delta},\, g_1^{z,\alpha,\delta}\right)_1| + \alpha^{-\eta} \left\| H_s g_2^{z,\alpha,\delta} - H_m g_1^{z,\alpha,\delta} \right\|^2_{L^2(\Sigma)} + \alpha^{-\eta}\delta \left\| g^{z,\alpha,\delta} \right\|^2 < \infty.$$

If $z \in D$, there exists $\delta_0(\alpha)$ such that for all $\delta(\alpha) \leq \delta_0(\alpha)$, $Hg^{z,\alpha,\delta(\alpha)}$ converges strongly to the solution v of (4.35) with $(f,g) = (\Phi_z, \frac{\partial \Phi_z}{\partial \nu})$ as α goes to zero.

4.3.2 A coerciviy result when $n-1$ changes sign inside D

In this subsection we provide a important extension of Theorem 6. First let us recall the equality related to the imaginary part of T

Lemma 8. *We have the following identity, for $\psi \in L^2(D)$ and T defined in (4.4) :*

$$\Im(T\psi,\, \psi) = k \int_{\mathbb{S}^{d-1}} |w^\infty|^2 + k^2 \int_D \Im(n) |w + \psi|^2.$$

Proof. The proof is similar to the one done in theorem 6. We recall that for any $\psi \in L^2(D)$ there is a unique $w \in H^1_{loc}(\mathbb{R}^d)$ that solves (4.1). The definition of T (4.4) gives:

$$(T\psi,\, \psi) = -k^2 \int_D (1-n)|\psi + w|^2 + k^2 \int_D (1-n)(\psi + w)\bar{w} \tag{4.36}$$

Using (4.1) and integrating by parts over a ball B_R such that $D \subset B_R$ we have:

$$-\int_{B_R} \nabla w \cdot \overline{\nabla w} - k^2 w\overline{w} + \int_{\partial B_R} \frac{\partial w}{\partial r}\overline{w} = k^2 \int_D (1-n)(w+\psi)\overline{w}$$

Substituting in (4.36), taking the imaginary part and letting R to $+\infty$ prove the lemma. □

The coercivity of T is given by the following theorem.

Theorem 23. *Let Ω be an open regular domain strictly included in D such that $\mathbb{R}^d \setminus \Omega$ is connected. Assume that there exist $\alpha, c \in \mathbb{R}^{*+}$ such that either $\Re(n-1) + \alpha\Im(n) \geq c$ or $\Re(1-n) + \alpha\Im(n) \geq c$ in $D \subset \Omega$. Then there exists μ such that the operator T defined in 4.4 verified*

$$|(T\psi,\, \psi)| \geq \mu \, \|\psi\|^2_{L^2(D)} \quad \forall \psi \in \overline{\mathcal{R}(H_s)}$$

Proof. Assume for instance the existence of a sequence $\psi_\ell \in \mathcal{R}(H_s)$ such that

$$\|\psi_\ell\|_{L^2(D)} = 1 \quad \text{and } |(T\psi_\ell, \psi_\ell)| \to 0 \text{ as } \ell \to \infty.$$

We denote by $w_\ell \in H^2_{\text{loc}}(\mathbb{R}^d)$ the solution of

$$\begin{cases} \Delta w_\ell + nk^2 w_\ell = -k^2(n-1)\psi_\ell \text{ in } \mathbb{R}^d, \\ \lim\limits_{r\to\infty} \int\limits_{|x|=r} \left| \frac{\partial w_\ell}{\partial r} - ikw_\ell \right|^2 ds = 0. \end{cases} \tag{4.37}$$

Elliptic regularities imply that $\|w_\ell\|_{H^2(D)}$ is bounded uniformly with respect to ℓ. Then up to changing the initial sequence, one can assume that ψ_ℓ weakly converges to some ψ in $L^2(D)$ and w_ℓ converges weakly in $H^2_{\text{loc}}(\mathbb{R}^d)$ and strongly in $L^2(D)$ to some $w \in H^2_{\text{loc}}(\mathbb{R}^d)$. It is then easily seen (using distributional limit) that w and ψ satisfies (4.37), and since $\psi_\ell \in \mathcal{R}(H_s)$

$$\Delta\psi + k^2\psi = 0 \quad \text{ in } D. \tag{4.38}$$

Lemma 8 and $|(T\psi_\ell, \psi_\ell)| \to 0$ imply that $w^\infty_\ell \to 0$ in $L^2(\mathbb{S}^{d-1})$ and therefore $w^\infty = 0$. The Rellich theorem and unique continuation principle imply $w = 0$ outside D and consequently $w \in H^2_0(D)$. With the help of equation (4.38) we get that $u = w+\psi \in L^2(D)$ and $v = \psi \in L^2(D)$ are such that $u - v \in H^2(D)$ and are solution of the interior transmission problem (4.35) with $f = g = 0$. We then infer that $w = \psi = 0$ (under Hypothesis 5).

We introduce a function $n_0 \in L^\infty(\mathbb{R}^d)$ with non negative imaginary part that is equal to n in $D \setminus \Omega$ and satisfies either $\Re(n_0 - 1) + \alpha\Im(n_0) \geq c$ or $\Re(1 - n_0) + \alpha\Im(n_0) \geq c$ in D. $n_0 - 1 \geq c > 0$ in all D (and $n_0 = 1$ outside D). Let us then introduce the intermediate (scattered) field $u^s_{0,\ell} \in H^2_{\text{loc}}(\mathbb{R}^d)$ that solves:

$$\begin{cases} \Delta u^s_{0,\ell} + n_0 k^2 u^s_{0,\ell} = k^2(1-n_0)\psi_\ell \text{ in } \mathbb{R}^d, \\ \lim\limits_{r\to\infty} \int\limits_{|x|=r} \left| \frac{\partial(u^s_{0,\ell})}{\partial r} - ik(u^s_{0,\ell}) \right|^2 ds = 0. \end{cases} \tag{4.39}$$

We denote by $u_{0,\ell} = u^s_{0,\ell} + \psi_\ell$ the associated total field. We also introduce u^s_ℓ (field scattered by D for an incident field given by $u_{0,\ell}$) which solves:

$$\begin{cases} \Delta u^s_\ell + nk^2 u^s_\ell = k^2(n_0 - n)u_{0,\ell} \text{ in } \mathbb{R}^d, \\ \lim\limits_{r\to\infty} \int\limits_{|x|=r} \left| \frac{\partial u^s_\ell}{\partial r} - iku^s_\ell \right|^2 ds = 0. \end{cases} \tag{4.40}$$

Clearly

$$w_\ell = u^s_{0,\ell} + u^s_\ell.$$

Using the same argument as for w_ℓ we get that $u^s_{0,\ell}$ converges strongly to zero in $L^2(D)$. Since Ω is strictly included inside D, we have that $u_{0,\ell}$ is bounded in $H^2(\Omega)$ (by interior elliptic regularity applied to ψ_ℓ). Therefore $u_{0,\ell}$ converges weakly to zero in $L^2(D)$ but strongly in $L^2(\Omega)$. We then conclude that u^s_ℓ converges strongly to zero in $L^2(D)$. Finally we can decompose:

$$\begin{aligned} |(T\psi_\ell, \psi_\ell)| &= k^2 \left| \int_D (1-n)(u^s_\ell + u_{0,\ell})\overline{\psi}_\ell dx \right| \\ &= k^2 \left| \int_D (1-n_0)u_{0,\ell}\overline{\psi}_\ell dx + \int_D (1-n)u^s_\ell \overline{\psi}_\ell dx + \int_\Omega (n_0 - n)u_{0,\ell}\overline{\psi}_\ell dx \right| \\ &\geq k^2 \left| \int_D (1-n_0)u_{0,\ell}\overline{\psi}_\ell dx \right| - k^2 \left| \int_D (1-n)u^s_\ell \overline{\psi}_\ell dx + \int_\Omega (n_0 - n)u_{0,\ell}\overline{\psi}_\ell dx \right| \end{aligned}$$

Therefore

$$\begin{aligned} |(T\psi_\ell, \psi_\ell)| \geq k^2 \left| \int_D (1-n_0)|\psi_\ell|^2 dx \right| - k^2 \left| \int_D (1-n_0)u^s_{0,\ell}\overline{\psi}_\ell dx \right| \\ - k^2 \left| \int_D (1-n)u^s_\ell \overline{\psi}_\ell dx \right| - k^2 \left| \int_\Omega (n_0 - n)u_{0,\ell}\overline{\psi}_\ell dx \right|. \end{aligned} \tag{4.41}$$

Previous strong convergence results imply that all terms on the right side of the inequality except the first one go to zero as $\ell \to \infty$. One then conclude with a contradiction exactly in the same way as in the proof of Theorem 6 using the properties of n_0. □

Remark 8. *To the best of our knowledge it is the first time that a coercivity result for T is given when n changes sign inside the domain. This proof requires the same set of hypothesis as the one needed in order to prove the solvability of the related interior transmission problem (except for a countable set of frequencies).*

Remark 9. *The strong convergences results for Herglotz waves when the samplin point is inside D in Theorems 21 and 22 allows us to apply the results from Chapter 3. This means that one can apply the algorithm for differential measurements imaging with limited aperture data (using obvious adaptation of the cost functional as proposed in this Chapter).*

4.4 Extension to near field data

We concentrated in the previous sections on incident plane waves and farfield measurement and raise the problem of non symmetric factorization in the case of limited aperture. The

theory we developed in section 4.2 is concerned with non symmetric factorizations of any type. There are two interesting cases for applications where one may have to deal with non symmetric factorization. In this section we consider the case of near field imaging and we will postpone the case of known heterogeneous background to Chapter 6 in order to treat the more general case of anisotropic background.

The total field is generated by point sources and the scattered field is recorded on a surface of $\mathbb{R}^d$ (usually where the point source lies). If we denote by $\partial\Omega$ the surface where lie the sources, we should consider an incident field $u^i(y,x) := \Phi(y,x)$ with $x \in \mathbb{R}^d$ and $y \in \partial\Omega$. We introduce $N : H^{-\frac{1}{2}}(\partial\Omega) \to H^{\frac{1}{2}}(\partial\Omega)$ defined by

$$Ng := \int_{\partial\Omega} u^s(y,x)g(y)ds(y),\ g \in H^{-\frac{1}{2}}(\partial\Omega),\ x \in H^{\frac{1}{2}}(\partial\Omega), \tag{4.42}$$

where $u^s(y,\cdot)$ is defined in 4.1 for an incident field $\psi = u^i(y,\cdot.)$ We introduce the compact operator $S : H^{-\frac{1}{2}}(\partial\Omega) \to L^2(D)$ (which plays the role of H_s) defined by

$$Sg := \int_{\partial\Omega} \Phi(y,x)g(y)ds(y),\ g \in H^{-\frac{1}{2}}(\partial\Omega),\ x \in D \tag{4.43}$$

and the (compact) operator $G : \overline{\mathcal{R}(S)} \subset L^2(D) \to H^{\frac{1}{2}}(\partial\Omega)$ defined by

$$G\psi := w|_{\partial\Omega},$$

where $\overline{\mathcal{R}(S)}$ denotes the closure of the range of S in $L^2(D)$ and w is defined as in section 4.1. Then clearly

$$N = GS. \tag{4.44}$$

In the case under consideration, since the scattered field has the following expression :

$$w(x) = -\int_{\mathcal{D}} \Phi(y,x)(1-n)k^2(\psi(y)+w(y))dy,$$

one simply has $G = \bar{S}^* T\psi$ where $\bar{S}^* : L^2(D) \to L^2(\partial\Omega)$ is the conjugate of the adjoint of S given by:

$$\bar{S}^*\varphi(x) = \int_{\mathcal{D}} \Phi(y,x)\varphi(y)dy,\ x \in \Gamma,$$

and T is defined by (4.4). Finally we get

$$N = \bar{S}^* T S. \tag{4.45}$$

As for the limited aperture case this factorization is non symmetric.

Point sources and point measurements on the same surface

The case where the point sources and the measurements are on the same surface can be solved without relying on the theory developed in section 4.2.2. At the cost of computing an operator C (introduced in the following) such that :

$$B = CF = H^* T H,$$

one can rely on the theory of section 4.2.1. In [40] an inf-criterion is proposed to tackle the case of near field full aperture, through the use of the corresponding farfield operator. We propose to adapt this idea to the setting of the GLSM and to revisit its analysis to avoid the use of the corresponding farfield operator. To do so we need to introduce the following operator, which is closely connected to S and a technical lemma.

$$S_{\partial\Omega} : H^{-\frac{1}{2}}(\partial\Omega) \to H^{\frac{1}{2}}(\partial\Omega), S_{\partial\Omega}(f)(x) = \int_{\Gamma} \Phi(x,y) f(y) ds(y), \ x \in \partial\Omega \tag{4.46}$$

Lemma 9. *If k^2 is not a Dirichlet eigenvalue of the Laplace operator in Ω, we have that:*

$$S^*_{\partial\Omega} S^{-1}_{\partial\Omega} \bar{S}^* = S^*$$

Proof. If k^2 is not a Dirichlet eigenvalue of the Laplace operator in Ω, we have that $\bar{S} S^{-1,*}_{\partial\Omega} S_{\partial\Omega}$ and S solves the Helmholtz equation in Ω. Straightforward calculations provide that $S^*_{\partial\Omega} = \bar{S}_{\partial\Omega}$ and that they share the same boundary values on $\partial\Omega$. Thus those two operators are equal and taking the adjoint concludes the proof of this lemma. □

Using (4.45) we found

$$B = S^*_{\partial\Omega} S^{-1}_{\partial\Omega} N = S^* T S$$

Remark 10. *Finally we should point out that in [37] it was shown that if Ω is a ball the operator C reduces to the conjugation operator.*

From this factorization one can either uses the framework developed in chapters 2 and 3 or in section 4.2.1 or the factorization method developed in [40].

Point sources and measurements lying on different surfaces

One can consider a limited aperture nearfield measurement by considering that the point sources are located on $\Gamma_s \subset \partial\Omega$ and the measurements are done on $\Gamma_m \subset \partial\Omega$. In this case similarly to the farfield case we obtain a factorization :

$$N = \bar{S}^*_m T S_s. \tag{4.47}$$

Let $G := \bar{S}^*_m T$ restricted to the closure of the range of S_s. As for the farfield case we have the following result which is proven in [40],

Lemma 10. *If Hypothesis 5 is verified, $\Phi_z \in \mathcal{R}(G)$ if and only if $z \in D$.*

Lemma 11. *If k is not a dirichlet eigenvalue of Ω we have that S_s is dense in $\{v \in L^2(D)$ s.t. $\Delta v + v = 0$ in $D\}$*

As already pointed out the operator T is not changed by the type of incident wave and measurement therefore it keeps the coercivity property proven in section 4.3.

The two previous lemmas, the coercivity of T and (4.47) are all the required ingredients to apply the framework of 4.2.2 with $V = S_s$, $U = \bar{S}_m$ and $F = N$. We therefore obtain the following corollary for the GLSM with nearfield measurements.

Corollary 4. *Assume that Hypothesis 5 hold, that $D \subset \Sigma$ and that T is a coercive operator. Then $z \in D$ if and only if*

- $|(Ng_2^{z,\alpha}, g_1^{z,\alpha})_1| + \alpha^{-\eta} \left\| S_s g_2^{z,\alpha} - \bar{S}_m g_1^{z,\alpha} \right\|^2_{L^2(\Sigma)}$ *remains bounded for $g_1^{z,\alpha}$ and $g_2^{z,\alpha}$ defined as in Section 4.2 with $\phi = \phi_z$*
- $R(g^{z,\alpha,\delta}, \alpha, \delta)$ *(defined in Theorem 19) remains bounded for $g^{z,\alpha,\delta}$ defined as in Section 4.2 with $\phi = \phi_z$, $V = S_s$ and $U = \bar{S}_m$.*

Moreover we have that one can extract a subsequence from the sequence of herglotz wave functions associated to $g^{z,\alpha}$ (resp. $g^{z,\alpha,\delta}$)which will converge strongly to the solution v of (4.35) with $(f, g) = (\Phi_z, \frac{\partial \Phi_z}{\partial \nu})$ as α goes to zero (resp. as α and δ go to zero for $\delta \leq \delta_0$).

4.5 Numerical Algorithm and results

In order to fix the ideas, we shall restrict ourselves to the two dimensional case and will introduce the algorithms for the discrete version of GLSM. We identify $\mathbb{S}^1$ with the interval $[0, 2\pi[$. In order to collect the data of the inverse problem we solve numerically (4.1) for N incident fields using the surface integral equation forward solver available in [35]. The discrete version of F is then the matrix F_{N}. We add some noise to the data to build a noisy far field matrix F_N^δ where $(F_{\mathrm{N}}^\delta)_{j,k} = (F_{\mathrm{N}})_{j,k}(1 + \sigma N_{ij})$ for $\sigma > 0$ and N_{ij} an uniform complex random variable in $[-1, 1]^2$. We denote $\Phi_{z,\mathrm{N}} \in \mathbb{C}^{\mathrm{N}}$, the vector defined by $\Phi_{z,\mathrm{N}}(j) = \phi_z(\frac{2\pi j}{\mathrm{N}})$ for $0 \leq j \leq \mathrm{N} - 1$.

4.5.1 Symmetric case

First we will look at the result given when $\Gamma_m = \Gamma_s$. This setting could be seen as a reference image as it does not introduce any new regularization term based on apriori knowledge (the choice of Σ). Moreover it can be formulated as a convex functional if one introduces $F_\#^\delta = |\Re(F^\delta)| + |\Im(F^\delta)|$, we introduce:

$$g_\#^{z,\alpha,\delta} = arg \min_{g \in \mathbb{C}^N} \alpha \left\| (F_\#^\delta)^{\frac{1}{2}} g \right\|^2 + \alpha^{1-\eta} \delta \|g\|^2 + \left\| F^\delta g - \phi_z \right\|^2$$

This minimization is solved using the normal equation:

$$g_\#^{z,\alpha,\delta} = (\alpha F_\# + \alpha^{1-\eta} \delta Id + F^{\delta,*} F^\delta)^{-1} F^{\delta,*} \phi_z$$

And finally we use the following indicator function to retrieve the D

$$\mathcal{I}_\#(z) = \frac{1}{\left\| (F_\#^\delta)^{\frac{1}{2}} g_\#^{z,\alpha,\delta} \right\|^2 + \alpha^{-\eta} \delta \left\| g_\#^{z,\alpha,\delta} \right\|^2}$$

To compare with setting where $\Gamma_m \neq \Gamma_s$ we also introduced :

$$g^{z,\alpha,\delta} = arg \min_{g \in \mathbb{C}^N} \alpha |\big(F^\delta g, g\big)| + \alpha^{1-\eta} \delta \|g\|^2 + \alpha^{1-\eta} |\big(F^\delta g - \phi_z, g\big)| + \left\| F^\delta g - \phi_z \right\|^2$$

and consider the following indicator function:

$$\mathcal{I}(z) = \frac{1}{|\left(F^\delta g^{z,\alpha,\delta},\, g^{z,\alpha,\delta}\right)| + \alpha^{-\eta}\delta \left\|g^{z,\alpha,\delta}\right\|^2}.$$

Computing $g^{z,\alpha,\delta}$ is much more challenging as the functional is not convex nor differentiable. In chapter 2, we used a first order gradient method, we improved the efficiency of this scheme by using a second order method. We give the formula of the gradient and the hessian explicitly in the more general case were $\Gamma_m \neq \Gamma_s$. However, we need a starting point for our descent method, point that we obtain by using the original LSM with Tikhonov regularization :

$$g_0^{z,\beta,\delta} = arg \min_{g\in\mathbb{C}^N} \beta \left\|g\right\|^2 + \left\|F^\delta g - \phi_z\right\|^2$$

where we choose β such that $\delta \left\|g_0^{z,\beta,\delta}\right\| = \left\|F_0^{z,\beta,\delta} - \phi_z\right\|$. From this choice of β as in chapter 2 we set $\alpha = \frac{\beta}{\left\|F_\#\right\|}$ or $\frac{\beta}{\|F\|}$.

We consider two examples one with two ellipses and one with a kite shape obstacle. The axis are labelled as multiple of the wave length of index of refraction $n = 0.2$. And we consider four apertures : $[0, 2\pi[$, $[\pi/2, 3\pi/2[$, $[3\pi/4, 5\pi/4[$ and $[7\pi/8, 9\pi/8[$ with a noise of one percent. All the results for full aperture are gather in figure 4.2. In figures 4.3 and 4.4, we show the results of $\mathcal{I}_\#$ and $\mathcal{I}$. In chapter 2 we observe that the optimization increases the quality of the results only when the two obstacles where close too each other and did not bring any improvement for the single kite. In figures 4.5 and 4.6 we show that improvement can be seen even for single obstacle and the improvement of optimization gets higher with smaller aperture.

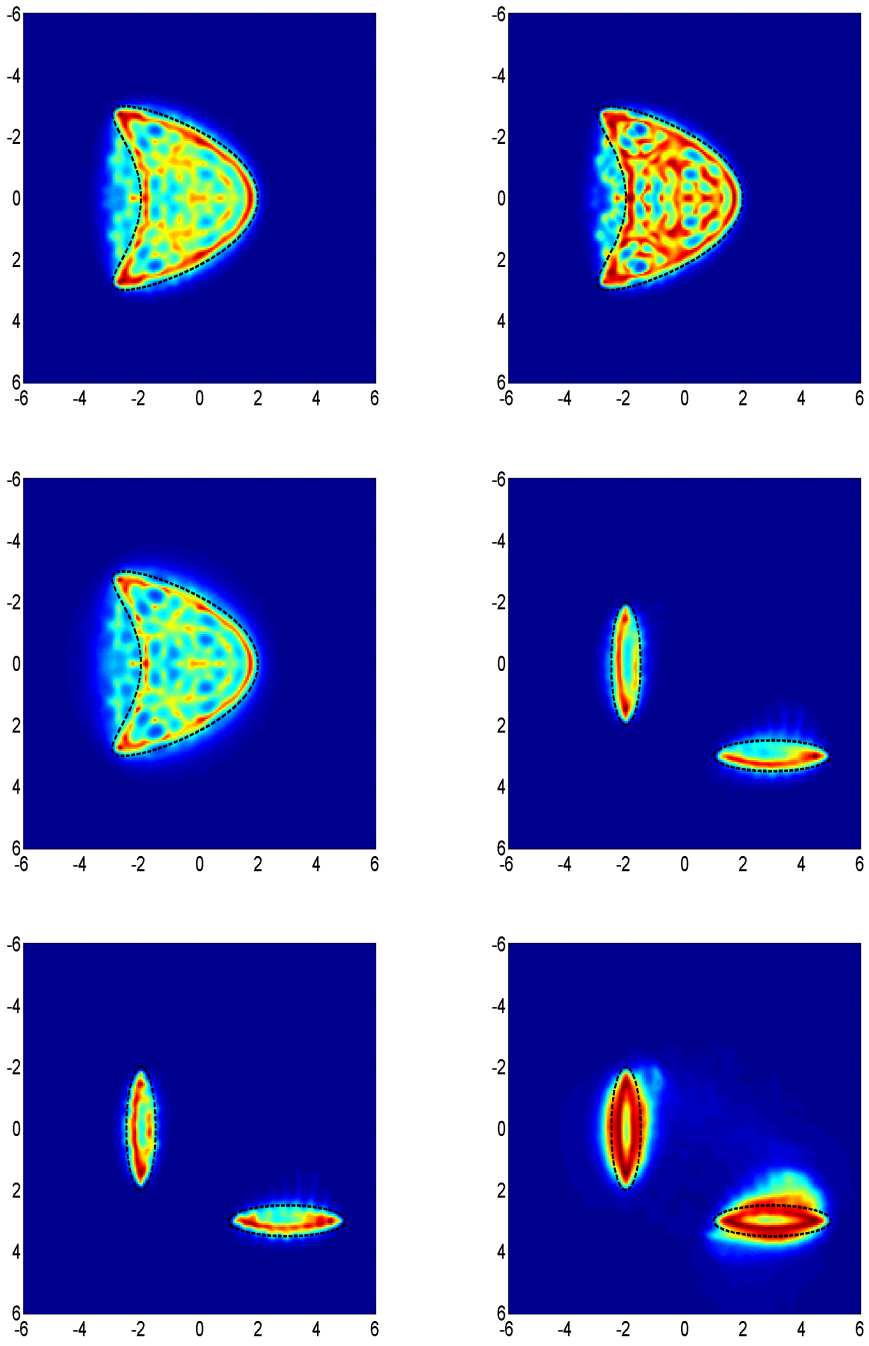

Figure 4.2: Results for full aperture.From up to down and left to right : $\mathcal{I}_{\#}$, $\mathcal{I}$ and $\mathcal{I}$ without optimization, for the Kite and $\mathcal{I}_{\#}$, $\mathcal{I}$ and $\mathcal{I}$ without optimization, for 2 ellipses.

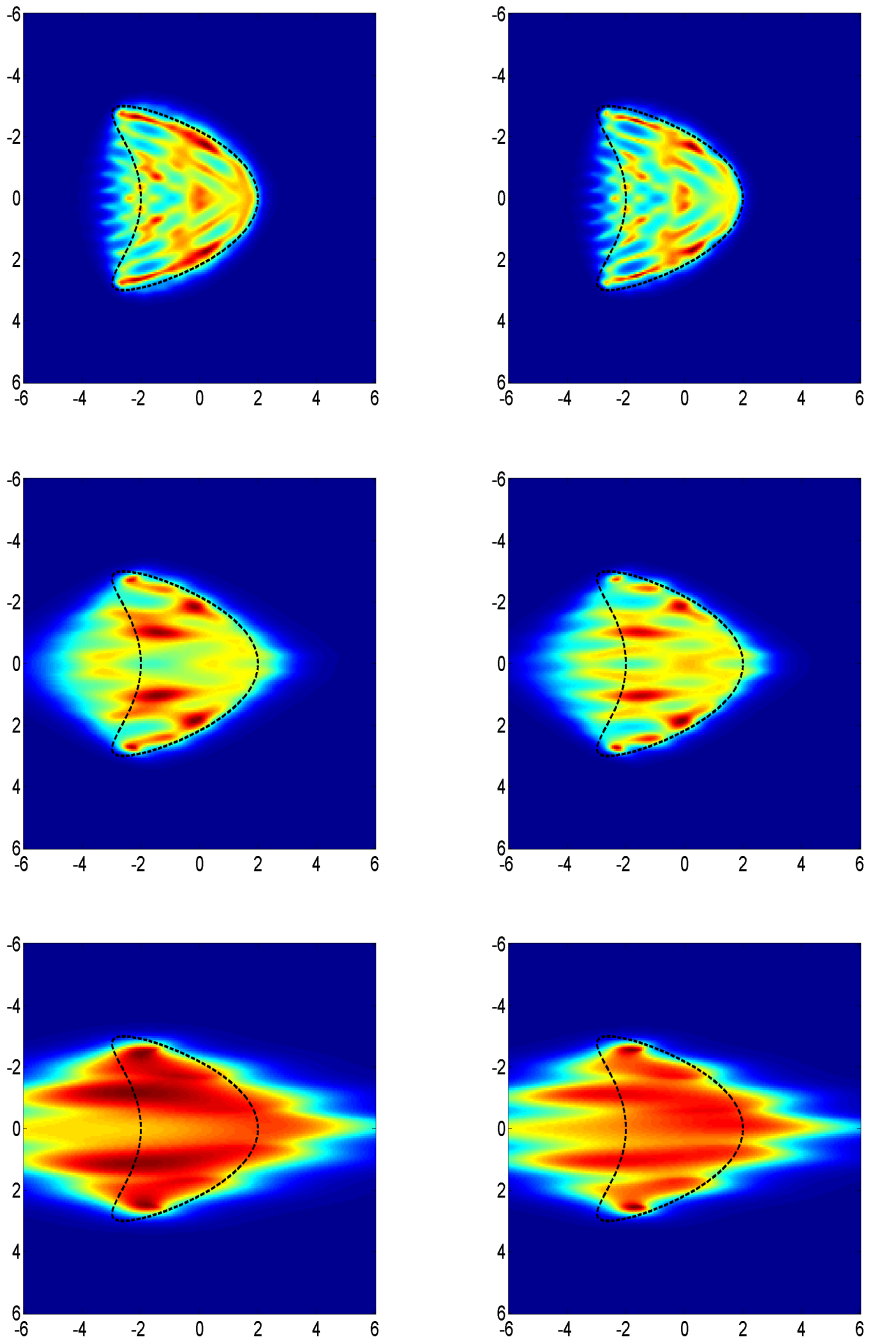

Figure 4.3: On the left $\mathcal{I}_{\#}$ and on the right $\mathcal{I}$. From up to down the aperture is : $[\pi/2, 3\pi/2[$, $[3\pi/4, 5\pi/4[$ and $[7\pi/8, 9\pi/8[$.

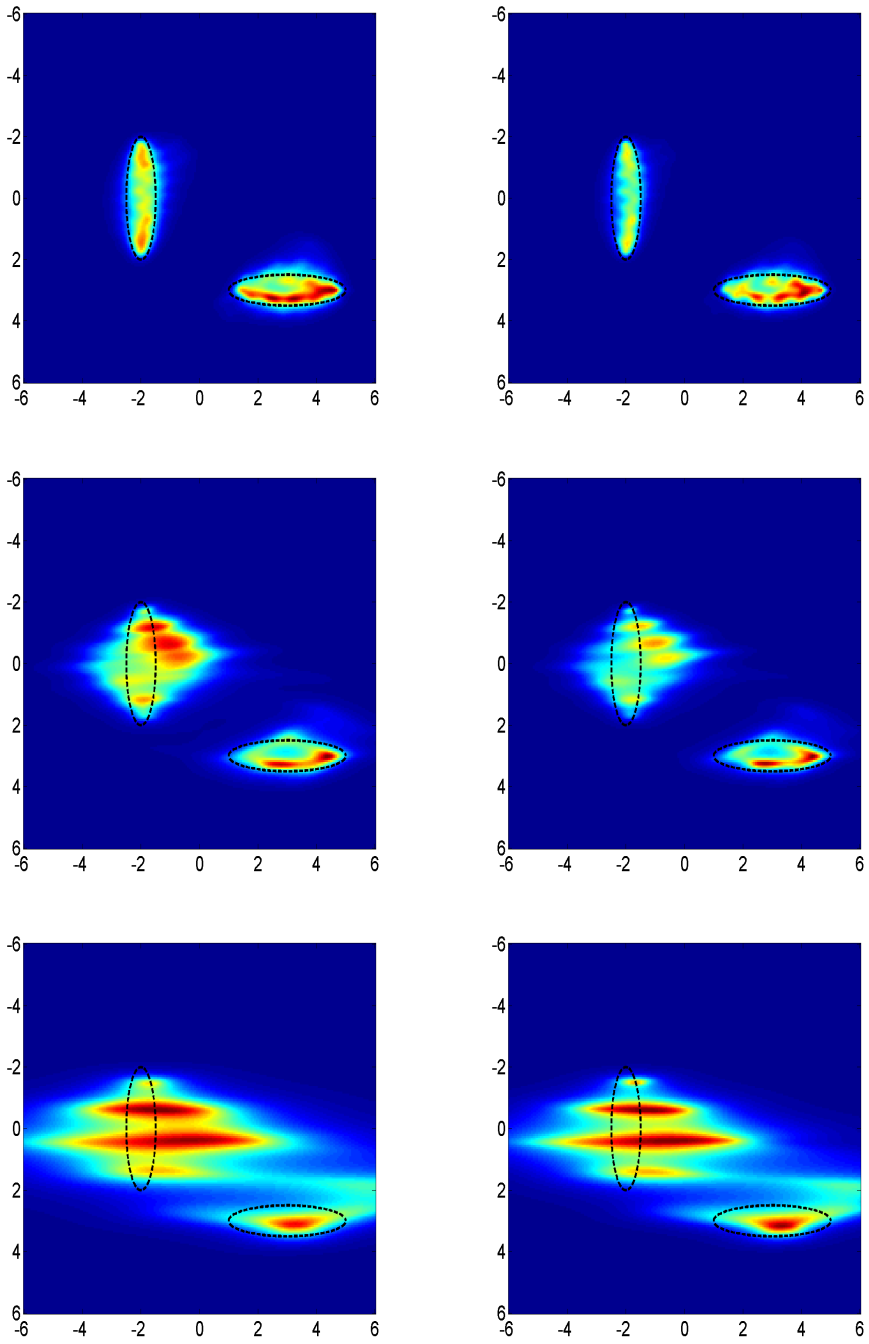

Figure 4.4: On the left $\mathcal{I}_{\#}$ and on the right $\mathcal{I}$. From up to down the apertures are : $[\pi/2, 3\pi/2[$, $[3\pi/4, 5\pi/4[$ and $[7\pi/8, 9\pi/8[$

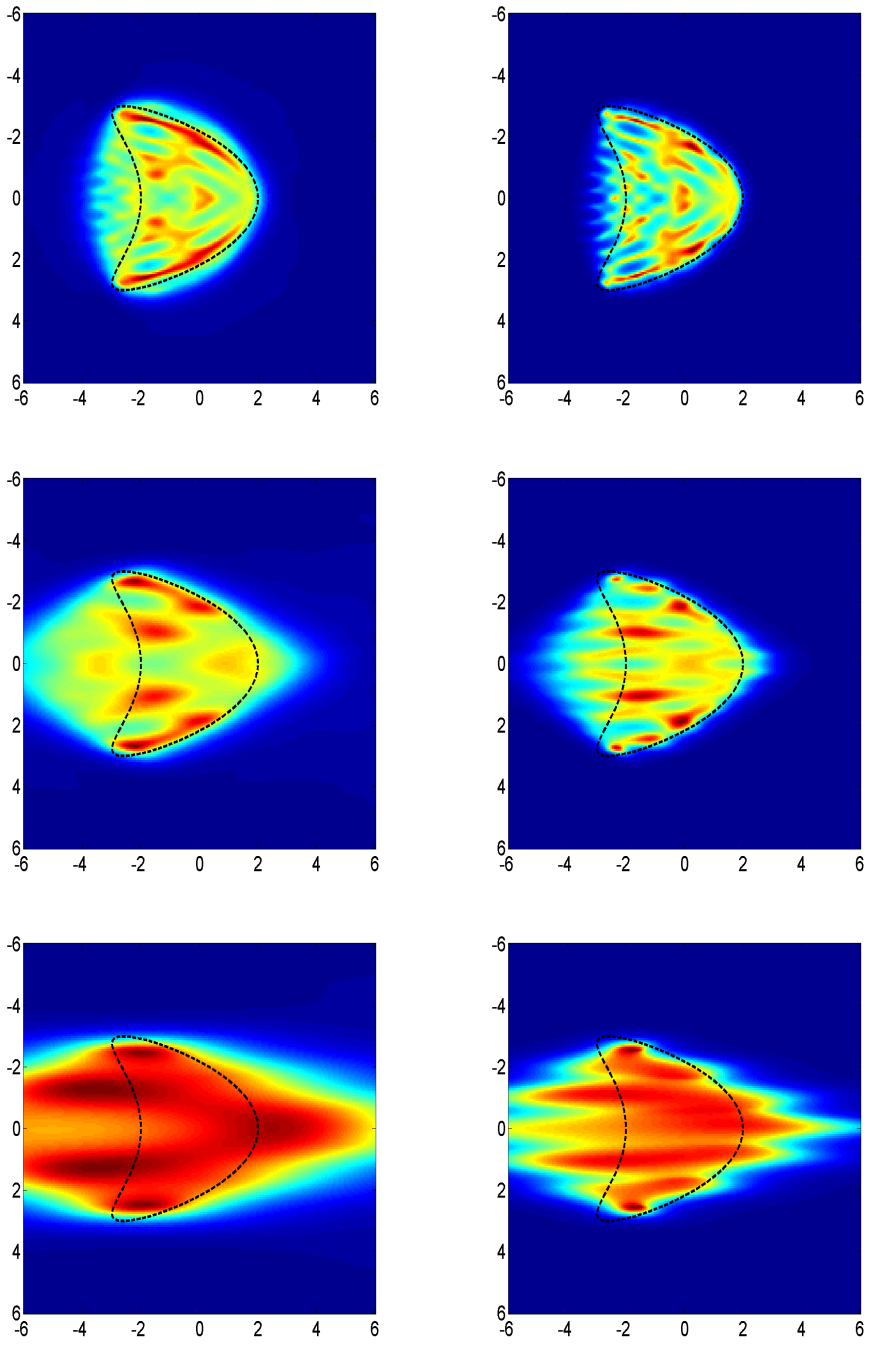

Figure 4.5: $\mathcal{I}$ computed without optimization on the left and with on the right. From up to down the apertures are : $[\pi/2, 3\pi/2[$, $[3\pi/4, 5\pi/4[$ and $[7\pi/8, 9\pi/8[$.

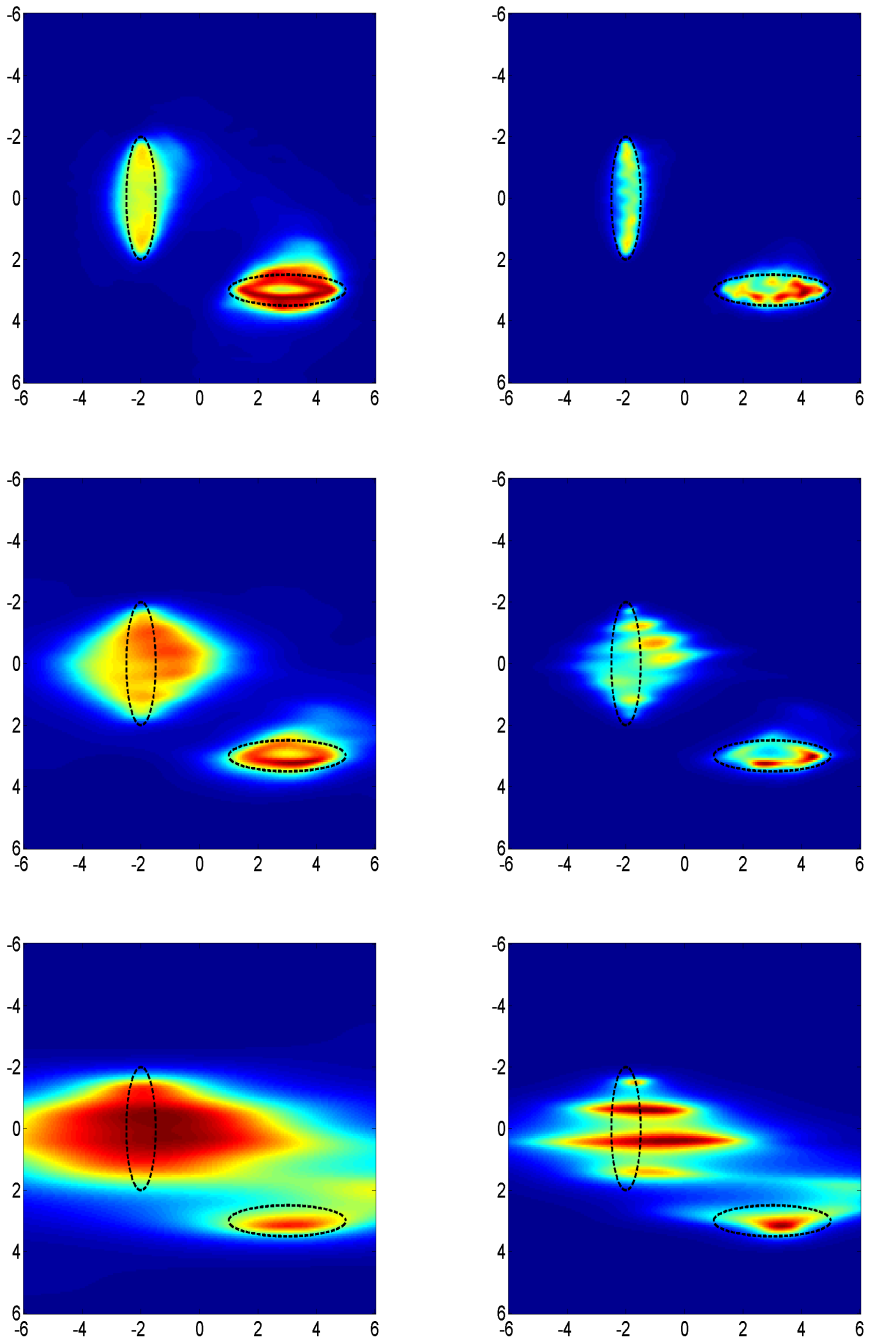

Figure 4.6: $\mathcal{I}$ computed without optimization on the left and with on the right. From up to down the apertures are : $[\pi/2, 3\pi/2[$, $[3\pi/4, 5\pi/4[$ and $[7\pi/8, 9\pi/8[$.

We also consider the case of differential measurement for limited aperture data. We consider a medium made of three disjoint component and we will consider three apertures : $[\pi/2, 3\pi/2[$,

$[3\pi/4, 5\pi/4[$ and $[7\pi/8, 9\pi/8[$. Figure 4.7 shows that the differential imaging method still work with limited aperture however it deteriorates faster with the aperture than the GLSM classical imaging functional.

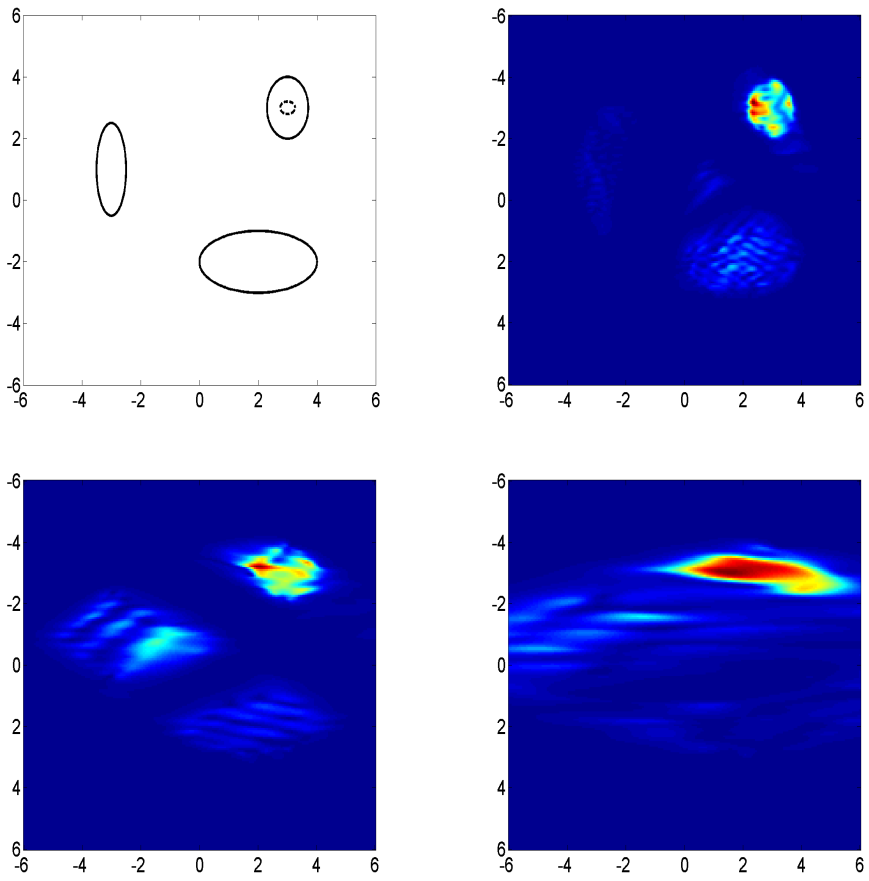

Figure 4.7: The first image is the medium, with the defect that appears depicted with a dashed line. The three other images show $\mathcal{I}_T$.From up to down and left to right, the apertures are : $[\pi/2, 3\pi/2[$, $[3\pi/4, 5\pi/4[$ and $[7\pi/8, 9\pi/8[$.

4.5.2 NonSymetric case

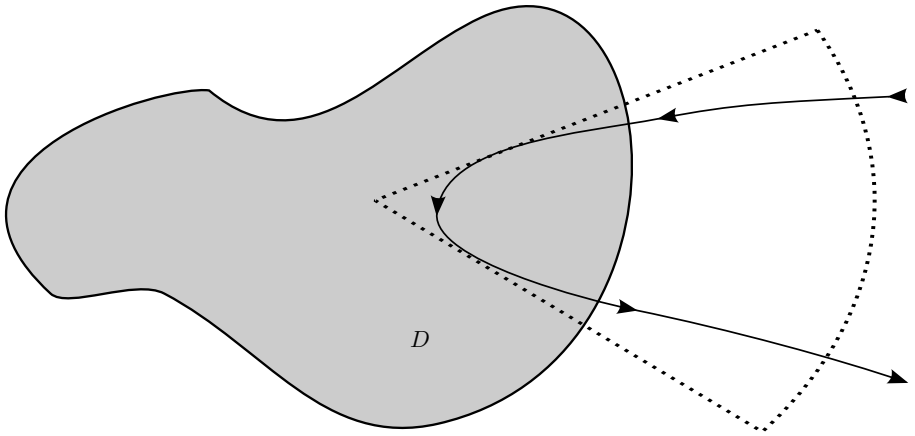

Figure 4.8: The arrow goes from the sources to the measurement in a backscattering manner.

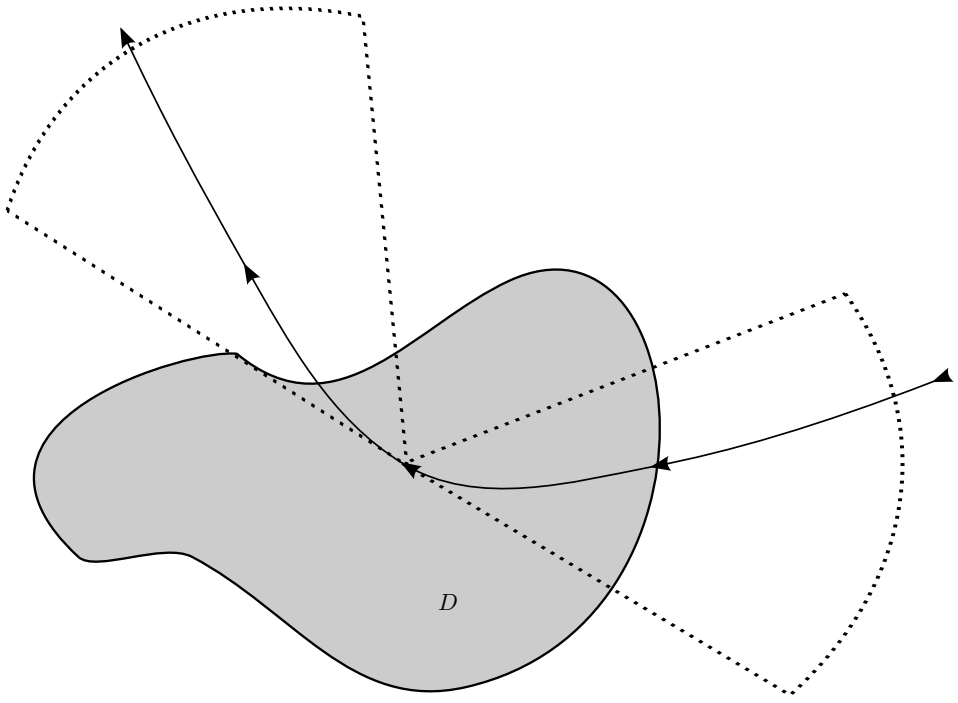

Figure 4.9: The arrow goes from the sources to the measurement.

We consider the case where $\Gamma_m \neq \Gamma_s$. In this case we have to define $g^{z,\alpha,\delta}$ as the minimizer of a non convex nor differentiable cost functional,

$$g^{z,\alpha,\delta} = arg \min_{g\in\mathbb{C}^N\times\mathbb{C}^N} \alpha|\big(F^\delta g_2,\, g_1\big)| + \alpha^{1-\eta}\delta \left\|g\right\|^2 + \alpha^{1-\eta}|\big(F^\delta g_2 - \phi_z,\, g_1\big)| \\ + \alpha^{1-\eta}\left\|H_s g_2 - H_m g_1\right\|^2 + \left\|F^\delta g_2 - \phi_z\right\|^2,$$

and we introduced the indicator function:

$$\mathcal{I}(z) = \frac{1}{|\Big(F^\delta g_2^{z,\alpha,\delta},\, g_1^{z,\alpha,\delta}\Big)| + \alpha^{-\eta}\delta\left\|g^{z,\alpha,\delta}\right\|^2 + \alpha^{-\eta}\left\|H_s g_2^{z,\alpha,\delta} - H_m g_1^{z,\alpha,\delta}\right\|^2}.$$

To minimize the cost functional we will rely on a second order descent method. We will choose the starting point of the descent , g_0, as

$$g_{0,2}^{z,\beta_2,\delta} = arg \min_{g\in\mathbb{C}^N} \beta_2 \left\|g\right\|^2 + \left\|F^\delta g - \phi_z\right\|^2$$

$$g_{0,1}^{z,\beta_1,\delta} = arg \min_{g\in\mathbb{C}^N} \beta_1 \left\|g\right\|^2 + \left\|H_m g - H_s g_{0,2}^{z,\beta,\delta}\right\|^2$$

where we choose β_2 such that $\delta\left\|g_{0,2}^{z,\beta_2,\delta}\right\| = \left\|F_{0,2}^{z,\beta_2,\delta} - \phi_z\right\|$ and β_1 such that $\left\|g_{0,1}^{z,\beta_1,\delta}\right\| = \left\|g_{0,2}^{z,\beta_2,\delta}\right\|$. This second choice is purely arbitrary, our purpose in setting β_1 is to avoid, $g_{0,1}^{z,\beta_1,\delta}$ to have an overwhelming norm which will dominate numerically all other quantities (or a very small influence).

The minimization of J_α^δ causes numerical problem. Indeed first numerically we have to be careful on the balance between the terms : $\left\|g_1\right\|^2$ and $\left\|H_m g_1 - H_s g_2\right\|$ because H_m is compact. This is even more important as $H_s g_2$ is not in the range of H_m. Since the theory does not give a strategy to set α, we proposed three equivalent strategies. Those strategies are based on the same idea that $\left\|g_1^{z,\beta_1,\delta}\right\|$ and $\left\|g_2^{z,\beta_1,\delta}\right\|$ should have the same order of magnitude. With a slight change of notation we have:

$$J_\alpha^\delta(g_1,g_2) = \alpha|\big(F^\delta g_2,\, g_1\big)| + \alpha_1\delta\left\|g_1\right\|^2 + \alpha_2\delta\left\|g_2\right\|^2 + \alpha^{1-\eta}|\big(F^\delta g_2 - \phi_z,\, g_1\big)| \\ + \alpha_3\left\|H_s g_2 - H_m g_1\right\|^2 + \left\|F^\delta g_2 - \phi_z\right\|^2$$

First one should remark that we have used the same parameter, η in front of all the terms but it could have been chosen with a different value for each term (as long as it stays between 0 and 1 for the theory). We use again our heuristic to set $\alpha = \frac{\beta_2}{\|F\|}$. We choose a specific balance between the terms involving g_1 and $H_m g_1$. We decide to choose $\alpha_1 = \alpha_2 = \alpha$ and $\beta_1 = \alpha\delta/\alpha_3$ and therefore keep the regularizing power used to find the initial guess. The parameters set, we used a newton method to minimize J_α^δ.

A second solution we have experienced is to alternatively minimize J_α^δ as a function of g_2 with $\alpha_3 = \alpha_1 = 0$ and to minimize the same Tikhonov functional we used to find an initial guess g_1. This will impose $\left\|g_1^{z,\beta_1,\delta}\right\| = \left\|g_2^{z,\beta_2,\delta}\right\|$ and limit the number of parameters to set.

A third solution closely related to our heuristic for symmetric factorization, we have set α_3 to 1 and $\alpha_1 = \alpha_2 = \alpha$ where α is chosen to be equal to $max(\beta_1,\beta_2)/\left\|F^\delta\right\|$

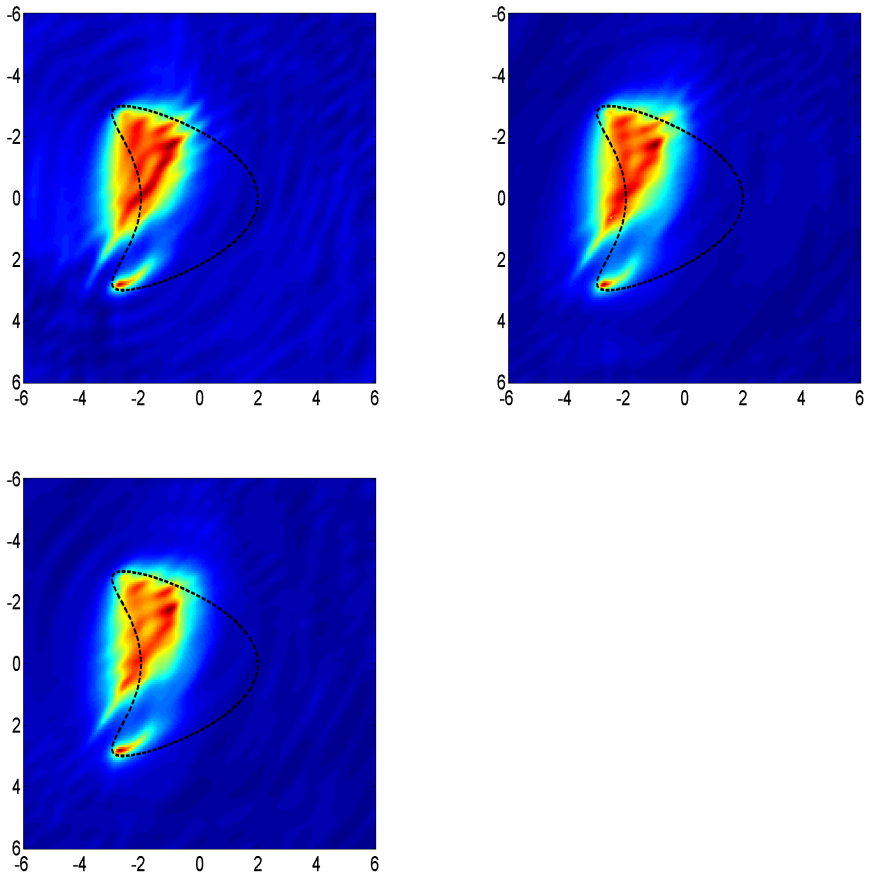

Figure 4.10: The three proposed methods for an aperture of $\Gamma_m = [\pi/4, 5\pi/4[$ and $Gamma_s = -\Gamma_m$.

All those three methods give similar results as shown on figure 4.10. In the following we will show only the results of the first method. In order to perform the Newton method we need to compute the gradient and the Hessian which we explicit in the following for the original cost functional, both gradient and Hessian can be easily derive from those formulas. If $\cdot$ is the dot product without conjugate, ^{t} the transposition and by * the classical transpose-conjugate, we can rewrite $J^\delta_\alpha(\phi, \cdot)$:

$$\alpha|\bar{g}^t \cdot (F^\delta g)| + \alpha^{1-\eta}|\bar{g}^t \cdot (F^\delta g - \phi)| + \delta\alpha^{1-\eta}\left\|F^\delta\right\| g^* \cdot g + \alpha^{1-\eta}(Hg)^* \cdot (Hg) + (F^\delta g - \phi)^* \cdot (F^\delta g - \phi)$$

where we use the matrix:

$$F^\delta = \begin{bmatrix} 0 & F^\delta_{\mathrm{N}} \\ 0 & 0 \end{bmatrix} \text{ and } H = \begin{bmatrix} H_m & -H_s \end{bmatrix} \text{ and } g = \begin{bmatrix} g_2 \\ g_1 \end{bmatrix} \text{ and } \phi = \begin{bmatrix} \Phi_z \\ 0 \end{bmatrix}$$

Using this notation we can compute following the framework of [50] the gradient

$$\delta\alpha^{1-\eta}\left\|F^{\delta}\right\| g + F^{\delta *}(F^{\delta}g-\phi) + \alpha^{1-\eta}H^{*}Hg + \alpha\frac{\overline{\bar{g}^{t}\cdot(F^{\delta}g)}F^{\delta}g + (\bar{g}^{t}\cdot(F^{\delta}g))F^{\delta *}g}{|\bar{g}^{t}\cdot(F^{\delta}g)|} + \alpha^{1-\eta}\frac{\overline{(\bar{g}^{t}\cdot(F^{\delta}g-\phi))}(F^{\delta}g-\phi) + (\bar{g}^{t}\cdot(F^{\delta}g-\phi))F^{\delta *}g}{|\bar{g}^{t}\cdot(F^{\delta}g-\phi)|}$$

and the Hessian,

$$\begin{aligned}
&\delta\alpha^{1-\eta}\left\|F^{\delta}\right\| Id + F^{\delta *}F^{\delta} + \alpha^{1-\eta}H^{*}H + \alpha\frac{\overline{\bar{g}^{t}\cdot(F^{\delta}g)}F^{\delta} + (\bar{g}^{t}\cdot(F^{\delta}g))F^{\delta *} + F^{\delta}gg^{*}F^{\delta *} + F^{\delta *}gg^{*}F^{\delta}}{|\bar{g}^{t}\cdot(F^{\delta}g)|}\\
&-\alpha\frac{(\overline{\bar{g}^{t}\cdot(F^{\delta}g)}F^{\delta}g + (\bar{g}^{t}\cdot(F^{\delta}g))F^{\delta *}g)(\overline{\bar{g}^{t}\cdot(F^{\delta}g)}F^{\delta}g + (\bar{g}^{t}\cdot(F^{\delta}g))F^{\delta *}g)^{*}}{2|\bar{g}^{t}\cdot(F^{\delta}g)|^{\frac{3}{2}}}\\
&+\alpha^{1-\eta}\frac{\overline{(\bar{g}^{t}\cdot(F^{\delta}g-\phi))}F^{\delta} + (\bar{g}^{t}\cdot(F^{\delta}g-\phi))F^{\delta *} + (F^{\delta}g-\phi)(g^{*}F^{\delta *}-\phi^{*}) + F^{\delta *}gg^{*}F^{\delta}}{|\bar{g}^{t}\cdot(F^{\delta}g-\phi)|}\\
&-\alpha^{1-\eta}\frac{(\overline{(\bar{g}^{t}\cdot(F^{\delta}g-\phi))}(F^{\delta}g-\phi) + (\bar{g}^{t}\cdot(F^{\delta}g-\phi))F^{\delta *}g)(\overline{(\bar{g}^{t}\cdot(F^{\delta}g-\phi))}(F^{\delta}g-\phi) + (\bar{g}^{t}\cdot(F^{\delta}g-\phi))F^{\delta *}g)^{*}}{2|\bar{g}^{t}\cdot(F^{\delta}g-\phi)|^{\frac{3}{2}}}
\end{aligned}$$

We apply those techniques to the case of back scattering data which is when $\Gamma_m = -\Gamma_s$, for apertures $\Gamma_s = [\pi/2, 3\pi/2[$, $[3\pi/4, 5\pi/4[$ and $[7\pi/8, 9\pi/8[$. The result are shown in figures 4.11 for the kite example and 4.12 for a domain Σ which occupies the whole image and the smallest rectangle that contains D. We also consider the case of Γ_s being either $[\pi/2, 3\pi/2[$, $[3\pi/4, 5\pi/4[$ and $[7\pi/8, 9\pi/8[$ and Γ_m being either $[0, \pi[$, $[\pi/4, 3\pi/4[$ and $[3\pi/8, 5\pi/8[$. The results are shown in figures 4.13 and 4.14. On those simulation the size of Σ has no clear impact therefore we will only show simulation for the large grid.

Figures 4.15,4.16,4.17,4.18,4.19 and 4.20 consider backscattering data from aperture of the same size as previously, but rotated around the obstacle. We see the strong dependency with the mean direction of the aperture. The fact that the results are coherent with the aperture we consider lets us think that non symmetric aperture is intrinsically worst than symmetric one. Connected to that subject in [27] they study invisibility for a finite number of incident direction and demonstrate that imposing invisibility in symmetric direction is equivalent to impose invisibility in all direction. Meaning that there is more information inside symmetric-factorization like farfield operator than any other setting of sources and measurements.

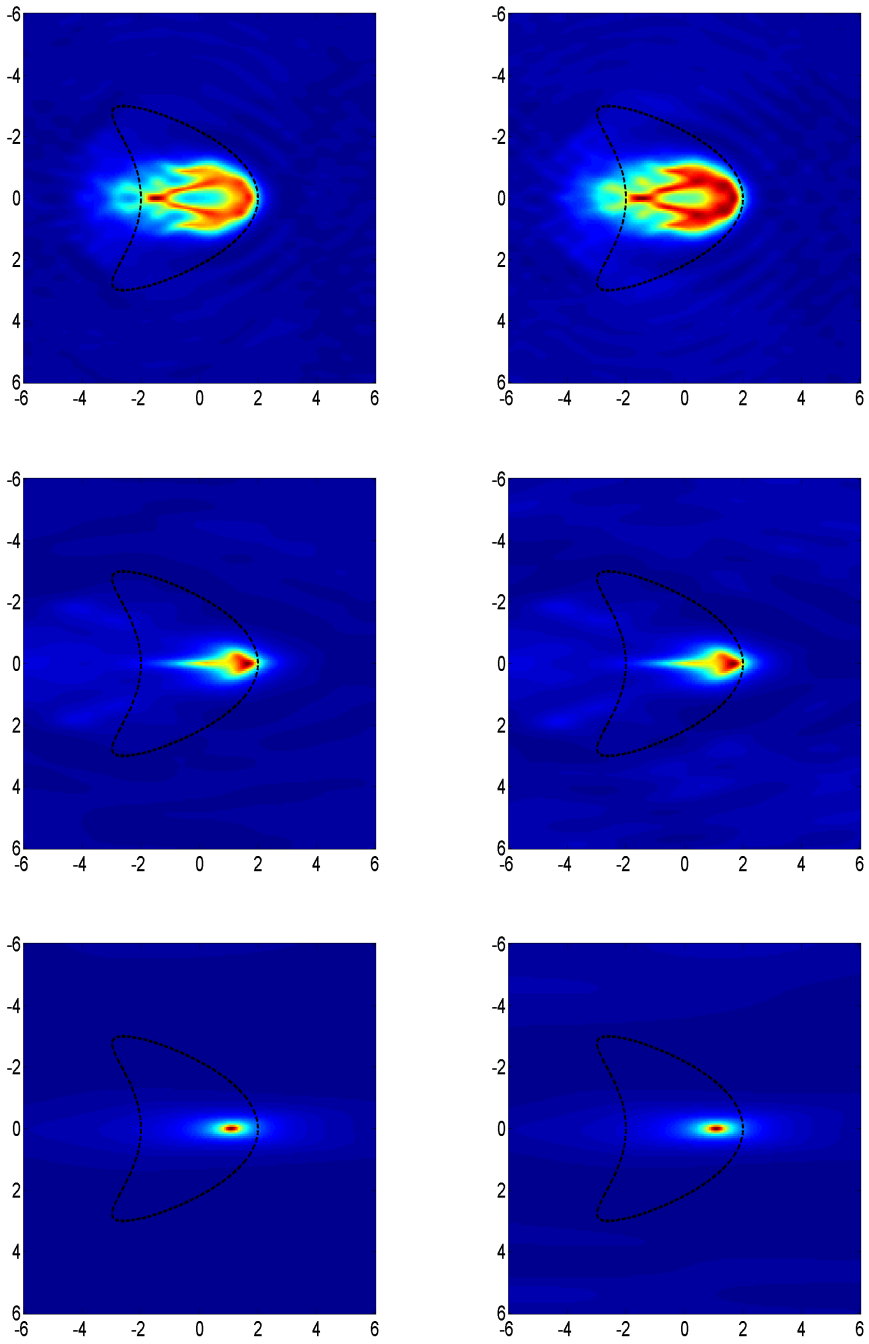

Figure 4.11: $\mathcal{I}$ computed on the left with a large Σ and with on the right with a small one. From up to down the apertures are : $\Gamma_s = [\pi/2, 3\pi/2[$, $[3\pi/4, 5\pi/4[$ and $[7\pi/8, 9\pi/8[$

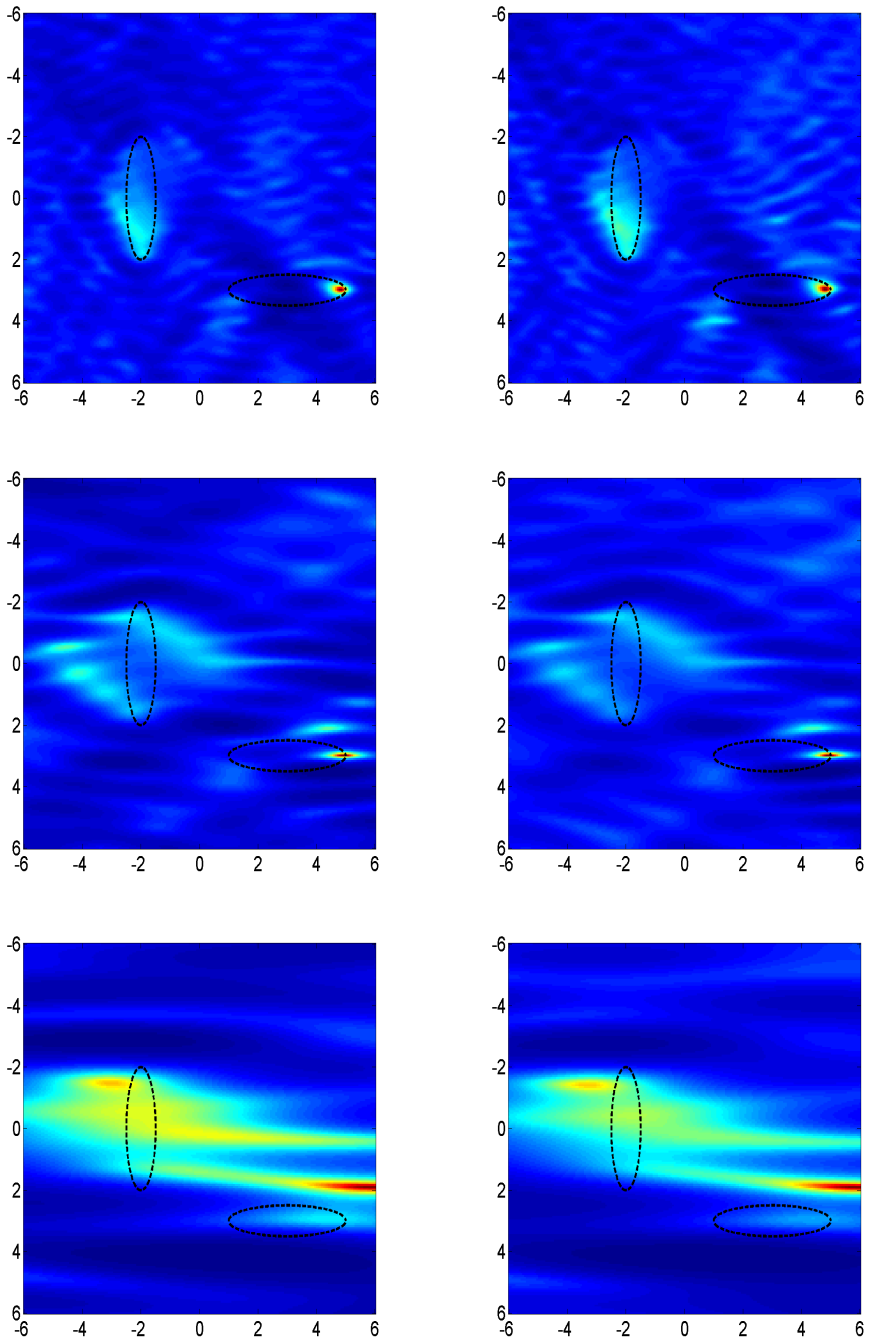

Figure 4.12: $\mathcal{I}$ computed on the left with a large Σ and with on the right with a small one. From up to down the apertures are : $\Gamma_s = [\pi/2, 3\pi/2[$, $[3\pi/4, 5\pi/4[$ and $[7\pi/8, 9\pi/8[$.

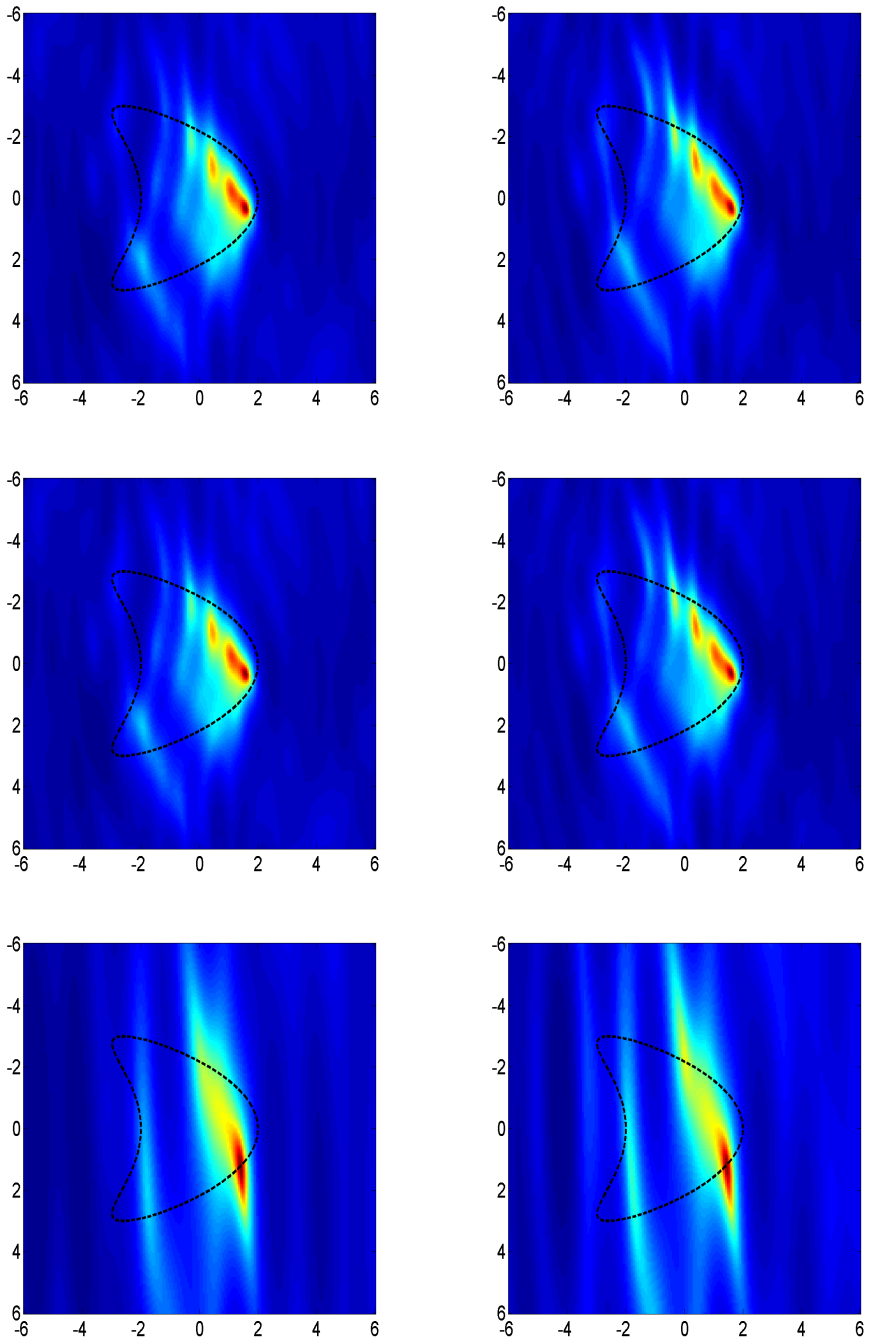

Figure 4.13: $\mathcal{I}$ computed on the left with a large Σ and with on the right with a small one. From up to down the apertures are :$\Gamma_s = [\pi/2, 3\pi/2[$, $[3\pi/4, 5\pi/4[$ and $[7\pi/8, 9\pi/8[$ and $\Gamma_m = [0, \pi[$, $[\pi/4, 3\pi/4[$ and $[3\pi/8, 5\pi/8[$

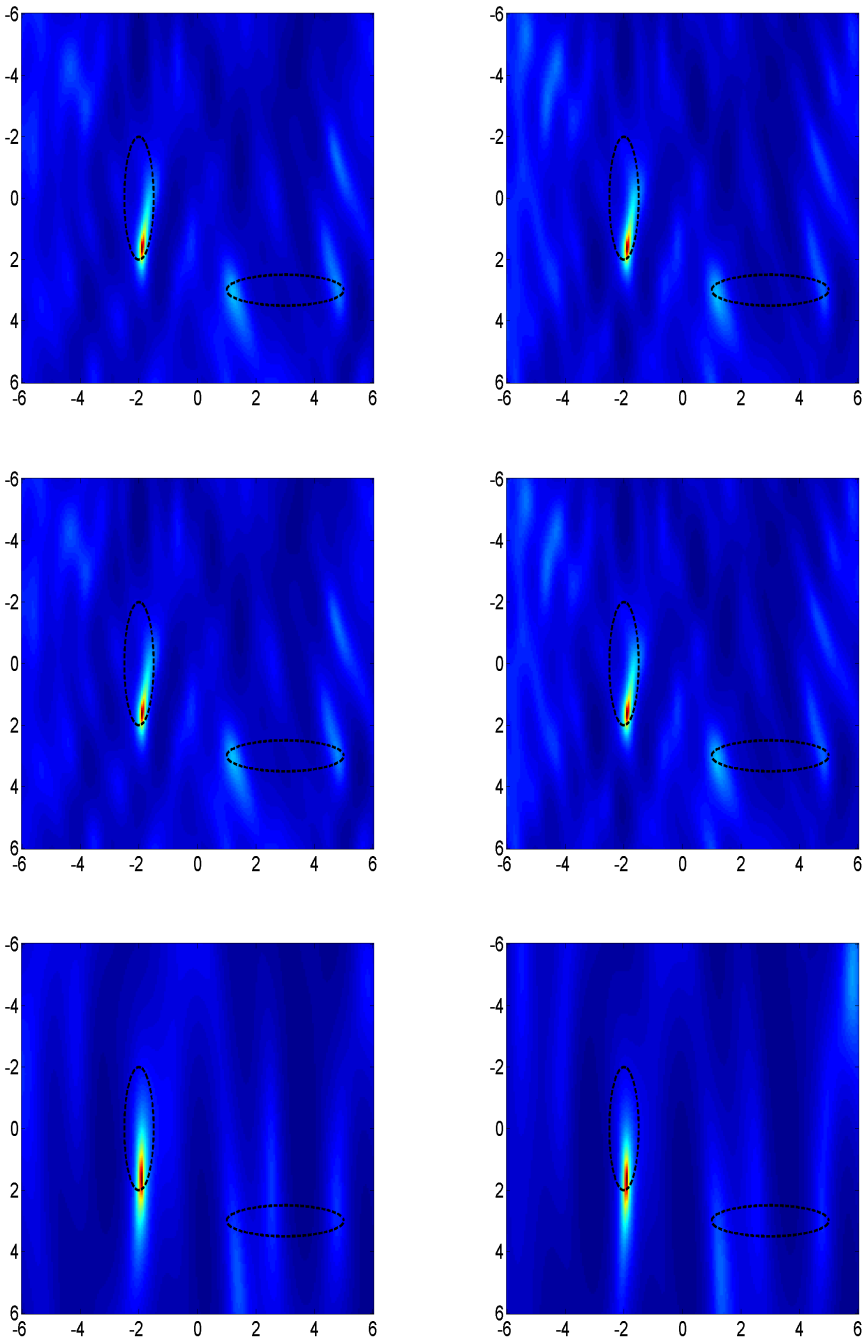

Figure 4.14: $\mathcal{I}$ computed on the left with a large Σ and with on the right with a small one. From up to down the apertures are :

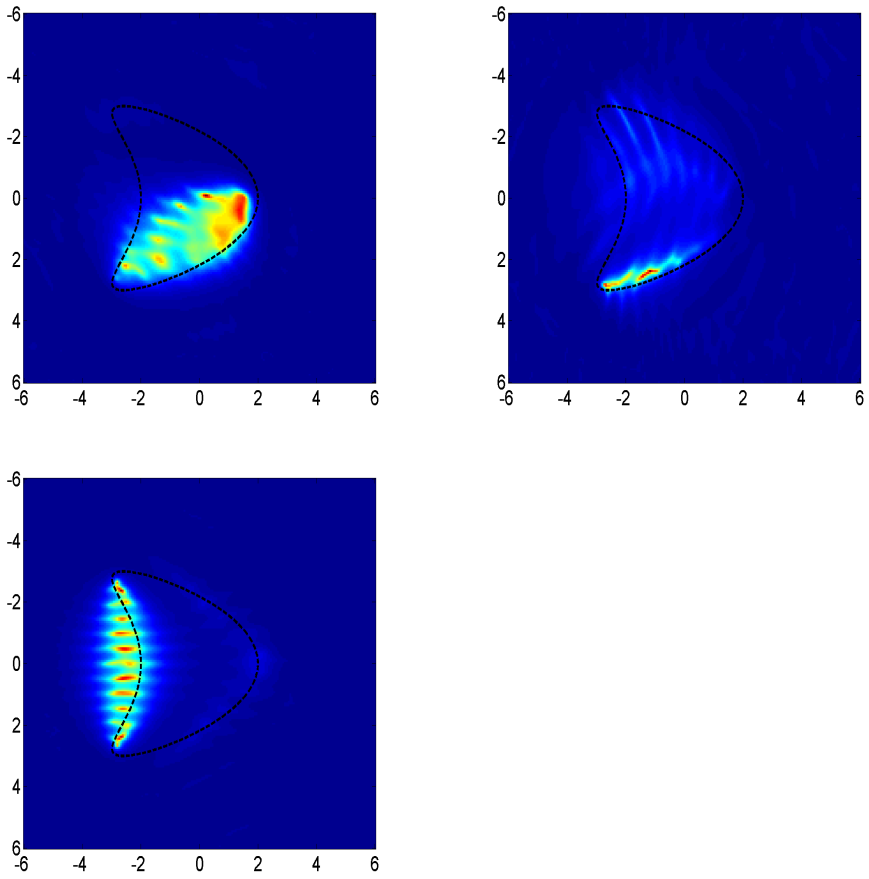

Figure 4.15: $\mathcal{I}$ computed with Σ equals the full grid. From left to right and up to down the aperture are : $\Gamma_s[3\pi/4, 7\pi/4[$, $[\pi, 2\pi[$ and $[-\pi/2, \pi/2[$ and $\Gamma_m = \Gamma_s + \pi$

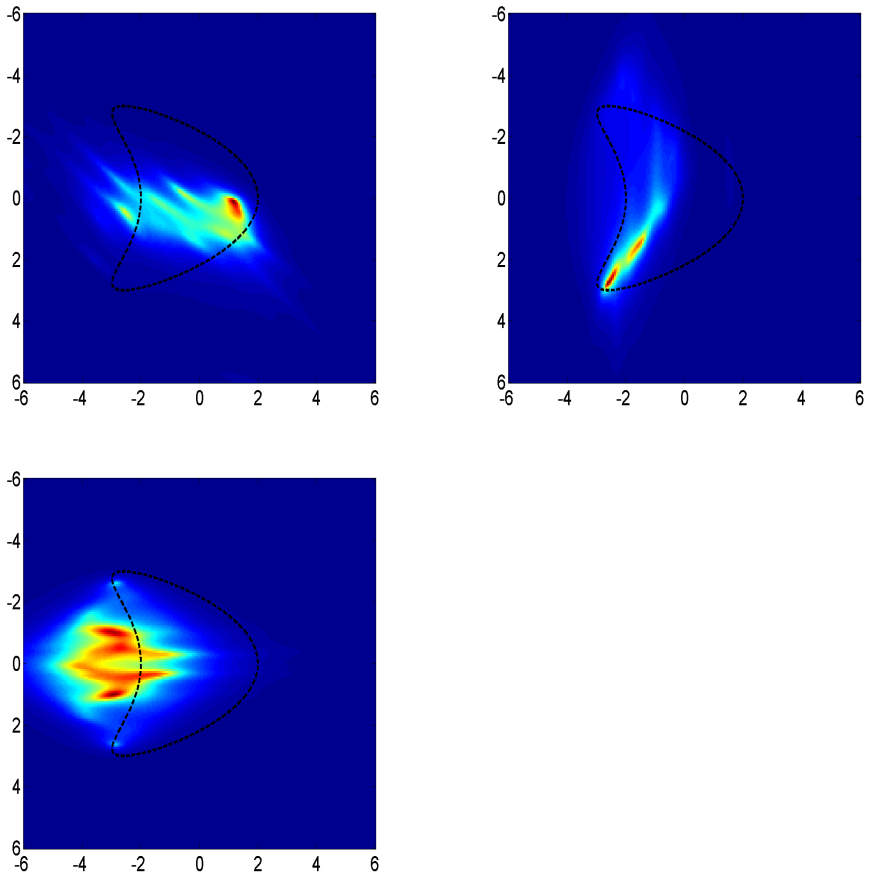

Figure 4.16: $\mathcal{I}$ computed with Σ equals the full grid. From left to right and up to down the aperture are : $\Gamma_s = [\pi, 3\pi/2[$, $[5\pi/4, 7\pi/4[$ and $[7pi/4, \pi/4[$ and $\Gamma_m = \Gamma_s + \pi$

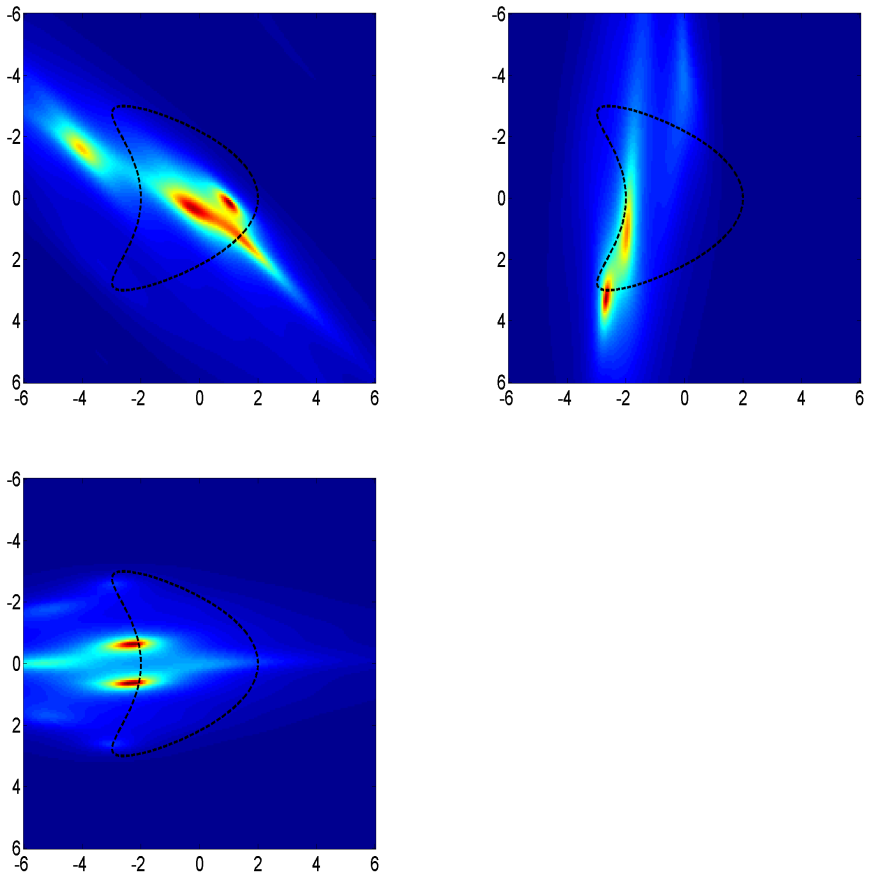

Figure 4.17: $\mathcal{I}$ computed with Σ equals the full grid. From left to right and up to down the aperture are : $\Gamma_s = [7\pi/8, 9\pi/8[$, $[11\pi/8, 13\pi/8[$ and $[-\pi/8, \pi/8[$ and $\Gamma_m = \Gamma_s + \pi$

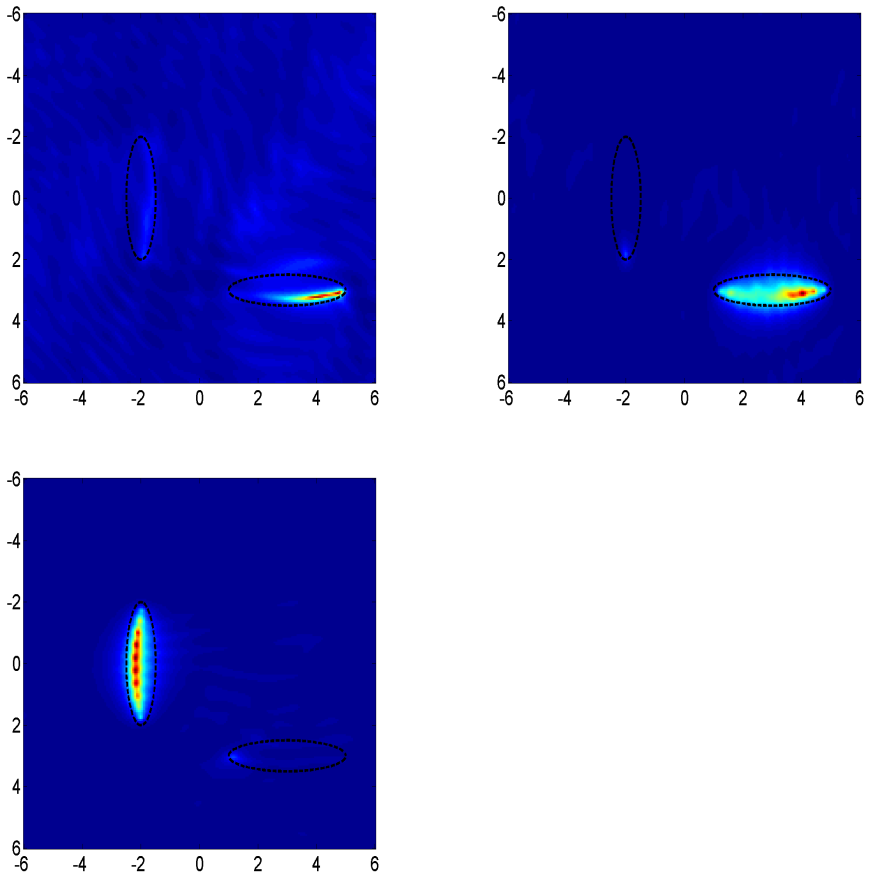

Figure 4.18: $\mathcal{I}$ computed with Σ equals the full grid. From left to right and up to down the aperture are : $\Gamma_s = [3\pi/4, 7\pi/4[$, $[\pi, 2\pi[$ and $[-\pi/2, \pi/2[$ and $\Gamma_m = \Gamma_s + \pi$

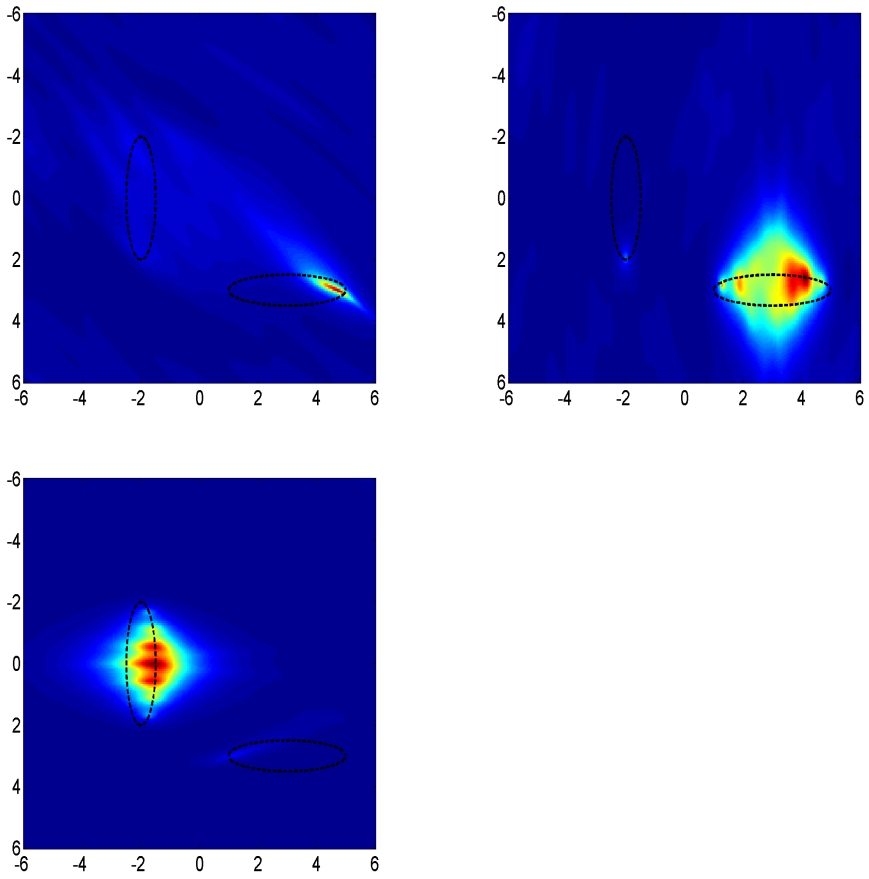

Figure 4.19: $\mathcal{I}$ computed with Σ equals the full grid. From left to right and up to down the aperture are : $\Gamma_s = [\pi, 3\pi/2[$, $[5\pi/4, 7\pi/4[$ and $[7\pi/4, \pi/4[$ and $\Gamma_m = \Gamma_s + \pi$

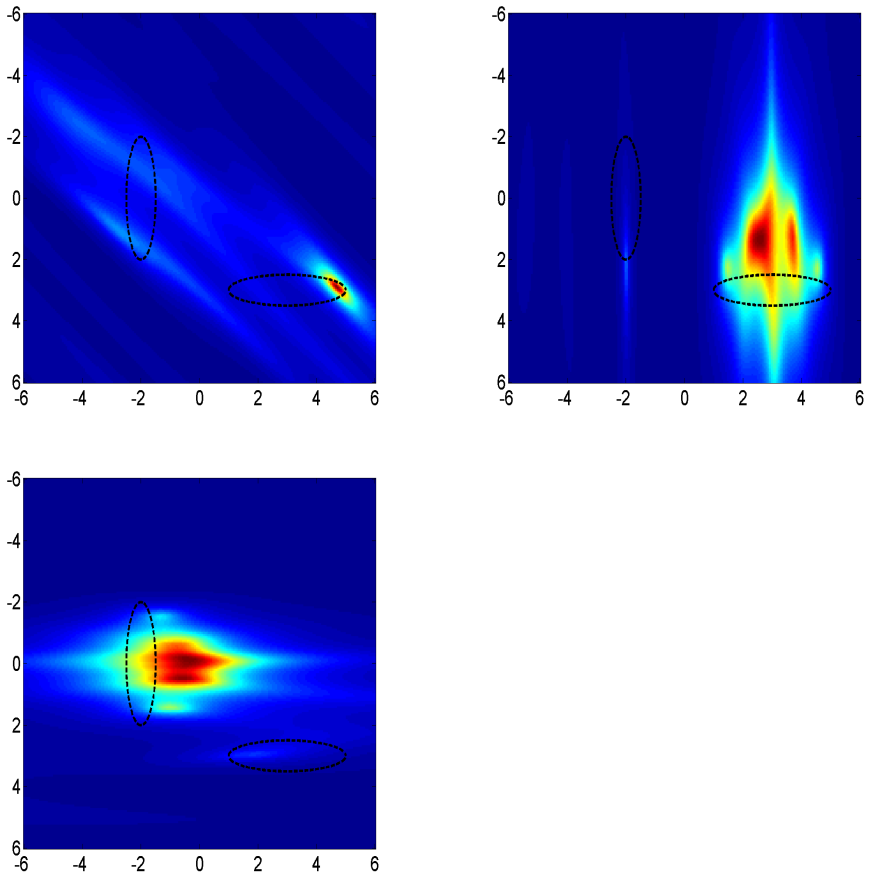

Figure 4.20: $\mathcal{I}$ computed with Σ equals the full grid. From left to right and up to down the aperture are : $\Gamma_s = [7\pi/8, 9\pi/8[$, $[11\pi/8, 13\pi/8[$ and $[-\pi/8, \pi/8[$ and $\Gamma_m = \Gamma_s + \pi$

We should mention that we have tried to use differential measurement with backscattering data but it did not work. At this point we do not know if this failure is due to the numerical difficulties in balancing the regularization term or to the intrinsic difficulties of this setting.

We believe that the numerical results could be improve if we have a better understanding of the optimal balance between all regularization terms. One may also think of an iterative scheme that will improve Σ using previously computed indicator function. An other way to simplify numerical simulation will be to have a term that enforce g_1 with a data fidelity term similar to the farfield equation.

Chapter 5

Numerical application to concrete

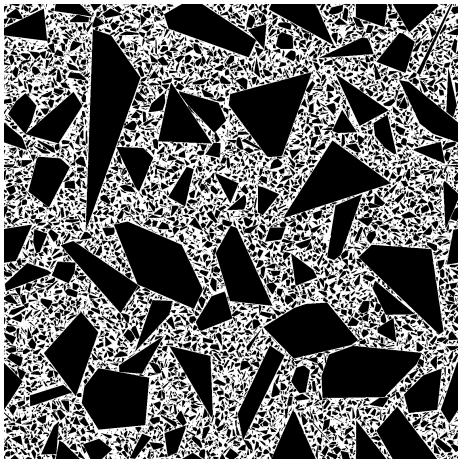

Contents

This chapter is divided into two main parts. In the first one we explain how we generate concrete like microstructures using the CAO software Salomé. This part of the thesis takes the form of a software that also can be used in the departement STEP of EDF R&D for other projects on concrete and non destructive testing. This software offers the possibility to fill a chosen volume with aggregates that respect a given distribution of size, which is assumed to be known from the engineering of concrete. In the second part of this chapter we give numerical examples of the application of the differential imaging technique introduced in chapter 3. We shall consider examples related to a change in the index of refraction of the medium and as a perspective we shall also numerically test the method for cracks that appeared between the two measurements campaigns. We give numerical results for both full and limited apertures.

5.1 Numerical generation of concrete like microstructures

The software that simulates realistic microstructures of concrete can generate a microstructure made of aggregates that follow a given size distribution. This microstructure can fill a given space in 3D. This space can be complex due to the presence of others inclusions such as reinforcing bars or defects. One should then be able to mesh the whole medium with proper labelling of the different components. The latter step is important for instance if one would like to use some finite element method to simulate wave propagation in the concrete structure.

This software is developed in Python as a module of the open-source CAO software Salomé. Its purpose is to construct numerically a realistic distribution of aggregates which we will call microstructure. The numerical microstructure should follow a given statistical distribution of size as this property is known in practice (and even mandatory through standards). We will also assume that the space is occupied by the aggregates uniformly with respect to their size. The algorithm takes as input a given region in space and a given statistical distribution of size. The global strategy is to fill the space from large to small aggregates by choosing random positions and by ensuring that aggregates do not intersect with the boundary of the domain and with previously inserted aggregates.

This strategy can be applied if one is able to test easily for intersections in 3D and if one has a fast generator of shapes of a given size.

5.1.1 Examples of Geometries

The "user-friendly" interface of Salomé makes it possible to easily specify a given canonical geometry. It also allows one to include interior components such as reinforcing steel bars in the case of concrete. We use this function to also insert defects that will not intersect the aggregates. The addition of structures inside the exterior shape before filling the space with aggregates is relevant for reinforcing steel bars. However this strategy seems more arguable for defects. We proceed in this way for three reasons. First it is more convenient from the practical point of view to put the defect in a known position. Second, considering rules on how one should incorporate defects inside a microstructure goes far beyond the scope of this thesis. Third, if the defect has a small volume, its influence on the microstructure would be negligible.

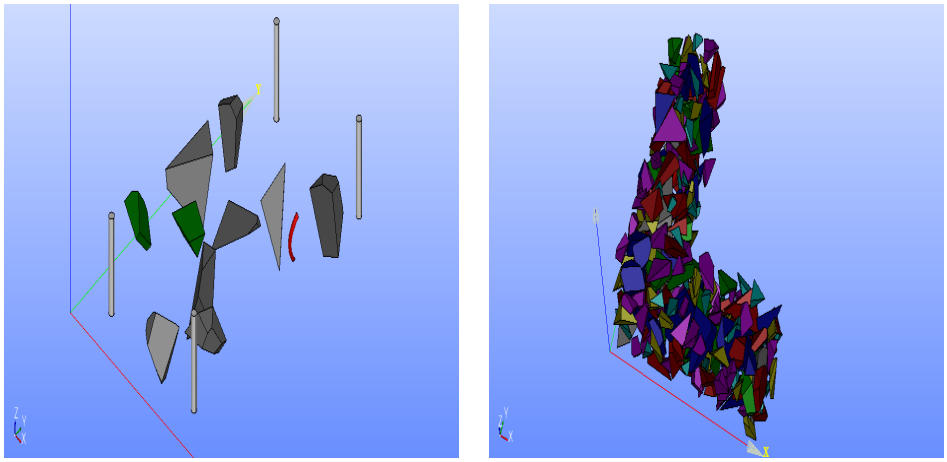

Figure 5.1: On the left we see a structure with 4 small grey cylinders and a red arc which are placed before the insertion of some aggregates. On the right we see an L-shape domain filled with aggregates.

5.1.2 Generation of shapes

We rely on previous works in the department of materials at EDF R&D to choose what might be an admissible shape for an aggregate. We consider two types of aggregates that feature two possible shape generation algorithms. We choose, as Julie Escoda's PhD [29], the radius of the larger sphere strictly included inside a shape as the characteristic size value that is used in the given distribution of size.

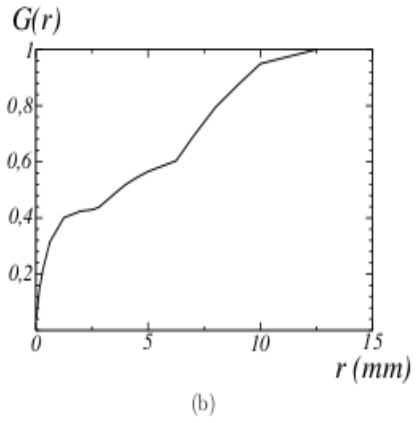

Figure 5.2: The cumulative distribution of size of aggregates. r is the radius of the largest ball strictly include inside the aggregate.

First we consider the case where one has a library of shapes. In our case we (have the chance to) use the library created by Julie Escoda during her PhD [29]. The generation of aggregate is

then easy as it reduces to choose (randomly) one of the shapes and to adjust its volume to the desired one. We should stress that there are two possible representations for a polyhedron: It can be stored either as the intersection of half spaces (meaning that one stores a plan and a side) or as a set of points and vertices. The second representation induces a significant gain of time in the test of intersections (using the intersection procedure describe below). The library was translated into this second representation as an offline computation, we also computed offline the radius for all shapes in the library.

The other possibility, proposed in the thesis of Francis Lavergne [42], is to generate the shape randomly when needed. In this setting he chose to generate points from lognormal distribution and to then construct a shape by taking the convex hull of the randomly generated points. Playing with the parameter of the lognormal distribution allows one to have different shapes of aggregates. For example, if one draws a large number of points from the lognormal distribution, the obtained shape is more likely to be smooth. From an implementation point of view, those steps (drawing points and taking the convex hull) can be done very efficiently using inbuilt function from SciPy package of Python. To adjust the shape to the desired size in order to comply with the distribution of size we need to have an efficient way to compute the radius of the larger sphere strictly included inside the shape. Finding this radius for a convex polyhedron can be cast to a Linear Programming problem as shown in [13] and can solved efficiently using the open source package LPSOLVE. To summarize, the algorithm to generate a shape "centered" at the origin is the following:

1. We randomly draw two angles $\theta \sim \mathcal{U}([0;\ 2\pi[)$ and $\phi \sim \mathcal{U}([0;\ \pi[)$, which gives a direction $D = [\sin\theta\cos\phi, \sin\theta\sin\phi, \cos\theta]$.

2. We draw from a lognormal distribution a distance from the origin, $d \sim Log - \mathcal{N}(\mu,\ \sigma^2)$.

3. We obtain a point $P = [d\sin\theta\cos\phi, d\sin\theta\sin\phi, d\cos\theta]$.

4. Repeat the previous steps N times and compute the convex hull of those points.

5. Use a linear program to determine the radius of the largest sphere contained inside the convex hull.

6. Build a Salomé object and compute its bounding box.

Finally we construct this shape as a polyhedron in the CAO framework of Salomé.

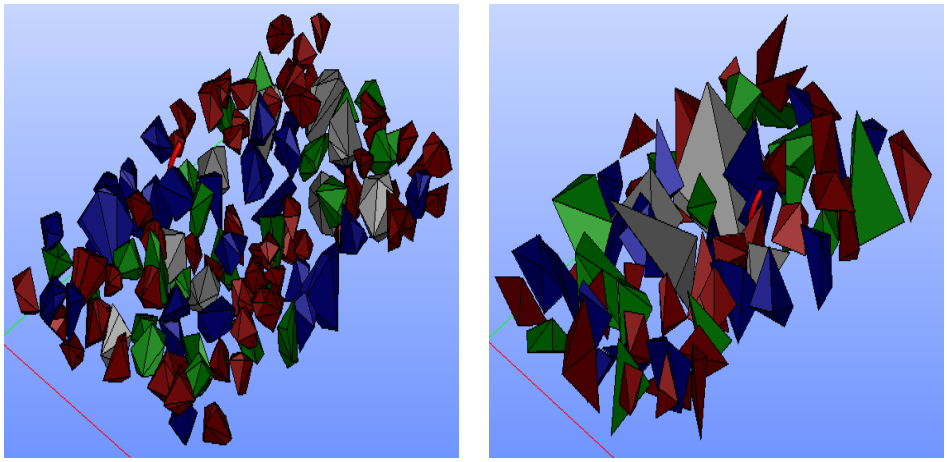

Figure 5.3: Smoother aggregates on the left, they are generated using more random points before taking their convex hull.

5.1.3 Insertion of aggregates

In the previous subsection we saw how we created the shapes aggregates. To obtain a microstructure that will follow a given distribution of radii we entirely fill the given volume (which might be complicated) starting from the largest radius to the smallest one. The algorithm follows these steps for each radius of the distribution

1. From the distribution and the proportion of aggregates compute the volume occupied by each class of aggregate.
2. Scale a shape (randomly generated as explained in 5.1.2) to comply with the current size of the distribution.
3. Draw at random uniformly a position in space for the shape.
4. Verifies that the current shape does not intersect any existing object (given exterior and interior objects or previously set aggregates)
    - If there is no intersection, then the shape is included as part of the microstructure and start again until all the distribution is finished.
    - If there is an intersection, then try another position or change the shape (after too many failures the algorithm just stops)

As we do not expect any specific position for the shape, we draw the position at random from a uniform distribution. The fact that we have to check for intersection with all existing objects requires an efficient procedure. In practice we actually use the built in distance function between two CAO object of Salomé and fix a minimal distance between objects bellow which we consider that there is an intersection. This minimal distance has no physical significance as far as we know.

Clearly our strategy will induce a bias when fitting the distribution as we only stop when we have reached the prescribe value, this induces a slight excess in the volume occupied by each class of aggregates. Moreover we can see on the figures that the presence of boundary induces that there is less large aggregates near them as there is less space available near a boundary. This fact is indeed a direct consequence of the filling procedure but it seems that this is also the case in real concrete.

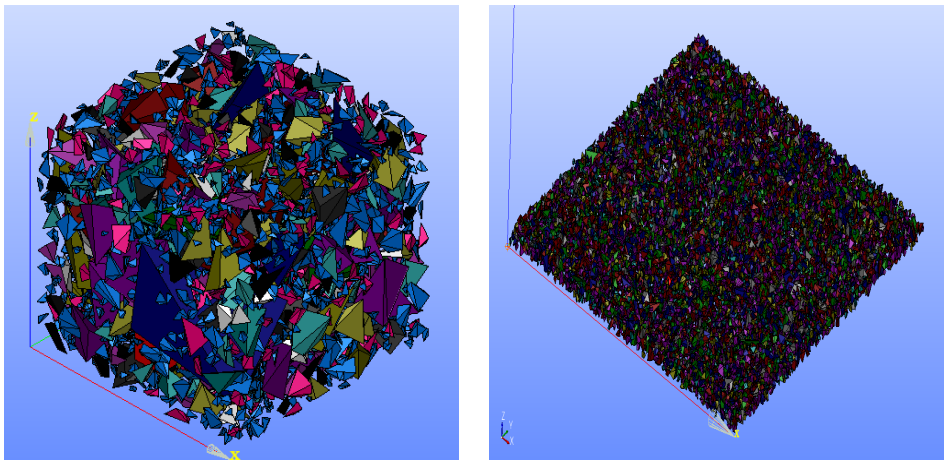

Figure 5.4: Two examples of microstructure

5.1.4 2D cut and meshing

Since our simulations are in 2D, we are interested in creating 2D configurations of concrete. These are simply obtained by taking the intersection of the 3D configuration with a plane. The obtained 2D cut is then meshed according to the frequency range of the numerical simulation and the physical parameters inside the object. In order to have a manageable mesh we also truncate the distribution of aggregates in order to avoid too small aggregates (with respect to the wavelength).

celerity	longitudinal	shear
mortar	$4300m.s^{-1}$	$2500m.s^{-1}$
aggregate	$5700m.s^{-1}$	$3200m.s^{-1}$

Table 5.1: Celerity of the two phases of concrete

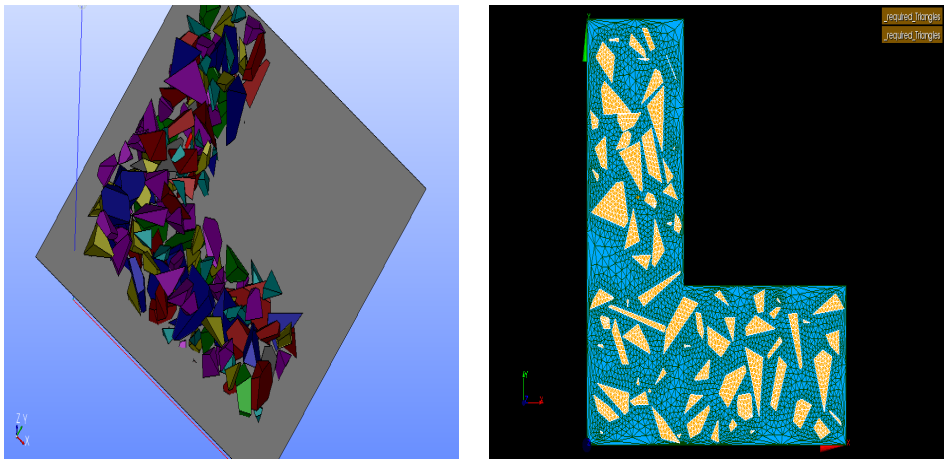

Figure 5.5: Cut of a microstructure by a plane on the left and a mesh of the 2D intersection (for visualization purposes the mesh is coarse)

Currently the mesh is labelled according to the material properties which means that the label of the region reflects the physical parameters that will used in the numerical simulation.

5.2 Numerical simulation and results related to concrete like microstructures

We restrict ourselves to two dimensions and to the scalar wave equation. In this setting taking the value of the celerity of pressure wave in concrete (Table 5.1), for a refractive index of one in cement paste we obtain a refractive index of 0.57 in the aggregates. We consider the medium shown in figure 5.7 and a frequency of 200kHz. This choice of frequency is motivated by the size of the defect we are looking for the experimental value used in [41] and the fact that taking a larger frequency is not realistic as the absorption in concrete gets higher above 500kHz, as shown in figure 5.6.

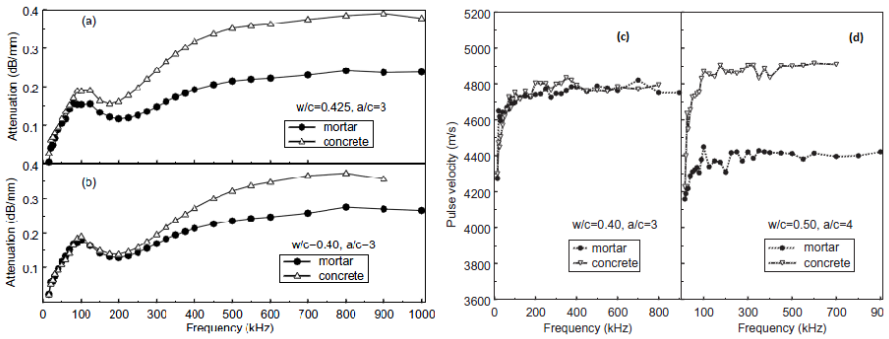

Figure 5.6: Experimental results of the absorption in concrete for a range of frequency [48].

For those numerical values the distribution of aggregates we consider occupies an area of approximately twelve by twelve centimeters, for a wavelength of approximately 2.1 centimeter. We used a finite element method implemented in FreeFem++ [36] to simulate the scattering of plane waves by such a medium. We implemented in FreeFem++ the variational formulation solved by the scattered field, u^s. The domain of computation will be a ball B_R that contains D and we used a Dirichlet-to-Neumann operator on the boundary of B_R to approximate the Sommerfeld radiation condition verified by u^s. For the Dirichlet-to-Neumann operator we used the implementation of Nicolas Chaulet from [22]. Finally the variational formulation we implemented is:

$$\int_{B_R} -\nabla u^s \nabla \psi + k^2 n u^s \psi + \int_{\partial B_R} DtN(u^s)\psi = \int_D k^2(1-n)u^i\psi$$

where the field is discretized using P1 nodal finite elements. Figure 5.7 shows the distribution of the index n in the domain of computation B_R.

Figure 5.7: The index of refraction used for the simulation

Let us consider a change in the medium index of refraction for two aggregates. This type of defect is covered by the theory presented in chapter 3. In figure 5.8 we show the aggregates that have been modified, the index of refraction inside these two aggregates is equal to 10% of the other aggregates index.We denote by F_0^δ and F^δ the multi-static noisy farfield operator associated with measurement before and after the change in the index of refraction of the aggregates. From chapter 3 we should consider :

$$g_0^{\alpha,\delta,z} = arg\min_g \alpha|\big(F_0^\delta g,\, g\big)| + \alpha^\gamma|\big(F_0^\delta g - \phi_z,\, g\big)| + \alpha^{1-\gamma}\delta\|F\|\,\|g\|^2 + \Big\|F_0^\delta g - \phi_z\Big\|^2$$
$$g_0^{\alpha,\delta,z} = arg\min_g \alpha|\big(F^\delta g,\, g\big)| + \alpha^\gamma|\big(F^\delta g - \phi,\, g\big)| + \alpha^{1-\gamma}\delta\|F\|\,\|g\|^2 + \Big\|F^\delta g - \phi\Big\|^2 .$$

As in chapter 4 we compute both minimizers using the second order scheme and we choose α using our heuristic from the Tikhonov-Morozov regularization. Finally we used the following imaging functional in order to retrieve the connected component that contains the change in the

index of refraction.

$$\begin{aligned}
\mathcal{A}(z) &= |\left(F^{\delta} g^{\alpha,\delta,z},\, g^{\alpha,\delta,z}\right)| + \alpha^{-\gamma}\delta \left\| g^{\alpha,\delta,z} \right\|^2, \\
\mathcal{A}_0(z) &= |\left(F_0^{\delta} g_0^{\alpha,\delta,z},\, g_0^{\alpha,\delta,z}\right)| + \alpha^{-\gamma}\delta \left\| g_0^{\alpha,\delta,z} \right\|^2, \\
\mathcal{D}(z) &= |\left(F_0^{\delta}(g_z^{\alpha,\delta,z} - g_0^{\alpha,\delta,z}),\, (g_z^{\alpha,\delta,z} - g_0^{\alpha,\delta,z})\right)| + \delta \left\| g_z^{\alpha,\delta,z} - g_0^{\alpha,\delta,z} \right\|^2 \\
\mathcal{I}(z) &= \frac{1}{\sqrt{\mathcal{A}_0(z) + \mathcal{A}(z)(1 + \mathcal{A}_0(z)\mathcal{D}(z)^{-1})}}.
\end{aligned}$$

In figure 5.9 we show the results obtained by applying the GLSM framework to each set of measurement independently (plot of $\mathcal{A}(z)^{-\frac{1}{2}}$ and $\mathcal{A}_0(z)^{-\frac{1}{2}}$) . Clearly the aggregates are not separated by the indicator function as they are close to each other with respect to the wavelength. In figure 5.10 we show the result obtained using the indicator function that combined both measurement (plot of $\mathcal{I}(z)$). We see that we localize the defect exactly and detect the fact that there are two components. However, the shape is not accurately reconstructed.

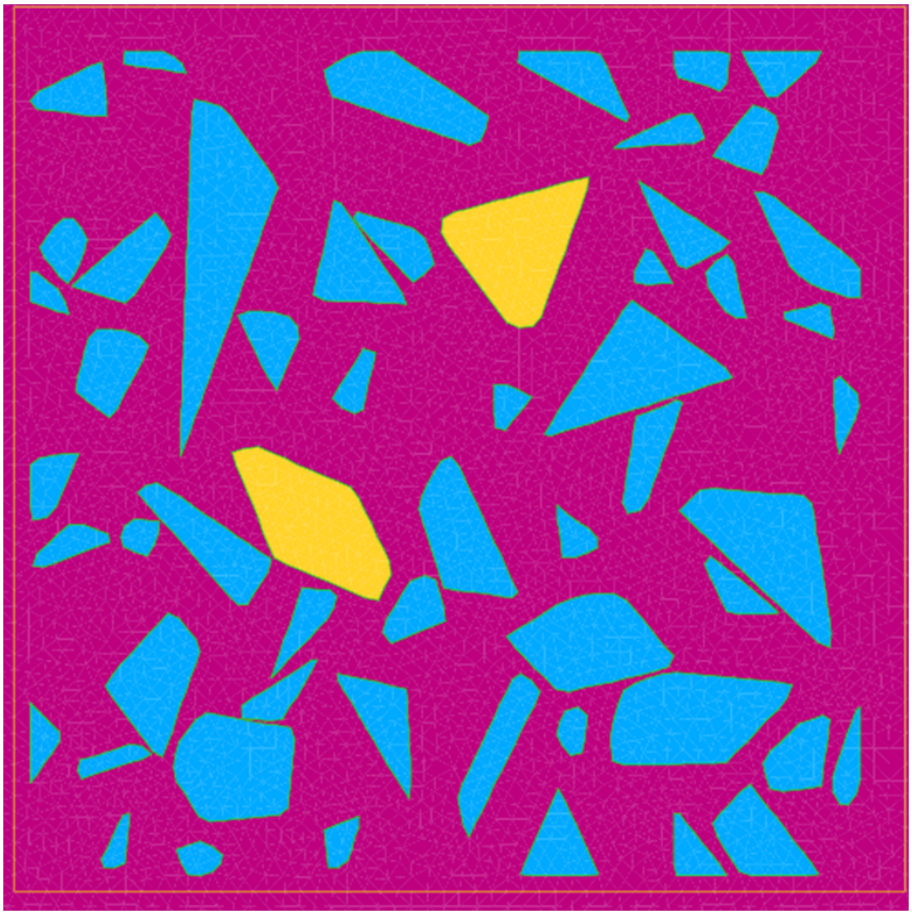

Figure 5.8: The modified aggregates

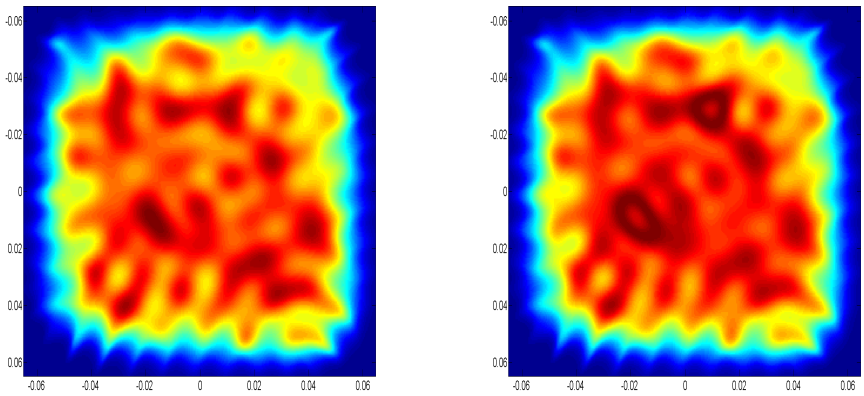

Figure 5.9: On the left the image obtain from the background dataset and on the right from the dataset with the modified aggregates

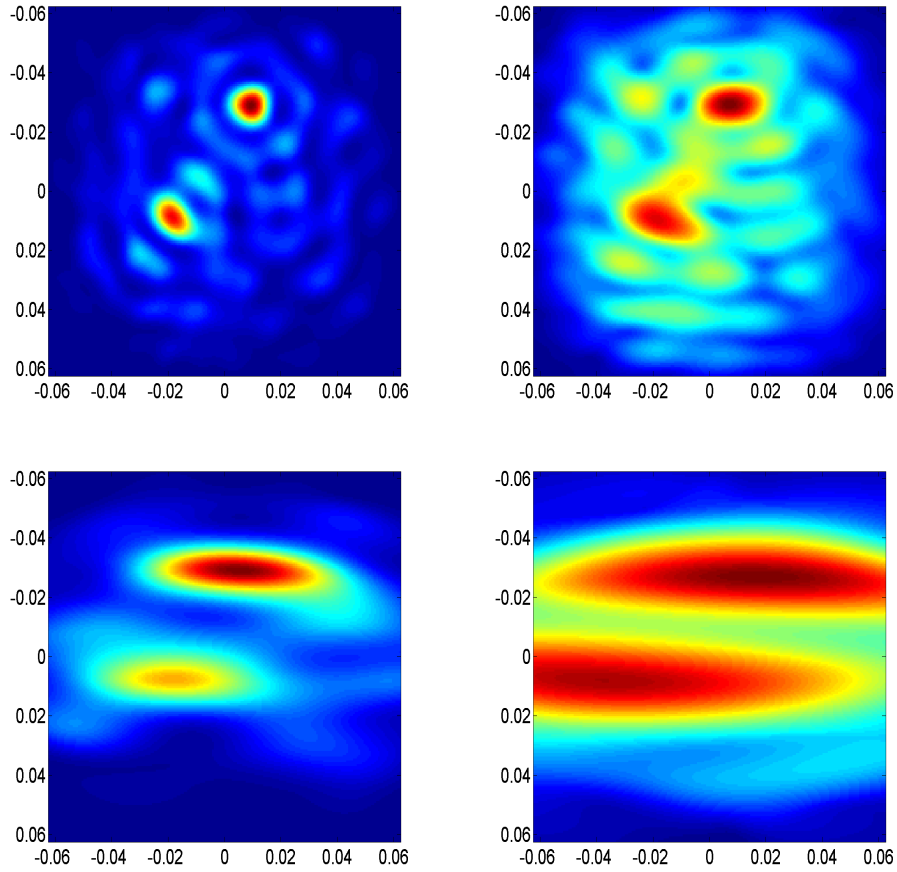

Figure 5.10: The differential indicator function for a change in the index of refraction of two aggregates figure 5.9.From left to right and up to down the apertures are : $[0, 2\pi[$, $[\pi/2, 3\pi/2[$, $[3\pi/4, 5\pi/4[$ and $[7\pi/8, 9\pi/8[$

5.3 Conclusion and perspectives

5.3.1 Numerical experiment with cracks

Defects in concrete are usually cracks therefore in the following we will consider the case of cracks either inside or outside the aggregates.

In figure 5.11 we show a crack with Neumann boundary conditions that appears inside an aggregate. This type of defect is not covered by the theory presented in this thesis. We believe that the coercivity of T should be verified in this case as the crack is stricly included inside the aggregates. The analysis of chapter 3 has to be done for a crack which will lead to the solvability of the interior transmission problem for a crack inside. Such an interior transmission problem has not been studied yet, the result of [17] on interior transmission problem with Dirichlet inclusion inside and the study of interior transmission problem using integral equation method [26] might be adapted to the case of cracks. In figure 5.12 we show that we localize correctly the crack but

with significant artefacts.

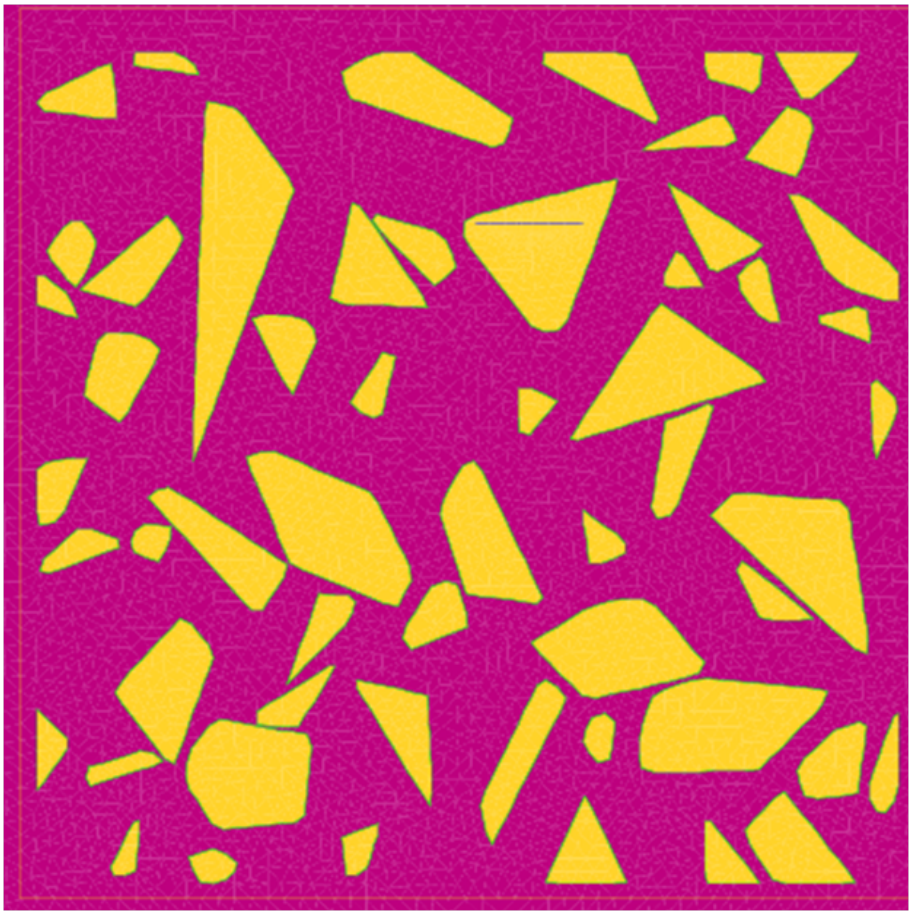

Figure 5.11: The modified medium with a crack inside one of the aggregates (located in the upper part of the figure))

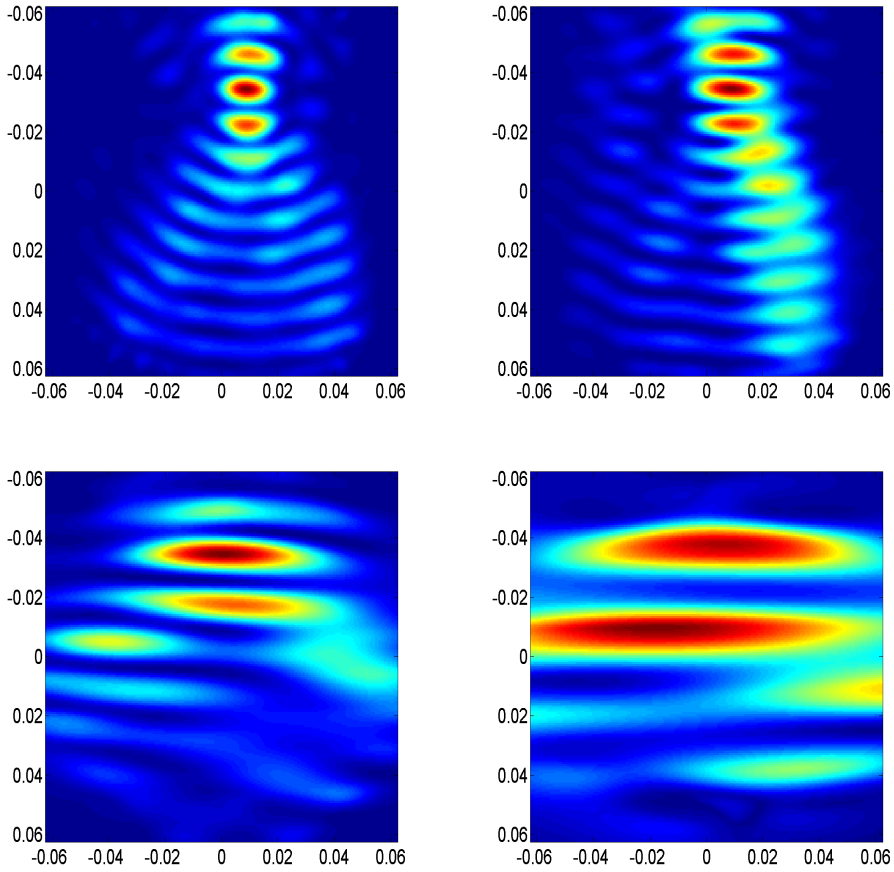

Figure 5.12: The indicator function for differential measurement associated to the defect shown in figure 5.11. From left to right and up to down the aperture are: $[0, 2\pi[$, $[\pi/2, 3\pi/2[$, $[3\pi/4, 5\pi/4[$ and $[7\pi/8, 9\pi/8[$

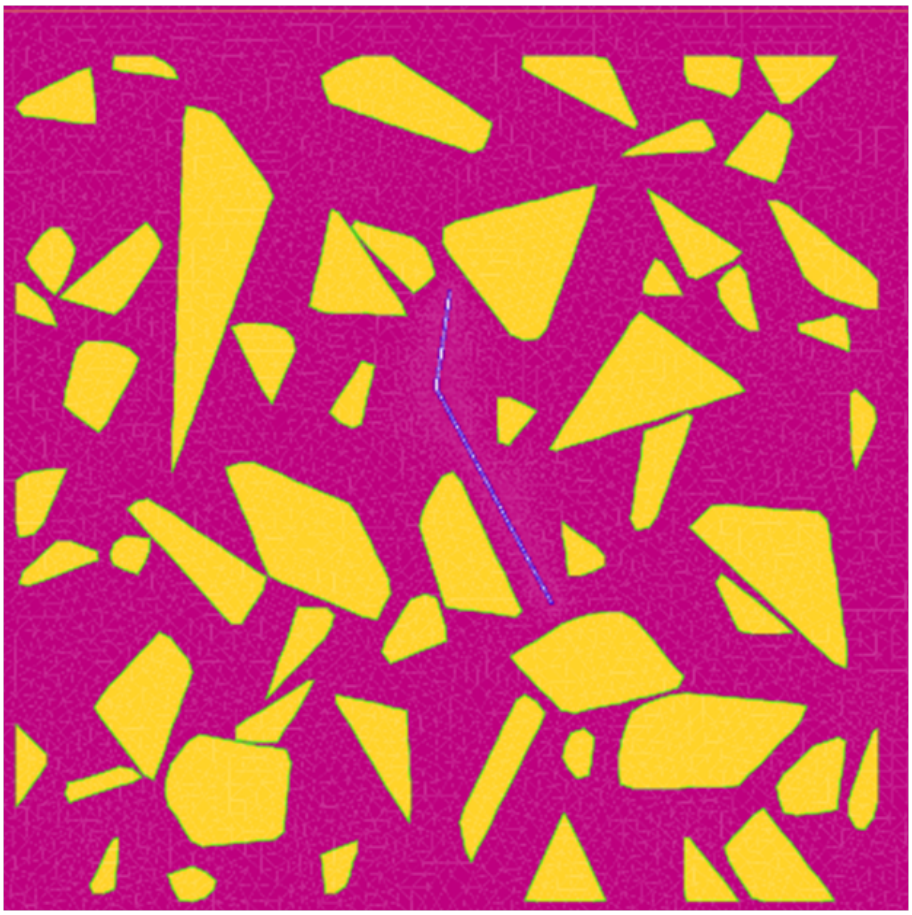

Figure 5.13: The modified medium with a crack outside the aggregates (located in the middle of the figure))

Finally we consider a crack outside the aggregates: Figure 5.13. Imaging of cracks in the vacuum using the factorization method has been studied in [12]. In this paper the factorization and the coercivity of T have been proven. In our case the crack is surrounded with aggregates therefore the coercivity of T will have to be proven in this case (there might be issues similar to the one in section 6.2.2). Since the crack is outside the aggregates as long as the coercivity of T is verified the theory of chapter 3 is valid if we sample with Φ_z. However in [12] they explained that one should consider the GLSM cost functional with $\partial_\nu \Phi_z^\infty$ instead of Φ_z, the analysis of chapter 3 should be verified. To respect their results on cracks, we minimized the GLSM cost functional for both $\partial_x \Phi_z^\infty$ and $\partial_y \Phi_z^\infty$ and we choose the orientation of the derivative of Φ_z^∞ for each z :

$$(u_z, v_z) = arg \min_{u,v \in \mathbb{R}_+ \ s.t. u^2+v^2=1} |\Big(F^\delta(ug_x^{\alpha,\delta,z} + vg_y^{\alpha,\delta,z},\ ug_x^{\alpha,\delta,z} + vg_y^{\alpha,\delta,z}\Big)| + \delta \left\| ug_x^{\alpha,\delta,z} + vg_y^{\alpha,\delta,z} \right\|^2$$

Figures 5.15 and 5.14 show the result of the differential imaging and what we obtain if the crack is not surrounded by aggregates.

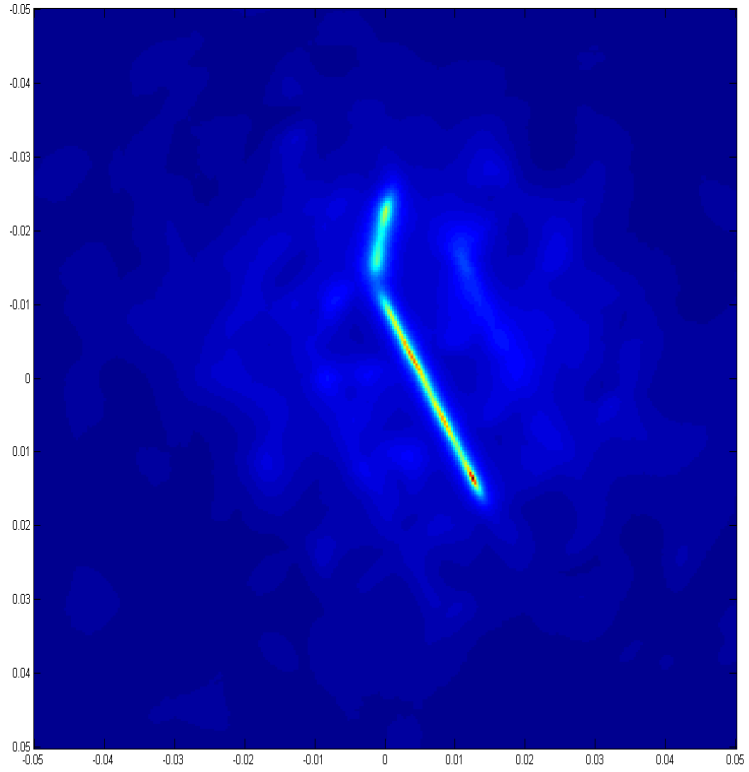

Figure 5.14: The reconstructed crack when there is no aggregates for a full aperture

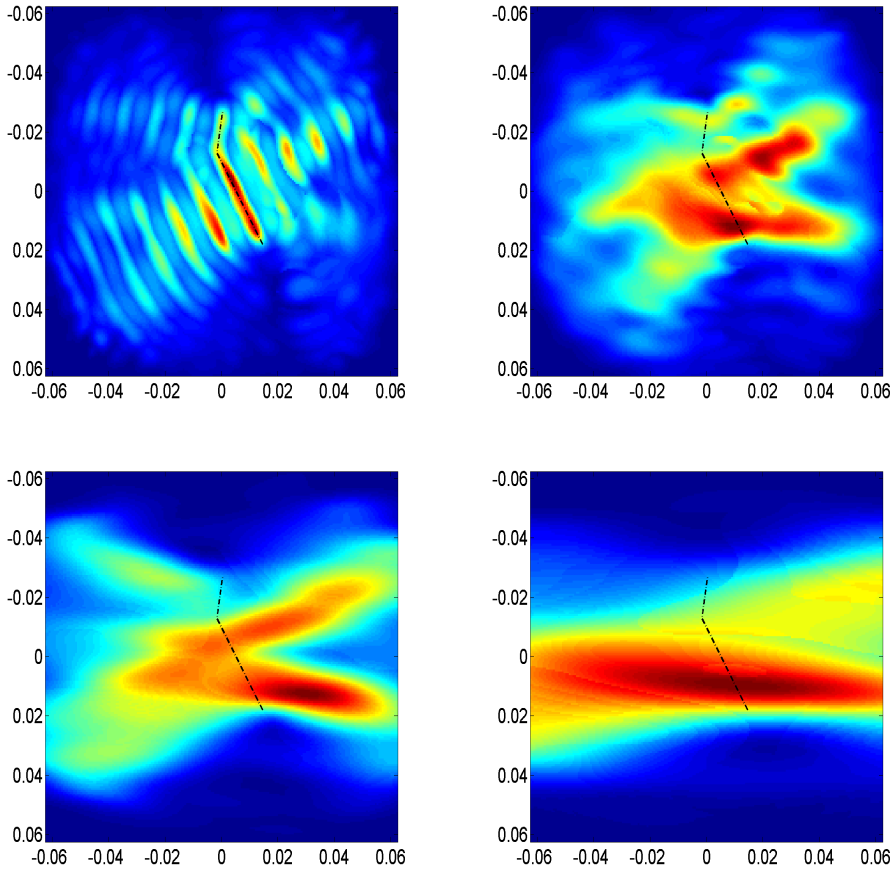

Figure 5.15: TThe indicator function for differential measurement associated to the defect shown in figure 5.13. From left to right and up to down the apertures are : $[0, 2\pi[$, $[\pi/2, 3\pi/2[$, $[3\pi/4, 5\pi/4[$ and $[7\pi/8, 9\pi/8[$

5.3.2 Perspectives

In this chapter we have presented the software that have been built to generate concrete-like microstructure and mesh them. As shown in Figure 5.16 which is taken from a piece of concrete from the mock up VERCORS, we omitted an important third phase in terms of volume which are the pores. In this figure we have segmented the pores using an image processing code that uses the shade to discriminate between pores and other contrasted structure in the image. Pores create a second microstructure made of voids in the figure which are actually mainly filled with water inside concrete. The software can with slight modification cope with this second type of objects, the modified algorithm will work similarly filling the space from large objects (either aggregates or pores) to small ones with the additional phase attribute to all objects. It would be also possible to choose pores from one type of shape and aggregates to another if one has a priori information on the properties of each phase. The main question is whether we will be able, using our current filling scheme, to obtain the density of objects we see on those pictures.

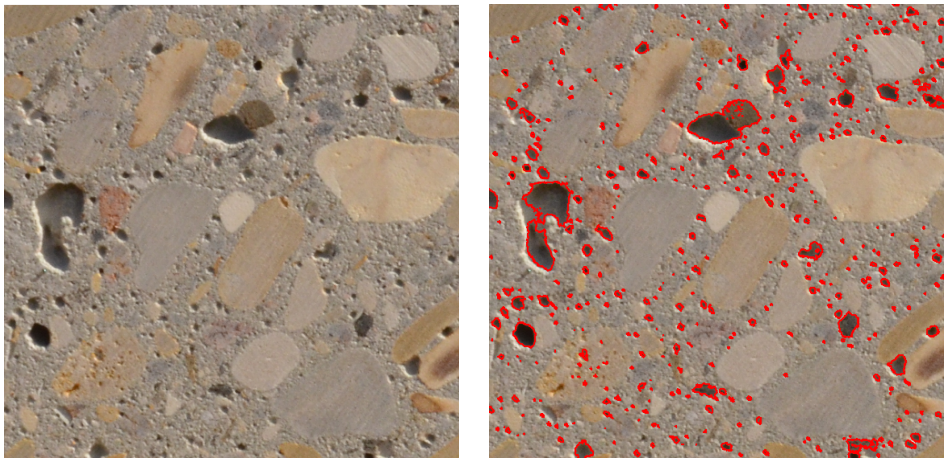

Figure 5.16: On the left we saw a picture of concrete and on the right the same image with a segmentation of pores

If we would like to mimic realistic microstructure we should study statistically the existence of long range correlation. For example on picture 5.17 we see that the orientation of the aggregates is not random but rather exhibit some pattern that we believe is a consequence of flow of liquid concrete. We believe such property could be enforced into our current code by using a uniform distribution in space but an a priori distribution of orientation within the volume.

Figure 5.17: On this image we saw how the right border influence the distribution of the aggregates compared to the part on the left under the horizontal (metallic) structure where we can see some preferred orientation of the aggregates.

As we already pointed out, it seems realistic to numerically fill a space where lies already existing reinforcing bars, especially as one bias of our algorithm is to put more small aggregates

near the boundary like in real concrete however it is questionable to insert the defect before filling the volume with aggregates (especially if it has a large size).

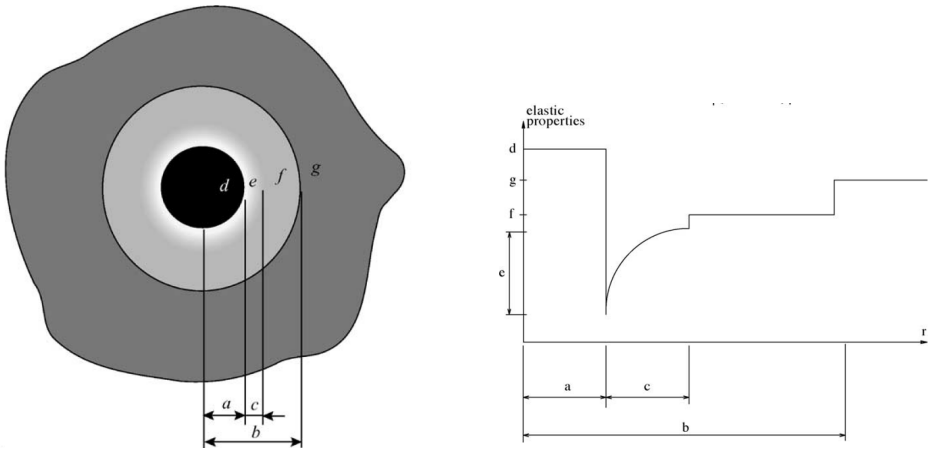

Figure 5.18: A scheme of the Interfacial Transition Zone and a typical variation of the elastic parameter μ and κ inside.

Finally we simplify concrete by modeling it as a two phases material. Actually each aggregate is surrounded by a small layer with different property which is referred to as the Interfacial Transition Zone (ITZ) (Figure 5.18 extracted from [46]). This ITZ has a real impact on the material as it changes the macroscopic behavior of concrete from a mechanical point of view. This property and the fact that defects appear first in this area supported the fact that we should take it into account in terms of non destructive testing. If we model this zone using Generalized Impedance Boundary conditions, it will only impact the current software by a careful labelling of the mesh in order to assign easily the Generalized Impedance Boundary condition in the finite element code. The main difficulty will certainly come from the actual modeling and numerical implementation and from the study of this type of scatterer within the framework of the GLSM for differential measurement (a study of this type of boundary and of the associated factorization method can be found in [21]).

Another aspect that is allowed by this software is to do numerical analysis of the differential imaging method with respect to the distribution of size, type of shapes, material properties, type of acquisition, overall size of the medium, etc... Such numerical experiments will be carried out in the near future in order to prepare an experiment on real data.

Chapter 6

Orthotropic medium

Contents

In this chapter we concentrate on the cases where the medium inside D may be anisotropic. The interest we have in looking at this type of media is two fold. First it provides a simplified version of the elasticity problem that will be addressed in a next chapter and second it can be seen as an appropriate model for non destructive testing of coarse-grained steel.

In Section 6.1 we introduce the scalar wave equation for orthotropic media and demonstrate that the farfield operator can be factorized in a similar way as for the isotropic case (although with some additional technicalities). The obtained factorization does not require any correlation between the supports of the isotropic parameters and the anisotropic ones (which then may be different). In Section 6.2 we demonstrate that the GLSM can be applied to such medium. The main point that has to be checked is the coercivity of the middle operator (denoted T) which is shown to hold true if the contrasts have fix (and compatible) sign in a neighborhood of the boundary of D. Following an idea of Kirsch and Grinberg [40] we also consider the application of GLSM to some cases where T cannot be coercive. These considered configurations are those where D is made of disjoint parts where the sign of the contrasts are different between at least two of the connected components. The GLSM allows us to treat this case without knowing the contrast sign in each component (but we still need to be able to regroup the components that have the same contrast sign). Finally we discuss the case of known heterogeneous media in Section 6.4 and of differential measurements in Section 6.3.

6.1 Model Problem

Similarly to Chapter 2 for a wave number $k > 0$, the total field solves the following scalar wave equation:

$$\operatorname{div}(A\nabla u) + k^2 n u = 0 \text{ in } \mathbb{R}^d$$

with $d = 2$ or 3 and with $n \in L^\infty(\mathbb{R}^d)$ denoting the refractive index such that the support of $n - 1$ is included into $\overline{D}_n$ with D_n a bounded domain with Lipschitz boundary and connected

complement and such that $\Im(n) \geq 0$. We assume that A is at least in $L^\infty(\mathbb{R}^d)^{d\times d}$ and that the support of $A - Id$ is included into $\overline{D}_A$ with D_A a bounded domain with Lipschitz boundary and connected complement and such that $\Im(A\zeta \cdot \bar{\zeta}) \leq 0$ and $\Re(A)\zeta \cdot \bar{\zeta} \geq c|\zeta|^2$ for $\zeta \in \mathbb{C}^d$ and for some positive constant c. We introduce a domain D such that $D_n \cup D_A \subset D$ with D a bounded domain with Lipschitz boundary and connected complement. In the following we will assume that the connected component of D will either have boundary where A is not equal to Id or n is not equal to one if A is identically equal to Id. Therefore we will have $D_n \cup D_A = D$.

We are interested in the cases where the total field is generated by plane waves, $u^i(\theta, x) := e^{ikx\cdot\theta}$ with $x \in \mathbb{R}^d$ and $\theta \in \Gamma_s$ ($\Gamma_s \subset \mathbb{S}^{d-1}$ the unit sphere) and we denote by u^s the scattered field defined by

$$u^s(\theta, \cdot) = u(\theta, \cdot) - u^i(\theta, \cdot) \quad \text{in } \mathbb{R}^d,$$

which is assumed to be satisfying the Sommerfeld radiation condition,

$$\lim_{r\to\infty} \int_{|x|=r} \left| \frac{\partial u^s}{\partial r} - iku^s \right|^2 ds = 0.$$

Our data for the inverse problem will be formed by noisy measurements of so called farfield pattern $u^\infty(\theta, \hat{x})$ defined by

$$u^s(\theta, x) = \frac{e^{ik|x|}}{|x|^{(d-1)/2}}(u^\infty(\theta, \hat{x}) + O(1/|x|))$$

as $|x| \to \infty$ for all $(\theta, \hat{x}) \in \Gamma_s \times \Gamma_m$, where Γ_m is a subset of $\mathbb{S}^{d-1}$ possibly different from Γ_s. The goal is to be able to reconstruct D from these measurements (without knowing n and A). Therefore the goal is to extend the results of Chapters 2 and 3 to the farfield operator $F : L^2(\Gamma_s) \to L^2(\Gamma_m)$, defined by

$$Fg(\hat{x}) := \int_{\Gamma_s} u^\infty(\theta, \hat{x}) g(\theta) ds(\theta), \ \hat{x} \in \Gamma_m$$

Let us define for $\psi \in \{f \in L^2(D) \ s.t \ f|_{D_A} \in H^1(D_A)$, the unique function $w \in H^1_{\text{loc}}(\mathbb{R}^d)$ satisfying

$$\begin{cases} \operatorname{div}(A\nabla w) + nk^2 w = -k^2(n-1)\psi - \operatorname{div}((A - Id)\nabla\psi) \text{ in } \mathbb{R}^d, \\ \lim\limits_{r\to\infty} \int\limits_{|x|=r} \left| \dfrac{\partial w}{\partial r} - ikw \right|^2 ds = 0. \end{cases} \tag{6.1}$$

By linearity of the forward scattering problem, Fg is nothing but the farfield pattern of w solution of (6.1) with $\psi = v_g$ in D , where

$$v_g(x) := \int_{\Gamma_s} e^{ikx\cdot\theta} g(\theta) ds(\theta), \ g \in L^2(\Gamma_s), \ x \in \mathbb{R}^d.$$

We introduce $X(D) = \{(f, g) \in L^2(D) \times L^2(D_A) \ s.t. \ g = \nabla f \ in \ D_A\}$, we identify X and its adjoint. Finally we consider the norm on $X(D)$ defined by

$$\|(f, g)\|_X = \|f\|_{L^2(D)} + \|g\|_{L^2(D_A)} = \|f\|_{H^1(D_A)} + \|f\|_{L^2(D_n)}$$

Now consider the (compact) operator $H_s : L^2(\Gamma_s) \to X$ defined by

$$H_s g := \begin{bmatrix} v_g|_{D_n} \\ \nabla v_g|_{D_A} \end{bmatrix}, \tag{6.2}$$

and the (compact) operator $G_m : \overline{\mathcal{R}(H_s)} \subset X \to L^2(\Gamma_m)$ defined by

$$G_m \begin{bmatrix} \psi \\ \nabla\psi \end{bmatrix} := w^\infty|_{\Gamma_m} \tag{6.3}$$

where w^∞ is the farfield of $w \in H^1_{\text{loc}}(\mathbb{R}^d)$ solution of (6.1) and where $\overline{\mathcal{R}(H_s)}$ denotes the closure of the range of H_s in X. Then clearly

$$F = G_m H_s$$

One can also decompose G_m to get the second factorisation of the farfield operator. More precisely, for the case under consideration, since the farfield pattern of w has the following expression ([15]):

$$w^\infty(\hat{x}) = -\int_{D_n} e^{-iky.\hat{x}}(1-n)k^2(\psi(y)+w(y))dy - \int_{D_A}(A-Id)\nabla_y e^{-iky.\hat{x}} \cdot \nabla(\psi(y)+w(y))dy,$$

one simply has $G_m = H_m^* T\psi$, where $H_m^* : X \to L^2(\Gamma_m)$ is the adjoint of H_m (defined similarly to H_s with Γ_s replaced by Γ_m) given by

$$H_m^* \begin{bmatrix} \varphi \\ \nabla\varphi \end{bmatrix}(\hat{x}) := \int_{D_n} e^{-iky.\hat{x}}\varphi(y)dy + \int_{D_A}(A-Id)\nabla_y e^{-iky.\hat{x}} \cdot \nabla\varphi dy,\ \varphi \in X,\ \hat{x} \in \Gamma_m,$$

and T: $X \to X$ is defined by

$$T \begin{bmatrix} \psi \\ \nabla\psi \end{bmatrix} := \begin{bmatrix} -k^2(1-n)(\psi+w) \\ -(A-Id)\cdot(\nabla\psi(y)+\nabla w(y) \end{bmatrix}, \tag{6.4}$$

with $w \in H^1_{\text{loc}}(\mathbb{R}^d)$ being the solution of (6.1)(with $\psi_1 = \psi$ and $\psi_2 = \nabla\psi$). Finally we get

$$F = H_m^* T H_s, \tag{6.5}$$

Remark 11. *Similarly to Chapter 4 we remark that T is independent of the type of incident waves (either plane waves, point sources or more complicated ones such as the one from known heterogeneous background).*

6.2 The application of GLSM

The factorization (6.5) is again "non symmetric" because of the limited aperture setting. This configuration is covered by Theorem 4.2. The main point that needs to be checked is the coercivity of T. Indeed if T is coercive one can apply Theorems 21 and 22 to image the defect.

6.2.1 Range characterization

First we assume that our obstacle D will be composed of several disjoint simply connected components. Those components will either have $A = Id$ and $n \neq 1$ or $A \neq Id$ in a neighborhood of their boundaries. As in Chapter 2 a key ingredient of the GLSM the characterization of the obstacle D in term of the range of G_m. This characterization is based on the solvability of the interior transmission problem (for given regular boundary values f and g):

$$\begin{cases} \mathrm{div} A\nabla u + k^2 n u = 0 \quad \text{in } D, \\ \Delta v + k^2 v = 0 \quad \text{in } D, \\ (u - v) = f \quad \text{on } \partial D, \\ \frac{\partial}{\partial \nu}(u - v) = g \quad \text{on } \partial D, \end{cases} \tag{6.6}$$

where $(u, v) \in \mathcal{Y}(D)$ and $\mathcal{Y}(D)$ is a space of solutions that will be specified later. We will assume that the following hypothesis holds true.

Hypothesis 6. *We assume that $k^2 \in \mathbb{R}_+$ is such that problem (6.6) has a unique solution for all regular ($C^\infty(\partial D)$) functions f and g.*

This hypothesis and the interior transmission problem stated above are incomplete in the sense that we did not specify $\mathcal{Y}(D)$. This space actually depends on the properties of A and n. For example if we assume that $D_n \subset D_A = D$, (6.6) can be studied for $(u, v) \in \mathcal{Y}(D) = H^1(D) \times H^1(D)$. In this case we know from [9] that hypothesis 6.6 is for instance true if $A - Id$ and $n - 1$ have the same sign and do not change sign in a neighborhood of ∂D. The case where $D_A = \emptyset$ has already been discussed in Chapter 4: System (6.6) holds for $(u, v) \in L^2(D) \times L^2(D)$ such that $u - v \in H^2(D)$. In this case Hypothesis 6 is true if $n - 1$ does not change sign in a neighborhood of ∂D. The case where $n = 1$ in a neighborhood of ∂D has been less studied in the literature and the only case where we know that hypothesis 6 is true is when $A - Id$ does not change sign in all D and $n = 1$ in D. Finally when $A = Id$ in a neighborhood of ∂D, but not in all D, and $n - 1$ does not change sign in a neighborhood of ∂D, there is no clearly stated result in the literature about this case. Let us mention however that surface integral method applied to (6.6) (as proposed in [26]) would be an appropriate tool to study this case.
As in the previous chapter we set

$$\phi_z(\hat{x}) := e^{-ik\hat{x}\cdot z}$$

and consider a known domain Σ such that $D \subset \Sigma$. We denote by $\hat{X}(\Sigma) := \{(f, g) \in L^2(\Sigma) \times L^2(\Sigma)\ s.t.\ g = \nabla f\ in \Sigma\}$ which can be identified with $H^1(\Sigma)$. Let $C > 0$ be a given constant (independent of α) and consider $\alpha > 0$ and $z \in \mathbb{R}^d$, $g^{z,\alpha} \in L^2(\Gamma_m) \times L^2(\Gamma_s)$ such that :

$$\begin{aligned} J_\alpha(\phi_z, g^{z,\alpha}) &= \alpha |(Fg_2^{z,\alpha},\, g_1^{z,\alpha})| + \alpha^{1-\gamma} \left\| H_s g_2^{z,\alpha} - H_m g_1^{z,\alpha} \right\|^2_{\hat{X}(\Sigma)} + \alpha^{1-\gamma} |(Fg_2^{z,\alpha} - \phi_z,\, g_1^{z,\alpha})| \\ &\quad + \left\| Fg_2^{z,\alpha} - \phi_z \right\|^2 \\ &\leq j_\alpha(\phi_z) + C\alpha, \end{aligned} \tag{6.7}$$

where $\gamma \in]0, 1[$ and

$$j_\alpha(\phi_z) = \inf_{g \in L^2(\Gamma_m) \times L^2(\Gamma_s)} J_\alpha(\phi_z, g).$$

Combining the results of Theorems 18 and 20 we obtain the following theorem:

Theorem 24. *Assume that Hypothesis 6 holds and that T verifies*

$$|(Th,\, h)| \geq \mu \|h\|^2_{X(D)}$$

for all $h \in \overline{\mathcal{R}(H_s)}$. Then $z \in D$ if and only if $\limsup_{\alpha\to 0} |(Fg_2^{z,\alpha},\, g_1^{z,\alpha})| + \alpha^{-\gamma} \|H_s g_2^{z,\alpha} - H_m g_1^{z,\alpha}\|^2_{\hat{X}(\Sigma)} < \infty$. Moreover, we have that the sequence of Herglotz wave functions associated with $g^{z,\alpha}$ converges strongly to the solution v of (6.6) with $(f,g) = (\Phi_z, \frac{\partial \Phi_z}{\partial \nu})$ as α goes to zero.

For the noisy case, consider $F^\delta : L^2(\Gamma_s) \to L^2(\Gamma_m)$ a compact operator such that:

$$\left\| F^\delta - F \right\| \leq \delta.$$

Then consider for $\alpha > 0$ and $\phi \in L^2(\Gamma_m)$ the functional $J^\delta_\alpha(\phi, \cdot) : L^2(\Gamma_s) \times L^2(\Gamma_m) \to \mathbb{R}$,

$$J^\delta_\alpha(\phi_z, g) = \alpha |\left(F^\delta g_2,\, g_1\right)| + \alpha^{1-\gamma} \|H_s g_2 - H_m g_1\|^2_{H^1(\Sigma)} + \alpha^{1-\gamma}\delta \|g\|^2 + \alpha^{1-\gamma} |\left(F^\delta g_2 - \phi_z,\, g_1\right)| + \left\| F^\delta g_2 - \phi_z \right\|^2$$

where $\gamma \in]0,1[$. Then as a direct consequence of Theorem 19 we obtain the following asymptotic characterization of D.

Theorem 25. *Assume that Hypothesis 6 holds and that T verifies*

$$|(Th,\, h)| \geq \mu \|h\|^2_{X(D)}$$

for $(h_1, h_2) \in \overline{\mathcal{R}(H_s)}$. For $z \in \mathbb{R}^d$ let us denote by $g^{z,\alpha,\delta}$ the minimizer of $J^\delta_\alpha(\phi, \cdot)$ over $L^2(\Gamma_s) \times L^2(\Gamma_m)$.
Then $z \in D$ if and only if $\limsup_{\alpha\to 0} \limsup_{\delta\to 0} |\left(F^\delta g_2^{z,\alpha,\delta},\, g_1^{z,\alpha,\delta}\right)| + \alpha^{-\gamma} \left\| H_s g_2^{z,\alpha,\delta} - H_m g_1^{z,\alpha,\delta} \right\|^2_{\hat{X}(\Sigma)} + \alpha^{-\gamma}\delta \left\| g^{z,\alpha,\delta} \right\|^2 < \infty$.
Moreover, there exists $\delta_0(\alpha)$ such that for all $\delta(\alpha) \leq \delta_0(\alpha)$, $Hg^{z,\alpha,\delta(\alpha)}$ converges strongly to the solution v of (6.6) with $(f,g) = (\Phi_z, \frac{\partial \Phi_z}{\partial \nu})$ as α goes to zero.

In the following subsection we will extend the coercivity result of Chapter 4. If we consider the connected components of D then we assume that they can be split into two categories. The first one is such that $A - Id$ does not equal zero on a neighborhood of the boundary and the second one is such that $A - Id = 0$ and $n - 1$ does not vanish on a neighborhood of the boundary. We will give a coercivity result for each of those two configurations and then merge them into a combined condition on n and A under which we have the coercivity of T defined in (6.4). We first state a classical identity.

Lemma 12. *We have the following identity, for $\psi = (\psi_1, \psi_2) \in L^2(D_n) \times L^2(D_A)^d$ and T defined in (6.4) :*

$$\Im(T\psi,\, \psi) = k \int_{\mathbb{S}^{d-1}} |w^\infty|^2 - \int_{D_A} \Im(A)(\nabla(w) + \psi_2) \cdot \overline{(\nabla(w) + \psi_2)} + k^2 \int_{D_n} \Im(n) |w + \psi_1|^2.$$

Proof. We recall that for any $\psi = (\psi_1, \psi_2) \in L^2(D_n) \times L^2(D_A)^d$ there exists a unique $w \in H^1_{loc}(\mathbb{R}^d)$ that solves (6.1). The definition of T (6.4) gives:

$$\begin{aligned}(T\psi,\, \psi) = &- \int_{D_A} (A - Id)(\psi_2 + \nabla w) \cdot (\overline{\psi_2 + \nabla w}) - k^2 \int_{D_n} (1-n)|\psi_1 + w|^2 \\ &+ \int_{D_A} (A - Id)(\psi_2 + \nabla w) \cdot (\overline{\nabla w}) + k^2 \int_{D_n} (1-n)(\psi_1 + w)\bar{w}\end{aligned} \tag{6.8}$$

Using (6.1) and integrating by parts over a ball B_R such that $D \subset B_R$ we have:

$$-\int_{B_R} \nabla w \cdot \overline{\nabla w} - k^2 w\overline{w} + \int_{\partial B_R} \frac{\partial w}{\partial r}\overline{w} = \int_{D_A} (A - Id)(\nabla w + \psi_2) \cdot \overline{\nabla w} + k^2 \int_{D_n} (1-n)(w + \psi_1)\overline{w}$$

Substituting in (6.8), taking the imaginary part and letting R to $+\infty$ prove the lemma. □

The case where $\overline{D_A} \subsetneq D_n$

We first consider the case where $\overline{D_A} \subsetneq D_n$ which can be seen as an extension of Theorem 23 that treats the case $D_A = \emptyset$. The Herglotz wave operator reduces to $Hg = [v_g|_D, \nabla v_g|_{D_A}]$.

Theorem 26. *If $\bar{D}_A \subsetneq D_n = D$ and if there exist $\alpha, c \in \mathbb{R}^{*+}$ such that either $\Re(n-1)+\alpha\Im(n) \geq c$ or $\Re(1-n)+\alpha\Im(n) \geq c$ in a neighborhood of ∂D, then there exists μ such that the operator T defined in 6.4 verifies*

$$|(T\psi,\, \psi)| \geq \mu \, \|\psi\|^2_{X(D)}\,,$$

for all $\psi \in \overline{\mathcal{R}(H_s)}$.

Proof. We introduce n_0 such that $n_0 = n$ in some domain $V \subset D$ and there exist $\alpha, c \in \mathbb{R}^{*+}$ such that either $\Re(n_0 - 1) + \alpha\Im(n_0) \geq c$ or $\Re(1 - n_0) + \alpha\Im(n_0) \geq c$ in D. We introduce $\Omega = supp(n_0) \cup D_A$. By assumption we have that $\Omega \subsetneq D$ and we can choose V such that $V \cap \Omega$.

Lemma 12 implies that $w^\infty \to 0$ in $L^2(\mathbb{S}^{d-1})$ and therefore $w^\infty = 0$. The Rellich theorem and the unique continuation principle imply that $w = 0$ outside D. Thus we have that u and v solve the interior transmission eigenvalue problem. Hypothesis 6 implies that that $u = v = w = 0$. We introduce the intermediate scattered fields

$$\begin{cases} \Delta u^s_{0,\ell} + k^2 n u^s_{0,\ell} = -k^2(n_0 - 1)\psi_\ell \text{ in } \mathbb{R}^d, \\ \lim\limits_{r\to\infty} \int\limits_{|x|=r} \left| \frac{\partial(u^s_{0,\ell})}{\partial r} - ik(u^s_{0,\ell}) \right|^2 ds = 0 \end{cases} \tag{6.9}$$

and

$$\begin{cases} \operatorname{div}(A\nabla u^s_\ell) + k^2 n u^s_\ell = -\operatorname{div}((A - Id)\nabla u_{0,\ell}) - k^2(n - n_0)u_{0,\ell} \text{ in } \mathbb{R}^d, \\ \lim\limits_{r\to\infty} \int\limits_{|x|=r} \left| \frac{\partial(u^s_{0,\ell})}{\partial r} - ik(u^s_\ell) \right|^2 ds = 0. \end{cases} \tag{6.10}$$

We have that $u_{0,\ell} \in H^2(\Omega)$ (for the same reason as in Theorem 23) which implies its strong convergence to zero in $H^1(\Omega)$ together with the continuity of the forward scattering problem

for u_ℓ^s, we deduce that u_ℓ^s converges strongly to zero in $H^1_{loc}(\mathbb{R}^d)$. Finally the interior elliptic regularity implies that ψ_ℓ strongly converges to zero in $H^1(\Omega)$. We have,

$$\begin{aligned}(T\psi_\ell,\, \psi_\ell) = &- \int_D (1-n_0)u_{0,\ell}\overline{\psi}_\ell - sign(\Re(1-n_0)) \int_\Omega |\nabla\psi_\ell|^2 - \int_\Omega (A-Id)\nabla(u_{0,\ell}+u_\ell^s)\nabla\overline{\psi}_\ell \\ &- \int_D (1-n)u_\ell^s\overline{\psi}_\ell - \int_\Omega (1-n_0)u_{0,\ell} + sign(\Re(1-n_0)) \int_\Omega |\nabla\psi_\ell|^2 - \overline{\psi}_\ell.\end{aligned}$$

Using the strong convergence results we deduce that the last four terms go to zero. Treating the first term on the right hand side as in Theorem 23 leads to a contradiction. □

The case $D_n = \emptyset$ and $D = D_A$

We now consider the case where $D_n = \emptyset$ and $D = D_A$ rather than the case $D_n \subset D_A = D$ in order to lighten the notation. The reader can easily see that the latter case can be treated in a similar way. In the following, $\|\|_{X(D)}$ will refer to the H^1 norm of the Herglotz wave function in D.

Theorem 27. *If $D_n = \emptyset$, $D = D_A$, A is C^1 in a neighborhood of ∂D that we denote by V and if there exist $\alpha, c \in \mathbb{R}^{*+}$ such that either $\Re(A - Id) - \alpha\Im(A) \geq c$ or $\Re(Id - A) - \alpha\Im(A) \geq c$ in V there exists μ such that the operator T defined in 6.4 verifies*

$$|(T\psi,\, \psi)| \geq \mu \, \|\psi\|_X^2$$

for all $\psi \in \overline{\mathcal{R}(H_s)}$.

Proof. We introduce A_0 such that $A_0 = A$ inside V and A_0 is such that either $\Re(A_0 - Id) - \alpha\Im(A_0) \geq c$ or $\Re(Id - A_0) - \alpha\Im(A_0) \geq c$ in D. Since we suppose that A is C^1 inside V we can choose A_0 to be C^1 inside all D. We also introduce $\Omega = supp(A - A_0)$, by construction $\Omega \subsetneq D$.

We will proceed by a contradiction argument, therefore we assume:

$$\|\psi_\ell\|_{X(D)} = 1 \quad \text{ and } |(T\psi_\ell, \psi_\ell)| \to 0 \text{ as } \ell \to \infty$$

and that ψ_ℓ weakly converges in $H^1(D)$ to ψ that satisfies

$$\Delta\psi + k^2\psi = 0 \text{ in } D.$$

The solution w_ℓ satisfying (6.1) with $v = \psi_\ell$ weakly converges in $H^1(D)$ to $w \in H^1(\mathbb{R}^d)$ satisfying (6.1) with $v = \psi$.

Lemma 12 implies that $w^\infty \to 0$ in ${}^2(\mathbb{S}^{d-1})$ and therefore $w^\infty = 0$. The Rellich theorem and unique continuation theorem imply that $w = 0$ outside D. Thus we have that u and v solve the interior transmission eigenvalue problem. Hypothesis 6 implies that that $u = v = w = 0$. Let us introduce the intermediate (scattered) field $u_{0,\ell}^s$ that solves:

$$\begin{cases} \operatorname{div}(A_0\nabla u_{0,\ell}^s) + k^2 u_{0,\ell}^s = -\operatorname{div}((A_0 - Id)\nabla\psi_\ell) \text{ in } \mathbb{R}^d, \\ \lim\limits_{r\to\infty} \int\limits_{|x|=r} \left| \frac{\partial(u_{0,\ell}^s)}{\partial r} - ik(u_{0,\ell}^s) \right|^2 ds = 0. \end{cases} \tag{6.11}$$

We denote by $u_{0,\ell} = u^s_{0,\ell} + \psi_\ell$ the total field. We also introduce u^s_ℓ that solves:

$$\begin{cases} \operatorname{div}(A\nabla u^s_\ell) + k^2 u^s_\ell = -\operatorname{div}((A - A_0)\nabla u_{0,\ell}) \text{ in } \mathbb{R}^d, \\ \lim\limits_{r\to\infty} \int\limits_{|x|=r} \left| \frac{\partial u^s_\ell}{\partial r} - iku^s_\ell \right|^2 ds = 0. \end{cases} \tag{6.12}$$

We clearly have

$$\begin{aligned} |(T\psi_\ell, \psi_\ell)| &= \left| \int_D (A - Id)\nabla(u^s_\ell + u_{0,\ell})\nabla\overline{\psi}_\ell dx \right| \\ &= \left| \int_D (A_0 - Id)\nabla u_{0,\ell}\nabla\overline{\psi}_\ell dx + \int_D ((A - Id)\nabla u^s_\ell \nabla\overline{\psi}_\ell dx + \int_\Omega (A - A_0)\nabla u_{0,\ell}\nabla\overline{\psi}_\ell dx \right| \\ &\geq \left| \int_D (A_0 - Id)\nabla u_{0,\ell}\nabla\overline{\psi}_\ell dx \right| - \left| \int_D ((A - Id)\nabla u^s_\ell \nabla\overline{\psi}_\ell dx + \int_\Omega (A - A_0)\nabla u_{0,\ell}\nabla\overline{\psi}_\ell dx \right| \\ &\geq \left| \int_D (A_0 - Id)\nabla u_{0,\ell}\nabla\overline{\psi}_\ell dx \right| - \left| \int_D (Id - A)\nabla u^s_\ell \nabla\overline{\psi}_\ell dx \right| - \left| \int_\Omega (A - A_0)\nabla u_{0,\ell}\nabla\overline{\psi}_\ell dx \right| \end{aligned} \tag{6.13}$$

Since $u_{0,\ell} \in H^1(D)$ satisfies $\operatorname{div}(A_0\nabla u_{0,\ell}) + k^2 u_{0,\ell} = 0$ in D, we infer by interior elliptic regularity that $u_{0,\ell} \in H^2(\Omega)$ (from [31] and the fact that A_0 is C^1) and therefore converges strongly to zero in $H^1(\Omega)$.
By continuity of the forward scattering problem verified by u^s_ℓ and the strong convergence of $u_{0,\ell}$ in $H^1(\Omega)$, we deduce that u^s_ℓ strongly converges to zero in $H^1(D)$. We therefore deduce that for ℓ large enough (6.13) becomes:

$$|(T\psi_\ell, \psi_\ell)| \geq \frac{1}{2} \left| \int_D (A_0 - Id)\nabla u_{0,\ell}\nabla\overline{\psi}_\ell dx \right| \tag{6.14}$$

To treat $|(T_0\psi_\ell, \psi_\ell)| = \left|\int_D (A_0 - Id)\nabla u_{0,\ell}\nabla\overline{\psi}_\ell dx\right|$ we need to consider two cases depending on the compatibility of the sign of $A_0 - Id$ and Id (as in [19]). First we consider the case when there exist $\alpha, c \in \mathbb{R}^{+,*}$ such that $\Re(A_0 - Id) - \alpha\Im(A_0) \geq c > 0$. Since $u^s_{0,\ell}$ solves (6.11) we deduce that:

$$\begin{aligned} (T_0\psi_\ell, \psi_\ell) = -\int_D (A_0 - Id)\nabla u_{0,\ell}\nabla\overline{u}_{0,\ell} + |u_{0,\ell}|^2 - \int_{\mathbb{R}^d} |\nabla u^s_{0,\ell}|^2 + |u^s_{0,\ell}|^2 + \int_D |u_{0,\ell}|^2 \\ + \int_{\mathbb{R}^d} |u^s_{0,\ell}|^2 + ik \int_{\mathbb{S}^{d-1}} |u^s_{0,\ell}|^2 \end{aligned} \tag{6.15}$$

The weak convergence of $u^s_{0,\ell}$ in $H^1_{loc}(\mathbb{R}^d)$ and $u_{0,\ell}$ in $H^1(D)$ imply the strong convergence in $L^2_{loc}(\mathbb{R}^d)$ and $L^2(D)$ respectively. Therefore the last three terms in the equality above go to zero. Moreover (6.14) implies that $|(T_0\psi_\ell, \psi_\ell)|$ go to zero. Therefore the first term in (6.15) goes also to zero. From the convergence to zero of its imaginary part we deduce that $\nabla u_{0,\ell}$ goes to zero on the support of $\Im(A_0)$. From the real part we deduce that the remaining part of $\|u_{0,\ell}\|^2_{H^1(D)}$ goes to zero as well as $\left\|u^s_{0,\ell}\right\|^2_{H^1_{loc}(\mathbb{R}^d)}$. This implies that $\|\psi_\ell\|^2_{H^1(D)} \to 0$ which is a contradiction. Then we consider the case when there exist $\alpha, c \in \mathbb{R}^{+,*}$ such that $\Re(Id - A_0) - \alpha\Im(A_0) \geq c > 0$.

We cannot use (6.15) since the term involving $u_{0,\ell}$ and $u^s_{0,\ell}$ do not have the same sign. From the definition of T_0 we have:

$$(T_0\psi_\ell,\psi_\ell) = -\int_D (A_0 - Id)\nabla\psi_\ell\nabla\overline{\psi}_\ell + |\psi_\ell|^2 - \int_D (A_0 - Id)\nabla u^s_{0,\ell}\nabla\overline{\psi}_\ell + \int_D |\psi_\ell|^2.$$

Using equation (6.1) verified by $u^s_{0,\ell}$ we have:

$$\begin{aligned}
(T_0\psi_\ell,\psi_\ell) =& -\int_D (A_0 - Id)\nabla\psi_\ell\nabla\overline{\psi}_\ell + + \int_{\mathbb{R}^d} \bar{A}_0\nabla\bar{u}^s_{0,\ell}\nabla u^s_{0,\ell} \\
& - 2i\int_D \Im(A_0)\nabla u^s_{0,\ell}\nabla\overline{\psi}_\ell - ik\int_{\mathbb{S}^{d-1}} |u^\infty_{0,\ell}|^2 \\
=& -\int_D \Re(A_0 - Id)\nabla\psi_\ell\nabla\overline{\psi}_\ell + \int_{\mathbb{R}^d} \Re(A_0)\nabla\bar{u}^s_{0,\ell}\nabla u^s_{0,\ell} \\
& - i\int_D (\Im(A_0)\nabla\psi_\ell\nabla\overline{\psi}_\ell + \Im(A_0)\nabla u^s_{0,\ell}\nabla\bar{u}^s_{0,\ell} + 2\Im(A_0)\nabla u^s_{0,\ell}\nabla\overline{\psi}_\ell) - ik\int_{\mathbb{S}^{d-1}} |u^\infty_{0,\ell}|^2 \\
=& -\int_D \Re(A_0 - Id)\nabla\psi_\ell\nabla\overline{\psi}_\ell + \int_{\mathbb{R}^d} \Re(A_0)\nabla\bar{u}^s_{0,\ell}\nabla u^s_{0,\ell} \\
& - i\int_D (\Im(A_0)(\nabla\psi_\ell + \nabla u^s_{0,\ell})(\nabla\overline{\psi}_\ell + \nabla\bar{u}^s_{0,\ell}) + 2i\Im(\Im(A_0)\nabla u^s_{0,\ell}\nabla\overline{\psi}_\ell) - ik\int_{\mathbb{S}^{d-1}} |u^\infty_{0,\ell}|^2 \\
=& \int_D \Re(Id - A_0)\nabla\psi_\ell\nabla\overline{\psi}_\ell + |\psi_\ell|^2 + \int_{\mathbb{R}^d} \Re(A_0)\nabla\bar{u}^s_{0,\ell}\nabla u^s_{0,\ell} + |u^s_{0,\ell}|^2 + 2\int_D \Im(\Im(A_0)\nabla u^s_{0,\ell}\nabla\overline{\psi}_\ell) \\
& - i\int_D (\Im(A_0)(\nabla\psi_\ell + \nabla u^s_{0,\ell})(\nabla\overline{\psi}_\ell + \nabla\bar{u}^s_{0,\ell}) - \int_D |\psi_\ell|^2 - ik\int_{\mathbb{S}^{d-1}} |u^\infty_{0,\ell}|^2 - \int_{\mathbb{R}^d} |u^s_{0,\ell}|^2
\end{aligned}$$

The last three terms go to zero and we will denote them by CT. Then

$$\begin{aligned}
|(T_0\psi_\ell,\psi_\ell)| \geq& \frac{1}{\sqrt{2}}\Big|\int_D \Re(Id - A_0)\nabla\psi_\ell\nabla\overline{\psi}_\ell + |\psi_\ell|^2 + \int_{\mathbb{R}^d} \Re(A_0)\nabla\bar{u}^s_{0,\ell}\nabla u^s_{0,\ell} + |u^s_{0,\ell}|^2 \\
& + 2\int_D \Im(\Im(A_0)\nabla u^s_{0,\ell}\nabla\overline{\psi}_\ell)\Big| + \frac{1}{\sqrt{2}}\left|\int_D (\Im(A_0)(\nabla\psi_\ell + \nabla u^s_{0,\ell})(\nabla\overline{\psi}_\ell + \nabla\bar{u}^s_{0,\ell})\right| - |CT|
\end{aligned}$$

From this last inequality we see that the first term will control the norm of the incident field and scattered field in the region where $\Im(A_0)$ is equal to zero and the second term ensures that the total field is zero in the region where $\Im(A_0)$ is equal to zero. It implies that the total field is equal to zero in all D and therefore by linearity of the forward scattering problem the scattered field is also equal to zero meaning that ψ_ℓ is equal to zero which is a contradiction. □

Remark 12. *One can weaken the regularity assumption on A in V (e.g. example piecewise C^1) as long as one obtain an interior regularity property (e.g. $u_{0,\ell} \in H^s(\Omega)$ where s is strictly larger than one) which implies strong convergence through compact embeddings [34].*

A final coercivity result

We introduce $D = \bigcup_i D^i_n \cup \bigcup_i D^i_A$ where the D_i are simply connected disjoint component. We assume that $A - Id$ is not zero in the neighborhood of the boundary D^i_A and $A - Id$ equals zero in the neighborhood of the boundary D^i_n. With those notation and the result of Theorems 27 and 26 we can give the final result under Hypothesis 6 in the case of many disjoint scatter.

Theorem 28. *Assume A has C^1 regularity in $D_A^i \cap V$ and there exist $c > 0$ and $\alpha > 0$ such that either $\Re(A - Id) - \alpha\Im(A) \geq c > 0$ in $\bigcup_i D_A^i \cap V$ and $\Re(1-n) + \alpha\Im(n) \geq c > 0$ in $\bigcup_i D_n^i \cap V$ or $\Re(Id - A) - \alpha\Im(A) \geq c > 0$ in $\bigcup_i D_A^i \cap V$ and $\Re(n-1) + \alpha Im(n) \geq c > 0$ in $\bigcup_i D_n^i \cap V$ is verified. We have that T defined by (6.4) verifies:*

$$|(T\psi,\, \psi)| \geq \mu \, \|\psi\|_X^2$$

where $\psi \in \overline{\mathcal{R}(H_s)}$.

Proof. We set $D_1 = \bigcup_i D_A^i$ and $D_2 = \bigcup_i D_n^i$. In this case we have that

$$(T\psi,\, \psi) = (T\psi|_{D_1},\, \psi|_{D_1}) + (T\psi|_{D_2},\, \psi|_{D_2})$$

By the linearity of the forward scattering problem, if we introduce the two total fields associated to the two incidents waves $\psi_1 = \psi|_{D_1}$ in D_1 and 0 in D_2 and $\psi_2 = \psi|_{D_2}$ in D_2 and 0 in D_1, denoted $u_1 = u_1^s + \psi_1$ and $u_2 = u_2^s + \psi_2$. Then we have:

$$\begin{aligned}(T\psi,\, \psi) =& (T_1\psi_1,\, \psi_1)_{D_1} + (T_2\psi_2,\, \psi_2)_{D_2} - \int_{D_1} (A - Id)\nabla u_2^s \cdot \nabla \bar{\psi}_1 + k^2(1-n)u_2^s\bar{\psi}_1 \\ &- \int_{D_2} k^2(1-n)u_1^s\bar{\psi}_2 + (A - Id)\nabla u_1^s \cdot \nabla \bar{\psi}_2\end{aligned}$$

where T_1 and T_2 are the operators corresponding to D_1 and D_2 respectively. We clearly see that the last two terms go to zero (by compactness argument). Therefore using the same argument as in the previous sections we have the coercivity of T if T_1 and T_2 have the same sign. The sign of T_1 and T_2 are given in the proofs of Theorems 27 and 26 respectively, which allows us to conclude. □

6.2.2 A priori known regions with different contrast signs

As we discussed in Section 6.2.1, the operator T is coercive under hypothesis on the physical parameter of the medium in the neighborhood of the boundary of D. However when there are several disjoint components, even if the operator T associated with a single part of D is coercive, the operator T associated with all of D might loose coercivity if the hypothesis of Theorem 28 are not verified. This problem is similar to the case of a mixture of Dirichlet and Neumann obstacles. In this section we would like to highlight that similarly to [40], it is possible to solve this problem if one has an a priori knowledge of subregions where contrast signs are incompatible. More precisely, we suppose that there exist two disjoint regions $D_- = \bigcup_i D_{n,-}^i \cup \bigcup_i D_{A,-}^i$ and $D_+ = \bigcup_i D_{n,+}^i \cup \bigcup_i D_{A,+}^i$ such that for a neighborhood V of ∂D we have $\Re(A - Id) - \alpha\Im(A) \geq c > 0$ in $\bigcup_i D_{A,+}^i \cap V$ and $\Re(1-n) + \alpha\Im(n) \geq c > 0$ in $\bigcup_i D_{n,+}^i \cap V$, and $\Re(Id - A) - \alpha\Im(A) \geq c > 0$ in $\bigcup_i D_{A,-}^i \cap V$ and $\Re(n-1) + \alpha Im(n) \geq c > 0$ in $\bigcup_i D_{n,-}^i \cap V$. Moreover we assume that we know a priori two regions Σ_- and Σ_+ such that $D_- \subset \Sigma_-$ and $D_+ \subset \Sigma_+$. We then introduce two cost functionals:

$$\begin{aligned}J_\alpha^+(\phi; g) :=& \alpha|(Fg_2,\, g_1)| + \alpha^{1-\gamma} \, \|H_s g_2 - H_m g_1\|_{\hat{X}(\Sigma_+)}^2 + \alpha^{1-\gamma}|(Fg_2 - \phi,\, g_1)| + \\ & \alpha^{1-\gamma}(\|H_s g_2 + \Phi_z\|_{\hat{X}(\Sigma_-)}^2 + \|H_m g_1 + \Phi_z^\infty\|_{\hat{X}(\Sigma_-)}^2) + \|Fg_2 - \phi\|^2 \\ & \forall g = (g_1, g_2) \in L^2(\Gamma_s) \times L^2(\Gamma_m)\end{aligned} \tag{6.16}$$

$$\begin{aligned} J_\alpha^-(\phi;g) :=& \alpha|(Fg_2,\, g_1)| + \alpha^{1-\gamma}\left\|H_s g_2 - H_m g_1\right\|^2_{\hat{X}(\Sigma_-)} + \alpha^{1-\gamma}|(Fg_2-\phi,\, g_1)|+ \\ & \alpha^{1-\gamma}(\left\|H_s g_2 + \Phi_z\right\|^2_{\hat{X}(\Sigma_+)} + \left\|H_m g_1 + \Phi_z\right\|^2_{\hat{X}(\Sigma_+)}) + \left\|Fg_2 - \Phi_z^\infty\right\|^2 \\ & \forall g = (g_1, g_2) \in L^2(\Gamma_s) \times L^2(\Gamma_m) \end{aligned} \tag{6.17}$$

Similarly to what we have done in Section 4.2, we can introduce g_α^+ and g_α^- two minimizing sequences of those functionals.

Theorem 29. *Under the hypothesis that k is not an interior transmission eigenvalue and that A and n verify the hypothesis above, we have the following characterization of D:*

- *for $z \in \Sigma_+$ we have that $z \in D_+$ if and only if $|\left(Fg_{\alpha,2}^+,\, g_{\alpha,1}^+\right)| + \alpha^{-\gamma}\left\|H_s g_{\alpha,2}^+ - H_m g_{\alpha,1}^+\right\|^2_{\hat{X}(\Sigma_+)} + \alpha^{-\gamma}(\left\|H_s g_{\alpha,2}^+ + \Phi_z\right\|^2_{\hat{X}(\Sigma_-)} + \left\|H_m g_{\alpha,1}^+ + \Phi_z\right\|^2_{\hat{X}(\Sigma_-)})$ stays bounded.*
- *for $z \in \Sigma_-$ we have that $z \in D_-$ if and only if $|\left(Fg_{\alpha,2}^-,\, g_{\alpha,1}^-\right)| + \alpha^{-\gamma}\left\|H_s g_{\alpha,2}^- - H_m g_{\alpha,1}^-\right\|^2_{\hat{X}(\Sigma_-)} + \alpha^{-\gamma}(\left\|H_s g_{\alpha,2}^- + \Phi_z\right\|^2_{\hat{X}(\Sigma_+)} + \left\|H_m g_{\alpha,1}^- + \Phi_z\right\|^2_{\hat{X}(\Sigma_+)})$ stays bounded.*

Moreover when $z \in D_+$ (resp. D_-) we can extract a sequence from g_α^+ (resp. g_α^-) such that the corresponding herglotz waves strongly converge to the solution of associated interior transmission problem.

Proof. The proof is the same for Σ_+ and Σ_-. We give details only for Σ_+.
If $z \in D_+$, we know that there exists v such that $\Phi_z^\infty = Gv$ and that v solves the interior transmission problem with $(f,g) = (\Phi_z, \frac{\partial \Phi_z}{\partial \nu})$. The interior transmission problem is independent on each disjoint set, particularly it can be analyzed separately in D_+ and D_-. In D_- we know that $v = -\Phi_z$ and $u = 0$. Therefore the denseness of the ranges of H_s and H_m and the fact that $z \notin \Sigma_-$ implies that one can construct $g_{0,1}$ such that :

$$\left\|H_s g_{0,1} - v\right\|_{X(D_+)} \leq \alpha$$

and

$$\left\|H_s g_{0,1} - v\right\|_{X(D_-)} \leq \left\|H_s g_{0,1} + \Phi_z\right\|_{\hat{X}(\Sigma_-)} \leq \alpha$$

where we have used the space $X(D_-)$ and $X(D_+)$ which are defined as $X(D)$ but for D_- and D_+ respectively. For the same reason we can construct $g_{0,2}$

$$\left\|H_s g_{0,1} - H_m g_{0,2}\right\|_{\hat{X}(\Sigma_+ \cup \Sigma_-)} \leq \alpha$$

which implies that

$$\begin{aligned} &\alpha\left[|\left(Fg_{\alpha,2}^+,\, g_{\alpha,1}^+\right)| + \alpha^{-\gamma}\left\|H_s g_{\alpha,2}^+ - H_m g_{\alpha,1}^+\right\|^2_{\hat{X}(\Sigma_+)} + \alpha^{-\gamma}(\left\|H_s g_{\alpha,2}^+ + \Phi_z\right\|^2_{\hat{X}(\Sigma_-)} + \left\|H_m g_{\alpha,1}^+ + \Phi_z\right\|^2_{\hat{X}(\Sigma_-)})\right] \\ &\leq J_\alpha^+(\Phi_z^\infty; g_0) \leq C\alpha. \end{aligned}$$

If $z \in \Sigma_+ \setminus \bar{D}_+$ and $|\left(Fg^+_{\alpha,2},\, g^+_{\alpha,1}\right)| + \alpha^{-\gamma}\left\|H_s g^+_{\alpha,2} - H_m g^+_{\alpha,1}\right\|^2_{\hat{X}(\Sigma_+)} + \alpha^{-\gamma}(\left\|H_s g^+_{\alpha,2} + \Phi_z\right\|^2_{\hat{X}(\Sigma_-)} + \left\|H_m g^+_{\alpha,1} + \Phi_z\right\|^2_{\hat{X}(\Sigma_-)})$ remains bounded, then

$$\left\|H_m g^+_{\alpha,1}\right\|^2_{X(D_-)} \leq \left\|H_m g^+_{\alpha,1}\right\|^2_{\hat{X}(\Sigma_-)} \leq C\alpha^\gamma + \|\Phi_z\|^2_{\hat{X}(\Sigma_-)},$$

$$\left\|H_s g^+_{\alpha,2}\right\|^2_{X(D_-)} \leq \left\|H_s g^+_{\alpha,2}\right\|^2_{\hat{X}(\Sigma_-)} \leq C\alpha^\gamma + \|\Phi_z\|^2_{\hat{X}(\Sigma_-)},$$

and

$$\begin{aligned}\left\|H_s g^+_{\alpha,2} - H_m g^+_{\alpha,1}\right\|^2_{X(D)} &\leq \left\|H_s g^+_{\alpha,2} - H_m g^+_{\alpha,1}\right\|^2_{\hat{X}(\Sigma_+)} + \left\|H_s g^+_{\alpha,2} + \Phi_z\right\|^2_{\hat{X}(\Sigma_-)} + \left\|H_m g^+_{\alpha,1} + \Phi_z\right\|^2_{\hat{X}(\Sigma_-)} \\ &\leq 2C\alpha^\gamma\end{aligned}$$

Following the idea of the proof of Theorem 28 we can split the operator T using T_+ and T_- which are associated to obstacles D_+ and D_- alone. Those operators are coercive as demonstrated in Theorem 28.

$$\left(TH_s g^+_{\alpha,2},\, H_s g^+_{\alpha,2}\right)_D = \left(T_+ H_s g^+_{\alpha,2},\, H_s g^+_{\alpha,2}\right)_{D_+} + \left(T_- H_s g^+_{\alpha,2},\, H_s g^+_{\alpha,2}\right)_{D_-} + \mathcal{C}$$

where $\mathcal{C}$ is a compact term. To explicitly define this term we introduce $\psi_+ = H_s g^+_{\alpha,2}$ in D_+ and 0 elsewhere and $\psi_- = H_s g^+_{\alpha,2}$ in D_- and 0 elsewhere, and u^s_+ and u^s_- the scattered fields associated to D_+ alone and D_- alone.

$$\begin{aligned}|\mathcal{C}| =& |-\int_{D_+}(A-Id)\nabla u^s_- \cdot \nabla\bar{\psi}_+ + k^2(1-n)u^s_-\bar{\psi}_+ - \int_{D_-} k^2(1-n)u^s_+\bar{\psi}_- + (A-Id)\nabla u^s_+ \cdot \nabla\bar{\psi}_-| \\ \leq& C\left\|H_s g^+_{\alpha,2}\right\|_{X(D^-)}\left\|H_s g^+_{\alpha,2}\right\|_{X(D^+)}\end{aligned}$$

where the inequality comes from the continuity of the forward scattering problem.
Combining those decomposition and the previous inequalities

$$\begin{aligned}\mu_{T_+}\left\|H_s g^+_{\alpha,2}\right\|^2_{X(D_+)} - C\,\|T_-\|\,\|\Phi_z\|^2_{\hat{X}(\Sigma_-)} - C\,\|\Phi_z\|^2_{\hat{X}(\Sigma_-)}\left\|H_s g^+_{\alpha,2}\right\|_{X(D^+)} &\leq |\left(TH_s g^+_{\alpha,2},\, H_s g^+_{\alpha,2}\right)| \\ &\leq |\left(TH_s g^+_{\alpha,2},\, H_m g^+_{\alpha,1}\right)| + \left\|H_s g^+_{\alpha,2} - H_m g^+_{\alpha,1}\right\|^2_{\hat{X}(\Sigma_+\cup\Sigma_-)}\end{aligned}$$

From which we conclude that $\left\|H_s g^+_{\alpha,2}\right\|^2_{X(D_+)}$ is bounded which is a contradiction.

□

Remark 13. *This functional shares some similarity with the case of limited aperture data in the sense that it uses an additional term to correct for the non coercivity of T (as we did for the non symmetric factorization). However for the case of limited aperture the a priori information is rather weak as we could set up Σ as being almost the whole space. For this case it is a very strong assumption since it assumes that we have a priori information on the location of the obstacles. In the approach proposed by Kirsch and Grinberg they also need to know what type of obstacle will be inside each region. However in our approach we do not need to know this apriori, we could have $D_- \subset \Sigma_+$ and $D_+ \subset \Sigma_-$.*

6.3 Analysis of differential measurements imaging

The result from Chapter 3 on the treatment of differential measurements relies on two main arguments: First the strong convergence of Herglotz waves to the solution of the underlying interior transmission problem (one for the background and one for the perturbed medium) and a careful comparison of ITP solutions between the two configurations of the medium. This comparison is possible if one can use a unique continuation principle and assume the solvability of an interior transmission problem.

The strong convergence of the sequence of Herglotz wave functions has been studied in the previous sections and basically relies on two sets of hypothesis: the first one ensures the solvability of the associated interior transmission problem and the second one ensures the coercivity of T. Unique continuation principle introduces a complementary hypothesis on A (for example $W^{1,\infty}$). We suppose in the following that all those hypothesis hold true.

Giving the proof of Theorem 13, the case of orthotropic medium will be either identical if we assume the solvability of all transmission eigenvalues that would appear in the proof or very painful, unclear and "combinatorial" if we want to specify the associated transmission problems since one has to go through all possible geometrical settings (as in Chapter 3) and all possible cases for A or A_0 (being equal to Id or not) and the same for n and n_0 (since each configuration requires to look for specific functional spaces and conditions on the parameters). We will rather highlight some specific cases that are either easy to handle or give rise to ITP that are not covered by existing literature.

We introduce the notation:

$$ITP(D,f,g,A,A_0,n,n_0) \equiv \begin{cases} \mathrm{div} A\nabla u + k^2 n u = 0 & \text{in } D, \\ \mathrm{div} A_0\nabla v + k^2 n_0 v = 0 & \text{in } D, \\ (u-v) = f & \text{on } \partial D, \\ (A\nabla u - A_0\nabla v)\cdot n = g & \text{on } \partial D, \end{cases} \tag{6.18}$$

and denote by $\sigma(D,A,A_0,n,n_0)$ the associated set of transmission eigenvalues.

The algorithm proposed in Chapter 3 exploits two sets of measurements that we will denote F and F_0 related to the perturbed medium and the background. From those two sets we can compute independently two sequences (indexed by α), $g_0^{\alpha,z}$ and $g^{\alpha,z}$, which lead to sequences $Hg^{\alpha,z}$ and $H_0 g_0^{\alpha,z}$ that converge strongly to v and v_0 where (u,v) and (u_0,v_0) are solutions of $ITP(D,\Phi_z,\partial_\nu\Phi_z,A,Id,n,1)$ and $ITP(D_0,\Phi_z,\partial_\nu\Phi_z,A_0,Id,n_0,1)$. In the following two examples we will see what are the hypothesis that should be needed to compare v and v_0. We will denote Ω the domain with Lipschitz boundary and connected complement such that $\{supp(n-n_0)\cup supp(A-A_0)\}\subset\Omega$.

The case Ω strictly included in D_0

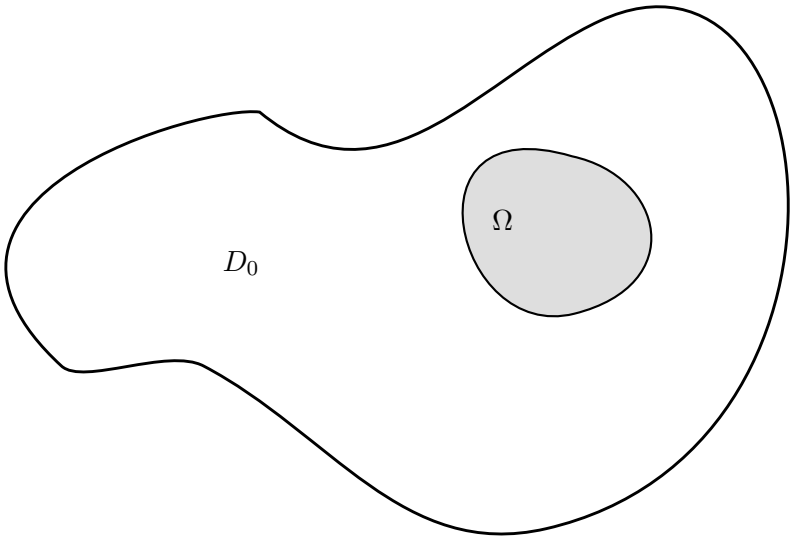

Figure 6.1: Schematic of the perturbation Ω

As a first case let us assume that D_0 and D are simply connected and that $\Omega \subsetneq D_0$ (which means that $D_0 = D$). In this case the perturbation that appears in between the two measurements takes place strictly inside a previously existing obstacle. To have convergence of the sequence of Herglotz wave functions that minimizes the GLSM cost functional to v and v_0, we should have $k \notin \{\sigma(D_0, A_0, Id, n_0, 1) \cup \sigma(D, A, Id, n, 1)\}$. This is a reasonable assumption if $\sigma(D_0, A_0, Id, n_0, 1) \cup \sigma(D, A, Id, n, 1)$ is discrete and countable with $+\infty$ as only accumulation point.

We know from [9] that $\sigma(D_0, A_0, Id, n_0, 1) \cup \sigma(D, A, Id, n, 1)$ is discrete for a solution in $H^1(D) \times H^1(D)$ if $A - Id$ and $1 - n$ have the same sign in a neighborhood of ∂D and $A_0 - Id$ and $1 - n_0$ have the same sign in a neighborhood of ∂D_0. We will assume that this is the case. In the proof of Theorem 13 we proceed using a contradiction argument, assuming that $v = v_0$ inside D_0. From this equality we deduce that the Cauchy data of u and u_0 are identical on $\partial D_0 = \partial D$. Then using a unique continuation argument (that's why we need some assumption on A and A_0) we deduce that u and u_0 solve $ITP(\Omega, 0, 0, A, A_0, n, n_0)$. To conclude that $u = u_0 = 0$ we need to assume that $k \notin \sigma(\Omega, A, A_0, n, n_0)$ which again is realistic if $\sigma(\Omega, A, A_0, n, n_0)$ is discrete. The latter problem has not been studied yet but it seems that a necessary condition (using the T-coercivity approach [9]) will be that $A - A_0$ and $n_0 - n$ should have the same sign near the boundary of Ω.

If we assume that $A = A_0$ in Ω, again the discreteness of $\sigma(\Omega, A, A_0, n, n_0)$ has not been studied. Following the work of [52] for $n - n_0$ that does not change sign in a neighborhood of $\partial\Omega$, it seems that the correct functional space could be $u, u_0 \in L^2(\Omega)$ and $u - u_0 \in H^2(\Omega)$. One immediately sees that above we assumed that $u, u_0 \in H^1(D)$, which means that to have $u - u_0 \in H^2(\Omega)$ using some elliptic regularity arguments one should assume that A and A_0 have C^1 regularity in a domain that strictly contains Ω.

Considering the case of $\Omega \subset D_0$ we quickly end up with an interior transmission problem that has not been clearly studied in the literature. Some of those problems might be treated

using already known techniques. However there is a tricky interplay between the spaces used to study $ITP(D_0, \Phi_z, \partial_\nu \Phi_z, A_0, Id, n_0, 1)$ and $ITP(D, \Phi_z, \partial_\nu \Phi_z, A, Id, n, 1)$ and the space one should use to study the solvability of $ITP(\Omega, 0, 0, A, A_0, n, n_0)$.

The case of Ω intersecting D_0

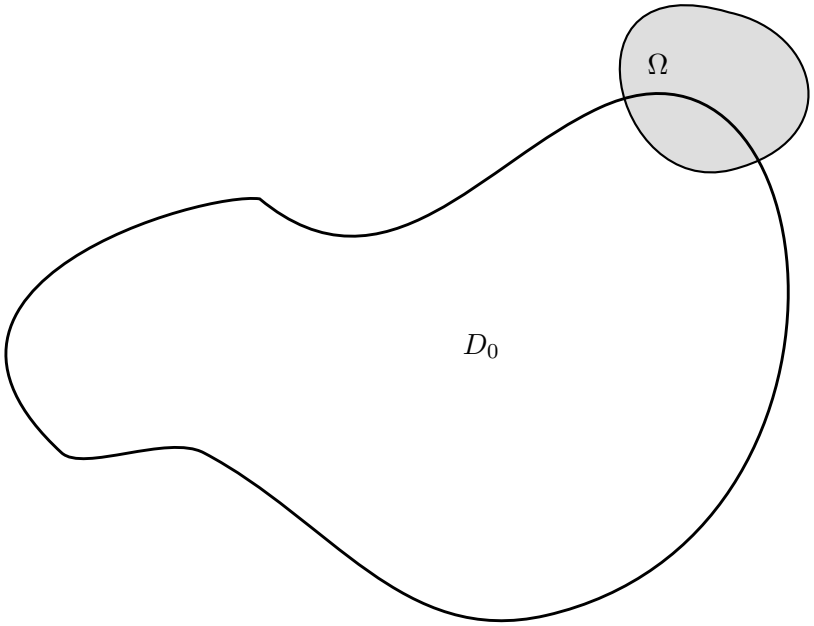

Figure 6.2: Schematic of the perturbation Ω

Let us assume that D_0 and D are simply connected and that $\Omega \cap D_0 \neq 0$ (which means that D_0 and Ω have non empty intersection). As in Chapter 3, we will assume that $\partial D_0 \cap \partial \Omega$ is of measure zero. Similarly to the previous section and Chapter 3 we obtain using the unique continuation principle that u and $\tilde{u}_0$ solves $ITP(\Omega, 0, 0, A, \tilde{A}_0, n, \tilde{n}_0)$ where we define:

$$\tilde{u}_0 = \begin{cases} u_0 & \text{in } D_0 \\ v + \Phi_z & \text{in } D \setminus D_0 \end{cases}, \tilde{A}_0 = \begin{cases} A_0 & \text{in } \tilde{D}_0 \\ Id & \text{in } D \setminus D_0 \end{cases}, \quad \tilde{n}_0 = \begin{cases} n_0 & \text{in } D_0 \\ 1 & \text{in } D \setminus D_0 \end{cases}.$$

If we assume that $A - Id$ and $1 - n$ have the same sign in a neighborhood of ∂D and $A_0 - Id$ and $1 - n_0$ have the same sign in a neighborhood of ∂D_0, we have that $\sigma(D_0, A_0, Id, n_0, 1) \cup \sigma(D, A, Id, n, 1)$ is discrete. As in the previous subsection we conjecture that $A - A_0$ and $n_0 - n$ having the same sign near the boundary of Ω is a sufficient condition for $\sigma(\Omega, A, \tilde{A}_0, n, \tilde{n}_0)$ to be discrete. Because Ω shares some boundary with D and D shares some boundary with D_0, we can deduce from the previous assumption that either $A > A_0 > Id$ and $n < n_0 < 1$ in neighborhood of ∂D or $A < A_0 < Id$ and $n > n_0 > 1$ in neighborhood of ∂D.

Considering other cases of contrast as in the previous subsection induces ITPs that are not solved in the literature and that exhibit complex interplay between the three possible different functional settings (known in the literature) for ITPs.

6.4 The case of known inhomogeneous backgrounds

In many applications the obstacle we try to image is embedded in a known heterogeneous background. Such configurations has been studied initially in [45] for electrical impedance tomography and then extended to isotropic Helmholtz equation in [33] and to anisotropic scalar waves in [19]. As for the near field case, the goal of those methods is to find an operator that will restore the symmetry of the second factorization in order to apply the factorization method. Since they consider incident plane waves they have restricted themselves to the case where $\Gamma_s = \Gamma_m$ (for reasons already discussed in Section 4.3). Using the framework of Section 4.2.2 we can extend their results to the case where $\Gamma_s \neq \Gamma_m$.

Even for full aperture measurements, the symmetry of the farfield operator has been successfully restored only when there is no absorption in the known heterogeneous medium and the support of the obstacle is inside the support of the background medium. In the following we would like to introduce the different quantities related to the case of known heterogeneous backgrounds. We consider a known background medium of physical parameters A_0 and n_0 and a unknown medium of physical parameters A and n. We introduce Ω such that support of $n - n_0$ and $A - A_0$ is include inside $\bar{\Omega}$. Moreover we assume that Ω is such that it has a Lipschitz boundary and connected complement in $\mathbb{R}^d$. We measure the farfield pattern of the scattered field $u^s(\hat{d}, \cdot)$ generated by A and n for an incident plane wave $\psi(\hat{d}, \cdot)$ for several directions. We denote by F the farfield operator associated to this medium. The condition on those directions of incidence and measurement can be either in the setting of full or limited aperture. Because the background medium is known we can also compute the far field pattern of $u_0^s(\hat{d}, \cdot)$ associated to A_0 and n_0 for $\psi(\hat{d}, \cdot)$. Therefore one has access to the farfield operator F_0 of the background medium. Those two scattered fields solve:

$$\begin{cases} \operatorname{div}(A\nabla u^s) + nk^2 u^s = -k^2(n-1)\psi - \operatorname{div}((A - Id)\nabla\psi) \text{ in } \mathbb{R}^d, \\ \lim\limits_{r\to\infty} \int\limits_{|x|=r} \left|\frac{\partial u^s}{\partial r} - iku^s\right|^2 ds = 0. \end{cases} \tag{6.19}$$

$$\begin{cases} \operatorname{div}(A_0\nabla u_0^s) + n_0 k^2 u_0^s = -k^2(n-1)\psi - \operatorname{div}((A_0 - Id)\nabla\psi) \text{ in } \mathbb{R}^d, \\ \lim\limits_{r\to\infty} \int\limits_{|x|=r} \left|\frac{\partial u_0^s}{\partial r} - iku_0^s\right|^2 ds = 0. \end{cases} \tag{6.20}$$

If we introduce $w = u^s - u_0^s$ and the total fields $u_0 = u_0^s + \psi$ and $u = u^s + \psi$, then after straightforward calculations we end up with

$$\begin{cases} \operatorname{div}(A_0\nabla w) + n_0 k^2 w = -k^2(n-n_0)u - \operatorname{div}((A - A_0)\nabla u) \text{ in } \mathbb{R}^d, \\ \operatorname{div}(A\nabla w) + nk^2 w = -k^2(n-n_0)u_0 - \operatorname{div}((A - A_0)\nabla u_0) \text{ in } \mathbb{R}^d, \\ \lim\limits_{r\to\infty} \int\limits_{|x|=r} \left|\frac{\partial w}{\partial r} - ikw\right|^2 ds = 0. \end{cases} \tag{6.21}$$

From those equations it is natural to introduce the following operators, $H : L^2(\Gamma_s) \to X(\Omega)$ defined by

$$Hg := \begin{bmatrix} \int_{\mathbb{S}} u_0(\hat{d}, x) g(\hat{d}) \\ \nabla \int_{\mathbb{S}} u_0(\hat{d}, y) g(\hat{d}) \end{bmatrix} \quad x \in \Omega_n \text{ and } y \in \Omega_A, \tag{6.22}$$

which plays the role of the Herglotz operator, and $K^* : X(\Omega) \to L^2(\Gamma_m)$ defined by

$$K^*\varphi = K^* \begin{bmatrix} \varphi \\ \nabla\varphi \end{bmatrix}(\hat{x}) := \int_{\Omega_n} \Phi^\infty_{n_0}(y,\hat{x})\varphi(y)dy + \int_{\Omega_A} (A - Id)\nabla_y \Phi^\infty_{n_0}(y,\hat{x}) \cdot \nabla\varphi dy, \ \varphi \in X(\Omega)$$

which plays the role of the adjoint Herglotz operator, and

$$T \begin{bmatrix} \psi \\ \nabla\psi \end{bmatrix} := \begin{bmatrix} -k^2(n_0 - n)(\psi + w) \\ -(A - A_0) \cdot (\nabla\psi(y) + \nabla(w(y)) \end{bmatrix}, \tag{6.23}$$

with $w \in H^1_{\text{loc}}(\mathbb{R}^d)$ being the solution of (6.21)(with $\psi = u_0$). We therefore obtain the following factorization

$$F - F_0 = W = K^*TH.$$

We see that we obtain again a non symmetric factorization. In order to apply the GLSM framework to this setting we should relate the range of $G = K^*T$ restricted to $\overline{\mathcal{R}H}$ to the support of Ω and then study the coercivity of T. To do so we need to introduce the following interior transmission problem defined for u and v in $H^1(\Omega)$,

$$\begin{cases} \text{div}A\nabla u + k^2 nu = 0 \quad \text{in } \Omega, \\ \Delta A_0 v + k^2 n_0 v = 0 \quad \text{in } \Omega, \\ (u - v) = f \quad \text{on } \partial\Omega, \\ (A\nabla u - A_0\nabla v) \cdot n = g \quad \text{on } \partial\Omega. \end{cases} \tag{6.24}$$

We assume that k is such that this problem is well posed.

Lemma 13. *If k is such that (6.24) is well posed the we have that $\Phi^\infty_{0,z} \in \mathcal{R}(G)$ if and only if $z \in \Omega$.*

Proof. The proof of this lemma is exactly the same as in the case of the vacuum as long as one can use the unique continuation principle in the background medium. □

The following lemma states an similar result as in Lemma 8 for the case of known background

Lemma 14. *We have the following identity, for $\psi = (\psi_1, \psi_2) \in L^2(\Omega_n) \times L^2(\Omega_A)^d$ and T defined in (6.23) :*

$$\Im(T\psi,\, \psi) = k \int_{\mathbb{S}^{d-1}} |w^\infty|^2 - \int_{\Omega_A} \Im(A - A_0)(\nabla(w) + \psi_2) \cdot (\overline{\nabla(w) + \psi_2}) + k^2 \int_{\Omega_n} \Im(n - n_0)|w + \psi_1|^2$$

We introduce $\Omega = \bigcup_i \Omega^i_n \cup \bigcup_i \Omega^i_A$ where the Ω_i are simply connected disjoint components. We assume that $A - A_0$ is not zero in the neighborhood of the boundary Ω^i_A and $A - Id$ equals zero in the neighborhood of the boundary Ω^i_n. We denote V neighborhood of $\partial\Omega$, $\Omega_1 = \bigcup_i \Omega^i_A$, $\Omega_2 = \bigcup_i \Omega^i_n$.

Theorem 30. *We assume that k is not a transmission eigenvalue of 6.24, $\Im(A - A_0) \leq 0$ and $\Im(n - n_0) \geq 0$ and A and A_0 are of regularity C^1 in $\bigcup_i \Omega^i_A \cap V$ and there exist $c > 0$ and $\alpha > 0$ such that either $\Re(A - A_0) - \alpha\Im(A - A_0) \geq c > 0$ in $\bigcup_i \Omega^i_A \cap V$ and $\Re(n_0 - n) + \alpha\Im(n - n_0) \geq c > 0$*

in $\bigcup_i \Omega_n^i \cap V$ *or* $\Re(A_0 - A) - \alpha\Im(A - A_0) \geq c > 0$ *in* $\bigcup_i \Omega_A^i \cap V$ *and* $\Re(n - n_0) + \alpha Im(n - n_0) \geq c > 0$ *in* $\bigcup_i \Omega_n^i \cap V$ *is verified. Then we have that* T *defined in* (4.4) *satisfies*

$$|(T\psi,\, \psi)| \geq \mu \, \|\psi\|^2_{X(\Omega)}$$

for all $\psi \in \overline{\mathcal{R}(H)}$.

The proof is again identical to the one of Section 4.3. As the background medium is known it is possible to compute H and K as operators from $L^2(\mathbb{S}^{d-1})$ to $\hat{X}(\Sigma) \times \hat{X}(\Sigma)^d$ where Σ is an a priori region such that $\Omega \subset \Sigma$. We can then finally state the exact characterization of Ω as a corollary of Theorems 18 and 19. One can apply Theorems 18 and 19 with $U = K$, $V = H$ and $\hat{Y} = \hat{X}(\Sigma)$, where $\Omega \subset \Sigma$.

Chapter 7

Elasticity

Contents

In this chapter we consider the scattering problem for linear elasticity. It turns out that in the case of full data, the formalism for previously introduced sampling methods is close to the one used in Chapter 6 and therefore we conclude in Sections 7.1 and 7.2 that the results from the previous chapters can be easily extended. In Section 7.4 we discuss the case of partial polarization data. The use of partial polarization data introduces new original problems that are still unsolved by the writing of this manuscript and constitute interesting perspectives. First the interior transmission problem is replaced with a problem that couples an interior transmission problem with an exterior one together with conditions on the polarization of the interior incident field and exterior scattered field. We were not able to demonstrate that this problem is of Fredholm type. The second problem arises when one considers that one polarization is used for the incident wave and the other polarization of the scattered field is measured. In this case the farfield pattern have a non symmetric factorization that does not verify the hypothesis of Chapter 4.

7.1 Model problem

We are interested in the inverse time harmonic scattering problem for linear elasticity. For a frequency $\omega > 0$ the total field, u, solves Navier equation:

$$\mathrm{div}(2\mu \mathrm{e}(u) + \lambda \mathrm{div}(u) Id) + \rho\omega^2 u = 0$$

where $\mathrm{e}(u) := \frac{1}{2}(\nabla u + \nabla u^\top)$ is the strain tensor, $\lambda \in L^\infty(\mathbb{R}^d)$ and $\mu \in L^\infty(\mathbb{R}^d)$ are the Lamé constants and $\rho \in L^\infty(\mathbb{R}^d)$ is the density. For the sake of simplicity we suppose that those physical parameters are such that the supports of the contrasts $\tilde{\lambda} = \lambda - \lambda_0$, $\tilde{\mu} = \mu - \mu_0$ and $\tilde{\rho} = \rho - \rho_0$ are all equal to $\overline{D}$ with D a bounded domain with Lipschitz boundary and connected complement. Moreover we assume that $\Im(\tilde{\rho}) \geq 0$,$\Im(3\tilde{\lambda} + 2\tilde{\mu}) \leq 0$, $\Im(\tilde{\mu}) \leq 0$ and $\Im(\rho_0) = \Im(\lambda_0) = \Im(\mu_0) = 0$. Finally for the sake of simplicity we restrict ourselves to the case where the supports of $\tilde{\mu}$, $\tilde{\lambda}$ and $\tilde{\rho}$ are exactly $\bar{D}$.

We are interested in the case where the total field is generated by plane waves. There are several types of plane waves considering the direction of incidence and the type of polarization. To have a unified representation we consider the extension of vector elastic fields to dyadic elastic fields. Using this representation a dyadic elastic plane wave with direction of incidence $\hat{d}$ is :

$$\mathbf{u^i}(\hat{d}, x) := e^{ik_p x.\hat{d}} \hat{d} \otimes \hat{d} + e^{ik_s x.\hat{d}} \left(I - \hat{d} \otimes \hat{d} \right)$$

A vector elastic field is then obtained by taking the dot product between the dyadic field and the desired polarization vector $\hat{p}$: $u^i(\hat{d}, x) = \mathbf{u^i}(\hat{d}, x) \cdot \hat{p} := e^{ik_p x.\hat{d}} (\hat{d} \cdot \hat{p}) \hat{d} + e^{ik_s x.\hat{d}} (\hat{\theta}_{\hat{d}} \cdot \hat{p}) \hat{\theta}_{\hat{d}} + e^{ik_s x.\hat{d}} (\hat{\varphi}_{\hat{d}} \cdot \hat{p}) \hat{\varphi}_{\hat{d}}$ with $x \in \mathbb{R}^3$, $\hat{d}, \hat{\theta}_{\hat{d}}, \hat{\varphi}_{\hat{d}} \in \mathbb{S}^2$ (formed an orthonormal system) and $k_p = \omega \sqrt{\frac{\rho_0}{2\mu_0 + \lambda_0}}$ and $k_s = \omega \sqrt{\frac{\rho_0}{\mu_0}}$. The extension to dyadic fields does not impact nor interact with the differential operator, it is only a convenient way to gather in one notation all the possible polarizations. Thus one can retrieve the corresponding vector field by simply projecting (dotted to the right) on the corresponding polarizations.

We denote by u^s the scattered field and denote by $\mathbf{u^s}(\hat{d}, \cdot) := \mathbf{u} - \mathbf{u^i}(\hat{d}, \cdot)$ its dyadic counter part. We can introduce the *pressure* and *shear* parts of the scattered field :

$$\mathbf{u_p^s} = -\frac{1}{k_p^2} \mathrm{grad}\ \mathrm{div} \mathbf{u^s}$$

$$\mathbf{u_s^s} = \frac{1}{k_s^2} \mathrm{curl}\ \mathrm{curl} \mathbf{u^s}$$

Using those two quantities we can formulate the radiation condition (also called Kupradze condition) verified by $\mathbf{u^s}$:

$$\begin{cases} \lim\limits_{R \to +\infty} \int_{|x|=R} \left| \dfrac{\partial \mathbf{u_p^s}}{\partial r} - ik_p \mathbf{u_p^s} \right|^2 ds = 0 \\ \lim\limits_{R \to +\infty} \int_{|x|=R} \left| \dfrac{\partial \mathbf{u_s^s}}{\partial r} - ik_s \mathbf{u_s^s} \right|^2 ds = 0 \end{cases} \tag{7.1}$$

Our data for the inverse problem will be formed by the noisy measurements of the so called farfield pattern defined by the following asymptotic expansion :

$$\mathbf{u^s}(\hat{d}, x) = \frac{e^{k_p |x|}}{|x|^{\frac{d-1}{2}}} \mathbf{u_p^\infty}(\hat{d}, \hat{x}) + \frac{e^{k_s |x|}}{|x|^{\frac{d-1}{2}}} \mathbf{u_s^\infty}(\hat{d}, \hat{x}) + O(1/|x|)$$

with $\mathbf{u_s^\infty}$ the shear-part (transverse waves) and $\mathbf{u_p^\infty}$ pressure-part (normal waves). They define the farfield pattern $\mathbf{u^\infty} = \mathbf{u_p^\infty} + \mathbf{u_s^\infty}$.

Let us define for all $v \in H^1(D)^d$ the unique function $w \in H^1_{loc}(\mathbb{R}^d)^d$ satisfying

$$\begin{cases} \mathrm{div}(2\mu \mathrm{e}(w) + \lambda \mathrm{div}(w) Id) + \rho\omega^2 w = -\mathrm{div}(2\tilde{\mu}\mathrm{e}(v) + \tilde{\lambda}\mathrm{div}(v)Id) - \tilde{\rho}\omega^2 v \\ w \text{ satisfies (7.1)} \end{cases} \tag{7.2}$$

The incident field is given by the Herglotz wave:

$$v_g(x) := \int_{\hat{d}\in\mathbb{S}^{d-1}} e^{ik_p x.\hat{d}} g_p(\hat{d}) + e^{ik_s x.\hat{d}} g_s(\hat{d})$$

where $g \in L^2(\mathbb{S}^{d-1})^d$ can be uniquely decomposed into $g = g_p + g_s$, with $g_p \in L_p(\mathbb{S}^{d-1})$ and $g_s \in L_s(\mathbb{S}^{d-1})$ and $L_p(\mathbb{S}^{d-1})$ and $L_s(\mathbb{S}^{d-1})$ respectively defined as $\{g \in L^2(\mathbb{S}^{d-1})^d \text{ s.t. } g(\hat{d}) \times \hat{d} = 0\}$ and $\{g \in L^2(\mathbb{S}^{d-1})^d \text{ s.t. } g(\hat{d}) \cdot \hat{d} = 0\}$. Using the dyadic form this can be written:

$$v_g(x) := \int_{\hat{d}\in\mathbb{S}^{d-1}} \mathbf{u^i}(x, \hat{d}) \cdot (g_s(\hat{d}) + g_p(\hat{d}))$$

By linearity of the forward scattering problem the farfield pattern of w solution of (7.2) (with $v = v_g$) is given by :

$$w^\infty(\hat{x}) := Fg(\hat{x}) := \int_{\hat{d}\in\mathbb{S}^{d-1}} \mathbf{u}^\infty(\hat{x}, \hat{d}) \cdot (g_s(\hat{d}) + g_p(\hat{d}))$$

where $F : L^2(\mathbb{S}^{d-1})^d \to L^2(\mathbb{S}^{d-1})^d$ is called the farfield operator and where w^∞ is the farfield of w.

Now we introduce the compact operator (closely related to v_g) $H : L^2(\mathbb{S}^{d-1})^d \to X(D)$, where $X(D) = \{(f, g, h) \in L^2(D)^d \times L^2(D) \times L^2(D)^{d\times d} \; s.t. \; g = \mathrm{div}(f) \; and \; h = \mathrm{e}(f)\}$, defined by

$$Hg(x) = \begin{bmatrix} v_g(x) \\ \mathrm{div}(v_g)(x) \\ \mathrm{e}(v_g)(x) \end{bmatrix} = \begin{bmatrix} v_g(x) \\ ik_p \int_{\hat{d}\in\mathbb{S}^{d-1}} e^{ik_p x.\hat{d}} \hat{d} \cdot g_p(\hat{d}) \\ \int_{\hat{d}\in\mathbb{S}^{d-1}} e^{ik_p x.\hat{d}} ik_p \hat{d} \otimes g_p(\hat{d}) + e^{ik_s x.\hat{d}} ik_s \hat{d} \otimes g_s(\hat{d}) \end{bmatrix} \tag{7.3}$$

for $x \in D$.

Remark 14. *Using the Korn inequality*

$$\|f\|_{H^1(D)^d} \leq C(\|\mathrm{e}(f)\|_{L^2(D)^{d\times d}} + \|f\|_{L^2(D)^d}), \tag{7.4}$$

on the third element of Hg we can conclude that the first element of Hg, namely v_g, is in $H^1(D)$. One other useful inequality relating the second and the third components of Hg is:

$$\|\mathrm{div}(f)\|_{L^2(D)} \leq 3 \|\mathrm{e}(f)\|_{L^2(D)^{d\times d}} \tag{7.5}$$

We can also define the compact operator $G : \mathcal{R}(H) \subset X \to L^2(\mathbb{S}^{d-1})^d$ defined by

$$Gv := w^\infty.$$

We then clearly have that:

$$F = GH.$$

This factorization together with lemma 15 leads to the Linear Sampling Method for elastic waves, more details about this can be found in [1].

The Green tensor fundamental solution of the Navier equation in free space is defined (in dyadic form)

$$\mathbf{\Gamma}(x,y) = \begin{cases} \frac{1}{\mu_0}\frac{e^{ik_s|x-y|}}{4\pi|x-y|}Id - \frac{i}{4\mu_0 k_s^2}\nabla_x \otimes \nabla_x \left[H_0^1(k_p|x-y|) - H_0^1(k_s|x-y|)\right] \text{ in } 2D \\ \frac{1}{\mu_0}\frac{e^{ik_s|x-y|}}{4\pi|x-y|}Id - \frac{1}{\mu_0 k_s^2}\nabla_x \otimes \nabla_x \left[\frac{e^{ik_p|x-y|}}{4\pi|x-y|} - \frac{e^{ik_s|x-y|}}{4\pi|x-y|}\right] \text{ in } 3D \end{cases}$$

for $x \in \mathbb{R}^d \setminus \{y\}$. And it has the following farfield:

$$\mathbf{\Gamma}_{\mathbf{p}}^{\infty}(\hat{x},y) = \begin{cases} \frac{e^{i\pi/4}}{(\lambda_0+2\mu_0)\sqrt{8\pi k_p}}e^{-ik_p\hat{x}\cdot y}\hat{x}\otimes\hat{x} \text{ in } 2D \\ \frac{k_p^2}{4\pi\rho_0\omega^2}e^{-ik_p\hat{x}\cdot y}\hat{x}\otimes\hat{x} \text{ in } 3D \end{cases}$$

$$\mathbf{\Gamma}_{\mathbf{s}}^{\infty}(\hat{x},y) = \begin{cases} \frac{e^{i\pi/4}}{\mu_0\sqrt{8\pi k_s}}e^{-ik_s\hat{x}\cdot y}(Id-\hat{x}\otimes\hat{x}) \text{ in } 2D \\ \frac{k_s^2}{4\pi\rho_0\omega^2}e^{-ik_s\hat{x}\cdot y}(Id-\hat{x}\otimes\hat{x}) \text{ in } 3D \end{cases}$$

The farfield pattern of w, solution of (7.2) also solves:

$$\begin{cases} \mathrm{div}(2\mu_0 \mathrm{e}(w) + \lambda_0 \mathrm{div}(w)Id) + \rho_0\omega^2 w = -\mathrm{div}(2\tilde{\mu}\mathrm{e}(v+w) + \tilde{\lambda}\mathrm{div}(v+w)Id) - \tilde{\rho}\omega^2(v+w) \\ w \text{ satisfies (7.1)} \end{cases} \tag{7.6}$$

Using the fundamental solution of the elasticity system, w can be expressed through the following Lippmann-Schwinger type equation:

$$w(x) = \int_D \tilde{\rho}\omega^2 \mathbf{\Gamma}(x,z)(w+v) - \tilde{\lambda}\mathrm{div}_z(\mathbf{\Gamma}(x,z))\mathrm{div}(w+v) - 2\tilde{\mu}\mathrm{e}_z(\mathbf{\Gamma}(x,z)) : \mathrm{e}(w+v)dV(z) \tag{7.7}$$

Taking the asymptotic expansion of the previous expression one simply has that $G = H^*T$ where $H^* : X \to L^2(\mathbb{S}^{d-1})^d$ is the adjoint of H defined by:

$$H^*[f, \mathrm{div}(f), \mathrm{e}(f)](\hat{x}) = \int_D \mathbf{\Gamma}^{\infty}(\hat{x},z)f(z) + \mathrm{div}_z\mathbf{\Gamma}^{\infty}(\hat{x},z)\mathrm{div}(f)(z) + \mathrm{e}(\mathbf{\Gamma}^{\infty}(\hat{x},z)) : \mathrm{e}(f)(z)dV(z) \tag{7.8}$$

and where $T : X \to X$ is defined by

$$T(f) = \begin{bmatrix} \tilde{\rho}\omega^2(w+f) \\ -\tilde{\lambda}(\mathrm{div}(w)+\mathrm{div}(f)) \\ -2\tilde{\mu}(\mathrm{e}(w)+\mathrm{e}(f)) \end{bmatrix} \tag{7.9}$$

with w defined as the weak radiating solution to : $\mathrm{div}(2\mu\mathrm{e}(w) + \lambda\mathrm{div}(w)Id) + \rho\omega^2 w = -\mathrm{div}(\tilde{\mu}\mathrm{e}(f) + \tilde{\lambda}\mathrm{div}(f)Id) - \tilde{\rho}\omega^2 f$.

7.2 Preliminary results for sampling methods

As for the acoustic case, sampling methods rely on the solvability of the interior transmission problem. For the Navier equations it takes the following form:

$$\begin{cases} \operatorname{div}(2\mu_0 \mathrm{e}(v) + \lambda_0 \operatorname{div}(v) Id) + \rho_0 \omega^2 v = 0 & D \\ \operatorname{div}(2\mu \mathrm{e}(u) + \lambda \operatorname{div}(u) Id) + \rho \omega^2 u = 0 & D \\ u - v = 0 & \partial D \\ T_{\mathbf{n}}(u) - T^0_{\mathbf{n}}(v) = 0 & \partial D \end{cases} \tag{7.10}$$

where

$$T_{\mathbf{n}}(u) := 2\mu \mathbf{n} \cdot \nabla u + \lambda \operatorname{div}(u)\mathbf{n} + \mu \mathbf{n} \times \operatorname{curl}(u)$$

is the surface stress vector and $\mathbf{n}$ is the outwardly directed unit normal on ∂D ($T^0_{\mathbf{n}}$ is defined similarly for the background medium corresponding with μ_0, λ_0 and ρ_0).
The functional spaces that should be used to study the ITP depend on the value of the contrast $\tilde{\lambda}$, $\tilde{\mu}$ and $\tilde{\rho}$. In [7] a study of the problem for different kind of material properties is given. In our case we assume that $\tilde{\lambda}$, $\tilde{\mu}$ and $\tilde{\rho}$ have the same support and therefore the appropriate solution space is $(u, v) \in H^1(D)^d \times H^1(D)^d$. The values of ω for which this problem has a non trivial solution are the interior transmission eigenvalues. As in the case of Helmholtz equation we state the two important lemmas related to the range of G and the coercivity of T.

Lemma 15. *For any polarization $p \in \mathbb{S}^{d-1}$ and if ω is not an interior transmission eigenvalue, $\Gamma^\infty(\cdot, z) \cdot p \in \mathcal{R}(G)$ if and only if $z \in D$. Moreover if $z \in D$ and $G\varphi = \Gamma^\infty(\cdot, z) \cdot p$ we have that the first component of φ, $\varphi_1 \in H^1(D)$ (because of $\varphi \in \overline{\mathcal{R}}(H)$) and $u \in H^1(D)$ solve*

$$\begin{cases} \operatorname{div}(2\mu_0 \mathrm{e}(\varphi_1) + \lambda_0 \operatorname{div}(\varphi_1) Id) + \rho_0 \omega^2 \varphi_1 = 0 & D \\ \operatorname{div}(2\mu \mathrm{e}(u) + \lambda \operatorname{div}(u) Id) + \rho \omega^2 u = 0 & D \\ u - v = \Gamma(\cdot, z)p & \partial D \\ T_{\mathbf{n}}(u) - T^0_{\mathbf{n}}(v) = T^0_{\mathbf{n}}(\Gamma(\cdot, z)p) & \partial D \end{cases} \tag{7.11}$$

Lemma 16. *Under the hypothesis that ω is not an interior transmission eigenvalue and that either*

- *there exist $\alpha, c > 0$ such that $\Re(\tilde{\lambda}) \leq 0$ and $\Re(2\tilde{\mu} + 3\tilde{\lambda}) - \alpha \Im(2\tilde{\mu} + 3\tilde{\lambda}) \geq c > 0$ in D,*
- *there exist $\alpha, c > 0$ such that $\Re(\tilde{\lambda}) \geq 0$ and $-\Re(2\tilde{\mu} + 3\tilde{\lambda}) - \alpha \Im(2\tilde{\mu} + 3\tilde{\lambda}) \geq c > 0$ in D,*

the operator T verifies:

$$|(Th,\, h)| \geq c \, \|h\|_X^2 \,,$$

for $h \in \overline{\mathcal{R}(H)}$.

Proof. First we prove an identity related to the imaginary part of T. Multiplying (7.6) with $\overline{w}$ and integrating by parts over B_R, a ball of radius R containing D,

$$\begin{aligned} &- \int_{B_R} \left[2\mu_0 |\mathrm{e}(w)|^2 + \lambda_0 |\operatorname{div}(w)|^2 - \rho_0 \omega^2 |w|^2 \right] dx + \int_{|x|=R} T^0_{\mathbf{n}}(w) \overline{w} \\ &= \int_D \left[2\tilde{\mu} \mathrm{e}(v+w) \mathrm{e}(\overline{w}) + \tilde{\lambda} \operatorname{div}(v+w) \operatorname{div}(\overline{w}) - \tilde{\rho} \omega^2 (v+w) \overline{w} \right]. \end{aligned} \tag{7.12}$$

One can easily show that the radiation condition implies that :

$$\int_{|x|=R} T^0_{\mathbf{n}}(w)\overline{w} = ik_p(\lambda_0+2\mu_0)\int_{|x|=1} w_p^\infty \overline{w_p^\infty} ds + ik_s\mu_0 \int_{|x|=1} w_s^\infty \overline{w_s^\infty} ds + O(\frac{1}{R})$$

Therefore, taking the imaginary part and letting $R \to \infty$ yields:

$$\begin{aligned} &\Im\Big(\int_D 2\tilde{\mu}\mathrm{e}(v+w)\mathrm{e}(\overline{w}) + \tilde{\lambda}\mathrm{div}(v+w)\mathrm{div}(\overline{w}) - \tilde{\rho}\omega^2(v+w)\overline{w} \\ &= -\int_{\mathbb{R}^d} \left[2\Im(\mu_0)|\mathrm{e}(w)|^2 + \Im(\lambda_0)|\mathrm{div}(w)|^2\right] dx + \int_{\mathbb{R}^d} \Im(\rho_0)\omega^2|w|^2 dx \\ &\quad + k_p(\lambda_0+2\mu_0)\int_{\mathbb{S}^{d-1}} w_p^\infty \overline{w_p^\infty} ds + k_s\mu_0 \int_{\mathbb{S}^{d-1}} w_s^\infty \overline{w_s^\infty} ds \end{aligned} \tag{7.13}$$

Consequently decomposing $(v+w)\overline{v} = |v+w|^2 - (v+w)\overline{w}$, we obtain the following important identity,

$$\begin{aligned} \Im(Tv,\, v) = &\int_D \left[-2\Im(\tilde{\mu})|\mathrm{e}(v+w)|^2 - \Im(\tilde{\lambda})|\mathrm{div}(v+w)|^2 + \Im(\tilde{\rho})\omega^2|v+w|^2\right] \\ &- \int_{\mathbb{R}^d} \left[2\Im(\mu_0)|\mathrm{e}(w)|^2 + \Im(\lambda_0)|\mathrm{div}(w)|^2\right] dx \\ &+ \int_{\mathbb{R}^d} \Im(\rho_0)\omega^2|w|^2 dx + k_p(\lambda_0+2\mu_0)\int_{\mathbb{S}^{d-1}} w_p^\infty \overline{w_p^\infty} ds + k_s\mu_0 \int_{\mathbb{S}^{d-1}} w_s^\infty \overline{w_s^\infty} ds \end{aligned} \tag{7.14}$$

From physical considerations, we know that $\Im(3\lambda+2\mu) \le 0$, $\Im(\mu) \le 0$ and $\Im(\rho) \ge 0$ and by assumption we have $\Im(\lambda_0) = 0$; $\Im(\mu_0)) = 0$ and $\Im(\rho_0) = 0$. If $\Im(\lambda) \le 0$ we immediately conclude that $\Im(Tv,\, v) \ge 0$. If $\Im(\lambda) > 0$ using (7.5) we can also obtain that $\Im(Tv,\, v) \ge 0$.
To prove the coercivity property we use a contradiction argument. Assume for instance the existence of a sequence $v_\ell \in \mathcal{R}(H)$ (to avoid complicated notation we will omit the subscript 1 in $v_{\ell,1}$) such that:

$$\|v_\ell\|_X = 1 \quad \text{and} \quad |(Tv_\ell,\, v_\ell)| \to 0 \text{ as } l \to \infty.$$

We denote by w_ℓ the solution of (7.2) for $v = v_\ell$. Using inequality (7.4) we have that $\|v_\ell\|_{H^1(D)^d}$ is also bounded and bounded away from 0 independently from ℓ. Then up to changing the initial sequence, one can assume that v_ℓ weakly converges to some v in $H^1(D)^d$. Elliptic regularity implies that $\|w_\ell\|_{H^1(D)^d}$ is bounded uniformly with respect to ℓ. It is then easily seen that w and v satisfy (7.2) and since $v_\ell \in \mathcal{R}(H)$, v satisfies

$$\mathrm{div}(2\mu_0\mathrm{e}(v) + \lambda_0\mathrm{div}(v)Id) + \rho_0\omega^2 v = 0$$

Identity (7.14) and $|(Tv_\ell,\, v_\ell)| \to 0$ implies that $w^\infty = 0$. The Rellich theorem and the unique continuation principle imply that $w = 0$ outside D. Therefore $u = w + v \in H^1(D)$ and v are solution of the interior transmission problem (7.10). Since we exclude the interior transmissions eigenvalues $w = u = v = 0$.
First we consider the case where $\Re(2\tilde{\mu}+3\tilde{\lambda}) - \alpha|\Im(2\tilde{\mu}+3\tilde{\lambda}) > 0$ and $\Re(\tilde{\lambda}) \le 0$. Identity (7.12)

implies that:

$$
\begin{aligned}
(Tv_\ell,\, v_\ell) = &- \int_D \left[2\tilde{\mu}|\mathrm{e}(v_\ell+w_\ell)|^2 + \tilde{\lambda}|\mathrm{div}(v_\ell+w_\ell)|^2 + |v_\ell+w_\ell|^2\right] - \int_{\mathbb{R}^d} \left[2\mu_0|\mathrm{e}(w_\ell)|^2 + \lambda_0|\mathrm{div}(w_\ell)|^2 + |w_\ell|^2\right] \\
&+ \int_{\mathbb{R}^d} (\rho_0\omega^2+1)|w_\ell|^2 dx + \int_D (\tilde{\rho}\omega^2+1)|v_\ell+w_\ell|^2 \\
&+ ik_p(\lambda_0+2\mu_0)\int_{\mathbb{S}^{d-1}} |w^\infty_{p,\ell}|^2 ds + ik_s\mu_0 \int_{\mathbb{S}^{d-1}} |w^\infty_{s,\ell}|^2 ds
\end{aligned}
\tag{7.15}
$$

The terms on the second line goes to zero due to the compact embedding from $H^1(D)^d$ to $L^2(D)^d$, $H^1_{loc}(\mathbb{R}^d)^d$ to $L^2_{loc}(\mathbb{R}^d)^d$ and $H^1_{loc}(\mathbb{R}^d)^d$ to $L^2(\mathbb{S}^{d-1})^d$. Putting all these terms under the notation CT we get:

$$
\begin{aligned}
|(Tv_\ell,\, v_\ell)| \geq &\Big| \int_D \left[2\tilde{\mu}|\mathrm{e}(v_\ell+w_\ell)|^2 + \tilde{\lambda}|\mathrm{div}(v_\ell+w_\ell)|^2 + |v_\ell+w_\ell|^2\right] \\
&+ \int_{\mathbb{R}^d} \left[2\mu_0|\mathrm{e}(w_\ell)|^2 + \lambda_0|\mathrm{div}(w_\ell)|^2 + |w_\ell|^2\right] \Big| - |CT| \\
&\geq \frac{1}{\sqrt{2}}\Big(\int_D \left[2\Re(\tilde{\mu})|\mathrm{e}(v_\ell+w_\ell)|^2 - \Re(-\tilde{\lambda})|\mathrm{div}(v_\ell+w_\ell)|^2 + |v_\ell+w_\ell|^2\right] \\
&+ \int_{\mathbb{R}^d} \left[2\mu_0|\mathrm{e}(w_\ell)|^2 + \lambda_0|\mathrm{div}(w_\ell)|^2 + |w_\ell|^2\right] dx \\
&+ \Big| \int_D 2\Im(\tilde{\mu})|\mathrm{e}(v_\ell+w_\ell)|^2 + \Im(\tilde{\lambda})|\mathrm{div}(v_\ell+w_\ell)|^2 \Big| - |CT|
\end{aligned}
$$

If $\Im(\tilde{\lambda}) \leq 0$ we find that

$$
\begin{aligned}
|(Tv_\ell,\, v_\ell)| \geq \frac{1}{\sqrt{2}}\Big(&\int_D \left[\Re(2\tilde{\mu}+3\tilde{\lambda})|\mathrm{e}(v_\ell+w_\ell)|^2 + |v_\ell+w_\ell|^2\right] + \int_{\mathbb{R}^d} \left[2\mu_0|\mathrm{e}(w_\ell)|^2 + \lambda_0|\mathrm{div}(w_\ell)|^2 + |w_\ell|^2\right] dx \\
&- \int_D 2\Im(\tilde{\mu})|\mathrm{e}(v_\ell+w_\ell)|^2 + \Im(\tilde{\lambda})|\mathrm{div}(v_\ell+w_\ell)|^2 \Big) - |CT|
\end{aligned}
$$

If $\Im(\tilde{\lambda}) > 0$ we find that

$$
\begin{aligned}
|(Tv_\ell,\, v_\ell)| \geq \frac{1}{\sqrt{2}}\Big(&\int_D \left[\Re(2\tilde{\mu}+3\tilde{\lambda})|\mathrm{e}(v_\ell+w_\ell)|^2 + |v_\ell+w_\ell|^2\right] + \int_{\mathbb{R}^d} \left[2\mu_0|\mathrm{e}(w_\ell)|^2 + \lambda_0|\mathrm{div}(w_\ell)|^2 + |w_\ell|^2\right] dx \\
&- \int_D \Im(2\tilde{\mu}+3\tilde{\lambda})|\mathrm{e}(v_\ell+w_\ell)|^2 \Big) - |CT|
\end{aligned}
$$

which finally leads (independently of the sign $\Im(\tilde{\lambda})$) for ℓ large enough (using (7.4)) to the same reasoning as in the proof of Theorem 27: the region where $\Im(2\tilde{\mu}+3\tilde{\lambda})$ is not zero will control some part of the total field and the real part will control the remaining part of the total field. This implies that v_ℓ strongly converges to zero in $H^1(D)^d$, which is a contradiction.
Now we consider the case $-\Re(2\tilde{\mu}+3\tilde{\lambda}) - \alpha\Im(2\tilde{\mu}+3\tilde{\lambda}) < 0$ and $\Re(\tilde{\lambda}) > 0$. We cannot use identity (7.15) as the sign of the contrast and the sign of the background physical parameter will not be compatible. Instead we will use:

$$
(Tv_\ell,\, v_\ell) = - \int_D \left[2\tilde{\mu}|\mathrm{e}(v_\ell)|^2 + \tilde{\lambda}|\mathrm{div}(v_\ell)|^2 - \tilde{\rho}\omega^2|v_\ell|^2\right] - \int_D \left[2\tilde{\mu}\mathrm{e}(w_\ell)\mathrm{e}(\bar{v}_\ell) + \tilde{\lambda}\mathrm{div}(w_\ell)\mathrm{div}(\bar{v}_\ell) - \tilde{\rho}\omega^2 w_\ell\bar{v}_\ell\right] dx
$$

Using equation (7.2) and integrating by parts we have:

$$-\int_{B_R} 2\mu \mathrm{e}(w)\mathrm{e}(\bar{w})+\lambda \mathrm{div}(w)\mathrm{div}(\bar{w})-\rho w\bar{w}+\int_{\partial B_R} T^0_{\mathbf{n}}(w)\bar{w} = \int_D \tilde{2}\mu \mathrm{e}(v)\mathrm{e}(\bar{w})+\tilde{\lambda}\mathrm{div}(v)\mathrm{div}(\bar{w})-\tilde{\rho}v\bar{w}$$

Now taking the conjugate and combining the two previous equations we get

$$\begin{aligned}(Tv_\ell,\, v_\ell) = &-\int_D \left[2\tilde{\mu}|\mathrm{e}(v_\ell)|^2+\tilde{\lambda}|\mathrm{div}(v_\ell)|^2-\tilde{\rho}\omega^2|v_\ell|^2\right]-\int_D \left[2\tilde{\mu}\mathrm{e}(w_\ell)\mathrm{e}(\bar{v}_\ell)+\tilde{\lambda}\mathrm{div}(w_\ell)\mathrm{div}(\bar{v}_\ell)-\tilde{\rho}\omega^2 w_\ell\bar{v}_\ell\right]dx\\ &\int_D 2\overline{\tilde{\mu}}\mathrm{e}(\bar{v}_\ell)\mathrm{e}(w_\ell)+\overline{\tilde{\lambda}}\mathrm{div}(\bar{v}_\ell)\mathrm{div}(w_\ell)-\overline{\tilde{\rho}}\bar{v}_\ell w_\ell+\int_{B_R} 2\bar{\mu}\mathrm{e}(\bar{w}_\ell)\mathrm{e}(w_\ell)+\bar{\lambda}\mathrm{div}(w_\ell)\mathrm{div}(\bar{w}_\ell)-\bar{\rho}w_\ell\bar{w}_\ell\\ &-\int_{\partial B_R}\overline{T^0_{\mathbf{n}}(w_\ell)}w_\ell\end{aligned}$$

By letting $R\to\infty$ and collecting the "compact terms" under the name CT (for the same reason as above) we finally obtain a formula similar to (7.15) but with the desired sign,

$$\begin{aligned}(Tv_\ell,\, v_\ell) = &-\int_D \left[2\tilde{\mu}|\mathrm{e}(v_\ell)|^2+\tilde{\lambda}|\mathrm{div}(v_\ell)|^2-|v_\ell|^2\right]+\int_{\mathbb{R}^d} 2\bar{\mu}|\mathrm{e}(w_\ell)|^2+\bar{\lambda}|\mathrm{div}(w_\ell)|^2+|w_\ell|^2\\ &-2i\int_D \left[2\Im(\tilde{\mu})\mathrm{e}(w_\ell)\mathrm{e}(\bar{v}_\ell)+\Im(\tilde{\lambda})\mathrm{div}(w_\ell)\mathrm{div}(\bar{v}_\ell)\right]dx+CT.\\ = &\int_D -\Re(2\tilde{\mu})|\mathrm{e}(v_\ell)|^2-\Re(\tilde{\lambda})|\mathrm{div}(v_\ell)|^2+\int_{\mathbb{R}^d} 2\Re(\mu)|\mathrm{e}(w_\ell)|^2\\ &+\Re(\lambda)|\mathrm{div}(w_\ell)|^2+2\int_D \Im(\Im(2\mu)\mathrm{e}(w_\ell)\overline{\mathrm{e}(v_\ell)})+\Im(\Im(\lambda)\mathrm{div}(w_\ell)\overline{\mathrm{div}(v_\ell)})\\ &-i\int_D \Im(2\mu)\mathrm{e}(w_\ell+v_\ell)\overline{\mathrm{e}(w_\ell+v_\ell)}+\Im(\lambda)\mathrm{div}(w_\ell+v_\ell)\overline{\mathrm{div}(w_\ell+v_\ell)}.\end{aligned}$$

From this inequality, using (7.4) and the hypothesis on the physical parameters, we deduce as in the first case that $|(Tv_\ell,\, v_\ell)|$ control the total field $v_\ell+w_\ell$. Therefore when ℓ goes to infinity the total field $v_\ell+w_\ell$ goes to zero in $H^1(D)^d$ which implies that the scattered field w_ℓ goes to zero in $H^1(D)^d$ (by continuity of the forward scattering problem (as in theorem 27)), implying that the incident field v_ℓ also goes to zero in $H^1(D)^d$ which is a contradiction. □

Remark 15. *If one considers the full anisotropic elastic wave equation, the total field will solve:* $\mathrm{div}(C:\mathrm{e}(u))+\rho\omega^2 u=0$. *The result of section 4.3 on the coercivity of T can be extended by doing the same type of calculations with C instead of A. Therefore in addition to the fact that ω is not an interior transmission eigenvalue, one can obtain the coercivity of T from assumptions on the sign of $C-Id$ and $\rho-1$ only on a neighborhood of the boundary of D.*

7.3 GLSM for elastic waves

We can apply the theory of Chapter 4 in order to obtain a theorem that gives an exact characterization of D in terms of farfield data. The framework developed in this chapter allows one to deal with non-symmetric factorization that appears for example when one consider the case of limited aperture data meaning that one is using only a subset of $\mathbb{S}^{d-1}$ as incident

directions but all polarizations within this subset. We did not consider the case of limited aperture in section 7.1 in order to avoid complicated notation. To state the more general result we consider Π_s the projector from $L^2(\mathbb{S}^{d-1})^d$ onto $L^2(\Theta_s)^d$, where Θ_s is the set of incident directions of the sources (and similarly for the measurement we introduce Π_m). Using these two projectors the farfield operator for the limited aperture case is $\Pi_m^* H^* T H \Pi_s$ where T and H are defined by (7.9) and (7.3). Lemma 15 remains valid if one considers the range of $\Pi_m^* H^* T$ instead of H^*T. Since $\overline{\mathcal{R}(H\Pi_s)} = \overline{\mathcal{R}(H)}$ the middle operator T is not modified in the case of limited aperture data and therefore lemma 16 remains valid. We can deduce from those remarks that the result from chapter 4 can be applied, if we know a priori a bounded region Σ such that $D \in \Sigma$.

If we denote $V = H\Pi_s$, $U = H\Pi_m$, and $F = \Pi_m^* H^* T H \Pi_s$, we introduce the following cost functional for $g = (g_1, g_2) \in L^2(\Theta_m)^d \times L^2(\Theta_s)^d$:

$$J_\alpha(\Gamma_z^\infty p; g) := \alpha |(Fg_2,\, g_1)_{\ell^2(\Theta_m)^d}| + \alpha^{1-\gamma} \|Vg_2 - Ug_1\|^2_{H^1(\Sigma)^d} + \alpha^{1-\gamma} |(Fg_2 - \phi,\, g_1)_{\ell^2(\Theta_m)^d}| + \|Fg_2 - \Gamma_z^\infty p\|^2_{\ell^2(\Theta_m)^d}$$

with a fixed parameter $\gamma \in]0,1[$ and a positive parameter α that is supposed to go to 0. We introduce

$$j_\alpha(\Gamma_z^\infty p) := \inf_{g \in L^2(\Theta_m)^d \times L^2(\Theta_s)^d} J_\alpha(\Gamma_z^\infty p; g)$$

and $g_\alpha^{z,p}$ such that:

$$J_\alpha(\phi; g_\alpha^{z,p}) \leq j_\alpha(\Gamma_z^\infty p) + p(\alpha)$$

where $0 < p(\alpha) \leq C\alpha$ for some constant C.

Corollary 5. *Under the hypothesis of previous Sections of this chapter and the result from Theorem 18 we have the following characterization of D*

- *$z \in D$ implies $\limsup_{\alpha \to 0} |(Fg_2^{\alpha,z,p},\, g_1^{\alpha,z,p})_1| + \alpha^{-\gamma} \|Vg_2^{\alpha,z,p} - Ug_1^{\alpha,z,p}\|^2_{H^1(\Sigma)^d} < \infty$*
- *$z \notin D$ implies $\liminf_{\alpha \to 0} |(Fg_2^{\alpha,z,p},\, g_1^{\alpha,z,p})_1| + \alpha^{-\gamma} \|Vg_2^{\alpha,z,p} - Ug_1^{\alpha,z,p}\|^2_{H^1(\Sigma)^d} = \infty$.*

In the case $\phi = G\varphi$, the sequences Vg_2^α and Ug_1^α converge strongly to φ_1 in $H^1(D)^d$.

Remark 16. *The noisy case will follow as in Chapter 4. Similar result can be obtained if the supports of $\tilde{\lambda}$, $\tilde{\mu}$ and $\tilde{\rho}$ are different or in the case of the fully non isotropic elastic wave equation.*

7.4 Partial polarization

In the case of partial polarization only some polarizations are used as incident waves and only some (others) are measured. Longitudinal and transversal elastic waves can be decoupled through the Helmholtz decomposition in homogeneous elastic medium, therefore it seems natural to consider the case of limited polarizations as the fact of using either one of those two types of waves as incident field and measuring also only one type. We can decompose the

operator H as $H = H_p + H_s$ where H_p (resp. H_s) is the compression part (resp. shear part) of the Herglotz wave defined by:

$$H\mathcal{P}_p(g) = H_p g_p(x) = H_p g(x) = \begin{bmatrix} \displaystyle\int_{\hat{d}\in\mathbb{S}^{d-1}} e^{ik_p x.\hat{d}}(\hat{d}\cdot g(\hat{d}))\hat{d} \\ \displaystyle ik_p \int_{\hat{d}\in\mathbb{S}^{d-1}} e^{ik_p x.\hat{d}}\hat{d}\cdot g(\hat{d}) \\ \displaystyle\int_{\hat{d}\in\mathbb{S}^{d-1}} e^{ik_p x.\hat{d}} ik_p (g(\hat{d})\cdot\hat{d})\hat{d}\otimes\hat{d} \end{bmatrix} \tag{7.16}$$

$$H_s g_s(x) = \begin{bmatrix} \displaystyle\int_{\hat{d}\in\mathbb{S}^{d-1}} e^{ik_s x.\hat{d}}\left((g(\hat{d})\cdot\hat{\theta})\theta + (g(\hat{d})\cdot\hat{\phi})\hat{\phi}\right) \\ 0 \\ \displaystyle\frac{1}{2}\int_{\hat{d}\in\mathbb{S}^{d-1}} e^{ik_s x.\hat{d}} ik_s \left((g(\hat{d})\cdot\hat{\theta})(\hat{d}\otimes\hat{\theta}+\hat{\theta}\otimes\hat{d}) + (g(\hat{d})\cdot\hat{\phi})(\hat{d}\otimes\hat{\phi}+\hat{\phi}\otimes\hat{d})\right) \end{bmatrix} \tag{7.17}$$

where $\mathcal{P}_p$ (resp. $\mathcal{P}_s$) is the projector from $L^2(\mathbb{S}^{d-1})^d$ onto $L_p(\mathbb{S}^{d-1})$ (resp. $L_s(\mathbb{S}^{d-1})$). Those Herglotz operators are dense in the space of shear waves and longitudinal waves. We recall that the farfield of w associated with an incident field v of either type solves:

$$w^\infty(\hat{x}) = \int_D \tilde{\rho}\omega^2 \mathbf{\Gamma}^\infty(\hat{x},z)(w+v) - \tilde{\lambda}\mathrm{div}_z(\mathbf{\Gamma}^\infty(\hat{x},z))\mathrm{div}(w+v) - 2\tilde{\mu}\mathrm{e}_z(\mathbf{\Gamma}^\infty(\hat{x},z))\mathrm{e}(w+v)dV(z) \tag{7.18}$$

where $\mathbf{\Gamma}^\infty = \mathbf{\Gamma}^\infty_\mathbf{p} + \mathbf{\Gamma}^\infty_\mathbf{s}$. Moreover we have for the longitudinal part,

$$\mathbf{\Gamma}^\infty_\mathbf{p}(\hat{x},y) = \frac{k_p^2}{4\pi\rho_0^2} e^{-ik_p\hat{x}\cdot y}\hat{x}\otimes\hat{x}$$

$$\mathrm{div}(\mathbf{\Gamma}^\infty_\mathbf{p})(\hat{x},y) = \frac{-ik_p^3}{4\pi\rho_0^2} e^{-ik_p\hat{x}\cdot y}\hat{x}$$

$$\mathrm{e}(\mathbf{\Gamma}^\infty_\mathbf{p})(\hat{x},y) = \frac{-ik_p^3}{4\pi\rho_0^2} e^{-ik_p\hat{x}\cdot y}\hat{x}\otimes\hat{x}\otimes\hat{x}$$

and for the shear part,

$$\mathbf{\Gamma}^\infty_\mathbf{s}(\hat{x},y) = \frac{k_s^2}{4\pi\rho_0^2} e^{-ik_s\hat{x}\cdot y}(I - \hat{x}\otimes\hat{x})$$

$$\mathrm{div}(\mathbf{\Gamma}^\infty_\mathbf{s})(\hat{x},y) = 0$$

$$\mathrm{e}(\mathbf{\Gamma}^\infty_\mathbf{s})(\hat{x},y) = \frac{-ik_s^3}{8\pi\rho_0^2} e^{-ik_s\hat{x}\cdot y}(\hat{\theta}\otimes(\hat{x}\otimes\hat{\theta}+\hat{\theta}\otimes\hat{x}) + \hat{\phi}\otimes(\hat{x}\otimes\hat{\phi}+\hat{\phi}\otimes\hat{x}))$$

Using those equations one can easily verify that $H^* = H_s^* + H_p^*$ where H_s^* (resp. H_p^*) is defined as H^* in (7.8) with the s-part of the Green tensor (resp. p-part). Therefore the farfield operator associated with longitudinal incident plane waves and measurements of the farfield shear part is given by $F_{sp} = H_s^* T_p H_p$. The middle operator T_p is defined using the same set of equations that we used to define T, however T_p should be considered as an operator from $\mathcal{R}(H_p)$ into X. Moreover $\mathcal{R}(H_p) \subset \mathcal{R}(H)$ therefore the coercivity property is still verified for limited polarization (under the same hypothesis as in Lemma 16).

7.4.1 Full incident polarizations and partially measured polarizations

First we state the following intermediate lemma which gives a characterization of the support of D in terms of the range of H_p^*T defined as an operator from $\overline{\mathcal{R}(H)}$ to $L^2(\mathbb{S}^{d-1})$ (in lemma 15 we use the range of $H^*T = (H_p + H_s)^*T$)

Lemma 17. *For any polarization $p \in \mathbb{S}^{d-1}$ and if ω is not a interior transmission eigenvalue, $\mathbf{\Gamma_s^\infty}(\cdot, z)p \in \mathcal{R}(H_s^*T)$ or $\mathbf{\Gamma_p^\infty}(\cdot, z)p \in \mathcal{R}(H_p^*T)$ if and only if $z \in D$.*

Proof. If $z \in D$ and for any polarization p, we introduce $\varphi \in \mathcal{R}(H)$ (and φ_1 its first component) and $u \in H^1(D)$ such that

$$\begin{cases} \operatorname{div}(2\mu_0 \mathrm{e}(\varphi_1) + \lambda_0 \operatorname{div}(\varphi_1) Id) + \rho_0 \omega^2 \varphi_1 = 0 \quad D \\ \operatorname{div}(2\mu \mathrm{e}(u) + \lambda \operatorname{div}(u) Id) + \rho \omega^2 u = 0 \quad D \\ u - \varphi_1 = \Gamma_p(\cdot, z)p \quad \partial D \\ T_{\mathbf{n}}(u) - T_{\mathbf{n}}^0(\varphi_1) = T_{\mathbf{n}}^0(\Gamma_p(\cdot, z)p) \quad \partial D \end{cases} \tag{7.19}$$

Clearly from those equations we have that $H_p^*T\varphi = \Gamma_p^\infty(\cdot, z)p$ (and the same for the shear part: $H_s^*T\varphi = \Gamma_s^\infty(\cdot, z)p$). If $z \notin D$ and for any polarization p, we assume that $H_s^*T\varphi = \Gamma_s^\infty(\cdot, z)p$. Therefore by the Rellich lemma $\Gamma_s(\cdot, z)p$ defines the shear part of scattered field w in $\mathbb{R}^d \setminus \{D \cup \{z\}\}$. Therefore,

$$\operatorname{curl}(\Gamma_s(\cdot, z)p) = \operatorname{curl}(w) \in L^2_{loc}(\mathbb{R}^d \setminus D),$$

which is a contradiction because $\operatorname{curl}(\Gamma_s(\cdot, z)p)$ is not in $L^2_{loc}(\mathbb{R}^d \setminus D)^d$. For longitudinal waves the same reasoning yields to $\operatorname{div}(\Gamma_p(\cdot, z)p) \in L^2_{loc}(\mathbb{R}^d \setminus D)$ which is impossible. □

The coercivity of T and the result of Lemma 17 are the first mandatory results in order to apply the framework of the GLSM. The other crucial ingredient is the existence of a term, built from the data, that controls the norm of the Herglotz wave function. From the previous chapters this term (for compressional wave measurement) will be of the form

$$\left(H_p^*THg, (P)_p g\right) = (TH_pg_p, H_pg_p) + (TH_sg_s, H_pg_p) = (THg, Hg) - (THg, H_sg_s)$$

From this obvious decomposition we see that this term will allow a control over the norm of $H_p(P)_p g$ and not Hg if we are able to have a control over the norm of H_sg_s. As we have a priori no way to infer the value of the shear part of φ_1 (defined in the previous lemma as a solution to the interior transmission problem), our only possible control over H_sg is through $\|H_sg\|_{H^1(\Sigma)}$ where D is included in Σ (following the idea of chapter 4). Such a control will induce that there

is a solution to the following problem:

$$\begin{cases} \operatorname{div}(2\mu_0 \mathrm{e}(v) + \lambda_0 \operatorname{div}(v) Id) + \rho_0 \omega^2 v = 0 \quad D \\ \operatorname{curl}(v) = 0 \quad D \\ \operatorname{div}(2\mu \mathrm{e}(u) + \lambda \operatorname{div}(u) Id) + \rho \omega^2 u = 0 \quad D \\ \operatorname{div}(2\mu_0 \mathrm{e}(w) + \lambda_0 \operatorname{div}(w) Id) + \rho_0 \omega^2 w = 0 \quad \mathbb{R}^d \setminus D \\ \operatorname{div}(w) = 0 \quad \mathbb{R}^d \setminus D \\ u - v = w + \Gamma_p(\cdot, z)p \quad \partial D \\ T_{\mathbf{n}}(u) - T^0_{\mathbf{n}}(v) = T^0_{\mathbf{n}}(\Gamma_p(\cdot, z)p + w) \quad \partial D \\ \lim_{R \to +\infty} \int_{|x|=R} \left| \frac{\partial w}{\partial r} - i k_s w \right|^2 ds = 0 \end{cases} \tag{7.20}$$

This problem is actually central in the case of Limited polarization both for the sources and the measurements. We will discuss in the next session how this problem arises. The case of shear part measurement will be similar.

7.4.2 Partial polarization for sources and measurements

In Lemma 17 we considered the operator $H_p^* T$. However if one has only access to p-wave as incident fields the corresponding operator is $H_p^* T_p$. In the proof of this lemma the reasoning for the case $z \notin D$ is still valid however when $z \in D$ the solution of the interior transmission problem is clearly not in the closure of the range of H_p (resp. H_s). The specific problem we should study to exhibit a solution in $\overline{\mathcal{R}(H_p)}$ that creates a scattered field equals to $\Gamma_p^\infty(\cdot, z)p$ is the following exterior-interior transmission problem:

$$\begin{cases} \operatorname{div}(2\mu_0 \mathrm{e}(\varphi_1) + \lambda_0 \operatorname{div}(\varphi_1) Id) + \rho_0 \omega^2 \varphi_1 = 0 \quad D \\ \operatorname{curl}(\varphi_1) = 0 \quad D \\ \operatorname{div}(2\mu \mathrm{e}(u) + \lambda \operatorname{div}(u) Id) + \rho \omega^2 u = 0 \quad D \\ \operatorname{div}(2\mu_0 \mathrm{e}(w_s) + \lambda_0 \operatorname{div}(w_s) Id) + \rho_0 \omega^2 w_s = 0 \quad \mathbb{R}^d \setminus D \\ \operatorname{div}(w_s) = 0 \quad \mathbb{R}^d \setminus D \\ u - \varphi_1 = \Gamma_p(\cdot, z)p + w_s \quad \partial D \\ T_{\mathbf{n}}(u) - T^0_{\mathbf{n}}(\varphi_1) = T^0_{\mathbf{n}}(\Gamma_p(\cdot, z)p) + T^0_{\mathbf{n}}(w_s) \quad \partial D \\ \lim_{R \to +\infty} \int_{|x|=R} \left| \frac{\partial w_s}{\partial r} - i k_s w_s \right|^2 ds = 0 \end{cases} \tag{7.21}$$

We so far did not succeed in verifying a Fredholm property for this problem. In the following we will denote $\varphi_1 = v$ and $w_s = w$ to simplify the notation and exhibit some difficulties we encountered in studying such a problem.

7.4.3 Variational formulation of the Int-ext transmission problem, a potential approach

If we can introduce $v = \nabla p$ and $w = \text{curl}(q)$, then without source term the system can be rewritten as:

$$\begin{cases} \Delta p + k_p^2 p = 0 \quad D \\ \text{div}(2\mu \text{e}(u) + \lambda \text{div}(u) Id) + \rho\omega^2 u = 0 \quad D \\ \text{curlcurl}(q) - k_s^2 q = 0 \quad \mathbb{R}^d \setminus D \\ u \cdot n - \dfrac{\partial p}{\partial n} = \text{curl}(q) \cdot n \quad \partial D \\ u \times n - \nabla p \times n = \text{curl}(q) \times n \quad \partial D \\ T_{\mathbf{n}}(u) - T^0_{\mathbf{n}}(\nabla p) = T^0_{\mathbf{n}}(\text{curl}(q)) \quad \partial D \\ \lim\limits_{R \to +\infty} \int_{|x|=R} |\text{curl} q \times \hat{x} - i k_s q|^2 \, ds(x) = 0 \end{cases} \tag{7.22}$$

The natural spaces will be $p \in H^1(D)$, $u \in H^1(D)^d$ and $q \in H_{curl,loc}(\mathbb{R}^d \setminus \overline{D})$
From [47], we have the formula:

$$\begin{aligned} \nabla u \cdot n =& \frac{\partial u_\Gamma}{\partial n} + \frac{u \cdot n}{\partial n} n \\ =& \text{curl}(u) \times n + \nabla_\Gamma (u \cdot n) - Ru + \text{div}(u) n - \text{div}_\Gamma(u_\Gamma) n - (u \cdot n) \text{div}(n) n \end{aligned}$$

$$\text{curl}(q) \cdot n = \text{curl}_\Gamma q \quad \textit{and } \nabla p \times n = \nabla_\Gamma p \times n$$

Using this formula we can compute the stress vectors:

$$\begin{aligned} T^0_{\mathbf{n}}(\nabla p) =& (\lambda_0 + 2\mu_0) \text{div}(\nabla p) n + 2\mu_0 (\nabla_\Gamma (\nabla p \cdot n) - R \nabla p - \text{div}_\Gamma(\nabla p_\Gamma) n - (\nabla p \cdot n) \text{div}(n) n) \\ =& - \rho_0 \omega^2 p n + 2\mu_0 (\nabla_\Gamma (u \cdot n) - \nabla_\Gamma \text{curl}_\Gamma q - R \nabla p \\ & - \text{div}_\Gamma(\nabla p_\Gamma) n - (u \cdot n) \text{div}(n) n + \text{curl}_\Gamma q \text{div}(n) n) \end{aligned}$$

$$\begin{aligned} T^0_{\mathbf{n}}(\text{curl}(q)) =& \mu_0 \text{curlcurl}(q) \times n + 2\mu_0 (\nabla_\Gamma (\text{curl}_\Gamma q) - R(n \times (\text{curl} q \times n)) \\ & - \text{div}_\Gamma(n \times (\text{curl} q \times n)) n - (\text{curl}_\Gamma q) \text{div}(n) n) \\ =& \rho_0 \omega^2 q \times n + 2\mu_0 (\nabla_\Gamma \text{curl}_\Gamma q - R(n \times (u \times n)) + R(n \times (\nabla_\Gamma p \times n)) \\ & - \text{div}_\Gamma(u_\Gamma) n + \text{div}_\Gamma(\nabla_\Gamma p) n - (\text{curl}_\Gamma q) \text{div}(n) n) \end{aligned}$$

Which finally give

$$\begin{aligned} T_{\mathbf{n}}(u) =& T^0_{\mathbf{n}}(\text{curl}(q)) + T^0_{\mathbf{n}}(\nabla p) \\ =& \rho_0 \omega^2 (q \times n - p n) + 2\mu_0 (\nabla_\Gamma (u \cdot n) - R u_\Gamma - \text{div}_\Gamma(u_\Gamma) n - (u \cdot n) \text{div}(n) n) \end{aligned}$$

If we take $(u', p', q') \in \mathcal{H}$ where $\mathcal{H} = \{(u', p', q') \in H^1(D)^d \times H^1(D) \times H_{curl,loc}(\mathbb{R} \setminus \overline{D}\}$ and integrate by parts :

$$0 = \int_D -\nabla p \nabla p' + k_p^2 p p' + \int_{\partial D} (u \cdot n - \text{curl}_\Gamma q) p' \tag{7.23}$$

$$0 = \int_D -2\mu \text{e}(u) : \text{e}(u') - \lambda \text{div}(u) \text{div}(u') + \rho\omega^2 u u') + \int_{\partial D} T_n(u) u' \tag{7.24}$$

$$0 = \int_{B_R\setminus\bar{D}} \mathrm{curl}(q)\mathrm{curl}(q') - k_s^2 qq' + \int_{\partial D} (u\times n)q' - (\nabla p\times n)q' - \int_{\partial B_R} (\mathrm{curl}(q)\times n)q' \quad (7.25)$$

These variational formulations and the formula of $T_{\mathbf{n}}(u)$ can be combined either to simplify the boundary term (if $p = p'$, $u = u'$ and $q = q'$) $((7.24) + ((7.25) + (7.23))\rho_0\omega^2)$:

$$\begin{aligned}
0 = &\int_D -2\mu \mathrm{e}(u) : \mathrm{e}(u') - \lambda \mathrm{div}(u)\mathrm{div}(u') + \rho\omega^2 uu' + \rho_0\omega^2 \int_D -\nabla p\nabla p' + k_p^2 pp' \\
&+ \rho_0\omega^2 \int_{B_R\setminus\bar{D}} \mathrm{curl}(q)\mathrm{curl}(q') - k_s^2 qq' \\
&+ \int_{\partial D} 2\mu_0(\nabla_\Gamma(u\cdot n)u' - \mathrm{div}_\Gamma(u_\Gamma)nu' - (u\cdot n)(u'\cdot n)\mathrm{div}(n) \\
&- R(u_\Gamma)u' - \int_{\partial D} \rho_0\omega^2(\mathrm{curl}_\Gamma(q)p' + (\nabla p\times n)q' \\
&+ \int_{\partial D} \rho_0\omega^2((u\times n)q' + p'n\cdot u) - \int_{\partial D} \rho_0\omega^2((u'\times n)q + pn\cdot u') - \int_{B_R} \rho_0\omega^2(\mathrm{curl}q\times e_r)q'
\end{aligned}$$

or to obtain the same sign in front of the leading order volume term $((7.24)+((7.23)-(7.25))\rho_0\omega^2$:

$$\begin{aligned}
0 = &\int_D -2\mu \mathrm{e}(u) : \mathrm{e}(u') - \lambda \mathrm{div}(u)\mathrm{div}(u') + \rho\omega^2 uu' + \rho_0\omega^2 \int_D -\nabla p\nabla p' + k_p^2 pp' \\
&- \rho_0\omega^2 \int_{B_R\setminus\bar{D}} \mathrm{curl}(q)\mathrm{curl}(q') - k_s^2 qq' \\
&+ \int_{\partial D} 2\mu_0(\nabla_\Gamma(u\cdot n)u' - \mathrm{div}_\Gamma(u_\Gamma)nu' - (u\cdot n)(u'\cdot n)\mathrm{div}(n) - R(u_\Gamma)u' \\
&- \int_{\partial D} \rho_0\omega^2(\mathrm{curl}_\Gamma(q)p' - (\nabla p\times n)q' \\
&+ \int_{\partial D} \rho_0\omega^2(-(u\times n)q' + p'n\cdot u) - \int_{\partial D} \rho_0\omega^2((u'\times n)q + pn\cdot u') + \int_{B_R} \rho_0\omega^2(\mathrm{curl}q\times e_r)q'
\end{aligned}$$

These variational formulations make sense as they involves boundary duality products. We were not able to demonstrate Fredholm property for these variational formulations because in each of them there are non compact terms with different signs.

7.4.4 Variational formulation of the Int-ext transmission problem, an full field approach

We also tried to obtain a variational formulation without using potential representation. The problem is:

$$\begin{cases} \operatorname{div}(2\mu_0 \mathrm{e}(v) + \lambda_0 \operatorname{div}(v) Id) + \rho_0 \omega^2 v = 0 & D \\ \operatorname{curl}(v) = 0 & D \\ \operatorname{div}(2\mu \mathrm{e}(u) + \lambda \operatorname{div}(u) Id) + \rho \omega^2 u = 0 & D \\ \operatorname{div}(2\mu_0 \mathrm{e}(w) + \lambda_0 \operatorname{div}(w) Id) + \rho_0 \omega^2 w = 0 & \mathbb{R}^d \setminus D \\ \operatorname{div}(w) = 0 & \mathbb{R}^d \setminus D \\ u - v = w & \partial D \\ T_{\mathbf{n}}(u) - T^0_{\mathbf{n}}(v) = T^0_{\mathbf{n}}(w) & \partial D \\ \lim_{R \to +\infty} \int_{|x|=R} \left| \frac{\partial w}{\partial r} - i k_s w \right|^2 ds = 0 \end{cases} \tag{7.26}$$

An solution space would be $(u, v, w) \in \mathcal{H} = \{(u, v, w) \in H^1(D)^d \times H^1(D)^d \times H^1_{loc}(\mathbb{R}^d \setminus \bar{D})$ s.t. $u - v = w$ *on* ∂D *and* $\operatorname{div}(w) = 0$ *and* $\operatorname{curl}(w) = 0\}$. The variational formulations for these equations are respectively

$$0 = \int_D -2\mu \mathrm{e}(u) : \mathrm{e}(u') - \lambda \operatorname{div}(u) \operatorname{div}(u') + \rho \omega^2 u u' + \int_{\partial D} T_n(u) u'$$

$$0 = \int_D -2\mu_0 \mathrm{e}(v) : \mathrm{e}(v') - \lambda_0 \operatorname{div}(v) \operatorname{div}(v') + \rho_0 \omega^2 v v' + \int_{\partial D} T^0_n(v) v'$$

$$0 = \int_{B_R \setminus \bar{D}} -2\mu_0 \mathrm{e}(w) : \mathrm{e}(w') - \lambda_0 \operatorname{div}(w) \operatorname{div}(w') + \rho_0 \omega^2 w w' - \int_{\partial D} T^0_n(w) w' + \int_{\partial B_R} T^0_n(w) w'$$

We can combine these three equalities in order to eliminate the boundary terms. If we substitute w by $u - v$ in the boundary terms we obtain:

$$\begin{aligned} &\int_D -2\mu \mathrm{e}(u) : \mathrm{e}(u') - \lambda \operatorname{div}(u) \operatorname{div}(u') + \rho \omega^2 u u' + \int_D -2\mu_0 \mathrm{e}(v) : \mathrm{e}(v') - \lambda_0 \operatorname{div}(v) \operatorname{div}(v') + \rho_0 \omega^2 v v' \\ &+ \int_{B_R \setminus \bar{D}} -2\mu_0 \mathrm{e}(w) : \mathrm{e}(w') - \lambda_0 \operatorname{div}(w) \operatorname{div}(w') + \rho_0 \omega^2 w w' + \int_{\partial B_R} T^0_n(w) w' \\ &+ \int_{\partial D} T_n(u) v' + T^0_n(v) u' \end{aligned}$$

Substituting v by $u - w$ leads to a sign incompatibility for volume integrals.

$$\begin{aligned} &\int_D -2\mu \mathrm{e}(u) : \mathrm{e}(u') - \lambda \operatorname{div}(u) \operatorname{div}(u') + \rho \omega^2 u u' - \int_D -2\mu_0 \mathrm{e}(v) : \mathrm{e}(v') - \lambda_0 \operatorname{div}(v) \operatorname{div}(v') + \rho_0 \omega^2 v v' \\ &+ \int_{B_R \setminus \bar{D}} -2\mu_0 \mathrm{e}(w) : \mathrm{e}(w') - \lambda_0 \operatorname{div}(w) \operatorname{div}(w') + \rho_0 \omega^2 w w' + \int_{\partial B_R} T^0_n(w) w' \\ &+ \int_{\partial D} T_n(u) w' + T^0_n(w) u' \end{aligned}$$

Similarly to the previous equality substituting u by $v + w$ leads to a sign incompatibility in volume integrals.

$$
\begin{aligned}
&- \int_D -2\mu \mathrm{e}(u) : \mathrm{e}(u') - \lambda \mathrm{div}(u)\mathrm{div}(u') + \rho\omega^2 uu' + \int_D -2\mu_0 \mathrm{e}(v) : \mathrm{e}(v') - \lambda_0 \mathrm{div}(v)\mathrm{div}(v') + \rho_0\omega^2 vv' \\
&+ \int_{B_R \setminus \bar{D}} -2\mu_0 \mathrm{e}(w) : \mathrm{e}(w') - \lambda_0 \mathrm{div}(w)\mathrm{div}(w') + \rho_0\omega^2 ww' + \int_{\partial B_R} T_n^0(w)w' \\
&+ \int_{\partial D} T_n^0(v)w' + T_n^0(w)v'
\end{aligned}
$$

7.4.5 Comments on the GLSM for limited polarization

As already discussed, the coercivity of T_p is a direct consequence of the coercivity of T. Finally in the case of longitudinal incident waves and measurements of the p-part of the farfield, we will have:

$$|\big(H_p^* T_p H_p g,\, g\big)| = |(T_p H_p g,\, H_p g)| \geq \mu \left\| H_p g \right\|^2$$

and similarly in the case of transversal incident waves and measurement of the s-part of the farfield we will have:

$$|(H_s^* T_s H_s g,\, g)| = |(T_s H_s g,\, H_s g)| \geq \mu \left\| H_s g \right\|^2$$

If we suppose that problem (7.21) is solvable we will obtain a lemma similar to 17 that will give a characterization of D using the range of $H_p^* T_p$. Therefore we will have the desired term in order to apply the framework from the GLSM. However, in the case of incident p-waves and measured s-waves, $F = H_s^* T_p H_p$ and we will obtain:

$$(H_s^* T_p H_p g_2,\, g_1) = (T_p H_p g_2,\, H_p g_2) - (T_p H_p g_2,\, H_p g_2 - H_s g_1)$$

It is impossible to control $H_p g_2 - H_s g_1$ on a larger geometrical domain as we did for the limited aperture case because H_s is not dense in the range of H_p (they are actually completely different as one gives rise to the curl-free field and the other to div-free field).

7.5 Conclusion

In this chapter we have extended our previous results to the case of elastic waves. The GLSM framework can be applied with assumptions on the material properties which are similar to the acoustic case. Our work on non-symmetric factorization can also be extended to the case of elastic waves. In elasticity the notion of polarization can be considered and it is therefore natural to study the case of partial polarization data. This type of data raises issues on the key ingredient of sampling methods: the range characterization of D. Instead of the interior transmission problem we have this time an interior-exterior problem which we tried to study using variational techniques without success. The second problem is that the regularization term that comes naturally in the GLSM framework does not have the required property if one is sending one type of polarization and measuring the other one. The design of a suited regularization term in this case remains an open problem.

Chapter 8

Conclusion

First we will synthesize the results and discuss the perspectives directly related to the work presented in this thesis. Then we will step back on our work to discuss further research issues related to non-destructive testing of concrete.

In chapter 2, we proposed a new mathematical justification of the linear sampling method. Our justification is based on the design of a well suited regularization term. This method shows improvement in the numerical experiment we have carried out. In chapters 3 and 4 we further investigated our method and we were able to obtain a strong convergence result for the sequence of Herglotz wave function to the solution of the so-called interior transmission problem. We also demonstrated that these results hold in the case of noisy data. Using regularization, it is natural to look for a priori rule to choose the regularization parameter with respect to the noise. However several technical problems arise that makes classical techniques such as Morozov principle, difficult to apply to our setting. Connected to regularization techniques convergence rate and stability results would be of great interest as they will help understanding the behaviour of our differential measurement imaging functional that relies on the strong convergence of the Herglotz wave functions. Stability result might also help to provide a better understanding of the behaviour of our indicator functions outside the obstacle.

In chapter 4 we concentrate on extending the GLSM framework to the case of non symmetric factorization. This issue is important as it contains the case of limited aperture data. Our theory works under the small assumption that one knows a priori a domain that contains the heterogeneity. Numerical examples of this chapter show that the GLSM functional improves the results over a Tikhonov regularization and that differential imaging works only for symmetric factorization. The numerical results show that the non symmetric case is more difficult. It is known that having symmetric factorization is favourable however we believe our results might be improved because the cost functional we use is difficult to handle numerically. Clearly results such as stability and convergence rate will help to choose properly the weights in the numerical implementation of the GLSM.

In chapter 3, we proposed a method to do differential imaging in a heterogeneous medium regardless of a priori on the properties of the material or the wavelength. The analysis is based on the comparison of the solutions to the interior transmission problems that arise from each measurement. An imaging functional is then proposed to exploit this comparison thanks to the strong convergence results of the GLSM. As already discussed more results from regularization theory of the GLSM functional is needed to understand more deeply the type of image one might expect. Extension to other type of scattering medium calls for a careful analysis of the related interior transmission problem such as the one depicted in chapter 6 for anisotropic medium and in chapter 5 for cracks.

The results from chapters 6 and 7 show that the GLSM theory is flexible and easy to extend

to other scattering settings. The case of limited polarization in elasticity raises a lot of interesting problems both from the theoretical and application point of view. We left open the design of a proper regularization term within the GLSM framework in the case of polarization of different kind for sources and measurements but more importantly the range characterization at the heart of sampling methods is still an open problem for limited polarization as we were not able to solve the interior-exterior transmission problem that arises in that case.

If we step back on our work and go back to non destructive testing in concrete like material, we have proposed and analysed a method to use differential measurement in order to do imaging in concrete that do not rely on any approximation of the behavior of waves. Simulation on concrete like material show promising results both on heterogeneous medium and cracks (which are not covered by the current theory). As theoretical analyses of the resolution of the technique seems to be out of reach, an extensive numerical study of its limitations in terms of sizes both of the defect and of the region to probe should be carried out. Ultimately if those numerical studies are conclusive an experimental mock up will be considered.

From the application point of view even if differential measurement is interesting, it would be interesting to see if one might infer the farfield operator of the background from a priori knowledge such as the distribution of aggregates in order to create imaging techniques that do not need two sets of measurements. Connection with the study of waves in random media [30] [10] might give fruitful idea on how to infer the farfield operator.

Application to concrete raises a lot of new research items. We believe that looking into the inter-facial transition zone that we briefly discussed in chapter 5 would be necessary as it is an important aspect of the material and as the majority of the defects took place inside this area. From a modelling view point it seems possible to take into account this property of concrete, the fact that it will verify the property required by the GLSM framework is rather unclear. The second important aspect of the application we did not look into is the type of defect. We believe that the content of this thesis would be applicable for cracks of size comparable to the wavelength however networks of small cracks might need to consider other techniques. It might be interesting to look at techniques related to assessing the properties of the medium using transmission eigenvalue, homogenization such as the one performed in [18] and [20] might be an interesting path to explore.

In this thesis we develop the GLSM method and try by studying the limited aperture case to get closer to the hypothesis of non destructive testing measurement. As the data from ultrasound measurement are in the time domain, we believe that looking to the time domain linear sampling method will be important to get closer to the type of data available in practice.

Bibliography

[1] Konstantinos A. Anagnostopoulos and Antonios Charalambopoulos. The linear sampling method for the transmission problem in 2D anisotropic elasticity. *Inverse Problems*, 22(2):553–577, 2006. (Cited on page 140.)

[2] Tilo Arens. Why linear sampling works. *Inverse Problems*, 20(1):163–173, 2004. (Cited on pages 8, 9, 11 and 14.)

[3] Tilo Arens and Armin Lechleiter. The linear sampling method revisited. *J. Integral Equations Appl.*, 21(2):179–202, 2009. (Cited on pages 4, 8, 14, 22 and 54.)

[4] Lorenzo Audibert, Alexandre Girard, and Houssem Haddar. Identifying defects in an unknown background using differential measurements. *Inverse Problems and Imaging*, 9(3):625–643, 2015. (Cited on page 33.)

[5] Lorenzo Audibert and Houssem Haddar. A generalized formulation of the linear sampling method with exact characterization of targets in terms of farfield measurements. *Inverse Problems*, 30(3):035011, 2014. (Cited on pages 8, 34, 36, 37, 38, 39, 40, 41, 49 and 52.)

[6] Guillaume Bal, Lawrence Carin, Dehong Liu, and Kui Ren. Experimental validation of a transport-based imaging method in highly scattering environments. *Inverse Problems*, 23(6):2527–2539, 2007. (Cited on pages 3 and 34.)

[7] Cédric Bellis, Fioralba Cakoni, and Bojan B. Guzina. Nature of the transmission eigenvalue spectrum for elastic bodies. *IMA J. Appl. Math.*, 78(5):895–923, 2013. (Cited on page 141.)

[8] Eemeli Blåsten, Lassi Päivärinta, and John Sylvester. Corners always scatter. *Communications in Mathematical Physics*, 331(2):725–753, 2014. (Cited on page 30.)

[9] Anne-Sophie Bonnet-Ben Dhia, Lucas Chesnel, and Houssem Haddar. On the use of T-coercivity to study the interior transmission eigenvalue problem. *C. R. Math. Acad. Sci. Paris*, 349(11-12):647–651, 2011. (Cited on pages 122 and 132.)

[10] L. Borcea, F. González del Cueto, G. Papanicolaou, and C. Tsogka. Filtering deterministic layer effects in imaging. *SIAM Rev.*, 54(4):757–798, 2012. (Cited on pages 34 and 154.)

[11] Liliana Borcea, Josselin Garnier, George Papanicolaou, and Chrysoula Tsogka. Enhanced statistical stability in coherent interferometric imaging. *Inverse Problems*, 27(8):085004, 33, 2011. (Cited on page 34.)

[12] Yosra Boukari and Houssem Haddar. The Factorization method applied to cracks with impedance boundary conditions. *Inverse Problems and Imaging*, 2013. To appear. (Cited on pages 21 and 113.)

[13] Stephen Boyd and Lieven Vandenberghe. *Convex Optimization*. Cambridge University Press, New York, NY, USA, 2004. (Cited on page 102.)

[14] Haim Brezis. *Functional analysis, Sobolev spaces and partial differential equations*. Universitext. Springer, New York, 2011. (Cited on page 38.)

[15] Fioralba Cakoni and David Colton. *Qualitative methods in inverse scattering theory*. Interaction of Mechanics and Mathematics. Springer-Verlag, Berlin, 2006. An introduction. (Cited on pages 8, 34, 41, 59 and 121.)

[16] Fioralba Cakoni, David Colton, and Houssem Haddar. On the determination of Dirichlet or transmission eigenvalues from far field data. *C. R. Math. Acad. Sci. Paris*, 348(7-8):379–383, 2010. (Cited on pages 30 and 31.)

[17] Fioralba Cakoni, Anne Cossonnière, and Houssem Haddar. Transmission eigenvalues for inhomogeneous media containing obstacles. *Inverse Probl. Imaging*, 6(3):373–398, 2012. (Cited on page 110.)

[18] Fioralba Cakoni, Houssem Haddar, and Isaac Harris. Homogenization of the transmission eigenvalue problem for periodic media and application to the inverse problem. 2014. (Cited on page 154.)

[19] Fioralba Cakoni and Isaac Harris. The factorization method for a defective region in an anisotropic material. *Inverse Problems*, 31(2):025002, 22, 2015. (Cited on pages 60, 126 and 134.)

[20] Fioralba Cakoni and Shari Moskow. Asymptotic expansions for transmission eigenvalues for media with small inhomogeneities. *Inverse Problems*, 29(10):104014, 2013. (Cited on page 154.)

[21] Mathieu Chamaillard, Nicolas Chaulet, and Houssem Haddar. Analysis of the factorization method for a general class of boundary conditions. 2013. Preprint. (Cited on pages 21 and 117.)

[22] Nicolas Chaulet. *Generalized impedance models and inverse scattering*. Theses, Ecole Polytechnique X, November 2012. (Cited on page 106.)

[23] David Colton, Houssem Haddar, and Michele Piana. The linear sampling method in inverse electromagnetic scattering theory. *Inverse Problems*, 19(6):S105–S137, 2003. Special section on imaging. (Cited on page 8.)

[24] David Colton and Andreas Kirsch. A simple method for solving inverse scattering problems in the resonance region. *Inverse Problems*, 12(4):383–393, 1996. (Cited on pages 4, 8 and 22.)

[25] David Colton and Rainer Kress. *Inverse acoustic and electromagnetic scattering theory*, volume 93 of *Applied Mathematical Sciences*. Springer, New York, third edition, 2013. (Cited on pages 8, 11, 34, 36 and 54.)

[26] Anne Cossonnière and Houssem Haddar. Surface integral formulation of the interior transmission problem. *J. Integral Equations Appl.*, 25(3):341–376, 2013. (Cited on pages 110 and 122.)

[27] Anne-Sophie Bonnet-Ben Dhia, Lucas Chesnel, and Sergei A Nazarov. Non-scattering wavenumbers and far field invisibility for a finite set of incident/scattering directions. *Inverse Problems*, 31(4):045006, 2015. (Cited on page 87.)

[28] Klaus Erhard and Roland Potthast. A numerical study of the probe method. *SIAM J. Sci. Comput.*, 28(5):1597–1612, 2006. (Cited on page 8.)

[29] Julie Escoda. *3D morphological and micromechanical modeling of cementitious materials*. Theses, Ecole Nationale Supérieure des Mines de Paris, 2012. (Cited on page 101.)

[30] Jean-Pierre Fouque, Josselin Garnier, George Papanicolaou, and Knut Sølna. *Wave propagation and time reversal in randomly layered media*, volume 56 of *Stochastic Modelling and Applied Probability*. Springer, New York, 2007. (Cited on pages 34 and 154.)

[31] David Gilbarg and Neil S. Trudinger. *Elliptic partial differential equations of second order*. Classics in Mathematics. Springer-Verlag, Berlin, 2001. Reprint of the 1998 edition. (Cited on page 126.)

[32] Giovanni Giorgi and Houssem Haddar. Computing estimates of material properties from transmission eigenvalues. *Inverse Problems*, 28(5):055009, 2012. (Cited on pages 4 and 30.)

[33] Y. Grisel, V. Mouysset, P.-A. Mazet, and J.-P. Raymond. Determining the shape of defects in non-absorbing inhomogeneous media from far-field measurements. *Inverse Problems*, 28(5):055003, 19, 2012. (Cited on pages 34, 52, 60 and 134.)

[34] P. Grisvard. *Elliptic problems in nonsmooth domains*, volume 24 of *Monographs and Studies in Mathematics*. Pitman (Advanced Publishing Program), Boston, MA, 1985. (Cited on page 127.)

[35] H. Haddar. Sampling 2d, Mars 2013. http://sourceforge.net/projects/samplings-2d/. (Cited on pages 22, 48 and 76.)

[36] F. Hecht. New development in freefem++. *J. Numer. Math.*, 20(3-4):251–265, 2012. (Cited on page 106.)

[37] Guanghui Hu, Jiaqing Yang, Bo Zhang, and Haiwen Zhang. Near-field imaging of scattering obstacles with the factorization method. *Inverse Problems*, 30(9):095005, 25, 2014. (Cited on page 75.)

[38] Masaru Ikehata. A new formulation of the probe method and related problems. *Inverse Problems*, 21(1):413–426, 2005. (Cited on page 8.)

[39] Andreas Kirsch. Characterization of the shape of a scattering obstacle using the spectral data of the far field operator. *Inverse Problems*, 14(6):1489–1512, 1998. (Cited on pages 8, 14 and 22.)

[40] Andreas Kirsch and Natalia Grinberg. *The factorization method for inverse problems*, volume 36 of *Oxford Lecture Series in Mathematics and its Applications*. Oxford University Press, Oxford, 2008. (Cited on pages 8, 14, 21, 34, 44, 70, 75, 119 and 128.)

[41] Digulescu A. PlanesT. Chaix J-F Mazerolle F. Larose E., Obermann A. and Moreau G. Locating and characterizing a crack in concrete with diffuse ultrasound : a four-point bending test. *J. Acoust. Soc. Am*, 2015. accepted. (Cited on pages 3 and 105.)

[42] F. Lavergne, K. Sab, J. Sanahuja, M. Bornert, and C. Toulemonde. Investigation of the effect of aggregates' morphology on concrete creep properties by numerical simulations. *Cement and Concrete Research*, 71(0):14 – 28, 2015. (Cited on page 102.)

[43] Armin Lechleiter. The factorization method is independent of transmission eigenvalues. *Inverse Problems and Imaging*, 3(1):123–138, 2009. (Cited on page 30.)

[44] Adrian I. Nachman, Lassi Päivärinta, and Ari Teirilä. On imaging obstacles inside inhomogeneous media. *J. Funct. Anal.*, 252(2):490–516, 2007. (Cited on page 8.)

[45] Adrian I. Nachman, Lassi Päivärinta, and Ari Teirilä. On imaging obstacles inside inhomogeneous media. *J. Funct. Anal.*, 252(2):490–516, 2007. (Cited on pages 34 and 134.)

[46] J.C. Nadeau. A multiscale model for effective moduli of concrete incorporating {ITZ} water–cement ratio gradients, aggregate size distributions, and entrapped voids. *Cement and Concrete Research*, 33(1):103 – 113, 2003. (Cited on page 117.)

[47] Jean-Claude Nédélec. *Acoustic and electromagnetic equations : integral representations for harmonic problems.* Applied mathematical sciences. Springer, New York, 2001. (Cited on page 149.)

[48] Audrey Quiviger. *Ultrasons diffus pour la caractérisation d'une fissure dans le béton. : approche linéaire et non linéaire.* PhD thesis, 2012. Thèse de doctorat dirigée par Garnier, Vincent Mécanique, physique, micro et nanoélectronique Aix-Marseille 2012. (Cited on pages 3 and 106.)

[49] B. P. Rynne and B. D. Sleeman. The interior transmission problem and inverse scattering from inhomogeneous media. *SIAM J. Math. Anal.*, 22(6):1755–1762, 1991. (Cited on pages 11 and 36.)

[50] L. Sorber, M. Barel, and L. Lathauwer. Unconstrained optimization of real functions in complex variables. *SIAM J. Optim.*, 22(3):879–898, 2012. (Cited on pages 26 and 86.)

[51] L. Sorber, M. Barel, and L. Lathauwer. Complex optimization toolbox v1.0, February 2013. http://esat.kuleuven.be/sista/cot/. (Cited on page 26.)

[52] John Sylvester. Discreteness of transmission eigenvalues via upper triangular compact operators. *SIAM J. Math. Anal.*, 44(1):341–354, 2012. (Cited on pages 11, 41, 70 and 132.)

Qualitative method for heterogeneous media

Abstract: This thesis focuses on non destructive testing of concrete using ultrasonic waves, and thus examines imaging in complex heterogeneous media. We assume that measurements are multistatic, which means that we record the total field on different points by using several sources. For this type of data we wish to build methods that are able to image inclusions or defects that contributed to the measured field. We focus in this work on the extension of so called sampling methods to deal with the over-mentioned application where the main additional difficulty is the lack of knowledge of the reference media (media without defects, also referred to as background media). The first part of this thesis consists of a new theoretical analysis of the Linear Sampling Method leading to new mathematically sound formulation of this method. Such analysis is done in the framework of regularization theory, and our main contribution is to provide and analyze a regularization term that ensures exact characterization of the shape in terms of measured data. We also prove that one is able to reconstruct from regularized solutions a sequence of functions that strongly converges to the solution of the so-called interior transmission problem. This result gives a central place to the interior transmission problem as it allows describing the asymptotic behaviour of our regularized problem. More importantly it also allows us to compare solutions coming from two different datasets. Based on the result of this comparison, we manage to produce an image of the connected components of the background that contain the defects appearing between two measurement campaigns and this is regardless of background "microstructure". This strategy is well suited for applications to concrete-like backgrounds as shown on several numerical examples with realistic concrete-like microstructures. Finally, we extend our theoretical results to the case of limited aperture, anisotropic medium and elastic waves, which correspond to the real physics of the ultrasounds.
Keywords: Inverse problems, Sampling Method.

Méthodes qualitative pour les milieux hétérogènes

Résumé : Motivée par le contrôle non destructif par ultrasons du béton cette thèse s'intéresse à la problématique de l'imagerie à l'aide d'ondes dans des milieux hétérogènes. On se place dans un contexte de mesures multistatiques, c'est-à-dire qu'il est possible de disposer du champ total en plusieurs points de mesure excités par des sources indépendantes. Il est alors proposé de développer des méthodes pour réaliser une image de l'inclusion ou du défaut qui a contribué au champ mesuré. Plus précisément on souhaite étendre les méthodes de sampling pour traiter cette application dans le cas où on manque de connaissance sur le milieu de référence (le milieu sans défaut). La première partie de cette thèse a consisté en une nouvelle analyse théorique de la Linear Sampling Method qui a conduit à une nouvelle formulation plus rigoureuse. Cette analyse est faite dans le cadre de la théorie de la régularisation, notre principale contribution est d'avoir proposé et analysé un terme de régularisation qui assure une caractérisation exacte de la forme du défaut en fonction des données mesurées. Nous avons également démontré que l'on peut construire à partir des solutions du problème régularisé une suite de fonction qui converge fortement vers la solution du problème de transmission intérieure. Cette propriété donne un rôle central au problème de transmission intérieure dans le sens où il permet de décrire le comportement limite de notre solution régularisé. Plus encore cela permet de comparer les solutions provenant de deux campagnes de mesure différentes. Pour ce faire, une méthode permettant de construire une image de la composante connexe du milieu qui contient le défaut qui est apparu entre deux campagnes de mesure est proposée et ce indépendamment du milieu dans lequel le défaut est apparu. Cette méthode d'imagerie différentielle est particulièrement adaptée aux milieux constitués d'un ensemble d'hétérogénéités disjointes, ce qui correspond au cas du béton. Des résultats numériques illustrent son application sur un milieu constitué d'une microstructure simulant le béton. Finalement, nous montrons que nos résultats, développés dans un cadre d'ondes acoustiques en milieu isotrope avec une émission/acquisition en ouverture totale, s'étendent aux mesures en ouverture limitée, aux milieux anisotropes et aux ondes élastiques qui correspondent à la physique réelle des ultrasons.
Mots-clés : Problèmes inverses, Sampling Méthodes.